

General Disclaimer

One or more of the Following Statements may affect this Document

- This document has been reproduced from the best copy furnished by the organizational source. It is being released in the interest of making available as much information as possible.
- This document may contain data, which exceeds the sheet parameters. It was furnished in this condition by the organizational source and is the best copy available.
- This document may contain tone-on-tone or color graphs, charts and/or pictures, which have been reproduced in black and white.
- This document is paginated as submitted by the original source.
- Portions of this document are not fully legible due to the historical nature of some of the material. However, it is the best reproduction available from the original submission.

Unclas
36520



PRELIMINARY DRAFT

CSC/TM-76/6003

**EVALUATION OF THE COMMUNICATIONS TECHNOLOGY
SATELLITE ATTITUDE ACQUISITION ALGORITHMS
AND PROCEDURES**

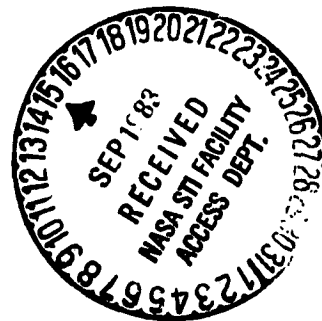
FINAL REPORT

**ORIGINAL PAGE IS
OF POOR QUALITY**

**Prepared for
GODDARD SPACE FLIGHT CENTER**

**By
COMPUTER SCIENCES CORPORATION**

**Under
Contract NAS 5-11999
Task Assignment 635**



Prepared by:

Approved by:

**Dr. G. M. Lerner
J. E. Keat
J. S. Legg, Jr.
Dr. K. Yong
B. T. Blaylock**

Dr. G. M. Lerner _____ **Date**
Technical Supervisor

D. J. Stewart _____ **Date**
Technical Area Manager

PRELIMINARY DRAFT

PREFACE

This preliminary version has been prepared to facilitate review and comment by cognizant GSFC personnel.

ORIGINAL PAGE 19
OF POOR QUALITY

PRECEDING PAGE BLANK NOT FILMED

PRELIMINARY DRAFT

ABSTRACT

This document describes the results of the study of the Communications Technology Satellite (CTS) attitude acquisition procedures. Models of spacecraft hardware and dynamics are also included.

ORIGINAL PAGE IS
OF POOR QUALITY

PRECEDING PAGE BLANK NOT FILMED

PRELIMINARY DRAFT

ORIGINAL PAGE 18
OF POOR QUALITY

TABLE OF CONTENTS

<u>Section 1 - Introduction and Summary</u>	1-1
<u>Section 2 - Hardware Modeling</u>	2-1
2.1 Non-Spinning Earth Sensor Assembly	2-1
2.1.1 Scan Plane Pointing Angle Generation	2-2
2.1.2 Cross Axis Pointing Angle Generation	2-4
2.1.3 Horizon Data Computation	2-4
2.1.4 NESR Region Identification	2-9
2.1.5 Sun Interference	2-14
2.2 Nonspinning Sun Sensors	2-17
2.3 Rate Gyros	2-22
2.4 Spinning Sun Sensors	2-24
2.5 Momentum Wheel	2-25
2.6 Thrusters	2 27
<u>Section 3 - Software Modifications</u>	3-1
3.1 GCAP Modifications	3-1
3.2 ADAMSSIM Modifications	3-1
3.3 FSD Modifications	3-5
3.3.1 Non-Graphics Version of FSD	3-7
3.3.2 FSD/CTS	3-7
3.3.3 GCAP Version of FSD	3-7
<u>Section 4 - Attitude Acquisition Studies</u>	4-1
4.1 ADAMSSIM Open Loop	4-1
4.2 ADAMSSIM Closed Loop	4-4
4.2.1 DESPIN	4-4
4.2.2 PREDAY	4-7
4.2.3 SUNAC	4-8
4.2.4 JETDEP	4-13
4.2.5 SPINUP	4-16
4.2.6 PRESUN	4-16
4.2.7 ERTLCK	4-30
4.3 FSD Open-Loop Study Results	4-35
4.3.1 Torque and Array Flexibility Models	4-35
4.3.2 Results of Simulation Runs	4-38

TABLE OF CONTENTS (Cont'd)

Section 4 (Cont'd)

4.4	FSD/GCAP Closed Loop Study Results	4-54
4.4.1	Momentum Wheel Spinup	4-54
4.4.2	PRESUN Precession Maneuver	4-58
4.4.3	Failure Mode	4-87

Appendix A - DOP Summary

Appendix B - Evaluation of GCAP Data Smoothing
Algorithm - Smooth

Appendix C - Summary of Meetings With SED On August 27 and 28

Appendix D - Loss of Sun Reference During Momentum Wheel
Spinup (LSL)

Appendix E - Attitude Acquisition Via Momentum Transfer (AAMT)

Appendix F - Determination of Phase Angle About Sun Line During
CTS Attitude Acquisition

Appendix G - Sign of Non-Spinning Earth Sensor (NESA) Transfer
Function

Appendix H - Summary of Meetings With SED On November 19 and 20

Glossary

References

PRELIMINARY DRAFT

ORIGINAL PAGE IS
OF POOR QUALITY

LIST OF ILLUSTRATIONS

Figure

1-1	CTS On-Station Configuration	1-2
2-1	NESA Scan Geometry	2-3
2-2	NESA Reference Frame Definition	2-5
2-3	Definition of Earth Sensor Angles. \hat{E}_B is the Earth Vector in Body Coordinates	2-10
2-4	Definition of NESA Field of View Using Output From Both NESA	2-11
2-5	NESA Region Breakdown Using EW ("A") Scanner Data	2-12
2-6	NESA Region Breakdown Using NS ("B") Scanner Data	2-13
2-7	Orientation of NSSS Boresights	2-19
2-8	NSES Reference Frame Definition	2-20
2-9	RGP Transfer Functions	2-23
3-1	ADAMSSIM/GCAP Data Flow.	3-6
3-2	FSD/GCAP Data Flow.	3-9
4-1	Definition of Sun Angles. X, Y, and Z are the Reference Axes in the Spacecraft Frame	4-12
4-2	Trajectory of Pitch Axis on Celestial Sphere During 180 Degree Precession	4-19
4-3	Phasing Relations for ω_x , ω_y , and δ for Spinning Wheel With $\pm X$ or $\pm Z$ Sun Locked.	4-21
4-4	Right Ascension Versus Time for the First Three Minutes of the SPINUP Maneuver	4-59
4-5	Declination Versus Time for the First Three Minutes of the SPINUP Maneuver.	4-60
4-6	ω_y Versus Time for the First Three Minutes of the SPINUP Maneuver	4-61
4-7	ω_x as a Function of Time During PRESUN Burns (#1, #2, #3).	4-65
4-8	ω_y as a Function of Time During PRESUN Burns (#1, #2, #3).	4-68
4-9	ω_z as a Function of Time During PRESUN Burns (#1, #2, #3).	4-71
4-10	Out-of-Plane Deflection of Solar Array #1 (23.79 Feet) During PRESUN Burn #1.	4-74
4-11	In-Plane Deflection of Solar Array #1 (23.79 Feet) During PRESUN Burn #1.	4-77
4-12	Out-of-Plane Deflection of Solar Array #2 (22.79 Feet) During PRESUN Burn #1.	4-80
4-13	In-Plane Deflection of Solar Array #2 (22.79 Feet) During PRESUN Burn #1.	4-83

PRELIMINARY DRAFT

ORIGINAL PAGE 19
OF POOR QUALITY

LIST OF TABLES

Table

2-1	Computation Logic for NESA Chord Lengths	2-8
2-2	NESA Region 0 to 5 Assignment	2-15
2-3	NESA Regions 6 to 9 Assignment	2-16
2-4	NSSS Alignment Angles	2-18
2-5	RGP Calibration Constants	2-24
2-6	Thruster Parameters	2-28
4-1	Efficiency of MODE-2 Damping as a Function of the Transverse Moment of Inertia Ratio	4-3
4-2	DESPIN Simulations	4-5
4-3	Nutation Build Up During DESPIN	4-6
4-4	PREDAY Performance at 58 RPM For Initial $\omega_1 = .38$ Degrees/Second	4-9
4-5	PREDAY Performance at 58 RPM For Initial $\omega_1 = 0.75$ Degrees/Second	4-10
4-6	PREDAY Performance at 58 RPM For Initial $\omega_1 = 1.50$ Degrees/Second	4-11
4-7	SUNAC Starting at End of PREDAY #2	4-14
4-8	JETDEP Profile	4-15
4-9	PRESUN - Test Case Simulation Parameters	4-17
4-10	PRESUN Performance as a Function of Initial Phase Angle	4-22
4-11	Details of Case 3 ϕ_s Determination	4-25
4-12	PRESUN Sensitivity to Thruster and Inertia Biases	4-27
4-13	Earth Lock Simulations	4-31
4-14	Variation in Attitude and Attitude Rates in Six Hours for Spin Rates of One and Two RPM	4-39
4-15	Effect of Magnetic Dipole Strengths Upon Attitude Drift During a Two-Hour Period	4-41
4-16	Z-Axis Drift After Array Deployment	4-43
4-17	Attitude Drift and Drift Rates Due to Slightly Asymmetric Arrays	4-45
4-18	Attitude Drift and Drift Rates Due to Drastically Asym- metric Arrays	4-47
4-19	Attitude Drift and Drift Rates as a Function of Spin Rate . . .	4-48
4-20	Attitude Drift and Drift Rates During Momentum Wheel Spinup	4-50
4-21	Attitude Drift and Drift Rates After Loss of Closed Loop Control During Momentum Wheel Spinup	4-51

PRELIMINARY DRAFT

ORIGINAL PAGE 18
OF POOR QUALITY

LIST OF TABLES (Cont'd)

Table

4-22	SPINUP Parameters	4-55
4-23	SPINUP Results	4-56
4-24	FSD/GCAP Results for the First Five Minutes of the SPINUP Maneuver	4-57
4-25	Flexible Solar Array Tip Deflections and Deflection Rates During the First Six Minutes of the PRESUN Precession Maneuver	4-62
4-26	A Comparison of Simulations With and Without Flexibility for the First Six Minutes of the PRESUN Precession Maneuver	4-63
4-27	PRESUN Burn Parameters	4-86
4-28	Spacecraft Motion With One Array at 23.79 Feet and One Array at 1.0 Foot, With Active δ -Controller For First One-Half Hour	4-88

PRELIMINARY DRAFT

ORIGINAL PAGE IS
OF POOR QUALITY

SECTION 1 - INTRODUCTION AND SUMMARY

The Communications Technology Satellite (CTS) is a joint United States and Canadian project to advance spacecraft communications systems by operating at broadcast frequencies in the 12 to 14 GHz bands at power levels significantly greater than those of existing spacecraft (Reference 1). Requisite power will be supplied by two large-area (10 m^2) deployable solar arrays. The CTS will be 3-axis stabilized using a momentum wheel aligned along the pitch axis (orbit normal) and an onboard, closed loop system utilizing roll or offset (roll-yaw) low thrust hydrazine engines (LTE). Error signals for the thruster control unit (TCU) are provided by two non-spinning Earth sensors assemblies (NESA), NESA-A and NESA-B. NESA-A scans in a nominal east-west (pitch) direction. NESA-B scans in a nominal north-south (roll) direction.

Figure 1-1 illustrates the CTS configuration on-station. The yaw axis is maintained along the local vertical with pitch and roll errors less than ± 0.1 degrees. Yaw errors will be maintained at less than 1.1 degrees via 1/4 orbit coupling.

The CTS mission may be divided into three phases: the first phase, primarily a NASA responsibility, is concerned with achieving the operational geostationary orbit; the second phase, primarily a Canadian Department of Communications/Communications Research Centre (CRC) responsibility, is concerned with achieving the operational 3-axis Earth-oriented attitude, with pitch, roll, and yaw angles and rates within the specifications of the onboard control system; and the third phase is concerned with meeting the experimental objectives of the project once orbit and attitude constraints have been satisfied.

This report documents the results of studies of Phase 2, hereafter denoted as attitude acquisition (AA), performed on Task 635 during the period July 1975 through January 1976. The task assignment was to evaluate the AA procedures developed by SED Systems Ltd. under contract to CRC and recommend analytical and procedural changes to the CTS Project. As part of the task, three trips

PRELIMINARY DRAFT

ORIGINAL PAGE 13
OF POOR QUALITY

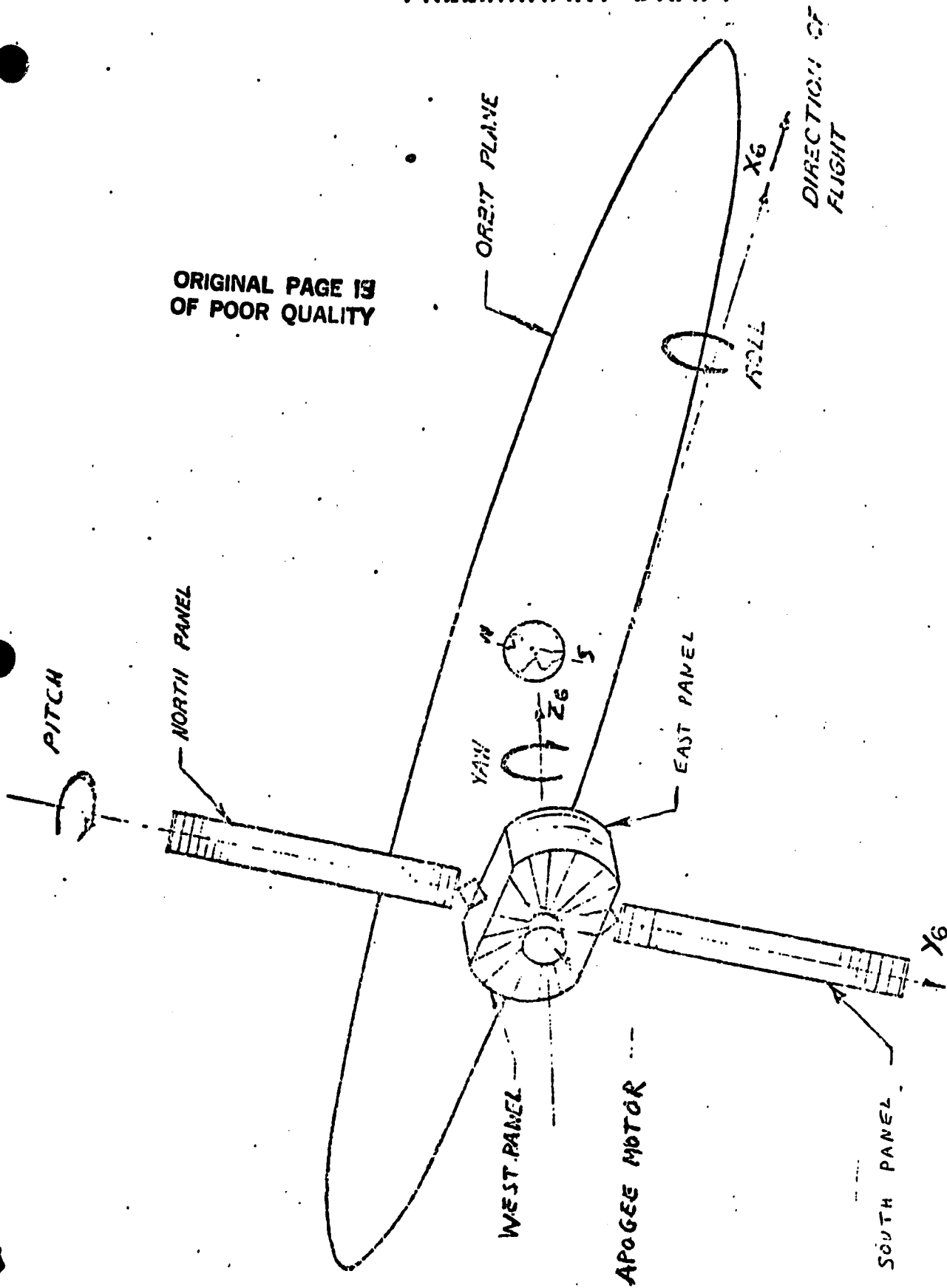


Figure 1-1. CTS On-Station Configuration

to Ottawa were taken (July, August, and November) to attend simulations and discuss procedures with SED/CRC.

Attitude acquisition refers to a series of dynamic maneuvers and the associated algorithms and procedures which are required to convert the CTS attitude state at the end of the NASA phase (a 60 ± 2 RPM spinner with the +Z axis along the southerly orbit normal) to the required on-station attitude state. These maneuvers and procedures are thoroughly documented in the detailed operating procedures (DOP) (Reference 2) document, and a summary of the DOP is reproduced in Appendix A for reference. Briefly, the DOP consist of the following major steps:

1. Phased spin down from 60 to 2 RPM with holds at 54, 16, and 8 RPM to perform calibration, subsystem checkout, and nutation damping functions.
2. Despin to zero RPM with acquisition of the sunline in the spacecraft yaw-roll plane, with the angle between the negative roll (-X) axis and the sunline approximately equal to the Sun declination. The attitude relative to the sunline is maintained by LTE control burns via a closed loop system with the ground computer.
3. Rotation about the pitch axis to place the sunline along the positive yaw (+Z) axis and maintenance of that attitude by LTE control burns.
4. Jettison of the body mounted solar arrays (JBSA) and deployment of the deployable solar arrays (DSA).
5. Spinup of the momentum wheel while dumping momentum with pitch control burns to maintain the positive yaw axis along the sunline; engagement of the onboard constant speed wheel control system after spinup is completed.
6. Rotation of the spacecraft about the inertially fixed pitch axis to acquire the Earth in the NESAs field of view (FOV) to permit a

determination of the phase angle of the pitch (wheel) axis about the sunline.

7. Precession about the sunline to place the pitch axis southerly.
8. Precession about the roll axis to place the yaw axis in the orbit plane.
9. Rotation about the pitch axis to acquire the Earth in the NESA field of view.
10. Trim precessions about roll and yaw and active nutation damping to reduce angular errors and rates to within the limits of the onboard controller.
11. Activation of the onboard controller.

The algorithms and procedures used to implement this sequence of maneuvers are embedded in the ground control algorithms and procedures (GCAP) software and the DOP.

The implementation plan for Task 635 consisted of the following steps:

- Evaluation of the attitude acquisition procedures and algorithms as documented in the DOP and implemented in the GCAP software
- Modification of the flexible spacecraft dynamics (FSD) program (Reference 3) to simulate the CTS configuration and to operate under the Graphic Executive Support System (GESS)
- Development of simulation models for CTS subsystems: rate gyro (RGP), non-spinning Sun sensors (NSSS), non-spinning Earth sensors (NESA), spinning Sun sensors (SSS), and thruster control unit (TCU)
- Modification of the Geodynamics Experimental Ocean Satellite (GEOS) dynamics program (ADAMSSIM) to accommodate thrusting

PRELIMINARY DRAFT

ORIGINAL PAGE IS
OF POOR QUALITY

- Modification of the FORTRAN (batch-mode simulation) version of the GCAP software (Reference 4) to permit operation in the S/360 environment and parameter modification via graphics or NAMELIST
- Integration of the dynamics program ADAMSSIM and the GCAP software (ADAMSSIM/GCAP) to permit closed loop evaluation of the proposed dynamic maneuvers.
- Integration of FSD and the GCAP software (FSD/GCAP) to permit an extension of the closed loop evaluation to include the effects of environmental torques (magnetic dipole, solar radiation pressure, and gravity gradient) and solar array flexibility.

At the outset of the task, CSC realized that the GCAP software to be evaluated differed in two respects from the HP-2100 assembly language code which would actually support AA (Reference 5): (1) most of the logic in the FORTRAN version of GCAP to determine the sequence of maneuvers and details of the selected maneuvers was not present in the HP-2100 assembly language version (flight dynamicists would make the decisions) and (2) significant changes in the DOP and the HP-2100 software had been made and were continuing to be made which were not (and could not) be reflected in the FORTRAN version. Despite these differences, the FORTRAN version of GCAP does contain the essence of the attitude acquisition procedure, and conclusions reached on the basis of its evaluation should be applicable, with few exceptions, to the HP-2100 software.

Due to the relatively short time between the initiation of the task and the nominal CTS launch date (January 13, 1976), periodic recommendations have been made in a series of memoranda (References 6 through 12) which are included, with some minor corrections and additional material, as Appendixes B-H. A review of previous CSC recommendations together with their status and several new recommendations is contained in Reference 12 and Appendix H. Several CSC proposals have been incorporated into the revised DOP; some of these changes

may have been inevitable, but others obviously have resulted solely or partly because of CSC's work. In particular:

1. The momentum wheel duty cycle during spinup has been reduced from 100 percent to 50 percent to ease attitude control during spinup
2. A nonstandard procedure (NSP) has been written to implement attitude acquisition via momentum transfer (AAMT) (Reference 9 and 13) in the event the NSSS subsystem fails. To aid in implementing this NSP, the revised DOP does not include the previously-planned precession of the yaw axis, after despin to 2 RPM, to place it normal to the sunline.
3. Revisions to the Damp Mode 2 algorithm have been made to permit nutation damping for the spinning wheel without Sun lock configuration (required for AAMT).
4. Precession to trim the pitch attitude to achieve $\phi_s \approx 270$ degrees will not be made unless adequate Earth search data is available and the Earth-Sun geometry will permit the accurate determination of ϕ_s .
5. Strict adherence to the extremely rigorous DOP schedule has been superseded by a more flexible approach which will permit additional time to be spent on the evaluation and preparation of maneuvers.

CSC has concluded that the current DOP are completely adequate to successfully support attitude acquisition under a wide range of hardware performance conditions. The basic philosophy is sound and considers all aspects of the problem: spacecraft dynamics, hardware and software performance, and spacecraft operations.

Approximations in the simulation model which have been examined by CSC (environmental torques; some aspects of flexibility; thruster alignment, calibration, and timing) do not have a significant impact on the nominal procedures.

However environmental torques do define an upper limit for maintaining non-nominal configurations as discussed in Section 4.3. The results of the environmental torque studies may be summarized as follows:

- Spin axis precession and nutation buildup at either 1 RPM or 2 RPM is negligible--less than 0.02 degree after 6 hours at 1 RPM.
- Yaw axis drift could be appreciable in the period between array deployment and wheel spinup if active attitude control is absent. The simulation studies indicate a 35-degree drift after 2 hours for a north-south array asymmetry of 6 inches.
- After array deployment, a spacecraft spin rate of 1 degree per second about yaw will reduce the yaw axis drift below 2 degrees in 12 hours if a holding attitude is required prior to momentum wheel spinup
- The presence of environmental torques will increase the offset angle and nutation cone described in Reference 9 for the AAMT non-standard procedure by 1 to 2 degrees.

The impact of an assumed 180-degree precession about the sunline to place the pitch (wheel) axis southerly (PRESUN) on the CTS orbit was examined. Parameter changes were:

$$\Delta a \text{ (semimajor axis)} = 0.24 \text{ km}$$

$$\Delta i \text{ (inclination)} = 0.00054 \text{ degree}$$

$$\Delta e \text{ (eccentricity)} = 0.000007$$

$$\Delta P \text{ (period)} = 0.75 \text{ second}$$

Since the PRESUN precession will cause, by far, the largest impulse during AA (despin burns, though longer, are pure couples and do not affect center-of-mass motion), orbit perturbations are concluded to be negligible.

While adequate for meeting attitude acquisition goals, the DOP are not optimal in a number of respects and will require alert and accurate response by dynamicists to overcome abnormal sensor or thruster performance. Two deficiencies which have been discussed previously, (References 6, 12, and 14) are inadequate preprocessing of sensor data and an inefficient attitude controller algorithm during spin up. Neither of these deficiencies is likely to cause serious problems, however, and it is questionable whether the required software changes could have been implemented without adversely affecting other pre-launch activities.

The detailed results of the study of the spinup attitude controller algorithm are contained in Reference 14, and the conclusions are summarized below:

1. The methods currently planned for the wheel spinup operation are concluded to be adequate.
2. The recent decision to employ a 0.5 duty cycle on the wheel torque pulses during spinup, rather than a unity duty cycle, alleviates the difficulty of maintaining α control during spinup.
3. While the algorithm planned for α control during spinup appears adequate, it is suboptimal in several respects: (a) it requires a larger number of jet pulses than necessary, (b) it depends heavily on operator interaction, and (c) it involves the possibility of "wrong direction" jet pulses due to the fact that the lower deadband is not deactivated.
4. If feasible, the ground support software should be modified to enable the lower deadband to be deactivated or, at least, removed sufficiently far away from the reference value of α that jet torque pulses in the wrong direction are not made. (This recommendation was made verbally during meetings in Ottawa in November 1975 (Reference 12).) Removing the lower α deadband would enable the

time durations of the jet pulses to be increased; a nominal rate command value, $\Delta\dot{\alpha}_c$, of approximately .55 to .65 degrees per second is recommended for computing the jet pulse time durations. The use of these longer pulses would lower the pulse frequency and should reduce the operator interaction requirements. Some operator interaction to trim up the $\Delta\dot{\alpha}$ command value one or more times during the maneuver, however, still would be desirable. The purpose of this trimming should be to place the α - $\dot{\alpha}$ dynamics in a limit cycle type of motion at the start of spinup and to maintain it, as necessary, in such motion throughout spinup.

5. The δ controller should be engaged at the start of spinup and it should not be disengaged until at least 600 to 1000 RPM is reached. Reasonably tight deadband limits are recommended. Widening the δ and $\dot{\delta}$ deadband limits at a given rpm is an alternative to disengagement of the controller.
6. Simulations performed at CSC showed that the original technique (utilizing wheel tachometer data) which SED developed, and abandoned, to control α during spinup performs considerably better at the new duty cycle of .5 than it did at the original 1.0 one. Therefore, it is believed that the original technique could be called upon during spinup, if there should be any reason for doing so.

The inadequate technique which is used to preprocess the sensor data can cause operational difficulties during periods of poor telemetry and possibly during rotations or precessions when the Sun traverses the field of view of two sensors. Occasional, erroneous controller burns can occur if Sun sensor data is poor. If Sun data errors persist over a prolonged period, alert operator action will be required to prevent large attitude errors.

PRELIMINARY DRAFT

ORIGINAL PAGE IS
OF POOR QUALITY

In several periods during attitude acquisition, particularly between the end of despin to 2 RPM and the conclusion of momentum wheel spinup, active ground control is required to maintain a power positive configuration and continuous telemetry communications. Ground support failures during this period are tolerable for periods ranging from only a few minutes (during spinup) up to an hour or more (between array deployment and spinup) without serious consequences. CSC therefore recommends that:

1. Every effort should be taken by SED to minimize the time required to resume operations after a ground support failure. Logs or checklists for parameter entry, keyed to DOP event, should be considered. A simulated failure of the GCAP computer (requiring use of the backup, display computer) should be included as a training exercise.
2. NASA/GSFC should be prepared to command the spacecraft if a failure occurs during a critical event. Only two commands would be necessary, and these would require only voice instructions from Ottawa.
 - a. Yaw burn of LTE to return to a spinner.
 - b. Activation of constant wheel speed (CWS) controller.

Attitude determination during events A32 and A33 prior to the large (up to 180 degrees) and trim precession maneuvers is expected to be difficult because of the inherent central body geometry (Earth and Sun in close proximity); the possibility of NESA Sun interference; and the poor NESA resolution outside the linear, ± 2.82 degrees, region. Because of these problems CSC has recommended (Reference 11) that for event A32 both α_E and δ_E data be used to determine the phase angle and that the trim maneuver, event A33, be delayed until sufficiently accurate Earth search data is available to justify a trim maneuver.

PRELIMINARY DRAFT

ORIGINAL PAGE IS
OF POOR QUALITY

The final recommendations concern the selection of thrusters and the procedures followed for precession commands particularly the initial, potentially 180 degree, precession about the Sun line. The present planning calls for the use of the roll thrusters to place the +Y axis southerly after wheel spinup. Unless the ϕ_s angle is near 0 or 180 degrees and/or telemetry problems occur, we recommend that a rotation to control $\pm X$ along the Sun line be performed after the ϕ_s determination and that a yaw couple be used to affect the precession. The reasons for this recommendation are as follows.

- The roll thrusters will be poorly calibrated having been used only for brief attitude controller (ATTCON) burns.
- The yaw thrusters will be well calibrated during the despin.
- The 90-degree orbit slot is favorable for $\pm X$ Sun lock, ϕ_s retermination, and timeline considerations.

Irrespective of the thruster selection, we recommend that (1) large precessions be preceded by short precessions in the desired direction to calibrate and validate the selected hardware and (2) expected ranges for telemetry parameters, such as Sun angles and rates, be established prior to each maneuver so that anomalies may be detected early and abnormal maneuvers may be aborted quickly.

PRELIMINARY DRAFT

ORIGINAL PAGE IS
OF POOR QUALITY

SECTION 2 - HARDWARE MODELING

The GCAP software requires input data from the NSSS, SSS, NESA, gyro, and wheel tachometer subsystems, and the dynamics software requires thruster and wheel reaction torque data. Simulation models for these subsystems were developed to interface between GCAP and either dynamics program, FSD or ADAMSSIM. The philosophy adopted in developing these models may be summarized as follows:

- Hardware specifications rather than simulator documentation were used wherever possible
- Dynamics considerations were emphasized for the momentum wheel and thrusters rather than detailed modeling of electronics and telemetry
- Existing SED subroutines or code were not used
- Details of the command implementation and timing were ignored.

The following subsections describe the subsystems and mathematical models developed for the interface module.

2.1 NON-SPINNING EARTH SENSOR ASSEMBLY (NESA)*

The Non Spinning CTS Earth Sensor Assembly is an infrared sensor which continuously scans across the Earth, measuring chords and angles to determine pitch and roll. It consists of two independent infrared Earth scanners. Each scanner is oriented so as to scan across a different Earth chord, in such a way that both pitch and roll information can be derived from either or both of the scanners.

*The NESA description is taken from a TRW specification document.

Figure 2-1 illustrates the basic scan geometry. In the figure, scanner EW generates pitch by measuring the difference between the two chord segments along the scan direction (scan output), while roll is generated by measuring the total chord and subtracting a preset chord length (cross output). For scanner NS, the computations are reversed. When both scanners are operating, all four outputs are generated; in this case, the scan outputs are the most precise and thus the preferred outputs.

The sensor head contains the infrared telescope with detector, the scanning mirror, Sun detector, and the preamplifiers and other electronics immediately associated with these devices. These subassemblies are described below.

The scanning of the instantaneous field of view is created by oscillating a polished flat beryllium mirror about an axis with an electromagnetic drive from a brushless DC torque motor. The scan frequency is 4.40 Hz.

A small Sun detector is located just ahead of the IR telescope to identify intrusion of the Sun in the field of view. This consists of a small mirror, two fixed mechanical apertures, and a silicon solar cell detector. The optical design is such that the Sun detector field of view is concentric with but larger than the infrared field-of-view. Whenever the Sun is within 3.5 degrees of the infrared FOV, the solar cell generates sufficient current to indicate Sun presence.

2.1.1 Scan Plane Pointing Angle Generation

Scan plane pointing angle computation is performed by using a binary up-down counter to accumulate encoder pulses from the scan mirror. Encoder pulses are counted during the time an Earth radiance logic signal is present with the direction of count established by the state of the reference position logic signal. Therefore for the case where the scan is centered, the up count and the down count are equal and a zero count or null pointing angle is generated.

To improve the overall accuracy, the up-down counter accumulates the count difference over a 0.9 second averaging interval (4 scans). At the end of each

PRELIMINARY DRAFT

ORIGINAL PAGE 15
OF POOR QUALITY

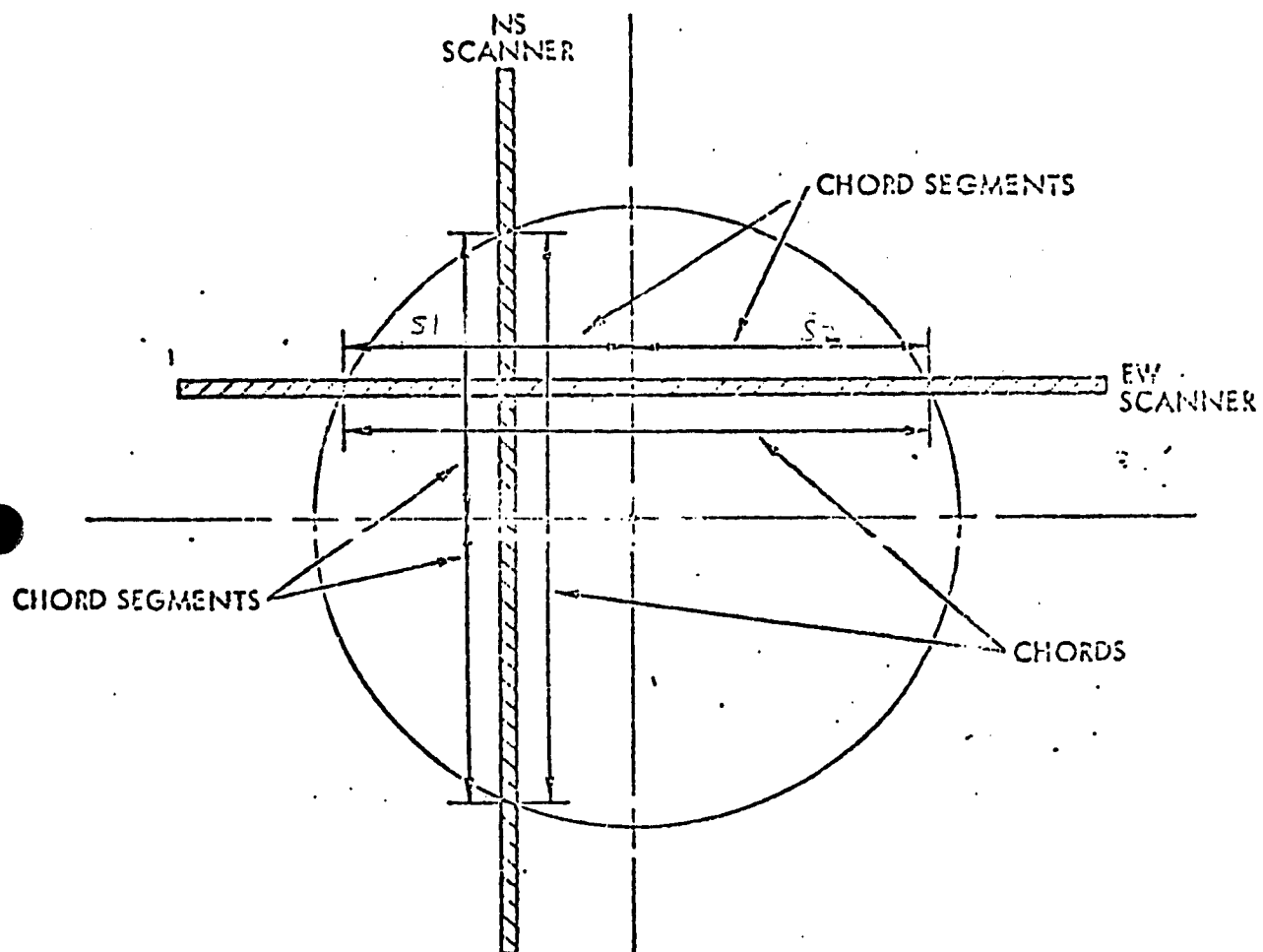


Figure 2-1. NESA Scan Geometry

4 scan period, the resultant pointing angle binary count is transferred to two 9 bit (8 data bits plus sign) storage registers. The control storage register has serial readout capability to provide the required data interface. Internal control logic inhibits any update of the register if a data readout is in progress. The telemetry storage register is part of the larger 24 bit telemetry word.

Internal data scaling results in a least significant bit weighting of 0.011 degrees with the data being presented in 2's complement natural binary form. The maximum output is ± 2.82 degrees. Should the computed angle exceed these angles, internal overflow detection logic causes the output register to be set at the appropriate extreme angle value.

2.1.2 Cross Axis Pointing Angle Generation

The pointing angle for the cross axis (perpendicular to the scan plane) is determined by comparing the length of the scanned chord with a fixed width.

The fixed width times eight is set into a binary down counter once every four scans. The encoder clock pulses are then counted whenever Earth radiance is present. The digital count in the counter at the end of the 4 scan interval is the difference in length between the fixed chord and the scanned chord averaged over a 0.9 second period. This value is again transferred to both a data shift register and a telemetry shift register to provide the output interface.

2.1.3 Horizon Data Computation

Input to the NESAs consists of the spacecraft to Earth (\hat{E}_I) and spacecraft to Sun (\hat{v}_I) vectors in inertial coordinates and the inertial to body transformation matrix (A). Output consists of NESAs region numbers (see Section 2.1.4) and Earth and Sun presence flags.

The NESA reference frame is shown in Figure 2-2. There are separate NESA reference frames for the NS and EW scanners. The boresight of each scanner oscillates with a frequency ω in its NESA x-y plane in the range $-13^\circ \leq \omega t \leq 13^\circ$. The boresight vector is

$$\hat{S}_{NESA} = (\cos \omega t, \sin \omega t, 0) \quad (2-1)$$

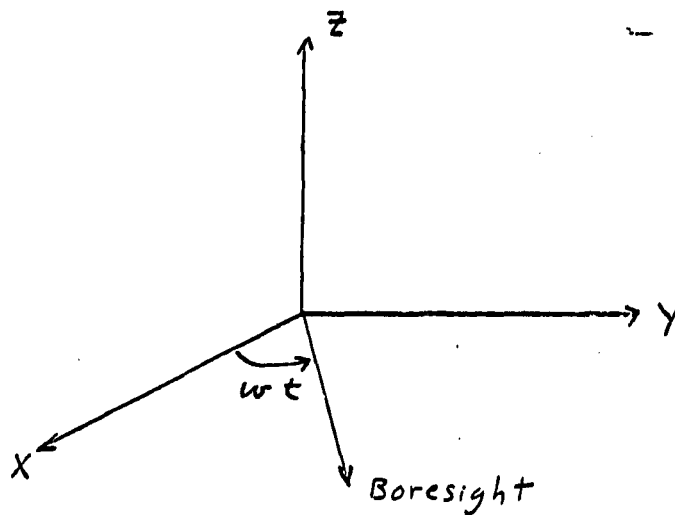


Figure 2-2. NESA Reference Frame Definition

The transformation from NESA to body coordinates for the EW scanner is

$$A_{EW} = \begin{pmatrix} 0 & -1 & 0 \\ \sin \phi & 0 & -\cos \phi \\ \cos \phi & 0 & \sin \phi \end{pmatrix} \quad (2-2)$$

where $\phi = 3.5$ degrees is the plane tilt.

PRELIMINARY DRAFT

ORIGINAL PAGE IS
OF POOR QUALITY

In body coordinates the boresight vector of the EW scanner is

$$\begin{aligned}\hat{S}_B^{EW} &= A_{EW} \hat{S}_{NEJA} \\ &= (-\sin \omega t, \sin \varphi \cos \omega t, \cos \varphi \cos \omega t)\end{aligned}\quad (2-3)$$

The scan is assumed to go from $\omega t = -13^\circ$ to $\omega t = +13^\circ$. (Note that the hardware averages the results of four cycles.)

The angles ωt corresponding to crossings of the Earth horizon are computed as follows. In body coordinates the spacecraft to Earth unit vector is given by $\hat{E}_B = A \hat{E}_I$ where \hat{E}_I is the spacecraft to Earth unit vector in inertial coordinates and A is the attitude matrix. Horizon vectors satisfy

$$\hat{H}_B \cdot \hat{E}_B = \cos \rho \quad (2-4)$$

where ρ is the angular radius of the Earth (8.686 degrees).

At a horizon crossing of the EW scanner, $\hat{S}_B^{EW} = \hat{H}_B$. Substitution of (2-3) into (2-4) thus yields at a horizon crossing

$$-\sin \omega t E_{B1} + \cos \omega t (\sin \varphi E_{B2} + \cos \varphi E_{B3}) = \cos \rho \quad (2-5)$$

with the solutions

$$\cos \omega t = \frac{bc \pm a(a^2 + b^2 - c^2)^{1/2}}{a^2 + b^2} \quad (2-6)$$

PRELIMINARY DRAFT

where

ORIGINAL PAGE IS
OF POOR QUALITY

$$\begin{aligned}a &= -E_{B1} \\b &= \sin \varphi E_{B2} + \cos \varphi E_{B3} \\c &= \cos \rho\end{aligned}\tag{2-7}$$

Note that $a^2 + b^2 - c^2 < 0$ implies no horizon intersection. Valid intersections satisfy

$$-13^\circ < \omega t < +13^\circ$$

The NS scanner boresight vector in body coordinates is given by

$$\hat{S}_B^{NS} = (-\sin \varphi \cos \omega t, \sin \omega t, \cos \varphi \cos \omega t)\tag{2-8}$$

Horizon intersections of the NS scanner satisfy Equation (2-6) with

$$\begin{aligned}a &= E_{B1} \\b &= \cos \varphi E_{B3} - \sin \varphi E_{B2} \\c &= \cos \rho\end{aligned}\tag{2-9}$$

Note that there are two solutions to Equation (2-6) corresponding to two horizon crossings. The quadrant of ωt is resolved using the relation

$$\sin \omega t = (c - b \cos \omega t) / a\tag{2-10}$$

together with Equation (2-6), and (2-7) or (2-9).

PRELIMINARY DRAFT

ORIGINAL PAGE IS
OF POOR QUALITY

2.1.3.1 Scanner Output

Defining the ordered horizon crossings as C1 and C2 where

$$C1 \text{ or } C2 = \tan^{-1} (\sin \omega t / \cos \omega t)$$

and $C2 > C1$, it remains to determine the sensor cross and scan outputs.

C1 and C2 are measured in the NESAs frame without restriction on the magnitude, i.e., C1 may be greater than 13 degrees, as computed, and C1 and C2 may both be on the same side of the null, i.e., $C1 < C2 < 0$. The chord segments, S1 and S2, as shown in Figure 2-1 are computed as follows.

Define the angle from acquisition of signal (AOS) to $\omega t = 0$ as S1 and from $\omega t = 0$ to loss of signal (LOS) as S2. The possibilities (a) to (g) in Table 2-1 need be considered in sequence.

Table 2-1. Computation Logic for NESAs Chord Lengths

	Logical Test Horizon Crossing Angles (degrees)		Chord length from AOS to zero and zero to LOS (degrees)		Earth Presence
	C1	C2	S1	S2	
(a)	$> + 13$		Undefined	Undefined	No
(b)		$< - 13$	Undefined	Undefined	No
(c)	$\leq - 13$		$13 + C2$	0	Yes
(d)		≥ 13	0	$13 - C1$	Yes
(e)		≤ 0	$C2 - C1$	0	Yes
(f)	≥ 0		0	$C2 - C1$	Yes
(g)			$- C1$	C2	Yes

If logical tests (a) to (f) are all false, S1 and S2 are as defined in (g), otherwise S1 and S2 are defined by the first test which is true.

Given the chord angles S1 and S2 the outputs are

$$\begin{aligned} \text{SCAN} &= - \left(\frac{S2 - S1}{2 * 2.82^\circ} \right) * 255 \\ \text{CROSS} &= \left(\frac{15.909^\circ - (S2 + S1)}{2.82^\circ} \right) * 255 \end{aligned} \quad (2-11)$$

The relations between the SCAN and CROSS outputs and the Earth angles α_E (pitch) and δ_E (roll) shown in Figure 2-3 are:

$$\begin{aligned} \alpha_E &= - \text{SCAN} * 2.82 / 255 \\ \delta_E &= \text{CROSS} * 2.82 / 255 \end{aligned} \quad (2-12)$$

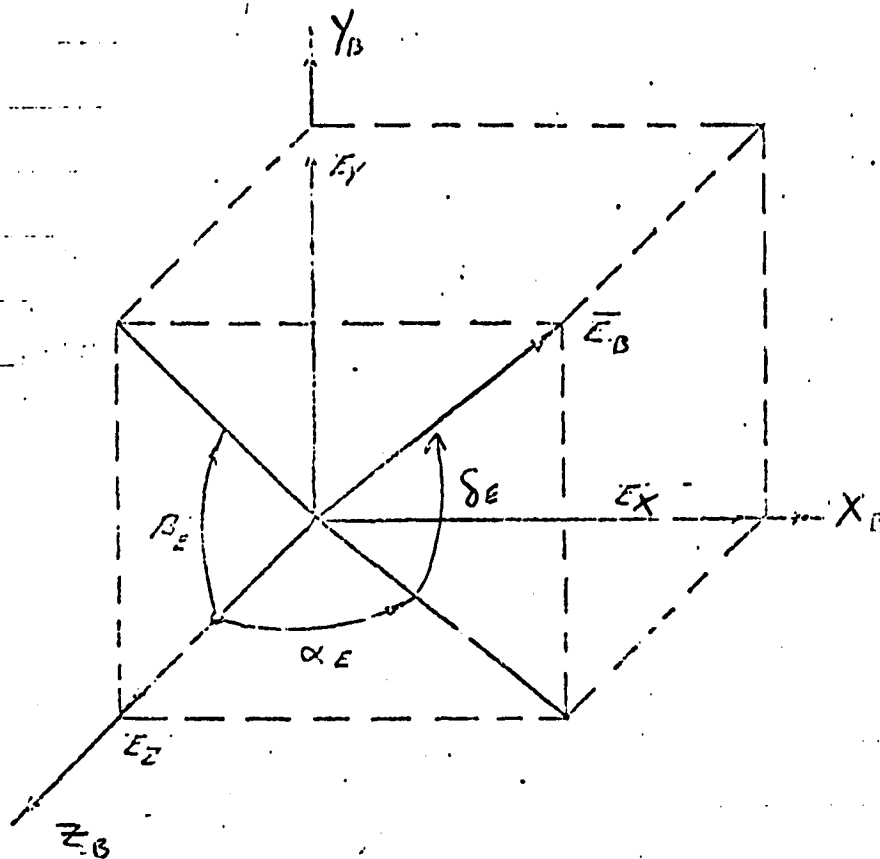
2.1.4 NESA Region Identification

The field of view of the NESA has been divided into regions. These regions (0 to 5, 6 to 7, and 8 to 9) and their subregions are shown in Figures 2-4 to 2-6, respectively. The individual regions are defined by the sign and magnitude of the scan and cross outputs and serve to provide an easily interpretable function of the NESA output in the event the Earth is outside the linear ± 2.82 degree field of view of either or both sensors.

The NESA region information is used by the GCAP (Batch Mode) modules PRESUN and ERTLCK to determine ϕ_S and compute precession directions. In flight, NESA regions are computed to provide operators with a visual aid and to compute ϕ_S .

PRELIMINARY DRAFT

ORIGINAL PAGE IS
OF POOR QUALITY



$$\alpha_E = \tan^{-1}(E_X / E_Z)$$

$$\beta_E = \tan^{-1}(E_Y / E_Z)$$

$$\delta_E = \sin^{-1}(E_Y) = \beta_E + O(\alpha_E)$$

Figure 2-3. Definition of Earth Sensor Angles. \hat{E}_B is the Earth Vector in Body Coordinates

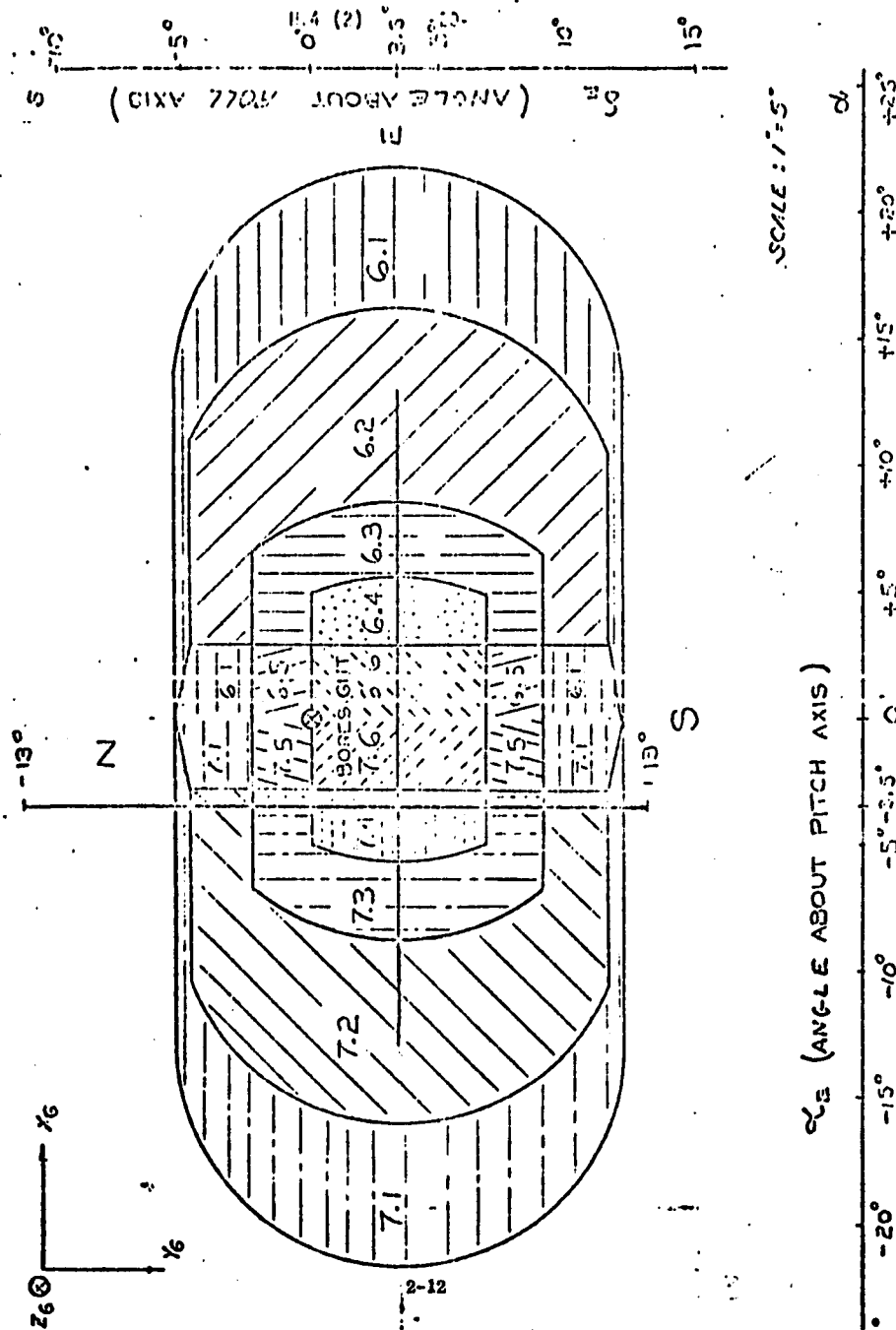
1. REGIONS IN TO IN ARE
2. REGION OF NORTH
3. REGION OF NORTH
4. REGION OF NORTH
5. REGION OF NORTH
6. REGION OF NORTH
7. REGION OF NORTH
8. REGION OF NORTH
9. REGION OF NORTH
10. REGION OF NORTH
11. REGION OF NORTH
12. REGION OF NORTH
13. REGION OF NORTH
14. REGION OF NORTH
15. REGION OF NORTH
16. REGION OF NORTH
17. REGION OF NORTH
18. REGION OF NORTH
19. REGION OF NORTH
20. REGION OF NORTH
21. REGION OF NORTH
22. REGION OF NORTH
23. REGION OF NORTH
24. REGION OF NORTH
25. REGION OF NORTH
26. REGION OF NORTH
27. REGION OF NORTH
28. REGION OF NORTH
29. REGION OF NORTH
30. REGION OF NORTH
31. REGION OF NORTH
32. REGION OF NORTH
33. REGION OF NORTH
34. REGION OF NORTH
35. REGION OF NORTH
36. REGION OF NORTH
37. REGION OF NORTH
38. REGION OF NORTH
39. REGION OF NORTH
40. REGION OF NORTH
41. REGION OF NORTH
42. REGION OF NORTH
43. REGION OF NORTH
44. REGION OF NORTH
45. REGION OF NORTH
46. REGION OF NORTH
47. REGION OF NORTH
48. REGION OF NORTH
49. REGION OF NORTH
50. REGION OF NORTH
51. REGION OF NORTH
52. REGION OF NORTH
53. REGION OF NORTH
54. REGION OF NORTH
55. REGION OF NORTH
56. REGION OF NORTH
57. REGION OF NORTH
58. REGION OF NORTH
59. REGION OF NORTH
60. REGION OF NORTH
61. REGION OF NORTH
62. REGION OF NORTH
63. REGION OF NORTH
64. REGION OF NORTH
65. REGION OF NORTH
66. REGION OF NORTH
67. REGION OF NORTH
68. REGION OF NORTH
69. REGION OF NORTH
70. REGION OF NORTH
71. REGION OF NORTH
72. REGION OF NORTH
73. REGION OF NORTH
74. REGION OF NORTH
75. REGION OF NORTH
76. REGION OF NORTH
77. REGION OF NORTH
78. REGION OF NORTH
79. REGION OF NORTH
80. REGION OF NORTH
81. REGION OF NORTH
82. REGION OF NORTH
83. REGION OF NORTH
84. REGION OF NORTH
85. REGION OF NORTH
86. REGION OF NORTH
87. REGION OF NORTH
88. REGION OF NORTH
89. REGION OF NORTH
90. REGION OF NORTH
91. REGION OF NORTH
92. REGION OF NORTH
93. REGION OF NORTH
94. REGION OF NORTH
95. REGION OF NORTH
96. REGION OF NORTH
97. REGION OF NORTH
98. REGION OF NORTH
99. REGION OF NORTH
100. REGION OF NORTH

4. SATURATED NITRA GROUP
ONE TO TEN PERCENT IN
ETHER SOLUBLE OILS
READY TO BE SENT TO
REGION 6.



PRELIMINARY DRAFT

ORIGINAL PAGE IS
OF POOR QUALITY



**ORIGINAL PAGE IS
OF POOR QUALITY**

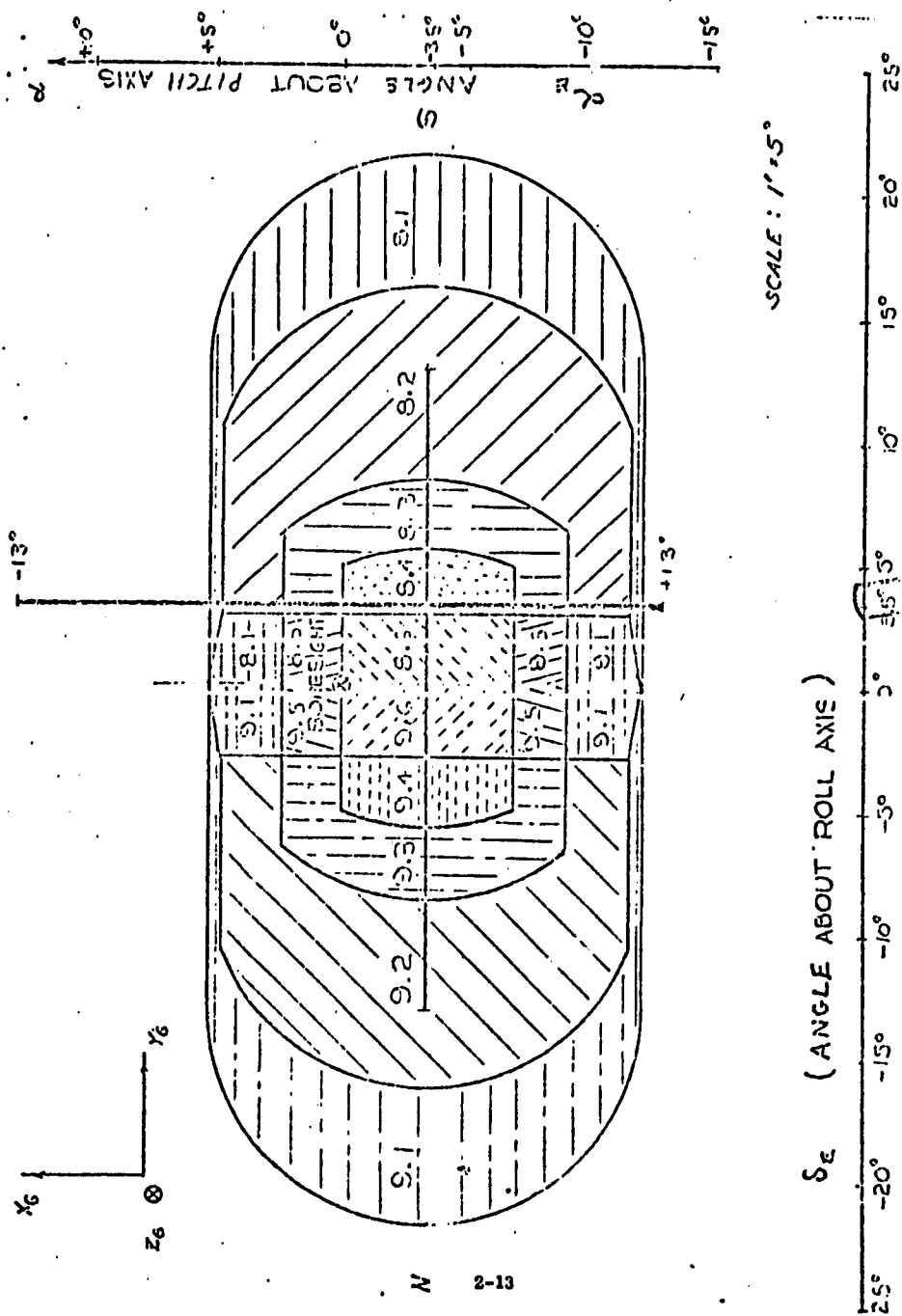


Figure 2-6. NESa Region Breakdown Using N.S. ("E") Scanner Data

PRELIMINARY DRAFT

ORIGINAL PAGE IS
OF POOR QUALITY

2.1.4.1 Regions 0 to 5

Regions 0 to 5 are defined in Figure 2-4 and are determined (with rare exceptions) by the scan output of both NESA-A (EW) and NESA-B (NS) as shown in Table 2-4.

2.1.4.2 Regions 6 and 7

Regions 6 and 7 are defined in Figure 2-5 and are determined by the scan and cross output of NESA-A as shown in Table 2-5.

2.1.4.3 Region 8 and 9

Regions 8 and 9 are defined in Figure 2-6 and are determined by the scan and cross output of NESA-B as shown in Table 2-6.

2.1.5 Sun Interference

A Sun interference flag is set aboard the spacecraft if the angle θ between the NESA boresight and Sun line (\hat{v}_B) is less than a critical value $\theta = \theta_x \approx 3.5$ degrees. For the East-West scanner,

$$\hat{s}_B^{EW} \cdot \hat{v}_B = \cos \theta \quad (2-13a)$$

Inserting Equation (2-3) yields

$$\begin{aligned} -\sin \omega t \, v_{B1} + \sin \phi \cos \omega t \, v_{B2} \\ + \cos \phi \cos \omega t \, v_{B3} = \cos \theta \end{aligned} \quad (2-13b)$$

or

$$f(\omega t) = \cos \theta \quad (2-13c)$$

PRELIMINARY DRAFT

ORIGINAL PAGE IS
OF POOR QUALITY

Table 2-2. NESA Region 0 to 5 Assignment

NESA Region	Earth Presence		Scan Output				Notes
	A(EW)	B(NS)	A(EW)		B(NS)		
			Sign	Saturated	Sign	Saturated	
0	F	F					
1.1	T	F	+				
1.2	T	T	+	Yes	-	Yes	
1.3	T	T	+		±	No	1.2
1.4	T	T	+	Yes	+	Yes	
2.1	F	T			+		
2.2	T	T	±	No	+	Yes	
3.1	T	F	-				
3.2	T	T	-	Yes	-	Yes	
3.3	T	T	-		±	No	3
3.4	T	T	-	Yes	+	Yes	
4.1	F	T			-		
4.2	T	T	±	No	-	Yes	
5.1	T	T	+	No	+	No	
5.2	T	T	-	No	+	No	3
5.3	T	T	-	No	-	No	3
5.4	T	T	+	No	-	No	1

- NOTES: (1) If EW scan is unsaturated, region 1.3 rather than 5.4 is selected if either cross output is saturated.
- (2) Region 1.3 selected rather than 5.1 if both cross outputs are saturated and both scan outputs are 201 counts or more.
- (3) Region 3.3 selected rather than 5.3 or 5.2 if either cross output is saturated.

PRELIMINARY DRAFT

ORIGINAL PAGE IS
OF POOR QUALITY

Table 2-3. NESA Regions 6 to 9 Assignment

<u>Region</u>	<u>Scanner A or B</u>	<u>SCAN Sign</u>	<u>Output Saturated</u>	<u>Cross Sign</u>	<u>Output Saturated</u>
6.1	A	+	No	±	Yes
6.2	A	+	Yes	±	Yes
6.3	A	+	Yes	+	No
6.4	A	+	Yes	-	No
6.5	A	+	No	+	No
6.6	A	+	No	-	No
7.1	A	-	No	±	Yes
7.2	A	-	Yes	±	Yes
7.3	A	-	Yes	+	No
7.4	A	-	Yes	-	No
7.5	A	-	No	+	No
7.6	A	-	No	-	No
8.1	B	-	No	±	Yes
8.2	B	-	Yes	±	Yes
8.3	B	-	Yes	+	No
8.4	B	-	Yes	-	No
8.5	B	-	No	+	No
8.6	B	-	No	-	No
9.1	B	+	No	±	Yes
9.2	B	+	Yes	±	Yes
9.3	B	+	Yes	+	No
9.4	B	+	Yes	-	No
9.5	B	+	No	+	No
9.6	B	+	No	-	No

Clearly θ is a minimum for $\cos \theta$ maximum; the minimum θ is the solution to

$$\frac{\partial (\cos \theta)}{\partial (\omega t)} = 0 \quad (2-13d)$$

Inserting Equation (2-13b), in (2-13d) yields for the East-West scanner

$$\omega t_m = \tan^{-1} \left(\frac{-N_{B1}}{\sin \varphi N_{B2} + \cos \varphi N_{B3}} \right) \quad (2-14)$$

Similarly, for the North-South scanner we obtain

$$\omega t_m = \tan^{-1} \left(\frac{N_{B2}}{\cos \varphi N_{B3} - \sin \varphi N_{B1}} \right) \quad (2-15)$$

The Sun interference flag is set at ωt_m if

$$\cos^{-1} (F(\omega t_m)) < \theta_x \approx 3.5^\circ \quad (2-16)$$

Degradation of the NESA output, caused by the Sun radiance adding counts to the S1 or S2 readings occurs at $\theta_x \approx 2.6$ degrees and causes a maximum addition to the chord output of 100 counts (1.2 degrees) for $\theta_x \leq 1$ degree.

The sign of ωt_m determines whether the scan output is increased or decreased by the Sun interference.

2.2 NONSPINNING SUN SENSORS (NSSS)

The NSSS system consists of five sensor heads and an electronics unit. The electronics unit selects the most intensely illuminated head and returns the

head ID and two Gray coded seven bit angles. Each sensor head is sensitive within a cone of half-angle 1° degrees from boresight. The boresights of the five sensors are distributed as shown in Figure 2-7 to yield 4π steradian coverage. Table 2-4 defines the orientation of each sensor frame $(\hat{x}_s, \hat{y}_s, \hat{z}_s)$ in the body frame $(\hat{i}, \hat{j}, \hat{k})$. As an example, Figure 2-8 defines the orientation of sensor 1.

Table 2-4. NSSS Alignment Angles

Sun Sensor	Sensor Axis		
	\hat{x}_s (Boresight)	\hat{y}_s	\hat{z}_s
1	\hat{i}	\hat{k}	$-\hat{j}$
2	$-\hat{i}$	\hat{k}	\hat{j}
3	$-\cos 30^\circ \hat{j} - \sin 30^\circ \hat{k}$	$\cos 30^\circ \hat{k} - \sin 30^\circ \hat{j}$	$-\hat{i}$
4	$\cos 30^\circ \hat{j} - \sin 30^\circ \hat{k}$	$\cos 30^\circ \hat{k} + \sin 30^\circ \hat{j}$	\hat{i}
5	\hat{k}	$-\hat{j}$	\hat{i}

The sensor reference angles, α and β , as defined in Figure 2-8 are related to the sensor outputs NA and NB through the equations:

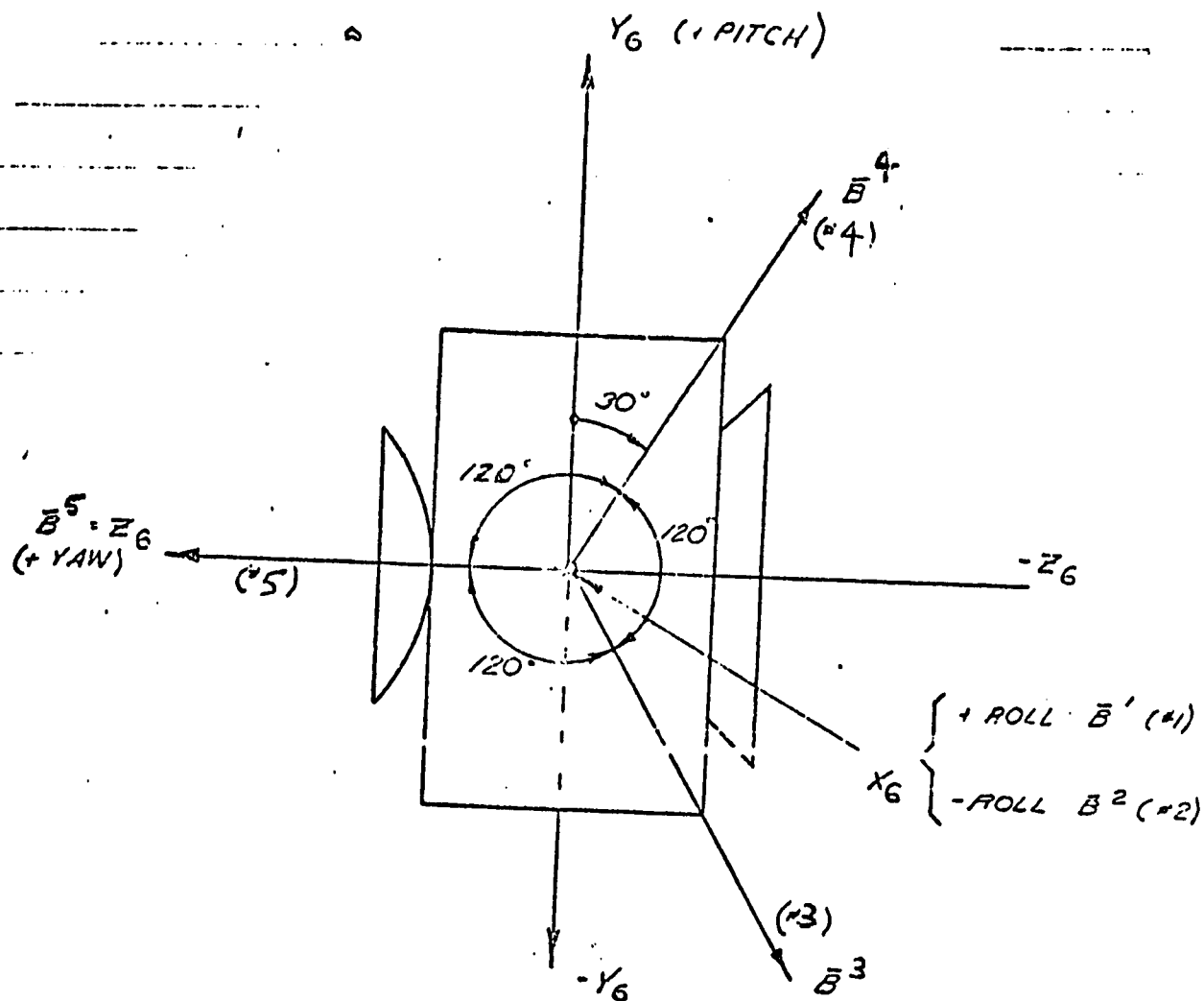
$$\begin{aligned} \tan \alpha &= n \rho / \theta \\ \tan \beta &= n \gamma / \theta \end{aligned} \quad (2-17)$$

where

$$\theta = [t^2 - (n^2 - 1)(\gamma^2 + \rho^2)]^{1/2}$$

PRELIMINARY DRAFT

ORIGINAL PAGE IS
OF POOR QUALITY



Note that the designation of sensors 3, 4, and 5 is different from that used in Reference 4.

Figure 2-7. Orientation of NSSS Boresights

PRELIMINARY DRAFT

ORIGINAL PAGE IS
OF POOR QUALITY

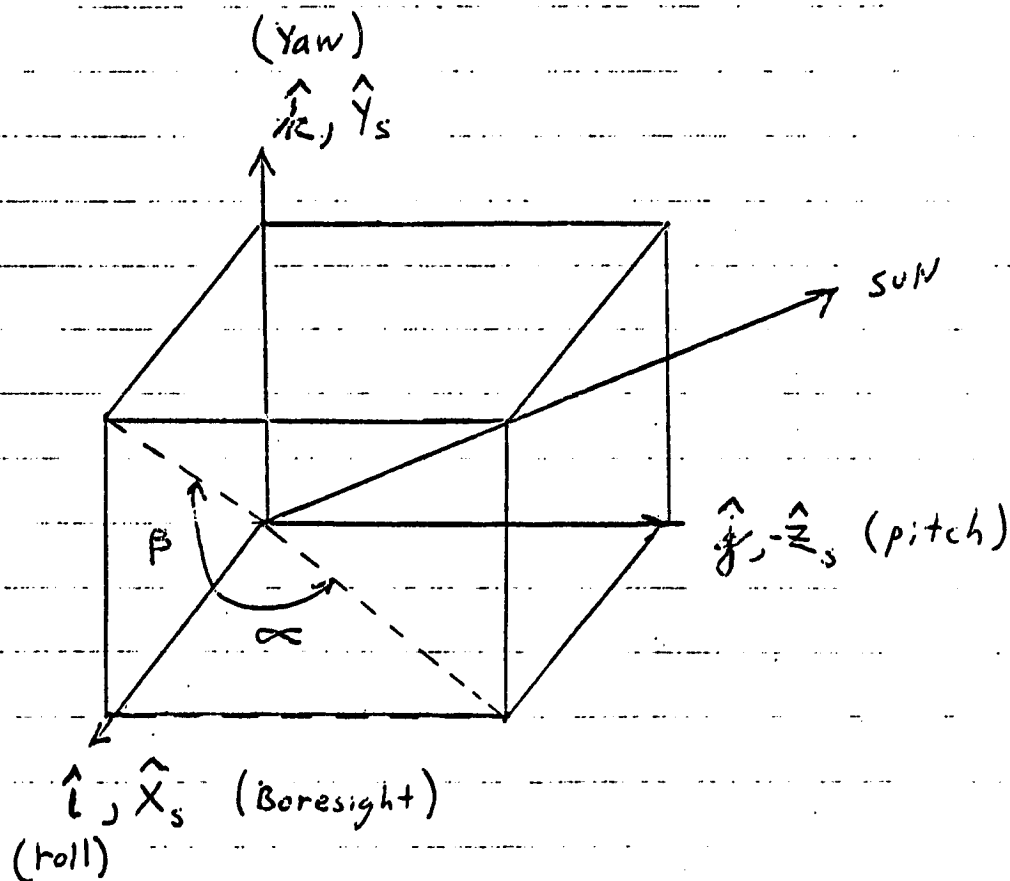


Figure 2-8. NSSF Reference Frame Definition and Orientation of Sensor 1

$$\rho = 0.00275 (|N_A| + 0.5) * \text{Sign}(N_A)$$

$$\gamma = 0.00275 (|N_B| + 0.5) * \text{Sign}(N_B)$$

$$h = 1.4553 \quad (2-18)$$

$$t^2 = 0.050176$$

The Sun vector in the sensor frame is

$$\hat{u}_{ss} = \frac{1}{[1 + \tan^2 \alpha + \tan^2 \beta]^{1/2}} \begin{pmatrix} 1 \\ \tan \beta \\ -\tan \alpha \end{pmatrix} \quad (2-19a)$$

and in body coordinates

$$\hat{u}_B = A^t \hat{u}_{ss} \quad (2-19b)$$

where the A^t matrix may be obtained from Table 2-4. For example, for Sensor 1,

$$A^t = \begin{pmatrix} 1 & 0 & 0 \\ 0 & 0 & -1 \\ 0 & 1 & 0 \end{pmatrix} \quad (2-19c)$$

The simulation model first uses the inverse of Equation (2-17) through (2-19) to compute N_A , N_B and the most intensely illuminated sensor identification and then uses Equations (2-17) through (2-19) to compute a "digitized" Sun vector (\hat{v}'_B) in body coordinates. The "digitized" Sun vector is used to compute the reference angles, $\alpha_S = \tan^{-1} (v'_{B3}/v'_{B1})$ and $\delta_S = \sin^{-1} (v'_{B2})$ which are used by the GCAP software.

Note that the equations employed and the definitions shown in Figure 2-8 differ from those in the Adcole literature. The present choice was made to conform to the SED definition of the NSSS reference frame.

2.3 RATE GYROS (RGP)

The rate gyro model was taken from the batch mode simulation document (Reference 4). A relation between the input axis rate and voltage output was assumed as shown in Figure 2-9.

Each of the three axes is assumed to have a separate calibration curve. Each calibration curve is broken into three segments as follows:

$$\begin{aligned} & W \leq D \Rightarrow N = F \\ (a) \quad & C \leq W \leq B \Rightarrow N = 0 \\ & W > A \Rightarrow N = E \end{aligned} \tag{2-20}$$

$$\begin{aligned} (b) \quad & D < W < C \\ & N = A2 - (A2 - F) * W / D \\ & A2 = CF / (C - D) \end{aligned} \tag{2-21}$$

$$\begin{aligned} (c) \quad & B < W < A \\ & N = A1 + (E - A1) * W / A \\ & A1 = BE / (B - A) \end{aligned} \tag{2-22}$$

The analog voltage data is digitized for transmission

$$N_n = N * (ADC) \tag{2-23}$$

PRELIMINARY DRAFT

ORIGINAL PAGE IS
OF POOR QUALITY

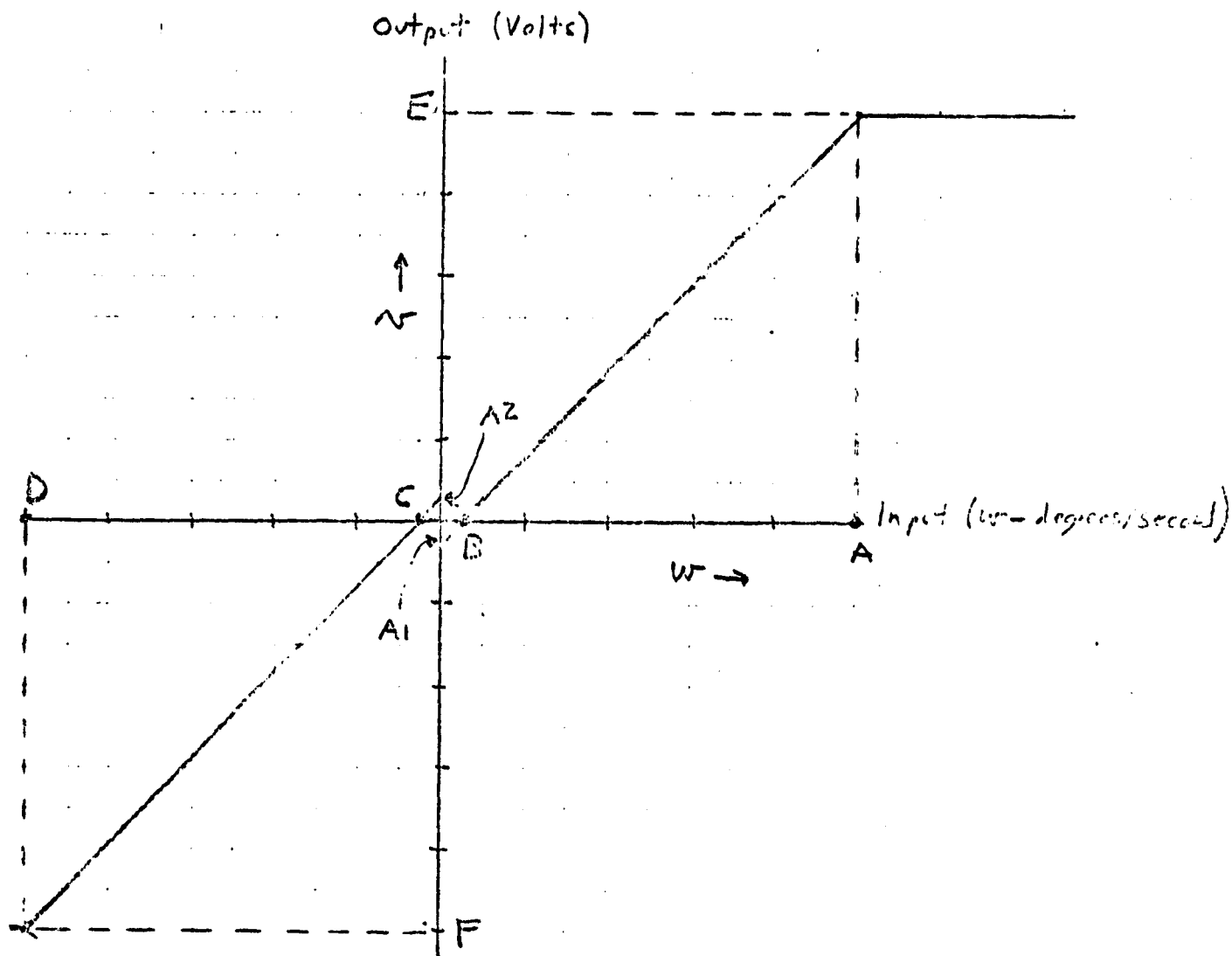


Figure 2-9. RGP Transfer Functions

PRELIMINARY DRAFT

ORIGINAL PAGE 19
OF POOR QUALITY

where $ADC = 127 \text{ counts}/5 \text{ volts}$, and n_v is truncated down to the next smaller integer.

The inverse transformation is given by

$$N = (n_v + 0.5) / ADC \quad (2-24)$$

and

$$\begin{aligned} (a) \quad N > 0 &\Rightarrow W = B + (A-B)N / E \\ (b) \quad N < 0 &\Rightarrow W = C + (D-C)N / F \end{aligned} \quad (2-25)$$

Nominal values of the constants A to F are given in Table 2-5.

Table 2-5. RGP Calibration Constants

<u>Gyro</u>	<u>A</u>	<u>B</u>	<u>C</u>	<u>D</u>	<u>E</u>	<u>F</u>
pitch	10	.02	-.02	-10	5	-5
roll	10	.02	-.02	-10	5	-5
yaw	10	.02	-.02	-10	5	-5

The RGP resolution or "bucket size" is $\pm 1/2$ count or ± 10 degrees/second /255 = ± 0.0394 degrees/second.

2.4 SPINNING SUN SENSORS

The spin mode Sun sensor assembly consists of two sensor heads mounted with boresights along the \pm roll axes. Sun sighting time pulses are output to the transfer orbit electronics (TOE) if the Sun angle (the angle from the Z-axis to

the Sun) is between 26 and 154 degrees. Sun angle measurements are provided if the Sun angle is between 58 and 122 degrees.

The model subroutine computes the time TSUN of the next Sun pulse

$$\begin{aligned} TSUN_{SSS1} &= \tan^{-1}(\nu_{B2} / \nu_{B1}) / \omega + T \\ TSUN_{SSS2} &= (\tan^{-1}(\nu_{B2} / \nu_{B1}) + \pi) / \omega + T \end{aligned} \quad (2-26)$$

where T is the time corresponding to the measurement $\hat{\nu}_B$, ω is the spin rate in radians per second and $\hat{\nu}_B = (\nu_{B1}, \nu_{B2}, \nu_{B3})$ is the Sun vector in body coordinates.

The time difference ΔT between successive Sun pulses is used to compute the spin rate (hi ω_z). The equations are

$$\begin{aligned} N &= \text{MOD}(C \cdot \Delta t, 32768) \\ \text{hi } \omega_z &= 60 \cdot C / (N + 0.5) \end{aligned} \quad (2-27)$$

where N = clock count

C = clock rate = 15.36 kHz

32768 = counter capacity (15 bits)

and hi ω_z is in RPM. The spin rate which is computed by the spinning Sun sensor data is valid, (i.e., unambiguous) for rates greater than 28.7 RPM; rates lower than this cause the counter capacity to be exceeded.

2.5 MOMENTUM WHEEL

The torque $\vec{\tau}_W$ exerted on the spacecraft by the momentum wheel and its motor is

$$\vec{\tau}_W = \vec{L} \times \vec{\omega} + \vec{\tau}_A \quad (2-28)$$

PRELIMINARY DRAFT

ORIGINAL PAGE IS
OF POOR QUALITY

where \vec{L} is the momentum of the wheel relative to the spacecraft (0 to 15 slug-ft²/s in the \hat{i} direction), $\vec{\omega}$ is the angular velocity of the spacecraft (radians per second) and $\vec{\tau}_B$ (slug-ft²/s²) is the net torque. At constant wheel speed, $\vec{\tau}_B = 0$; during spinup $\vec{\tau}_B$ is along $+\hat{j}$; and during spindown $\vec{\tau}_B$ is along $-\hat{j}$.

The magnitude, τ_B , of $\vec{\tau}_B$, is computed in the simulation by

$$\tau_B = a \cdot x / 511 - b > 0 \quad (2-29)$$

where x is the commanded wheel torque bias (0 to 511)

a is the motor torque (~ 0.036)

b is the bearing friction torque (~ 0.008)

The wheel momentum is updated in the simulation using the relation

$$L = L + \Delta t \cdot \tau_B \quad (\text{slug-ft}^2/\text{s}) \quad (2-30)$$

where Δt is the elapsed time (seconds) since the last update. The wheel speed, S , is

$$S = 30 \cdot L / (\pi \cdot I_w) \quad (2-31)$$

where I_w is the wheel inertia (nominally 0.0382 slug ft²), and S is in RPM.

The reaction torque, $\vec{\tau}_W$, of the momentum wheel on the spacecraft during spinup is computed using the basic equation listed at the start of this subsection with the directions of $\vec{\tau}_B$ and \vec{L} along $+\hat{j}$ and $-\hat{j}$ respectively as noted above. The result is

$$\vec{\tau}_W = (-\omega_z L, \tau_B, \omega_x L) \quad (2-32)$$

PRELIMINARY DRAFT

ORIGINAL PAGE IS
OF POOR QUALITY

2.6 THRUSTERS

Thruster firings are simulated by summing the torque vectors of all sixteen LTE under the assumption that the pulse profiles are rectangular. The net torque vector $\vec{\tau}$ is defined by the relation

$$\vec{\tau} = \sum_{i=1}^{16} \delta_i \cdot F_i \cdot \vec{r}_i \times \hat{F}_i \quad (2-33)$$

where $\delta_i = \begin{cases} 0 \\ 1 \end{cases}$ for $\begin{cases} \text{Thruster off} \\ \text{Thruster on} \end{cases}$

f_i = force level for ith thruster (lbs)

\vec{r}_i = position vector from spacecraft center of mass to ith thruster (feet)

\hat{F}_i = Thrust unit direction for ith thruster

The quantities f_i , \vec{r}_i , and \hat{F}_i above are independent from those used in the GCAP software to determine thruster selection and thrust duration. The nominal values are listed in Table 2-6.

Table 2-6. Thruster Parameters

Thruster	Hex ¹	i	f _i (lbs)	\vec{r} (feet)			\hat{r}		
				x	y	z	x	y	z
P1	FE8000	1	0.1	3.125	0	-.73667	0	0	1
P2	FE4000	2	0.1	-3.125	0	-.73667	0	0	1
P3	FE2000	3	0.1	3.000	0	-.73667	0	0	1
P4	FE1000	4	0.1	-3.000	0	-.73667	0	0	1
R1	FE0800	5	0.1	0	-2.4268	-1.0498	0	.2588	.9659
R2	FE0400	6	0.1	0	2.4268	-1.0498	0	-.2588	.9659
Y1	FE0200	7	0.1	-3.1373	-.20783	0	.5	.8660	0
Y2	FE0100	8	0.1	-3.1373	.20783	0	.5	-.8660	0
Y3	FE0080	9	0.1	3.1373	.20783	0	-.5	-.8660	0
Y4	FE0040	10	0.1	3.1373	-.20783	0	-.5	.8660	0
O1	FE0020	11	0.1	-.1835	2.4268	-1.0508	.1677	.2549	.9523
O2	FE0010	12	0.1	-.1835	-2.3118	-1.0508	.1677	-.2549	.9523
O3	FE0008	13	0.1	-.1835	-2.3118	-1.0508	.1677	.2549	.9523
O4	FE0004	14	0.1	-.1835	2.3118	-1.0508	.1677	-.2549	.9523
East	FE0002	15	0.1	3.139	0	0	-1.0	0	0
West	FE0001	16	0.1	-3.189	0	0	1.0	0	0

¹ Simultaneous thruster firing commands are computed by adding the individual FE commands. For example, a Y1 - Y3 couple is FE0280.

PRELIMINARY DRAFT

ORIGINAL PAGE IS
OF POOR QUALITY

SECTION 3 - SOFTWARE MODIFICATIONS

This section describes the modifications to GCAP, ADAMSSIM, and FSD which were required to develop the simulators used in the dynamic studies.

3.1 GCAP MODIFICATIONS

Source code for the GCAP modules DESPIN, PREDAY, SUNAC, JETDEP, SPINUP, PRESUN, and ERTLCK was received during the initial meeting with SED in July 1975. These basic modules together with subsidiary subroutines such as DAMP and ATTCON* were modified by CSC to operate on S/360 computers under the GESS. Although several minor errors were detected and corrected, the bulk of the software changes consisted of removing constants from the executable code and DATA statements and placing them in labeled COMMON, BLOCK DATA, NAMELIST, and GESS tables to facilitate parameter modification and permit numerous sensitivity studies without wasteful and time consuming recompilations. The only really substantive changes which were made to GCAP were modifications to ATTCON when investigating the utility of various controller algorithm for wheel spinup (Reference 14).

It is noted that two sets of hardware parameters were maintained in the simulators - one in the GCAP software and another in the hardware models and dynamic programs.

3.2 ADAMSSIM MODIFICATIONS

ADAMSSIM is the dynamics program which was used to perform prelaunch studies for GEOS-3. It is an outgrowth of a dynamics program initially developed for RAE-2. ADAMSSIM utilizes an Adams-Moulton fourth order predictor-corrector to integrate Euler's equations for the motion of a rigid

*ATTCON was the "new" FORTRAN version which had been modified in mid 1975:

body (Reference 15). This integration yields the components of the spacecraft's angular velocity vector $\vec{\omega}$ along the body-principal axes. Euler's equations are

$$\begin{aligned} I_1 \dot{\omega}_1 &= (I_2 - I_3) \omega_2 \omega_3 + \tau_1 \\ I_2 \dot{\omega}_2 &= (I_3 - I_1) \omega_3 \omega_1 + \tau_2 \\ I_3 \dot{\omega}_3 &= (I_1 - I_2) \omega_1 \omega_2 + \tau_3 \end{aligned} \tag{3-1}$$

where I_1 , I_2 , and I_3 are the principal moments of inertia of the spacecraft; ω_1 , ω_2 , and ω_3 are the components of $\vec{\omega}$ along the body-principal axes; and τ_1 , τ_2 , and τ_3 are the components, along the body-principal axes, of the vector sum $\vec{\tau}$ of the external torques.

To obtain the orientation of the body axes with respect to an inertial reference frame, additional parameters are needed. Let A be the rotation matrix which transforms vectors from inertial to body coordinates, i.e., $\vec{v}_B = A\vec{v}_I$. The A matrix can be written in terms of the 3-1-3 (ϕ - θ - ψ) Euler angles or in terms of the Euler symmetric parameters (y_1 , y_2 , y_3 , y_4). The Euler parameters are defined in terms of the Euler angles by the relations:

$$\begin{aligned} y_1 &= \sin \frac{\theta}{2} \cos \left(\frac{\phi - \psi}{2} \right) \\ y_2 &= \sin \frac{\theta}{2} \sin \left(\frac{\phi - \psi}{2} \right) \\ y_3 &= \cos \frac{\theta}{2} \sin \left(\frac{\phi + \psi}{2} \right) \\ y_4 &= \cos \frac{\theta}{2} \cos \left(\frac{\phi + \psi}{2} \right) \end{aligned} \tag{3-2}$$

Differentiating these equations with respect to time, using the relations,

$$\begin{aligned}\omega_1 &= \dot{\phi} \sin \theta \sin \psi + \dot{\theta} \cos \psi \\ \omega_2 &= \dot{\phi} \sin \theta \cos \psi - \dot{\theta} \sin \psi \\ \omega_3 &= \dot{\phi} \cos \theta + \dot{\psi}\end{aligned}\tag{3-3}$$

and performing a considerable amount of algebraic manipulation yields

$$\begin{aligned}\dot{y}_1 &= \frac{1}{2} (\omega_3 y_2 - \omega_2 y_3 + \omega_1 y_4) \\ \dot{y}_2 &= \frac{1}{2} (-\omega_3 y_1 + \omega_1 y_3 + \omega_2 y_4) \\ \dot{y}_3 &= \frac{1}{2} (\omega_2 y_1 - \omega_1 y_2 + \omega_3 y_4) \\ \dot{y}_4 &= \frac{1}{2} (\omega_1 y_1 + \omega_2 y_2 + \omega_3 y_3)\end{aligned}\tag{3-4}$$

Equations (3-1) and (3-4), when integrated, provide a complete description of the dynamic behavior of the satellite under the influence of external torques.

Note that the norm of the Euler parameters is unity: $y_1^2 + y_2^2 + y_3^2 + y_4^2 = 1$.

ADAMSSIM integrates Equations (3-1) and (3-4) using a variable stepsize constrained between an upper bound (DELMAX) and a lower bound (DELMIN) to achieve selected tolerance limits on the state vector $\vec{x} = (\omega_1, \omega_2, \omega_3, y_1, y_2, y_3, y_4)$ which are specified by an upper (DXU) and a lower (DXL) bound on the difference between the predicted and corrected states.

PRELIMINARY DRAFT

ORIGINAL PAGE 18
OF POOR QUALITY

External torques for CTS were limited to gravity-gradient

$$\vec{\tau}_{gg} = \frac{3\mu}{R^3} (\hat{R} \times (\hat{I} \cdot \hat{R})) \quad (3-5)$$

where \hat{I} is the moment of inertia tensor, and \hat{R} is the normalized radius vector from the center of the Earth to the center of mass of the spacecraft. Gravity-gradient torque was the dominant torque on the GEOS spacecraft, and it was included for CTS because of the negligible computational time required. Larger torques, such as solar radiation pressure torque, which is the dominant disturbance torque for CTS, and magnetic dipole torque which is comparable to gravity-gradient torque were not included; the former was not available in the program, and the latter was felt to require too much CPU time to justify inclusion.

A two body orbit generator, FASTOX (Reference 16), was used to generate the spacecraft to Earth vector using the following Keplerian parameters.

$$\begin{aligned} a &= 42200 \text{ km} \\ e &= 0 \\ i &= 0.9 \text{ degrees} \end{aligned} \quad (3-6)$$

Solar ephemeris was supplied via NAMELIST parameters for the inertial right ascension (α_{SI}) and declination (δ_{SI}). The orbit slot was computed using the relation

$$\phi_e = \frac{180}{\pi} (\tan^{-1}(R_2, R_1) - \alpha_{SI} + \pi) \quad (3-7)$$

where $\vec{R} = (R_1, R_2, R_3)$ is the unnormalized vector from the Earth center to the spacecraft.

The only significant change to ADAMSSIM required for the CTS application was to include torques generated by the thrusters. Logic was added to apply one or more square wave torques at selected (via NAMELIST) times by specifying the thrust vector, and thrust duration. Accuracy limits were maintained by switching to a fixed-step integrator with a reduced step size several normal integration steps preceding the thrust and maintaining the small steps until several normal integration steps after the thrust. This was accomplished by controlling the DELMIN and DELMAX parameters of the Adams-Moulton integrator during the thrust.

Closed loop control is simulated by calling, at selected intervals, an interface subroutine (FSDGCP) with the attitude state and ephemeris vectors as input. FSDGCP, in turn, calls the sensor models to compute simulated telemetry data and then calls the appropriate GCAP module. GCAP commands are then decoded by FSDGCP and a thruster, jettison, or momentum wheel torque returned to the integrator. The interface routine is called at approximately one second intervals to simulate the CTS telemetry rate. This was accomplished by setting DELMAX = 1 second.

GCAP commanded burns are processed by ADAMSSIM in the same manner as NAMELIST burns by switching to a small integration step size just prior, during, and just after the burn. Figure 3-1 illustrates the data flow for the ADAMSSIM/GCAP simulator. This simulator - though initially developed to unit test logic for handling thrusts, unit testing the interface modules and GCAP, and performing open loop simulations of nutation damping or momentum transfer - proved very useful for closed loop evaluation of GCAP.

3.3 FSD MODIFICATIONS

Three basic versions of FSD were used in performing the simulations discussed in this document. The modifications required for these versions are discussed in the following subsections.

PRELIMINARY DRAFT

ORIGINAL PAGE IS
OF POOR QUALITY

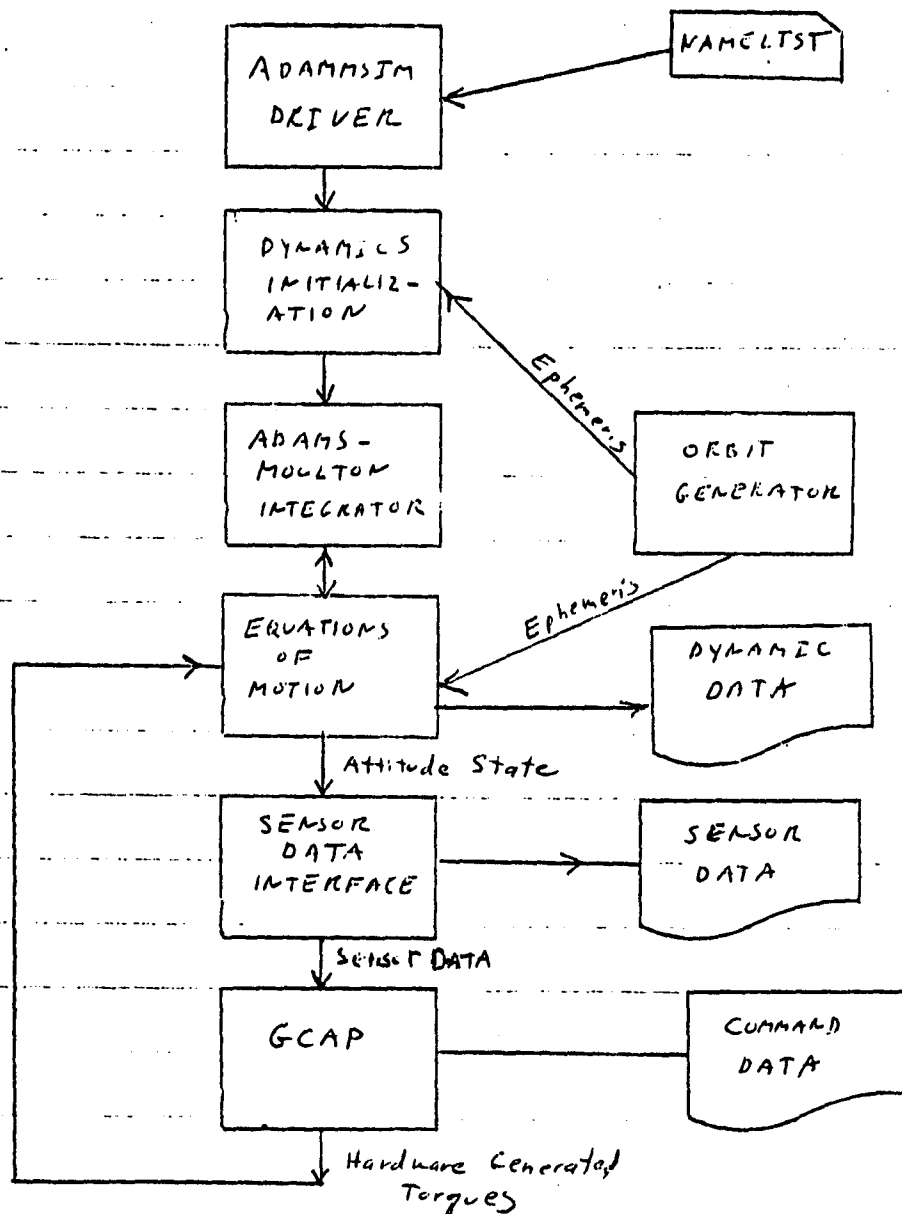


Figure 3-1. ADAMSSIM/GCAP Data Flow

3.3.1 Non-Graphics Version of FSD (Orbit Perturbation Studies)

An existing version of FSD (Reference 21) which was not modified for CTS was used for spacecraft-independent studies to determine the effects of thruster firing on the spacecraft's orbit during the PRESUN precession maneuver. This version of FSD computes the effect of thruster firings on both orbit and attitude. Thruster data is supplied externally via data cards which contain the thruster orientation, force level, thrust duration and burn initiation time. The input data were supplied by first running the ADAMSSIM/GCAP simulator for the desired precession and punching cards with the required format for each GCAP command. The results of these simulations are discussed in Subsection 4.3.2.8.

3.3.2 FSD/CTS (Open Loop Simulator)

The open loop simulator was derived from the version described in the previous Subsection as follows:

- Input modules were modified to accommodate FORTRAN NAMELIST
- The GESS executive structure was added to provide interactive and display table capabilities
- Input NAMELIST display tables and output vector plots were added to facilitate parameter entry and evaluation of the dynamic results
- The necessary modifications were made to model the solar arrays as flat plates for the solar radiation pressure studies

3.3.3 GCAP Version of FSD (Closed Loop Simulator)

The modifications made for the closed loop version of FSD included the following:

- Periodic calls (at nominal 1 second intervals) to an interface routine (FSDGCP) which translates the FSD attitude state and ephemeris

information into simulated sensor data, calls GCAP, and returns thruster, array deployment, and momentum wheel reaction torques

- Modification to the FSD/CTS equations of motion to accept externally generated torques
- Addition of models to simulate the DSA autotrack subsystem

The resulting FSD/GCAP system is depicted in Figure 3-2.

PRELIMINARY DRAFT

ORIGINAL PAGE 13
OF POOR QUALITY

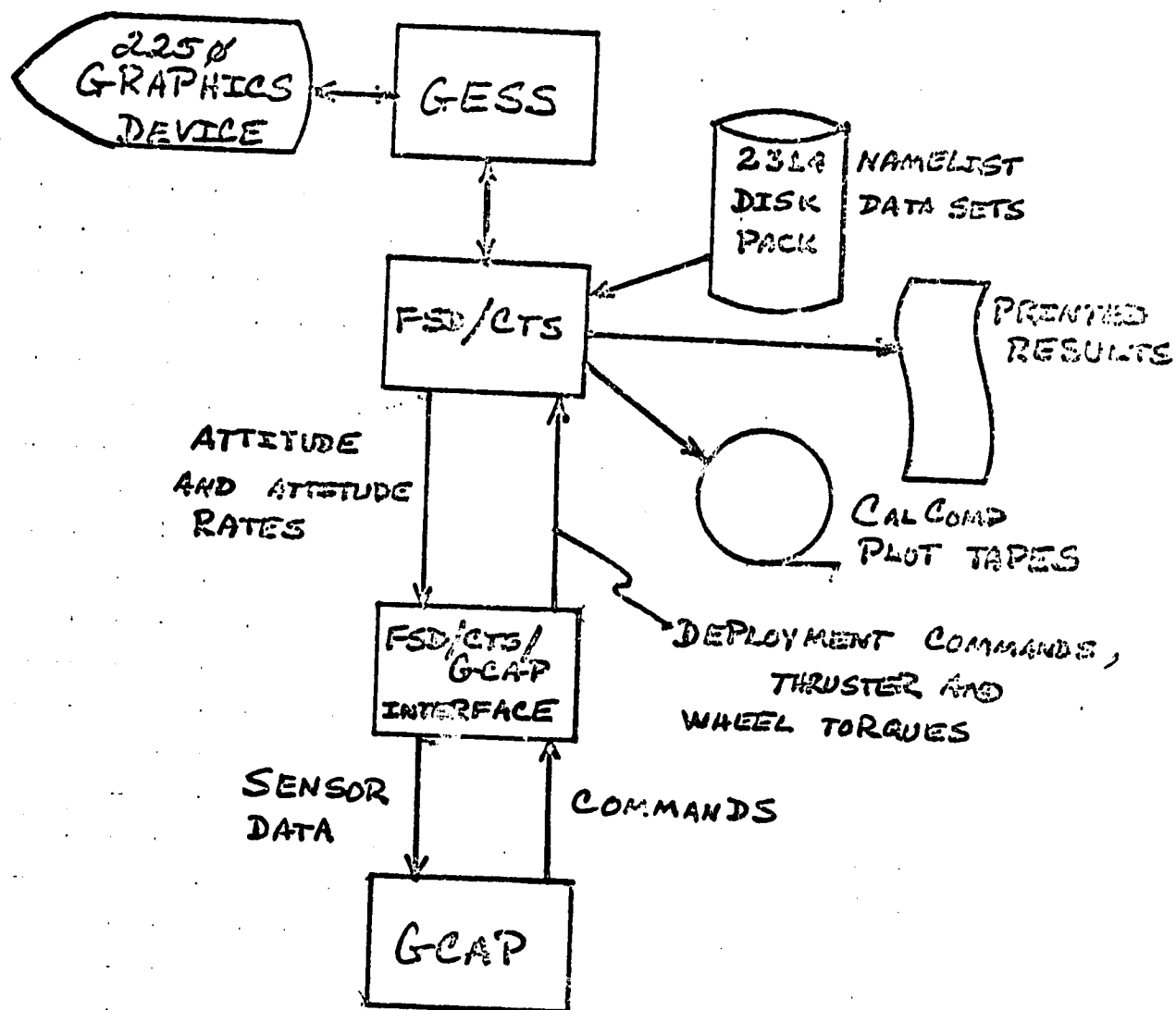


Figure 3-2. FSD/GCAP Data Flow

PRELIMINARY DRAFT

ORIGINAL PAGE 13
OF POOR QUALITY

SECTION 4 - ATTITUDE ACQUISITION STUDIES

This section describes the results of the analysis and simulations performed during the task assignment. The section is divided into four subsections as described below:

1. ADAMSSIM Open Loop--Simulations utilizing the open loop version of ADAMSSIM were performed to evaluate active nutation damping and the attitude acquisition via momentum transfer sequence.
2. ADAMSSIM Closed Loop (ADAMSSIM/GCAP)--This simulator was used to evaluate the performance of the GCAP modules and the various attitude controller algorithms for spinup.
3. FSD Open Loop--This simulator was used to evaluate the impact of environmental torques and array flexibility on various CTS configurations during attitude acquisition without consideration of GCAP generated commands.
4. FSD Closed Loop (FSD/GCAP)--This simulator was used to evaluate the impact of environmental torques, array flexibility and GCAP thruster firings on various nominal and non-nominal configurations during attitude acquisition.

4.1 ADAMSSIM OPEN LOOP

The initial application of this simulator was to evaluate the efficiency of the MODE-1 and MODE-2* active nutation damping algorithms developed by SED. These algorithms are derived in Reference 17 under two basic assumptions:

1. The transverse inertias, I_1 and I_2 , are equal
2. Thrust profiles (force versus time) are rectangular

*MODE-2 damps nutation optimally regardless of the achieved final attitude. MODE-1 selects the thruster and burn initiation time to move the Z-axis attitude more nearly normal to the Sunline and consequently does not remove the nutation as efficiently.

The second assumption appears to be less restrictive than the first one, since pulse durations for damping burns are typically less than one second and the achieved total impulse, $\Delta \vec{L}_1 = \int \vec{r}_1 \times \vec{I}_1(t) dt$, and burn timing are more important than the detailed profile. The first assumption initially appeared to be seriously in error because the actual inertias, $I_1 = 69.0 \text{ slug-ft}^2$ and $I_2 = 94.1 \text{ slug-ft}^2$, indicated considerably more asymmetry than the nominal inertias available during algorithm development.

A series of MODE-2 damping burn runs were performed as a function of the transverse inertia ratio. The results are shown in Table 4-1.

Although the pattern in Table 4-1 is somewhat obscured by the differing magnitudes of initial nutation, it is clear that the success of the algorithm decreases as the asymmetry increases. The first case in the table is included as a test of the algorithm and thrust implementation logic. The failure to completely dominate nutation is a consequence of the integrator step size and the inability to achieve precisely the desired burn duration. In these examples, a step size of 0.02 times the burn duration was employed during the burn; this implies roughly a 2 percent error. The conclusion reached from this study is that for the CTS configuration, roughly 90 percent of the nutation can be removed with a single burn and deficiencies in the algorithm may be neglected.

Timing errors of up to two seconds were introduced into the nutation burns without appreciable effect (the period of the nutation is 70 to 80 seconds).

A study of the momentum transfer attitude acquisition sequence and the nutation damping algorithm for the spinning wheel configuration was performed and is described in Appendix E.

Table 4-1. Efficiency of MODE-2 Damping as a Function
of the Transverse Moment of Inertia Ratio

Inertias		I_2/I_1	Initial Nutation Amplitude (Degrees)		Burn Duration (Seconds)	Initial Burn Phase (Degrees)	Percent Nutation Reduction
I_1	I_2						
<hr/>							
80.58	80.58	1.000	0.86	0.02	0.377	145.0	98
85.0	76.39	1.113	0.86	0.03	0.354	171.3	97
90.0	72.14	1.248	1.08	0.14	0.461	176.4	87
94.1	69.0	1.374	1.75	0.19	0.614	177.0	89
100.0	64.93	1.540	0.93	0.22	0.338	158.5	76
110.0	59.03	1.863	2.80	0.85	0.895	183.1	70

4.2 ADAMSSIM CLOSED LOOP (ADAMSSIM/GCAP)

This simulator was used to evaluate the performance of the GCAP modules under a variety of nominal and non-nominal conditions. Non-nominal conditions which were investigated included:

- Thruster misalignments (both position vectors and force vectors)
- Thruster miscalibrations (force)
- Incorrect inertias (assumed to be caused by an incomplete deployment of the south array)
- Systematic errors in sensor output, particularly NSSS data

With the exception of the impact of the loss of Sun data on the δ controller performance during spinup, adverse impact on software performance due to these anomalies was judged to be negligible.

4.2.1 DESPIN (Despin to 2 RPM)

Tables 4-2 and 4-3 summarize the results of the DESPIN study. The despin consisted of 4 burns:

- A brief (10 second) burn to clear the yaw thruster nozzles
- A calibration burn to 54 RPM (about 2 minutes)
- The major despin burn to approximately 8 RPM
- The final despin burn to 2 RPM

Table 4-2 demonstrates that for a wide range of initial conditions (nutation amplitudes of 0.05 to 0.2 degrees) and thruster misalignments, a final spin rate very close to 2 RPM or 12 degrees per second is achieved.

The final nutation amplitude is approximately a multiple of the initial nutation amplitude

$$\gamma_{\frac{1}{2}}(\text{final}) = \gamma_{\frac{1}{2}}(\text{initial}) \frac{\omega_3(\text{initial})}{\omega_3(\text{final})} \quad (4-1)$$

PRELIMINARY DRAFT

ORIGINAL PAGE IS
OF POOR QUALITY

Table 4-2. DESPIN Simulations*

Case	ω_1 (Initial) °/Sec	ω_1 (Final) °/Sec	ω_2 (Final) °/Sec	ω_3 (Final) °/Sec	Thruster Misalignment \hat{r}	Thruster Offset \hat{f}
1	0.38	.3619	.2920	12.02	0°	0°
2	0.38	.2674	.2119	12.00	2°	0°
3	0.38	.4719	.3656	11.98	0°	2°
4	0.38	.6024	.4600	11.98	2°	2°
5	0.75	.7425	.5844	12.00	0°	0°
6	0.75	.8414	.6701	12.05	2°	0°
7	0.75	.8373	.6507	12.03	0°	2°
8	0.75	.9359	.7237	11.96	2°	2°
9	1.50	1.4888	1.1676	12.06	0°	0°
10	1.50	1.5824	1.2564	12.05	2°	0°
11	1.50	1.5815	1.2370	12.05	0°	2°
12	1.50	1.7325	1.3426	11.99	2°	2°

*Initial conditions all cases

$\omega_2 = 0.0$ °/sec Thruster force level = 0.1 lb.

$\omega_3 = 372.0$ °/sec. = 62 RPM

PRELIMINARY DRAFT

ORIGINAL PAGE IS
OF POOR QUALITY

Table 4-3. Nutation Build Up During DESPIN*

<u>Case</u>	<u>$\gamma_{1/2}$ Initial (deg)</u>	<u>$\gamma_{1/2}$ Final (deg)</u>	<u>$\gamma_{1/2}$ Final/ $\gamma_{1/2}$ Initial</u>
1	0.0480	1.416	29.50
2	0.0480	1.408	29.33
3	0.0480	1.853	38.60
4	0.0480	2.365	49.27
5	0.0948	2.910	30.69
6	0.0948	3.280	34.60
7	0.0948	3.274	34.53
8	0.0948	3.681	38.83
9	0.1897	5.806	30.61
10	0.1897	6.177	32.56
11	0.1897	6.173	32.54
12	0.1897	6.797	35.83

*Despin nutation cone half angles were computed using

$$\gamma_{\frac{1}{2}} = \tan^{-1} \left\{ \left[(I_1 \omega_1)^2 + (I_2 \omega_2)^2 \right]^{1/2} / [I_3 \omega_3] \right\}$$

where $\omega_3(\text{initial})$ and $\omega_3(\text{final})$ are the initial and final Z-axis rate. The validity of Equation (4-1) is illustrated by the computer simulations listed in Table 4-3. The equation implies that the effect of thruster misalignment tends to average out over a large number of spin periods. Note, however, that for Case 4 and to a lesser degree Cases 8 and 12, the nutation buildup was appreciable when larger errors in both \vec{r} and \vec{f} were included.

No difference in DESPIN performance was noted for initial spin rates above or below 60 rpm nor for thrust levels twice or half the expected value.

The expected nutation amplitude at 60 rpm is 0.05 degrees or less because a passive nutation damper is specified to attenuate larger amplitudes. If the passive damper performs nominally, nutation at 2 rpm will be, at most, 2 to 3 degrees and will present no difficulty.

At high spin rates, nutation is observable most easily in the variation of the angular output of the spinning Sun sensor; the resolution of this output, however, is ± 0.25 degrees - considerably larger than expected nutation and consequently nominal performance of the passive damper cannot be verified. The present study thus indicates that marginally observable levels of nutation at 60 rpm can yield unacceptably large nutation amplitudes - 5 degrees or more. Nutation buildup, therefore, should be monitored during despin.

Present planning calls for a hold at 16 rpm to observe and if necessary remove, the nutation before despin to 8 and 2 rpm, and consequently nutation buildup should not cause any difficulty.

4.2.2 PREDAY (Precession to Place Yaw Axis Normal to Sunline)

PREDAY commands precessions at 2 rpm to place the spin axis normal to the Sunline to maximize power input to the body solar arrays. This maneuver is no longer part of the nominal DOP and will be performed only if specifically required for power or thermal reasons.

Tables 4-4 to 4-6 illustrate the sequence of precession and damping maneuvers utilized by PREDAY in the simulation studies for various initial conditions. In brief, the result of the studies of PREDAY performance may be summarized as follows:

- Two nutation burns are required after each precession because of the inefficiency of DAMP MODE-1; only about 2/3 of the nutation is removed in a single burn.
- Imprecision in the precession and damping burns coupled with Sun sensor resolution limit the accuracy of the maneuvers to about 2 degrees.
- The PREDAY module requirement that the Sun angle be maintained at 90 ± 2.5 degrees could not be achieved. Attempting to meet the requirement resulted in the continual generation of futile precessions. This difficulty, of course, would not occur when precession decisions are made external to the module.

4.2.3 SUNAC (Sun Acquisition Along Positive Yaw Axis)

SUNAC uses the spinning Sun sensor to provide a timing pulse so that the final despin will terminate with the -X axis along the Sun line. The significant Sun angles are defined in Figure 4-1.

The desired Sun angles after the final (43.5 second) burn are $\alpha_s = 180^\circ$ and $\delta_s =$ Sun declination; i.e., it is desired to perform the despin in such a manner that the Sunline lies in the X-Z plane after despin with -X offset from the Sunline by the Sun's declination value. Following this despin, SUNAC commands a brief burn to generate a rotation of (90-Sun declination) about pitch. This burn places +Z along the Sunline.

Table 4-4. PREDAY Performance at 58 RPM For Initial $\omega_1 = .38$ Degrees/Second

<u>Seconds Into Simulation</u>	<u>Seconds Since Last Burn</u>	<u>Thrust Duration in Seconds</u>	<u>Objective</u>
42.13	-	8.64	Precess 15°
290.45	248.32	5.00	Damp $A_0 = 2.47^\circ/\text{sec}^*$
531.82	241.37	3.27	Damp $A_0 = 0.854^\circ/\text{sec}$
669.37	137.55	5.01	Precess 8.8816°
874.87	205.50	3.63	Damp $A_0 = 1.64^\circ/\text{sec}$
1082.64	207.77	1.87	Damp $A_0 = 0.49^\circ/\text{sec}$
1209.17	126.53	1.42	Precess 2.5449°
1456.86	247.69	2.09	Damp $A_0 = 0.55^\circ/\text{sec}$
1628.40	171.54	1.42	Precess 2.5530°
1832.67	204.27	1.19	Damp $A_0 = 0.42^\circ/\text{sec}$
1987.75	155.08	1.44	Precess 2.5584°

$$*A_0 = 2 \left\{ \left[(I_1 \omega_1)^2 + (I_2 \omega_2)^2 \right]^{1/2} \right\} / (I_1 \omega_2)$$

PRELIMINARY DRAFT

ORIGINAL PAGE 13
OF POOR QUALITY

Table 4-5. PREDAY Performance at 58 RPM For Initial
 $\omega_1 = 0.75$ Degrees/Second

<u>Seconds Into Simulation</u>	<u>Seconds Since Last Burn</u>	<u>Thrust Duration In Seconds</u>	<u>Objective</u>
42.39	-	8.55	Precess 15°
250.82	208.43	5.00	Damp $A_0 = 2.27^\circ/\text{sec}$
461.51	210.69	2.506	Damp $A_0 = 0.66^\circ/\text{sec}$
617.64	156.13	3.56	Precess 6.4081°
869.18	251.54	4.62	Damp $A_0 = 1.21^\circ/\text{sec}$

PRELIMINARY DRAFT

ORIGINAL PAGE 19
OF POOR QUALITY

Table 4-6. PREDAY Performance at 58 RPM For
Initial $\omega_1 = 1.50$ Degrees/Second

<u>Seconds Into Simulation</u>	<u>Seconds Since Last Burn</u>	<u>Thrust Duration In Seconds</u>	<u>Objective</u>
30.05	-	8.55	Process 15°
236.49	206.44	5.00	Damp $A_0 = 3.96^\circ/\text{sec}$
435.29	198.80	4.809	Damp $A_0 = 1.26^\circ/\text{sec}$
598.27	162.98	3.97	Precess 7.0959°
827.91	229.64	5.00	Damp $A_0 = 1.21^\circ/\text{sec}$
1094.11	266.2	1.53	Damp $A_0 = 0.66^\circ/\text{sec}$
1261.86	167.75	1.39	Precess 2.5019°
1511.42	249.55	2.88	Damp $A_0 = 0.76^\circ/\text{sec}$
1681.33	169.91	1.75	Precess 3.1761°
1889.05	207.72	1.62	Damp $A_0 = 0.74^\circ/\text{sec}$
2045.71	156.66	1.41	Precess 2.5450°

PRELIMINARY DRAFT

ORIGINAL PAGE 13
OF POOR QUALITY

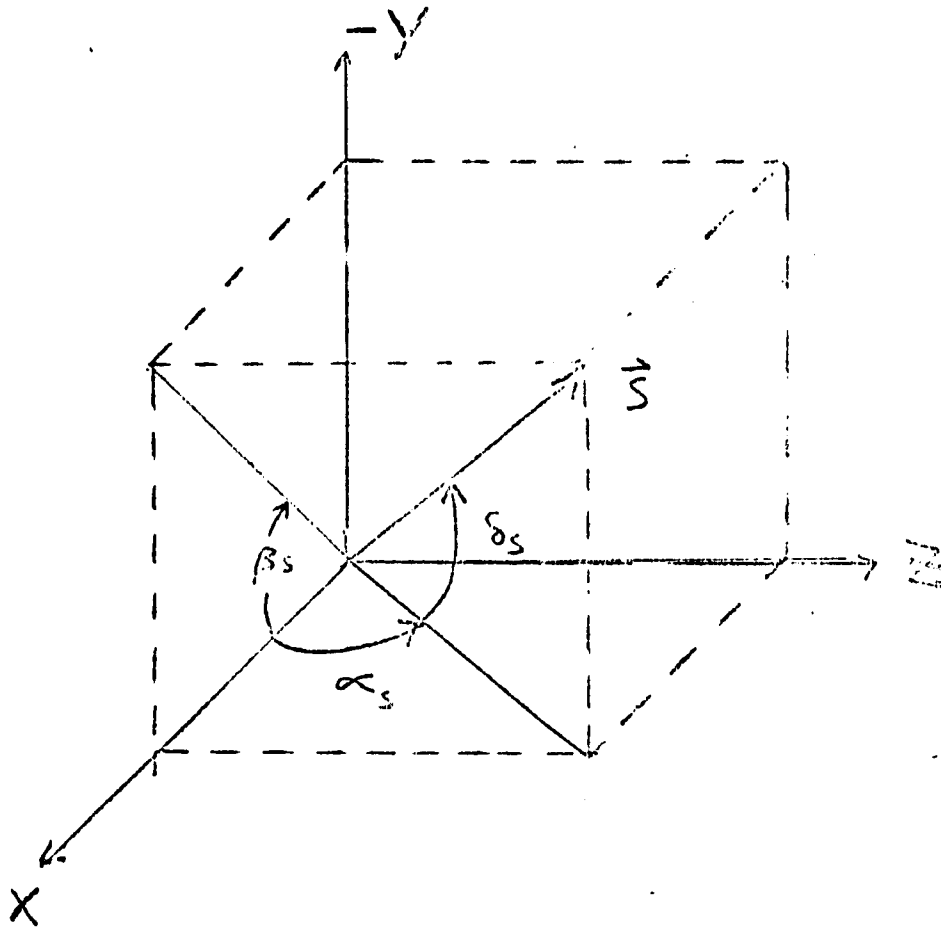


Figure 4-1. Definition of Sun Angles. X , Y , and Z are the Reference Axes in the Spacecraft Frame

The procedure described previously is slightly different from that which is specified in the most recent (11/75) DOP. In the earlier DOP, the desired Sun angles after despin were $\alpha_s = 180^\circ$ and $\delta_s = 0^\circ$; i.e., -X along the Sunline. The rotation about pitch to place +Z along the Sunline then had a value of 90 degrees.

The simulated SUNAC sequence was accomplished without problems as illustrated in Table 4-7.

4.2.4 JETDEP (Jettison and Deploy)

JETDEP refers to the jettison of the body mounted solar arrays (JBSA) and the extension of the deployable solar arrays (DSA). Only the former maneuver was considered here. The latter was simulated utilizing FSD/GCAP to permit inclusion of flexibility and solar radiation pressure torque.

Table 4-8 illustrates the performance of the controller during a "worst case" impulse of $\Delta \vec{L} = (0.0093, 0, 0.0133)$ ft-lb-s. This impulse assumes a near symmetric release of both seven pound panels at velocities of 6 feet per second along the geometric $\pm Y$ axes. The center of mass offset is about 3 inches.

The controller had no difficulty maintaining α_s and δ_s near the deadhand values because the jettison impulse is small compared to the typical 0.1 ft-lb-s controller burns. The initial yaw rate was 0.17 degrees per second and increased to 0.28 degrees per second after jettison. Since the yaw rate after jettison remained below the third axis rate controller threshold (0.3 degrees/second), no yaw burns were commanded. Because excessive yaw rates can be observed only with the yaw gyro, it is important to calibrate the gyro prior to jettison to ensure that array deployment occurs at permissible rates. (Specified tolerances for the array deployment, however, are several degrees per second - well above conceivable rates after jettison.)

Table 4-7. SUNAC Starting at End of PREDAY #2

Sec Into Simulation	Seconds Since Last Burn	Duration (seconds)	Objective*	Sun Angles	
				α_s (degrees)	δ_s
84.45	-	43.56	final despin		
137.32	52.77	.23	α_c	185.67	-9.68
150.86	13.54	.23	α_c	187.68	-3.57
157.41	6.55	1.73	δ_c	187.67	-0.51
169.44	12.03	.23	α_c	188.69	1.53
185.99	16.55	.45	δ_c	187.67	2.55
208.43	22.44	.23	α_c	187.67	0.51
222.97	14.54	1.53	$+\omega_2$ Rotation		
229.53	6.56	.23	δ_c	184.61	-2.56
243.08	13.55	.23	δ_c	178.46	-3.58
271.62	28.54	.23	δ_c	165.20	-4.53
308.17	36.55	.23	δ_c	149.26	-4.31
344.72	36.55	.47	δ_c	132.42	-4.99
381.25	36.53	.47	δ_c	115.84	-5.37
417.78	36.53	.47	δ_c	98.71	-5.60
431.31	13.53	1.53	$-\omega_2$ Stop Rotation		
464.86	33.55	.47	α_c	87.44	-3.58
501.40	36.54	.23	α_c	87.44	-1.53
582.95	81.55	.47	δ_c	90.51	2.56

* α_c , δ_c , and ω_2 refer to α (pitch), δ (roll), and ω_2 (pitch rate) control burns respectively.

PRELIMINARY DRAFT

ORIGINAL PAGE 19
OF POOR QUALITY

Table 4-8. JETDEP Profile

Sec Into Simulator	Seconds Since Last Burn	Thrust Duration	Objective	α_s	δ_s
3.0		0.01	Jettison*	92.56	1.535
22.54		0.469	δ_c	91.537	3.581
59.07	36.53	0.469	δ_c	90.513	3.582
97.60	38.53	0.234	α_c	88.464	2.559
163.14	21.55	0.234	α_c	91.536	- .0512
184.69	21.55	0.469	δ_c	90.512	-1.535
272.22	87.53	0.234	α_c	88.465	0.512
320.77	48.55	0.469	δ_c	90.512	1.536
334.30	13.53	0.234	α_c	91.536	0.512
376.84	42.54	0.469	δ_c	90.512	1.535
444.37	67.53	0.234	α_c	88.465	- .512
504.92	60.55	0.234	α_c	91.536	0.512
512.47	7.55	0.469	δ_c	91.536	1.535

*A burn of duration 0.01 seconds was used to yield an impulse of $\overline{\Delta L} =$
(0.0093, 0, 0.0133) ft-lb-s .

Additional JETDEP simulations were performed for various burn durations and larger impulses which assumed jettison of a single solar panel rather than a symmetric, simultaneous jettison. Controller performance was, in all cases, comparable to that shown in Table 4-7.

4.2.5 SPINUP (Momentum Wheel Spinup)

A complete description of the wheel spinup study is contained in References 8 and 14.

4.2.6 PRESUN (Precession of the Pitch Axis About the Sun Line)

PRESUN refers to the sequence of maneuvers which begins with a rotation about pitch to obtain Earth strike data in the 21.7 degree NESR field of view and ends with a precession to place the yaw axis in the orbit plane and the pitch axis along the southerly orbit normal. A description of the attitude determination geometry for PRESUN is contained in Reference 11 and Appendix F.

Table 4-9 contains the parameters which were used in the simulation. The initial attitude is specified as a 3-1-3 (ϕ - θ - ψ) Euler rotation from inertial to body coordinates. In each case the initial attitude placed the Sun along the +Z axis; Cases 1 to 4 correspond to various orientations of the pitch axis (+Y) about the Sunline.

PRESUN precessions are achieved by pairs of roll (yaw) burns for $\pm Z$ ($\pm X$) along the Sunline. The first burn induces nutation of the pitch axis about the total angular momentum vector and the second, opposite burn cancels the induced nutation. During the maneuver there is a net yaw (roll) rate which yields the desired precession. The time between burns, Δt , is half the precession period and is computed by PRESUN using the relation

$$\Delta t = \pi / \omega = 177 \text{ seconds} \quad (4-2)$$

PRELIMINARY DRAFT

ORIGINAL PAGE 13
OF POOR QUALITY

Table 4-9. PRESUN - Test Case Simulation Parameters

All test cases were run using the following initial conditions:

Initial Orbit Slot	2.7 degrees
Sun Right Ascension	$313.70^{\circ} (\alpha_{SI})$
Sun Declination	$-17.40^{\circ} (\delta_{SI})$

Satellite parameters

Wheel speed = 3715 rpm.

$$\begin{aligned}
 I_{xx} &= 825.10 \text{ slug-ft}^2 \\
 I_{yy} &= 68.20 \text{ slug-ft}^2 \\
 I_{zz} &= 845.60 \text{ slug-ft}^2 \\
 \omega_x &= 0.05^{\circ}/\text{sec} \\
 \omega_y &= 0.0^{\circ}/\text{sec} \\
 \omega_z &= 0.0^{\circ}/\text{sec} \\
 \phi &= 43.70^{\circ} = \alpha_{SI} + 90^{\circ} \\
 \theta &= 107.40^{\circ} = 90^{\circ} - \delta_{SI}
 \end{aligned}$$

Case 1: $\psi = 60^{\circ} = \phi_S - 90^{\circ}$

Case 2: $\psi = 180^{\circ}$

Case 3: $\psi = 240^{\circ}$

Case 4: $\psi = 300^{\circ}$

PRELIMINARY DRAFT

where $\alpha = h_W/l$
 $h_W = 15 \text{ slug-ft}^2/\text{sec}$
 $l = 843 \text{ slug-ft}^2$

ORIGINAL PAGE IS
OF POOR QUALITY

Figure 4-2 illustrates the serpentine path of the pitch axis on the celestial sphere during a 180 degree precession from the north to the south pole. The dashed line is the minimum, great circle, trajectory.

The precession method is further illustrated in Figure 4-3 which shows the phase relationship between ω_x , ω_z , and δ , the latter for the four possible Sun locked attitudes.

A positive yaw precession is induced by a $+T_x$ burn at $t = 0$ and a $-T_x$ burn at $\Delta t = 177$ seconds later. During this half nutation period, the average ω_x rate is zero, and the average ω_z rate is positive as required. Similarly, a negative roll precession is induced by a $+T_z$ burn followed by a $-T_z$ burn 177 seconds later. The impulse is computed from the desired half-nutation cone amplitude, N (radians) and the wheel momentum

$$\Delta L = h_w N = T_x \Delta t_B \quad (4-3)$$

where T_x is the thruster torque and Δt_B is the burn duration.

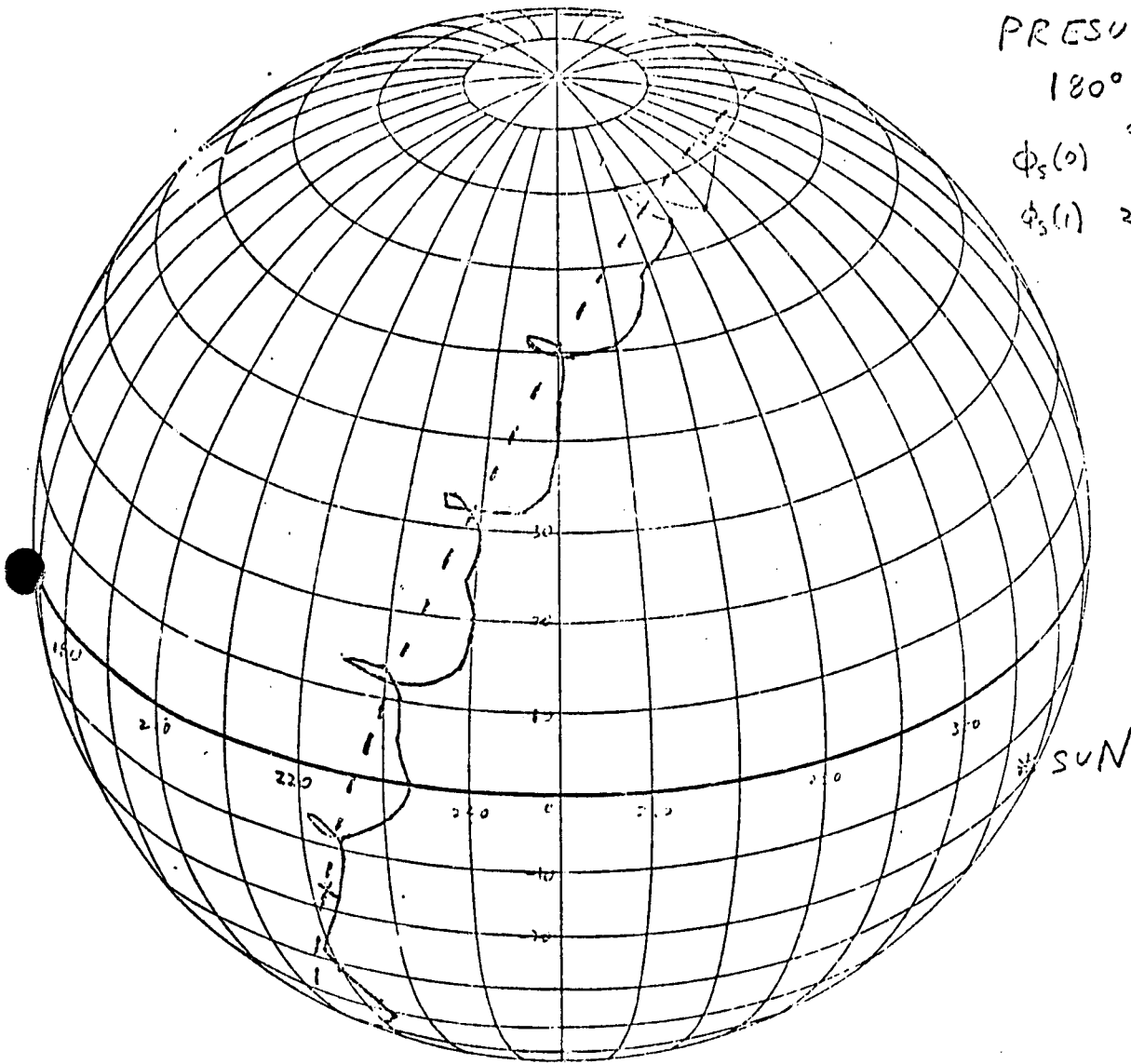
For a 15 degree half cone and a 0.5 ft-lb torque

$$\Delta t_B = 15 \times 15 / (57 \times 0.5) = 8 \text{ seconds} \quad (4-4)$$

Table 4-10 summarizes the simulation results for the four cases defined previously in Table 4-9. In all four cases PRESUN performance was excellent. (Case 2 began with the correct attitude.) The computed ϕ_S angles were within 5 degrees of the actual angles, and the final values for ϕ_S were within 5 degrees of the desired value, $\phi_S = 270$ degrees.

PRELIMINARY DRAFT

ORIGINAL PAGE IS
OF POOR QUALITY



PRESUN

180° precession
actual comput

$\phi_s(0)$ 90 94

$\phi_s(1)$ 288 282

Figure 4-2. Trajectory of Pitch Axis on Celestial Sphere
During 180 Degree Precession (1 of 2)

PRELIMINARY DRAFT

ORIGINAL PAGE IS
OF POOR QUALITY

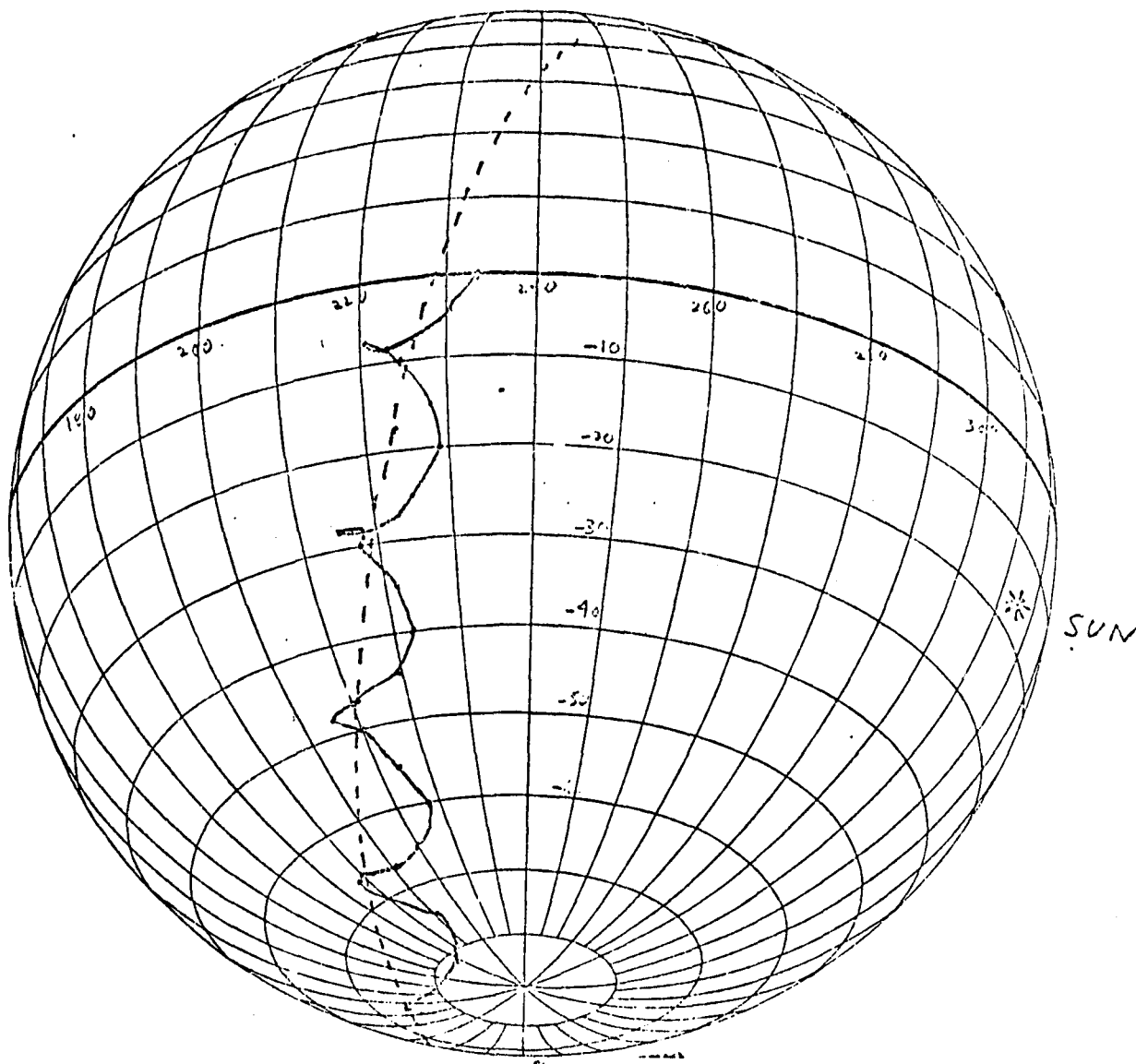


Figure 4-2. Trajectory of Pitch Axis on Celestial Sphere
During 180 Degree Precession (2 of 2)

PRELIMINARY DRAFT

ORIGINAL PAGE 19
OF POOR QUALITY

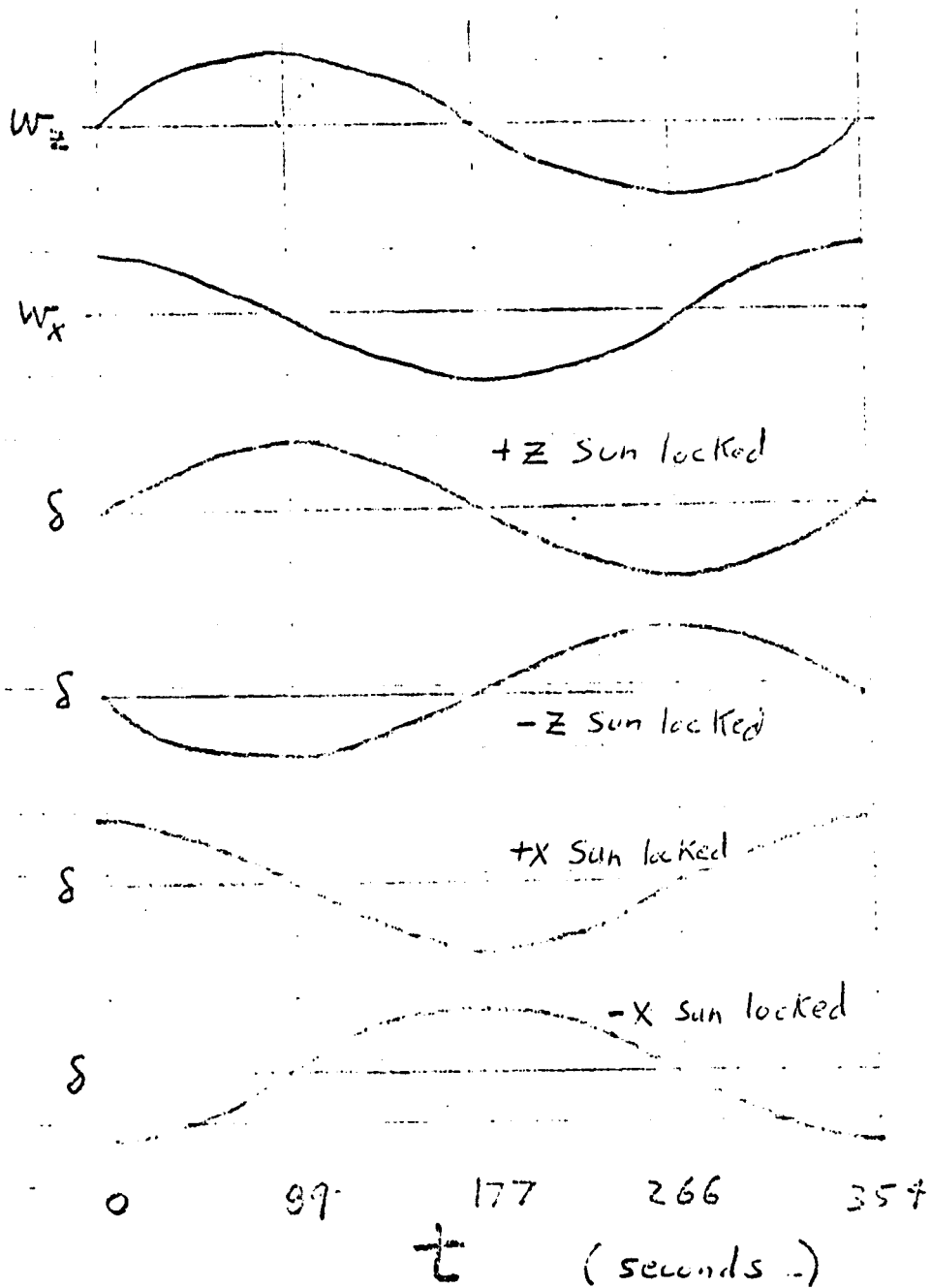


Figure 4-3. Phasing Relations for ω_x , ω_z , and δ for Spinning Wheel With $\pm X$ or $\pm Z$ Sun Locked

PRELIMINARY DRAFT

ORIGINAL PAGE IS
OF POOR QUALITY

Table 4-10. PRESUN Performance as a Function of Initial Phase Angle (1 of 2)

Event	Case 1	Case 2	Case 3	Case 4
ϕ_S at beginning of simulation	150.00°	270.00°	330.00°	30.00°
Start ROTAP for Earth search	3.00 sec	3.00 sec	3.00 sec	3.00°
Stop ROTAP	126.03 sec	41.03 sec	256.41 sec	237.41 sec
ϕ_S computed by GCAP	149.98°	271.53°	328.34°	32.88°
Start ROTAP for Sun lock	134.72 sec	49.72 sec	265.10 sec	246.10 sec
Stop ROTAP	252.41 sec	83.41 sec	355.79 sec	317.79 sec
ϕ_S at end of ROTAP	152.81°	272.33°	330.02°	30.31°
Start PRECES to place pitch southerly	350.40 sec	end of run	454.10 sec	416.25 sec
Stop PRECES	2456.10 sec		1513.57 sec	2535.20 sec
Duration of precession	2105.70 sec		1059.47 sec	2118.95 sec
Activate DAMP	2465.87 sec		1523.57 sec	2545.23 sec
DAMP ends	2754.88 sec		1880.03 sec	2963.23 sec
Minimum δ_S angle	-3.5816°		-3.5810°	-2.5586°
Maximum δ_S angle	6.6477°		1.5353°	1.5356°
Nutation Cone Amplitude	10.2293°		5.1163°	4.0942°
DAMP commands burn at	2830.07 sec		1928.37 sec	2997.42 sec

ORIGINAL PAGE IS
OF POOR QUALITY

Table 4-10. PRESUN Performance as a Function of Initial Phase Angle (2 of 2)

Event	Case 1	Case 2	Case 3	Case 4
ϕ_S after damping burn	269.80°		274.19°	272.29°
Start ROTAP for Earth search	2838.83 sec		1933.42 sec	3001.88 sec
Stop ROTAP for Earth search	2925.05 sec		1989.46 sec	309p.77 sec
ϕ_S computed by GCAP	272.87°		270.31°	272.56°
Start ROTAP for Sun lock	2934.04 sec		1998.47 sec	3100.88 sec
Stop ROTAP	3013.43 sec		2089.03 sec	3185.99 sec
ϕ_S at end of ROTAP	269.54°		275.14°	273.45°

An analysis now will be presented of the comparison between the ϕ_S determination accuracy achieved in the simulation with the accuracy estimation of Reference 11.

Consider Case 3 for the initial and final determination of ϕ_S as shown in Table 4-11. Several angles are used as input for the ϕ_S determination algorithm from NESA-B Earth data.

1. DLEMIN--Minimum roll angle from NESA-B region at closest approach to Earth center.
2. DLEMAX--Maximum roll angle from NESA-B region at closest approach to Earth center.
3. ALPHA-1 and ALPHA-2--Angle from spacecraft +yaw axis to projection of Sun line on roll-yaw plane at first and last Earth presence in NESA-B during rotation about pitch.
4. DALPM--Pitch angle from Sun to Earth center computed from ALPHA-1, ALPHA-2 and the 3.5 degree scanner offset computed from the Sun declination and orbit slot.

As discussed in Reference 11, ϕ_S may be computed from the Sun declination, orbit slot, and either δ_E or α_E . The observed value of δ_E (α_E) may be computed by averaging DLEMIN and DLEMAX (ALPHA1 and ALPHA2 ± 3.5 degrees) and computing ϕ_S for the mean value or, equivalently, by computing ϕ_S at the extremes and then taking the mean. The second approach, evidently used by SED for δ_E , assumes that the dependency $\phi_S(\alpha_E)$ or $\phi_S(\delta_E)$ is linear. As shown in Reference 11, the linear assumption is severely in error for many geometrical conditions.

The best value for ϕ_S may be obtained by considering the relative accuracy of the α_E and δ_E data together with the sensitivity of the computed ϕ_S , to errors in α_E and δ_E . The δ_E accuracy is determined from the region of Earth

PRELIMINARY DRAFT

ORIGINAL PAGE IS
OF POOR QUALITY

Table 4-11. Details of Case 3 ϕ_S Determination

	<u>Initial Search</u>	<u>Final Search</u>
ϕ_S (actual)	330.0	274.2
ϕ_S (computed)	328.3	270.3
$\Delta\phi_S$ (error)	1.7	3.9
Orbit slot	3.6	10.8
δ_E (actual)	-6.5	-17.6
δ_E (observed)	-5.77 to -8.68	-16.00 to -21.68
α_E (actual)	-16.9	-11.0
α_E (observed)	-14.7	-9.7
$\Delta\delta_E$ (error)	+0.7	+1.2
$\Delta\alpha_E$ (error)	-2.2	-1.3
$\partial\phi_S/\partial\delta_E$	-3.4	-5.0
$\partial\phi_S/\partial\alpha_E$	-11.0	-3.3
DALPM	17.7	11.6
θ_D	-17.4	-17.4

strike and the reliability of the region determination as shown in Figure 2-6. Errors may range from ± 1.4 degrees in region 8.6 or 9.6* to ± 2.9 degrees in regions 8.1 or 9.1. The α_E accuracy is determined from the Sun sensor resolution (± 0.5 degrees) and the reliability of the first and last Earth presence times. In general, the error in α_E should not be greater than ± 2 degrees.

The sensitivity of ϕ_S to errors in δ_E or α_E is strongly dependent on orbit slot, ϕ_S , and Sun declination. From Table 4-11, it is clear that the determination of ϕ_S , after the initial search using the observed value of α_E will yield a 24 degree error whereas using the observed δ_E will yield a 2 degree error. In contrast, determination of ϕ_S after the final search will yield a 4 degree error using α_E and a 6 degree error using δ_E .

The apparent success of PRESUN in computing ϕ_S seems to indicate that both α_E and δ_E data are considered; however the details of the algorithm used are obscure and, further, the inflight method involves the use of tables, graphs and overlays. CSC recommends that careful, equal consideration be given to α_E and δ_E data, using the sensitivity equations in Reference 11, for the most precise determination of ϕ_S .

The sensitivity of PRESUN to errors in the assumed moments of inertia and roll thruster calibration were investigated as shown in Table 4-12. PRESUN uses the expected roll thruster force to compute burn durations and the expected moments of inertia to determine the burn timing. Since roll thruster calibration maneuvers are not planned, and the inertias depend strongly on the array lengths, two source of error were considered:

1. 10 percent roll thruster miscalibration
2. 48 slug-ft² error in transverse (I_{xx} and I_{zz}) inertias (corresponding to roughly a 6 inch error in array length)

*Although δ_E accuracies in region 8.6 or 9.6 are ± 0.02 degrees, PRESUN only uses the information that δ_E is in the 2.82 degree linear region.

PRELIMINARY DRAFT

ORIGINAL PAGE 13
OF POOR QUALITY

Table 4-12. PRESUN Sensitivity to Thruster and Inertia Biases (1 of 3)

Maneuver	Nominal	Roll Thrusters 0.11 lb (expected 0.1 lb)	I_{xx}, I_{zz} off by 48 slug-ft ²	Roll Thrusters 0.11 lb I_{xx}, I_{zz} off by 48 slug-ft ²
ϕ_S at beginning of simulation	90.0°	90.0°	90.0°	90.0°
Start ROTAP for Earth search	3.00 sec	3.00 sec	3.00 sec	3.00 sec
Stop ROTAP	54.03 sec	54.03 sec	54.03 sec	54.03 sec
ϕ_S computed by GCAP	78.9113°	78.9113°	78.9113°	78.9113°
Start ROTAP for Sun lock	62.72 sec	62.72 sec	62.72 sec	62.72 sec
Stop ROTAP	109.41 sec	109.41 sec	109.41 sec	109.41 sec
ϕ_S at end of ROTAP	94.35°	94.35°	94.35°	94.35°
Start PRECES to place pitch southerly	207.10 sec	207.10 sec	207.10 sec	207.10 sec
Stop PRECES	3211.96 sec	3195.89 sec	3034.73 sec	3047.20 sec
Duration of precession	3004.86 sec	2988.79 sec	2827.63 sec	2840.10 sec
Activate DAMP	3222.26 sec	3205.66 sec	3044.85 sec	3058.13 sec
DAMP ends	3634.26 sec	3605.66 sec	3437.19 sec	3431.13 sec
Maximum δ_S angle	2.5590°	2.5589°	1.5356°	1.5356°
Minimum δ_S angle	-3.5816	-5.6261°	-5.6261°	-5.6261°
Nutation cone	6.1406°	8.185°	7.1617°	7.1617°

PRELIMINARY DRAFT

ORIGINAL PAGE 13
OF POOR QUALITY

Table 4-12. PRESUN Sensitivity to Thruster and Inertia Biases (2 of 3)

Maneuver	Nominal	Roll Thrusters 0.11 lb (expected 0.1 lb)	I_{xx}, I_{zz} off by 48 slug-ft ²	Roll Thrusters 0.11 lb I_{xx}, I_{zz} off by 48 slug-ft ²
DAMP commands burn at	3683.95 sec	3661.85 sec	3571.38 sec	3560.16 sec
ϕ_S after damping burn	283.14°	267.17°	278.91°	261.43°
Start ROTAP for Earth search	3690.37 sec	3669.44 sec	3577.80 sec	3566.02 sec
Stop ROTAP for Earth search	3803.40 sec	3748.95 sec	3721.13 sec	3651.91 sec
ψ_S computed by GCAP	284.2927°	266.8618°	278.6790°	261.7576
Start ROTAP for Sun lock	3812.40 sec	3757.95 sec	3730.24 sec	3660.58 sec
Stop ROTAP	3922.08 sec	3836.22 sec	3813.35 sec	3738.69 sec
ϕ_S at end of ROTAP	283.33°	267.03°	279.83°	263.65°
Start trim PRECES	4021.21 sec	Trim not needed	Trim not needed	Trim not needed
Stop trim PRECES	4195.26 sec			
Duration of PRECES	174.05 sec			
Start DAMP	4207.95 sec			
DAMP ends	4632.10 sec			
	DAMP ran out of monitoring time			

PRELIMINARY DRAFT

ORIGINAL PAGE IS
OF POOR QUALITY

Table 4-12. PRESUN Sensitivity to Thruster and Inertia Biases (3 of 3)

Maneuver	Nominal	Roller Thrusters 0.11 lb (expected 0.1 lb)	I_{xx} , I_{zz} off by 48 slug-ft ²	Roll Thrusters 0.11 lb I_{xx} , I_{zz} off by 48 slug-ft ²
ϕ_S after DAMP	273.40°			
Start ROTAP for Earth search	4638.22 sec			
Stop ROTAP	4789.30 sec			
ϕ_S computed by GCAP	270.0278°			
Start ROTAP for Sun lock	4798.29 sec			
Stop ROTAP	4887.73 sec			
ϕ_S after ROTAP	272.70°			
Start PRECES into orbit plane	5172.24 sec	3936.59 sec	3913.48 sec	3838.77 sec
Stop PRECES	5351.82 sec	4300.00 sec	4257.68 sec	4184.94 sec
Duration of PRECES	179.58 sec	363.41 sec	344.20 sec	346.17 sec
Start DAMP	5358.82 sec	4307.40 sec	4264.07 sec	4194.11 sec
DAMP ends	5735.30 sec	4731.83 sec	4629.60 sec	4595.83 sec
	CONE < 4.0°	ran out of time	CONE < 4.0°	ran out of time
Time required for maneuver	95 min 35.30 sec	78 min 51.83 sec	77 min 8.60 sec	76 min 35.83 sec
Number of α_C ATCON burns issued	73	48	57	60
Duration of α_C thrusting	17.109 sec	11.250 sec	13.359 sec	14.003 sec

PRESUN performance was unaffected by either or both of these errors; in fact, the biased runs performed somewhat better and did not require a ϕ_S trim. It is noted that the initial ϕ_S determination error was 11 degrees because of the high sensitivity of ϕ_S to δ_E errors for this geometry.

4.2.7 ERTLCK (Earth Lock)

ERTLCK refers to the series of rotations about pitch and precessions about roll (and possibly yaw) which are performed to reduce the angular errors and rates to within the limits of the onboard controller.

The results of the ERTLCK simulations are summarized in Table 4-13. The runs denoted in Table 4-13 correspond to continuations of the PRESUN simulation runs denoted earlier on Table 4-12.

The nominal case achieved Earth lock in 13 minutes requiring only a 23 degree rotation about pitch and two nutation damping burns (MODE-4, spinning wheel, α_E controlled).

Run 2, corresponding to a 10 percent miscalibrated roll thruster which was used for the PRESUN precession and nutation damping, achieved Earth lock in a similar fashion after 10 minutes.

Run 3, which used incorrect moments of inertia for computing nutation periods and consequent timing of precession burns, required a precession about roll and two additional damping burns to achieve Earth lock after 21 minutes.

Run 4, which used a miscalibrated roll thruster and incorrect moments of inertia, also required a roll precession but only a single damping burn and achieved Earth lock after 12 minutes.

The overall performance of Earth lock was extremely good and no problems were observed.

PRELIMINARY DRAFT

ORIGINAL PAGE IS
OF POOR QUALITY

Table 4-13. Earth Lock Simulations (1 of 4)

ERTLCK Run #1 Nominal Case*

Time of Event in Seconds	Event	Pitch ^b (degrees)	Roll	NESA Regions		
				A-B 0 to 5	B 6 to 7	A 8 to 9
3.00	Start ROTAP	28.0	0.4	0.0	0.0	0.0
95.40	Stop ROTAP	- 0.73	0.08	5.4	6.6	8.5
100.40	Start DAMP	- 0.73	0.08	5.4	6.6	8.5
423.68	Stop DAMP	0.29	0.08	5.3	7.6	8.6
	† β max = -0.0774° β min = -1.0174° Center = -0.5474°					
774.51	DAMP burn	- 0.61	0.12	5.4	6.6	8.5
779.74	Set Torque Bias	- 0.60	0.12	5.4	6.6	8.5
784.74	Enable PWC	- 0.60	0.12	5.4	6.6	8.5

*18 α_C burns with 1.969 seconds total duration

† β denotes the pitch angle

PRELIMINARY DRAFT

ORIGINAL PAGE IS
OF POOR QUALITY

Table 4-13. Earth Lock Simulations (2 of 4)

ERTLCK Run #2* Roll thruster R_1 force = 0.11 lbs

Time of Event in Seconds	Event	Pitch (degrees)	Roll (degrees)	NESA Regions		
				A-B 0 to 5	B 6 to 7	A 8 to 9
3.00	Start ROTAP	20.3	-2.0	0.0	0.0	0.0
70.41	Stop ROTAP	- 0.48	-1.88	5.1	6.5	9.5
74.58	Start DAMP	- 0.81	-1.85	5.1	6.5	9.5
393.51	Stop DAMP	0.30	-2.07	5.2	7.5	9.6
	β max = 2.067					
	β min = 1.1722					
	Center = 1.6201					
558.11	DAMP burn	- 0.08	-1.23	5.1	6.5	9.5
563.72	Set Torque Bias	- 0.08	-1.23	5.1	6.5	9.5
568.89	Enable PWC	- 0.36	-1.23	5.1	6.5	9.5

*13 α_C burns for 1.422 seconds total duration

PRELIMINARY DRAFT

ORIGINAL PAGE IS
OF POOR QUALITY

Table 4-13. Earth Lock Simulations (3 of 4)

ERTLCK Run #3* - I_{xx} and I_{zz} based on arrays 6-inches short

Time of Event in Seconds	Event	Pitch (degrees)	Roll	NESA Regions		
				A-B 0 to 5	B 6 to 7	A 8 to 9
3.00	Start ROTAP	25.8	2.1	0.0	0.0	0.0
107.31	Stop ROTAP	0.1	3.3	4.2	7.6	8.4
115.48	Start PRECES	0.1	3.4	4.2	7.6	8.4
282.54	Stop PRECES	0.72	3.3	2.2	7.1	9.4
288.02	Start DAMP	0.75	-3.4	2.2	7.1	9.4
623.22	Stop DAMP	2.5	-2.82	2.2	7.1	9.4
	β max: 3.2903 β min: 1.1833 Center: 2.2368					
839.88	DAMP burn	3.6	-0.95	3.3	7.3	9.6
846.41	Start ROTAP	3.6	-0.95	3.3	7.3	9.6
860.42	Stop ROTAP	0.18	-0.82	5.2	7.5	9.6
865.49	Start DAMP	0.21	-0.80	5.2	7.5	9.6
1105.20	Stop DAMP	0.13	-1.15	5.2	7.5	9.6
	β max 1.1611 β min 0.6414 Center .9013					
1261.00	DAMP Burn	-0.36	-0.41	5.1	6.5	9.5
1263.40	Set Torque Bias	-0.33	-0.40	5.1	6.5	9.5
1268.74	Enable PWC	-0.33	-0.40	5.1	6.5	9.5

*4 α_C burns for 0.438 seconds total duration

PRELIMINARY DRAFT

ORIGINAL PAGE IS
OF POOR QUALITY

Table 4-13. Earth Lock Simulations (4 of 4)

ERTLCK Run #4* - Roll thruster R_1 force - 0.11 lbs

I_{xx} and I_{zz} based on arrays 6-inches short

Time of Event in Seconds	Event	Pitch (degrees)	Roll (degrees)	NESA Regions		
				A-B 0 to 5	B 6 to 7	A 8 to 9
3.00	Start ROTAP	19.4	-4.7	0.0	0.0	0.0
56.31	Stop ROTAP	9.9	-5.2	2.2	7.1	9.2
64.28	Start PRECES	10.3	-5.2	2.2	7.1	9.2
231.54	Stop PRECES	- 2.9	2.27	1.3	6.4	8.1
240.35	Start ROTAP	- 2.70	2.46	1.3	6.6	8.1
252.13	Stop ROTAP	- 0.25	2.60	5.4	6.6	8.5
256.83	Start DAMP	- 0.32	2.65	5.4	6.6	8.5
	β max 0.09953					
	β min -2.7205					
	Center -1.3105					
732.51	DAMP burn	- 0.41	0.39	5.4	6.6	8.5
738.49	Set Torque Bias	- 0.49	0.22	5.4	6.6	8.5
743.07	Enable PWC	- 0.58	0.03	5.4	6.6	8.5

*14 α_C burns for 1.906 seconds total duration

4.3 FSD OPEN-LOOP STUDY RESULTS

Should ground-based attitude control be lost at any point during attitude acquisition, it is important that ground personnel have some reliable estimate of the direction and rate of attitude drift during the period prior to reacquisition of attitude control. Such estimates permit determination of (1) when control is regained if telemetry data are also lost during the loss of control, and (2) how long the power and thermal constraints will be satisfied.

The main environmental torques which generate attitude drift are the following:

- Residual magnetic dipole torque
- Gravity-gradient torque (after solar array deployment)
- Solar radiation pressure torque (after solar array deployment)

The models for these three torques and their effects on CTS are discussed in detail in subsequent sections.

After the solar arrays have been deployed, they are assumed to be rigid plates to a first approximation, but in reality they are flexible and oscillate in response to environmental and applied torques. The effects of this flexibility on both attitude drift and thruster activity were included in the study, and the results also are discussed.

4.3.1 Torque and Array Flexibility Models

The models and parameters used for the environmental torques are described in the following subsections.

4.3.1.1 Residual Magnetic Dipole Torque

If the spacecraft is not magnetically clean after launch, the residual magnetic dipole will interact with the Earth's magnetic field and cause a sustained drift in the spacecraft's attitude. The magnitude and direction of this drift will be dependent upon the orientation of the dipole in the spacecraft; experimental measurements of this property will not be made prior to launch. In lieu of such

data, a realistic magnetic dipole was simulated, using the following typical values:*

- 450 pole-cm along the spacecraft +X-axis
- 400 pole-cm along the spacecraft -Y-axis
- 500 pole-cm along the spacecraft +Z-axis

Simulations using ten times and one-tenth these values were also conducted for comparison; the results are discussed in Section 4.3.2.2.

The model used for the Earth's magnetic field was the International Geophysical Reference Field (IGRF) (1965). The average value of the Earth's field for the CTS orbit is approximately 0.11×10^{-2} gauss.

4.3.1.2 Gravity-Gradient Torque

Gravity-gradient torques were included in the simulations conducted after solar array deployment. The gravitational field model which was used was one which incorporated the first zonal harmonic correction to the point mass gravitational potential including oblateness. This model currently is used for many operational spacecraft. The orbital parameters which were used were as follows:

Semi-major axis = 41704.0 km

Eccentricity = 0.0

Inclination = 0.9°

Longitude of ascending node = 270.0°

Argument of perigee = 180.0°

The principal moments of inertia were assumed to be:

$$I_x = 93.3 \text{ slug-ft}^2$$

$$I_y = 69.8 \text{ slug-ft}^2$$

$$I_z = 114.3 \text{ slug-ft}^2$$

*Typical torques for this dipole strength are $\sim 10^{-7}$ ft-lbs

PRELIMINARY DRAFT

prior to solar array deployment, and

ORIGINAL PAGE IS
OF POOR QUALITY

$$I_x = 822.5 \text{ slug-ft}^2$$

$$I_y = 69.8 \text{ slug-ft}^2$$

$$I_z = 845.5 \text{ slug-ft}^2$$

after solar array deployment.

4.3.1.3 Solar Radiation Pressure Torque

The effects of solar radiation pressure were studied, and were found to contribute appreciably to a gradual drift in the spacecraft's orbit. The spacecraft was modeled as a spherical hub with flat plates as the solar arrays. The arrays were assumed to be actively directed by the auto-track mechanism so that they always faced the Sun. In this configuration there is no "propellor effect," but there is a slight translational motion in the spacecraft's center of mass, resulting in gradual alterations to the orbital elements. The solar pressure coefficient was assumed to be $0.189 \times 10^{-6} \text{ lb/ft}^2$. Solar pressure produces no effect on the attitude unless the solar arrays are asymmetric in either length or orientation.

4.3.1.4 Momentum Wheel Spinup Reaction Torque

As the momentum wheel is spun up, reactive torques will cause the spacecraft to rotate in a direction opposite to that of the momentum wheel, and the net result will depend on both the final wheel speed and the duty cycle with which it is accelerated. The studies which were performed for various examples of momentum wheel activity are discussed in detail in Section 4.3.2.6. The moment of inertia of the momentum wheel was assumed to be 0.0382 slug-ft^2 along the negative pitch axis.

4.3.1.5 Array Flexibility

In the simulations which included flexibility effects, the attached solar array booms were assumed to be cantilevered beams with one end fixed rigidly to the spacecraft body (this end is maintained normal to the body surface) and the

other end is free to oscillate. The stiffness of the arrays was taken to be 2322 ft-lb^2 (Reference 18) for both in-plane and out-of-plane motion. Flexure damping of solar array booms was included (Reference 19), and the arrays were assumed to have no twisting motion.

4.3.2 Results of Simulation Runs

The results of the simulations will be discussed in the following subsections. The simulations are discussed in the order in which the maneuvers will occur during the mission.

4.3.2.1 Spin Axis Precession (DOP Events A.14 and A.15)

Analog simulations have previously been performed by CRC (Reference 20), in which estimates of attitude drift were verified. These simulations resulted in the current version of the Detailed Operating Procedures (DOP), in which a spin rate of two rpm is maintained between Day 1 and Day 2 activities.

The open loop version of FSD/CTS described in Subsection 3.3.1 was used to verify and quantify the CRC results. Spin rates of one and two rpm were simulated, including all environmental torques. The +Z-axis was initially one degree off the south orbit normal. A small nutation angle (0.16° for one rpm and 0.30° for two rpm) was simulated. The resulting attitude drift after six hours is summarized in Table 4-14. In this and following tables, the angles ϕ , θ , and ψ are the conventional Euler angles for a 3-1-3 rotation sequence. $\gamma_{1/2}$ is the half-cone angle of nutation. Deviations above and below nominal values are included where applicable so that biases may be observed. ω_x , ω_y and ω_z are the body rates about the X-, Y-, and Z-axes, respectively.

The environmental disturbances which contribute the most to spacecraft nutation during this phase are the gravity-gradient and residual magnetic dipole. Since the magnitude and direction of the residual dipole will not be known, it will be impossible to predict the direction of drift. With the dipole simulated

PRELIMINARY DRAFT

ORIGINAL PAGE IS
OF POOR QUALITY

Table 4-14. Variation in Attitude and Attitude Rates in Six Hours
for Spin Rates of One and Two RPM

	<u>1 RPM</u>	<u>2 RPM</u>
$\gamma_{1/2}$ (Half-Cone Angle of Nutation)	-0.32 to 0.27 ⁰	-0.17 to 0.13 ⁰
θ	0.30 ⁰ (constant)	0.156 ⁰ (constant)
ω_x (Body Rate About X-Axis)	$\pm 0.08^0/\text{sec}$ (constant)	$\pm 0.02^0/\text{sec}$ (constant)
ω_y (Body Rate About Y-Axis)	0.016 ⁰ /sec	0.063 ⁰ /sec
ω_z (Body Rate About Z-Axis)	6.00 ⁰ /sec (constant)	12.00 ⁰ /sec (constant)

in the study, the drift is negligible and should prove to be of no significance to the mission at this point. Solar radiation pressure was included, but is of no significance to attitude drift until the solar arrays are deployed, and even then it contributes only to translational motion unless the auto-track mechanism causes unequal rotation of the arrays relative to the Sunline or the arrays are of unequal length.

4.3.2.2 Pre-Solar Array Deployment Drift (DOP Events A.22 and A.23)

After despinning from two rpm to zero, gyroscopic stability is lost and the spacecraft attitude would undergo large drift if active attitude control were absent. Were attitude control to be lost, the spacecraft would be expected to undergo motion similar to that described in the following two subsections.

4.3.2.2.1 -X-Axis Parallel to the Sunline

In these simulations the spacecraft initially had no rotational motion. After approximately two hours, in the absence of any active attitude control, the Z-axis of the spacecraft drifted 1.1 degrees from its initial direction along the south orbit normal. The major contributor to this drift is the residual magnetic dipole. Consequently more simulations were performed using dipole strengths ten times larger than the one just described, and one-tenth as large. Results of these simulations are summarized in Table 4-15.

4.3.2.2.2 +Z-Axis Parallel to the Sunline

In these simulations, as in the preceding ones, the spacecraft initially had no rotational motion. After approximately two hours, the spacecraft Z-axis drifted about 1.0 degrees. As expected, the residual magnetic dipole contributed more to the drift than any other environmental torques.

In summary, the spacecraft Z-axis may be expected to drift one or two degrees in a few hours if active attitude control is lost. It would appear that loss of active control would not constitute much of a problem during this phase of the mission.

PRELIMINARY DRAFT

ORIGINAL PAGE IS
OF POOR QUALITY

Table 4-15. Effect of Magnetic Dipole Strengths Upon Attitude Drift
During a Two-Hour Period

<u>M_x</u> <u>(pole-cm)</u>	<u>M_y</u> <u>(pole-cm)</u>	<u>M_z</u> <u>(pole-cm)</u>	<u>Z-Axis Drift From</u> <u>Nominal Direction (degrees)</u>
45	-40	50	0.01
450	-400	500	1.1
4500	-4000	5000	7.9

4.3.2.3 Solar Array Deployment

Simulations of solar array deployment under the influence of environmental torques and array flexibility were conducted. A deployment rate of 1 inch/sec (Reference 4) was employed. The spacecraft Z-axis was initially parallel to the Sunline, and an initial yaw rate of 0.3 degree/sec prior to deployment was assumed. From this simulation it was found that the spacecraft roll angle varied 0.01 degrees, with a roll rate of 0.12×10^{-3} deg/sec. The pitch angle varied 1.2 degrees, and a yaw rate of 0.8×10^{-2} deg/sec was induced due to environmental torque effects. The solar array boom deflection induced during deployment was negligible and did not adversely affect the spacecraft attitude. Environmental torques induce 1.2 degrees of drift about the body Z-axis during deployment.

4.3.2.4 Post-Solar Array Deployment

Sensitivity studies were performed during the post deployment phase of the mission to determine the attitude drift due to environmental and applied torques. The spacecraft Z-axis was parallel to the Sunline, and the solar arrays always faced the Sun. The initial attitude rates were zero.

The spacecraft behaves as a dipole satellite with minimum moment of inertia about the body Y-axis; the natural stable spacecraft attitude is with the body Y-axis along the local vertical. For different phase angles the spacecraft will undergo different rotations to achieve this stable configuration. The final attitude resulting therefrom is predictable. The amount of time required for the spacecraft to achieve the gravity-gradient stable attitude depends on the initial phase angle, but is much longer than the time periods under consideration here. For example, Table 4-16 illustrates variations to the spacecraft Z-axis pointing direction during a two-hour period for various phase angles. Drifts are on the order of a few degrees.

PRELIMINARY DRAFT

ORIGINAL PAGE 12
OF POOR QUALITY

Table 4-16. Z-Axis Drift After Array Deployment

<u>Phase Angle (degrees)</u>	<u>Z-Axis Drift After Two Hours (degrees)</u>
0	2.5
90	1.35
180	2.5
270	1.35

PRELIMINARY DRAFT

ORIGINAL PAGE 19
OF POOR QUALITY

The post-solar array deployment simulation discussed above assumed the arrays were rigid. Simulations were performed assuming flexible arrays, and the results were virtually identical. Rigid arrays are consequently assumed to represent adequately the expected motion during this phase of the mission and were used in all further simulations.

In all cases where the arrays are symmetric, there is no torque resulting from solar radiation pressure. However, in the event of unequal array lengths, solar radiation pressure torques not only affect, but dominate, the spacecraft's attitude drift. Consequently, simulations were performed to study the drift rates expected for various asymmetric configurations, as discussed in the following subsections.

4.3.2.4.1 One Array Slightly Shorter Than the Other

A situation in which one array is slightly shorter than the other was considered as a realistic possibility, and was investigated during this phase of the mission. The results are summarized in Table 4-17.

Simulations were performed for the case of one array six inches shorter than the other, and the case of one array one foot shorter than the other. The nominal lengths of the array booms were taken to be 23.79 feet, and the Z-axis of the spacecraft was parallel to the Sunline. The initial drift rates were zero, and the simulations covered a period of two hours. The numbers shown on the table are variations from the nominal values.

As one would expect, the attitude drift in θ and ϕ is proportional to the north-south array length difference, and attitude drift about the Z-axis is negligible. Attitude constraints can be maintained with normal control, but should active attitude control be lost in such a configuration, considerable drift can be expected within a matter of hours.

PRELIMINARY DRAFT

ORIGINAL PAGE IS
OF POOR QUALITY

Table 4-17. Attitude Drift and Drift Rates Due to
Slightly Asymmetric Arrays

<u>Attitude Drift and Drift Rates (after two hours)</u>	<u>One Boom Six Inches Too Short</u>	<u>One Boom One Foot Too Short</u>
ψ	0.0 to 0.3°	0.3 to 0.1°
θ	-35.0 to -0.9°	-65.0 to 0.1°
ϕ	-6.6 to 0.0°	-13.4 to 0.0°
ω_x	0.0 to 0.01°/sec	0.0 to 1.6°/sec
ω_y	-0.01 to 0.0°/sec	-0.004 to 0.0°/sec
ω_z	-0.001 to 0.0°/sec	-0.001 to 0.0°/sec

PRELIMINARY DRAFT

ORIGINAL PAGE IS
OF POOR QUALITY

4.3.2.4.2 One Array Drastically Shorter Than the Other

This contingency is considered unlikely, but a crude idea of what to expect in such an eventuality was determined. Table 4-18 contains attitude drift and drift rates similar to those in Table 4-17, for the case of one array one-half and three-fourths its nominal length.

As in the case of Table 4-17, the θ and ϕ drift rates are proportional to the asymmetry. Unlike Table 4-17, however, motion is induced about the Z-axis as well as X and Y. This is due to the coupling of the motion about the three axes.

4.3.2.4.3 Solar Radiation Pressure Summary

The preceding results may be summarized as follows:

- If one array is slightly shorter (one foot) than the other, significant attitude drift can be expected within a few hours if attitude control is lost, with little motion induced about the Z-axis.
- If one array is drastically shorter (three-fourths nominal length) than the other, attitude drift about the X and Y axes is only slightly greater than the slightly asymmetric, but significantly more motion is induced about the Z-axis.

4.3.2.5 Effect of Spin Rate on Attitude Drift

A sensitivity study was performed to investigate attitude stability as a function of spin rate. The solar arrays were fully (and symmetrically) deployed to 23.79 feet. Table 4-19 contains the results of this study, after twelve hours (half the orbital period).

The study indicates that a small yaw rate of 1-degree per second is sufficient for maintaining a power positive configuration for several hours but 5-degrees per second may be required to maintain a holding attitude for 24 hours.

PRELIMINARY DRAFT

ORIGINAL PAGE 18
OF POOR QUALITY

Table 4-18. Attitude Drift and Drift Rates Due to Drastically Asymmetric Arrays

<u>Attitude Drift and Drift Rates After Two Hours</u>	<u>One Boom Three-Fourths Its Nominal Lengths</u>	<u>One Boom One-Half Its Nominal Length</u>
ψ	-169.1 to 0.0°	-261.0 to 0.0°
θ	-44.5 to 17.2°	-70.2 to 1.5°
ϕ	0.0 to 271.1°	0.0 to 239.2°
ω_x	-0.005 to 0.03°/sec	-0.05 to 0.05°/sec
ω_y	-0.08 to 0.04°/sec	-0.03 to 0.02°/sec
ω_z	0.0 to 0.04°/sec	-0.004 to 0.02°/sec

Table 4-19. Attitude Drift and Drift Rates As a
Function of Spin Rate

Attitude Drift and Drift Rates After Twelve Hours	Spin Rate About Yaw Axis (ω_z)		
	$1^\circ/\text{sec}$	$2^\circ/\text{sec}$	$5^\circ/\text{sec}$
θ	0.2°	0.1°	Negligible
ϕ	1.67°	0.66°	0.21°
ω_x	$\pm 0.83 \times 10^{-3} \text{ }^\circ/\text{sec}$	$\pm 0.42 \times 10^{-3} \text{ }^\circ/\text{sec}$	$\pm 0.16 \times 10^{-3} \text{ }^\circ/\text{sec}$
ω_y	$\pm 0.6 \times 10^{-3} \text{ }^\circ/\text{sec}$	$\pm 0.3 \times 10^{-3} \text{ }^\circ/\text{sec}$	$\pm 0.12 \times 10^{-3} \text{ }^\circ/\text{sec}$

PRELIMINARY DRAFT

ORIGINAL PAGE IS
OF POOR QUALITY

4.3.2.6 Momentum Wheel Spinup (DOP Event A.30)

Simulations were performed to study the attitude drift and drift rates during spinup of the momentum wheel. A nominal spinup was found to be perfectly acceptable as planned in the DOP. When flexibility was introduced for the solar arrays, the drift and drift rates presented in Table 4-20 were obtained for the case of spinup during loss of active attitude control. The figures shown are deviations from nominal Sun-locked values.

The out-of-plane array tip deflections were 10^{-4} feet, the in-plane deflections were 10^{-1} feet, and the deflection rates were 10^{-4} feet/second.

A series of simulations was made to determine how much attitude drift could be expected if active attitude control were lost during wheel spinup, and how much effect the flexibility of the solar arrays would contribute to such drift. It was assumed that active attitude control was lost during spinup, and that shortly thereafter (~60 seconds) the wheel was commanded to maintain constant wheel speed. The attitude drift and solar array deflections were studied during the delay and for approximately 20 minutes thereafter. The +Z-axis was initially parallel to the Sunline. The results from this study for the case of rigid arrays are summarized in Table 4-21.

The numbers in Table 4-21 indicate that attitude drift and drift rates during loss of attitude control will not adversely affect the mission during this phase, even at intermediate momentum wheel speeds.

4.3.2.7 Momentum Transfer

An option has been suggested by CSC (Reference 9) which could be used for attitude acquisition should the procedures in the DOP prove untenable for any reason. This option, referred to as Attitude Acquisition via Momentum Transfer (AAMT), has been investigated and is presented here for completeness. The

PRELIMINARY DRAFT

ORIGINAL PAGE 13
OF POOR QUALITY

Table 4-20. Attitude Drift and Drift Rates During
Momentum Wheel Spinup

<u>Attitude Drift and Drift Rates</u>	<u>Deviations From Nominal Sun-Locked Values</u>
θ	-1.3 to 1.40°
ϕ	-1.3 to 1.40°
ω_x	-10 ⁻³ to 10 ⁻³ °/sec
ω_y	0.0 to 11.1 °/sec
ω_z	-10 ⁻³ to 10 ⁻³ °/sec

Table 4-21. Attitude Drift and Drift Rates After Loss of Closed Loop Control During Momentum Wheel Spinup

Case No.	Wheel Speed at Loss of Attitude Control rpm (deg/sec)	Delay Before Command Constant Wheel Speed Controller (sec)	Final Wheel Speed Maintained rpm (deg/sec)	θ (degrees)		ω (degrees per second)		
				θ	ϕ	ω_x	ω_y	ω_z
1	1000(6000)	10	1060(6360)	-0.9 ~ 0.9	-0.9 ~ 0.9	$-10^{-5} \sim 10^{-5}$	0.0 ~ 0.2	$-10^{-5} \sim 10^{-5}$
2	1000(6000)	30	1180(7080)	-0.9 ~ 0.9	-0.9 ~ 0.9	$-10^{-5} \sim 10^{-5}$	0.0 ~ 0.5	$-10^{-5} \sim 10^{-5}$
3	1000(6000)	60	1360(8160)	-0.9 ~ 0.9	-0.9 ~ 0.9	$-10^{-5} \sim 10^{-5}$	0.0 ~ 0.9	$-10^{-5} \sim 10^{-5}$
4	1000(6000)	120	1720(10,320)	-0.9 ~ 0.9	-0.9 ~ 0.9	$-10^{-5} \sim 10^{-5}$	0.0 ~ 1.6	$-10^{-5} \sim 10^{-5}$
5	100(600)	10	150(960)	-0.9 ~ 0.9	-0.9 ~ 0.9	$-10^{-5} \sim 10^{-4}$	0.0 ~ 0.2	$-10^{-4} \sim 10^{-4}$
6	100(600)	30	280(1680)	-0.9 ~ 0.9	-0.8 ~ 0.9	$-10^{-4} \sim 10^{-5}$	0.0 ~ 0.5	$-10^{-4} \sim 10^{-5}$
7	100(600)	60	460(2760)	-0.9 ~ 0.9	-0.9 ~ 0.9	$-10^{-4} \sim 10^{-4}$	0.0 ~ 0.9	$-10^{-4} \sim 10^{-5}$
8	199(600)	120	820(4920)	-0.9 ~ 0.9	-0.9 ~ 0.9	$-10^{-4} \sim 10^{-4}$	0.0 ~ 1.5	$-10^{-4} \sim 10^{-4}$

ORIGINAL PAGE IS
OF POOR QUALITY

AAMT requirements are less stringent than the nominal acquisition procedure requirements, with regard to ground support for both commands and attitude determination. Subsystem failures such as the nonspinning Sun sensor (NSSS) can be tolerated within the framework of this option, and fewer maneuvers and commands are required.

The disadvantages of using AAMT include a reliance on the momentum wheel under conditions of low duty cycle and substantial transverse body rates, and acceleration of the wheel for a prolonged period prior to solar array deployment requiring a substantial portion of the available power.

Simulations utilizing AAMT were performed with environmental torques included, using a 50 percent duty cycle for the wheel spinup motor. Prior to the damping burn, the attitude offset in θ was 8.9 degrees, and a nutation half-cone angle of 9.8 degrees was observed. These angles are approximately 1-degree larger than the corresponding ADAMSSIM runs which ignored environmental torques.

It is believed that the AAMT option remains a viable alternative should it be required, and environmental disturbances should present no complications thereto.

4.3.2.8 Orbit Perturbations During PRESUN Precession

Simulations were performed using the nongraphics version of FSD to determine the effect of the PRESUN precession maneuvers on the spacecraft's orbit. Prior to the maneuver the attitude and attitude rates were as follows:

$$\begin{array}{ll} \phi = 44.5^\circ & \omega_x = -0.0472^\circ/\text{sec} \\ \theta = 105.9^\circ & \omega_y = 0.00003^\circ/\text{sec} \\ \psi = 5.36^\circ & \omega_z = 0.0263^\circ/\text{sec} \end{array}$$

PRELIMINARY DRAFT

ORIGINAL PAGE IS
OF POOR QUALITY

The corresponding orbital parameters were:

Semimajor Axis (a)	41704.0 km
Eccentricity (e)	0.0
Inclination (i)	0.9°
Longitude of Ascending Node (Ω)	270°
Argument of Perigee (ω)	180°

The principal moments of inertia were:

$$\begin{aligned}I_{xx} &= 825.1 \text{ slug-ft}^2 \\I_{yy} &= 58.2 \text{ slug-ft}^2 \\I_{zz} &= 845.6 \text{ slug-ft}^2\end{aligned}$$

The maneuver is designed to change the phase angle ψ by 180 degrees, maintaining the Z-axis parallel to the Sunline. In separate simulations of this maneuver GCAP had issued 21 long duration burns and 123 short duration α controller burns. Only the 21 long burns were input to FSD as an approximation to the thrusts to be expected (the thrust time of each long burn was 12.52 seconds, whereas the thrust time of a short α control burn was only 0.23 second). The simulated maneuver resulted in the following changes in the orbital parameters by the end of the maneuver.

$$\begin{aligned}\Delta a &= 0.18 \text{ km} \\ \Delta e &= 0.6 \times 10^{-5} \\ \Delta i &= 0.8 \times 10^{-3} \text{ degrees} \\ \Delta T &= 0.75 \text{ seconds (period)}\end{aligned}$$

The maximum deviations in semimajor axis and eccentricity during the maneuver occur when the phase angle ψ is approximately 90 degrees; at this time in the maneuver the departures from nominal were:

$$\begin{aligned}\Delta a &= 0.58 \text{ km} \\ \Delta e &= 1.6 \times 10^{-5}\end{aligned}$$

The largest deviation in inclination occurs at the end of the maneuver.

Since the α controller burns were not included in the simulation, the Sun angle drifted by approximately 10 degrees--this drift would affect the resulting changes in orbital elements by a slight amount, but they are negligibly small anyway.

It is concluded that the PRESUN precession maneuver will not affect the spacecraft's orbit appreciably.

4.4 FSD/GCAP CLOSED LOOP STUDY RESULTS

The closed loop version of FSD/GCAP described in Subsection 3.3.3 was used to investigate GCAP attitude control capabilities under the influence of environmental torques, the effects of solar array boom flexibility, and possible anomalies such as unequal solar array lengths.

4.4.1 Momentum Wheel Spinup (SPINUP)

Several SPINUP simulations were performed to assess the impact of solar radiation pressure and array flexibility on the maneuver. The influence of torque due to solar radiation was investigated by assuming the south array deployed to 22.79 feet and the north array to a full 23.79 feet. The controller parameters listed in Tables 4-22 to 4-24 are believed representative of the planned maneuver. Initial attitude angles placed the yaw axis along the Sunline and attitude rates were 0.06 degree/second for all three body axes.

The results of SPINUP simulations, with and without flexibility, are compared to an ADAMSSIM/GCAP simulation (no solar radiation pressure or residual magnetic torque) in Tables 4-23 and 4-24. The data in the table covers SPINUP and 30 minutes thereafter; the δ controller is deactivated after the CWS controller command. Several items in the table are worth noting:

1. Flexibility has a minor impact on the controller performance.
2. Solar radiation pressure substantially increases the required number of delta controller burns and consequently delta control is necessary if the arrays deploy asymmetrically.

PRELIMINARY DRAFT

ORIGINAL PAGE IS
OF POOR QUALITY

Table 4-22. SPINUP Parameters

α deadband	3.0°
δ deadband	1.5°
$\dot{\alpha}$ command	$0.35^{\circ}/\text{sec}$
$\dot{\delta}$ command	$0.06^{\circ}/\text{sec}$
Wheel duty cycle	50%
Spinup time	1637 sec (27.3 minutes)

PRELIMINARY DRAFT

ORIGINAL PAGE IS
OF POOR QUALITY

Table 4-23. SPINUP Results

<u>Parameter</u>	<u>ADAMSSIM/GCAP</u>	<u>FSD/GCAP (no flexibility)</u>
α -burns*	35	39
δ -burns*	10	23
α -duration*	47.0 seconds	52.4 seconds
δ -duration*	39.4 seconds	90.6 seconds
α -burns†	26	27
ϕ	152.5 to 167.9°	260° to 270°
θ	47.7 to 58.2°	84° to 94°
ω_x	-0.09 to 0.09°/sec	-0.07 to 0.06°/sec
ω_y	-0.24 to 0.11°/sec	-0.3 to 0.3°/sec
ω_z	-0.09 to 0.09°/sec	-0.05 to 0.07°/sec
ψ	180 to 190°	180° to 265°

*Prior to activation of CWS controller.

†30 minutes following activation of CWS controller.

PRELIMINARY DRAFT

ORIGINAL PAGE IS
OF POOR QUALITY

Table 4-24. FSD/GCAP Results for the First Five Minutes
of the SPINUP Maneuver

<u>Parameter</u>	<u>Without Flexibility</u>	<u>With Flexibility</u>
α -burns	8	6
α -duration	1.344 sec	1.792 sec
δ -burns	7	7
δ -duration	3.938 sec	3.938 sec
ϕ	260.9 to 264.4 $^{\circ}$	260.6 to 265.2 $^{\circ}$
θ	86.3 to 90.5 $^{\circ}$	86.1 to 90.0 $^{\circ}$
ψ	181.1 to 200.3 $^{\circ}$	180.0 to 198.4 $^{\circ}$
ω_x	-0.065 to 0.060 $^{\circ}$ /sec	-0.1 to 0.1 $^{\circ}$ /sec
ω_y	-0.174 to 0.151 $^{\circ}$ /sec	-0.06 to 0.085 $^{\circ}$ /sec
ω_z	0.056 to 0.068 $^{\circ}$ /sec	0.00 to 0.07 $^{\circ}$ /sec

3. The phase angle drift is substantial, 85 degrees, even in the absence of a "propeller effect."

Figures 4-4 to 4-6 illustrate the attitude behavior for the first 3 minutes of SPINUP. Note the impact of the controller burns on the attitude angles and rates is coupled because the controlled angles are relative to the Sunline in body coordinates and the plotted angles are inertial.

4.4.2 PRESUN Precession Maneuver

A simulation was performed using the output attitude and rates from the wheel spinup maneuver as input values for the precession maneuver following spinup. Flexibility was included in the first simulation, then another one was performed without flexibility for comparison. The results of the two were not significantly different. The solar array lengths were taken to be 23.79 and 22.79 feet, as in the SPINUP maneuver. The moments of inertia were:

$$I_{xx} = 778.2 \text{ slug ft}^2$$

$$I_{yy} = 69 \text{ slug ft}^2$$

$$I_{zz} = 798.6 \text{ slug ft}^2$$

The in-plane and out-of-plane solar array boom tip deflections and deflection rates are illustrated in Table 4-25 for a period of six minutes.

As a comparison of the results from the flexible and non-flexible simulations, maximum and minimum values of several pertinent parameters are given in Table 4-26. The only significant difference in the flexible simulation is that slightly more alpha controller burns are required to maintain the desired attitude, as one might expect. GCAP had no trouble maintaining the desired attitude throughout the simulation.

PRELIMINARY DRAFT

ORIGINAL PAGE 19
OF POOR QUALITY

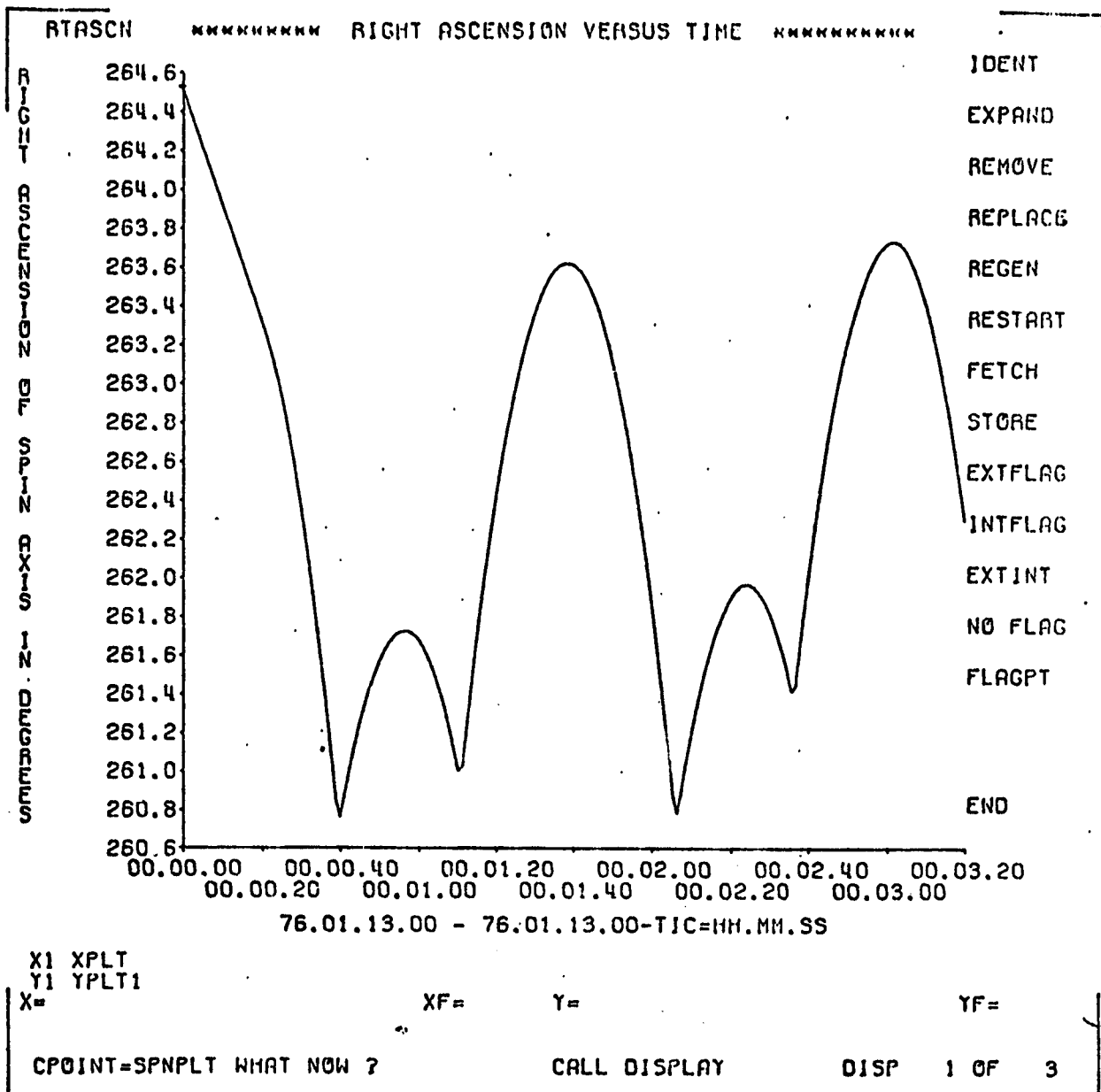


Figure 4-4. Right Ascension Versus Time for the First Three Minutes of the SPINUP Maneuver

PRELIMINARY DRAFT

ORIGINAL PAGE IS
OF POOR QUALITY

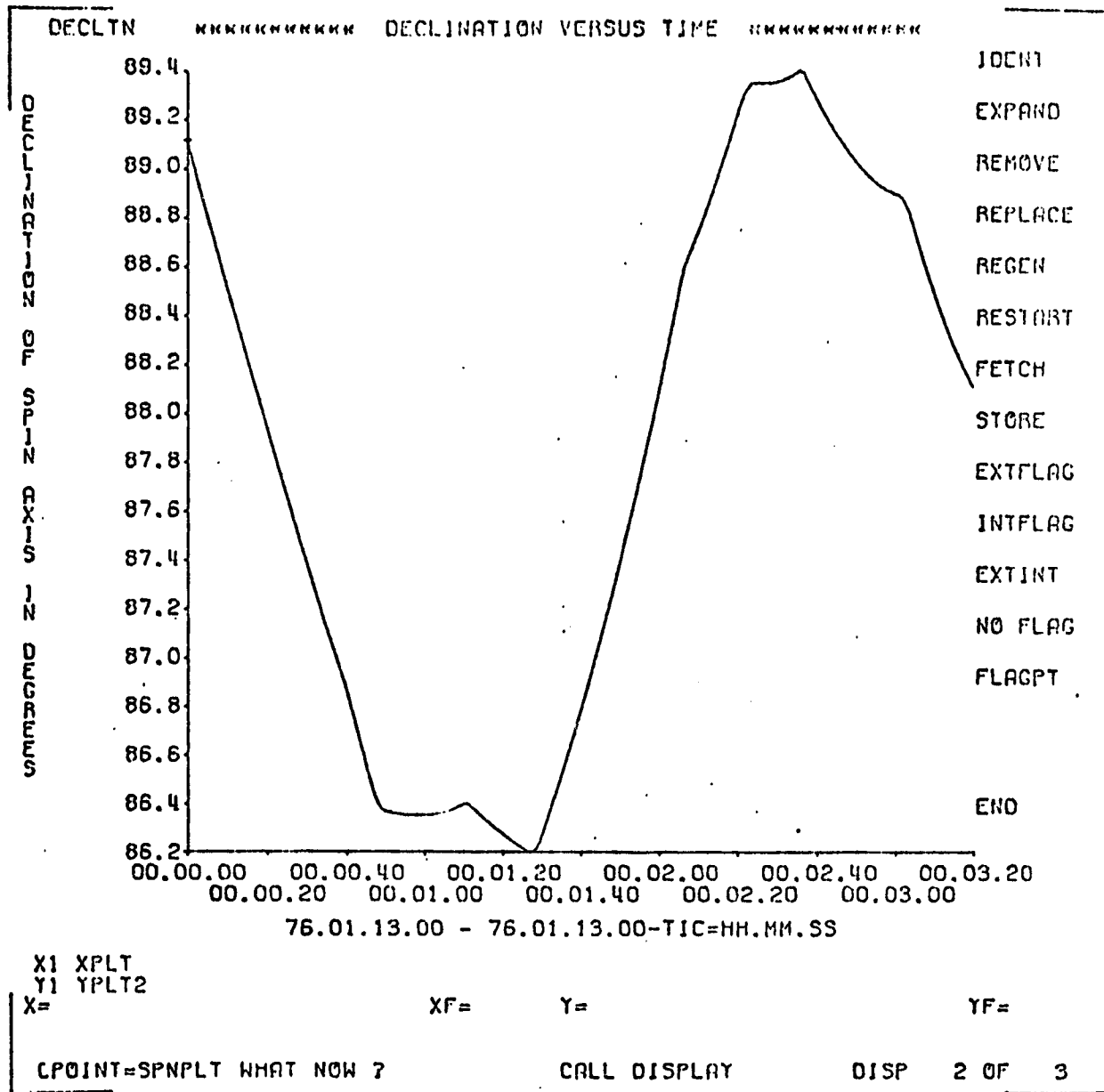


Figure 4-5. Declination Versus Time for the First Three Minutes of the SPINUP Maneuver

PRELIMINARY DRAFT

ORIGINAL PAGE IS
OF POOR QUALITY

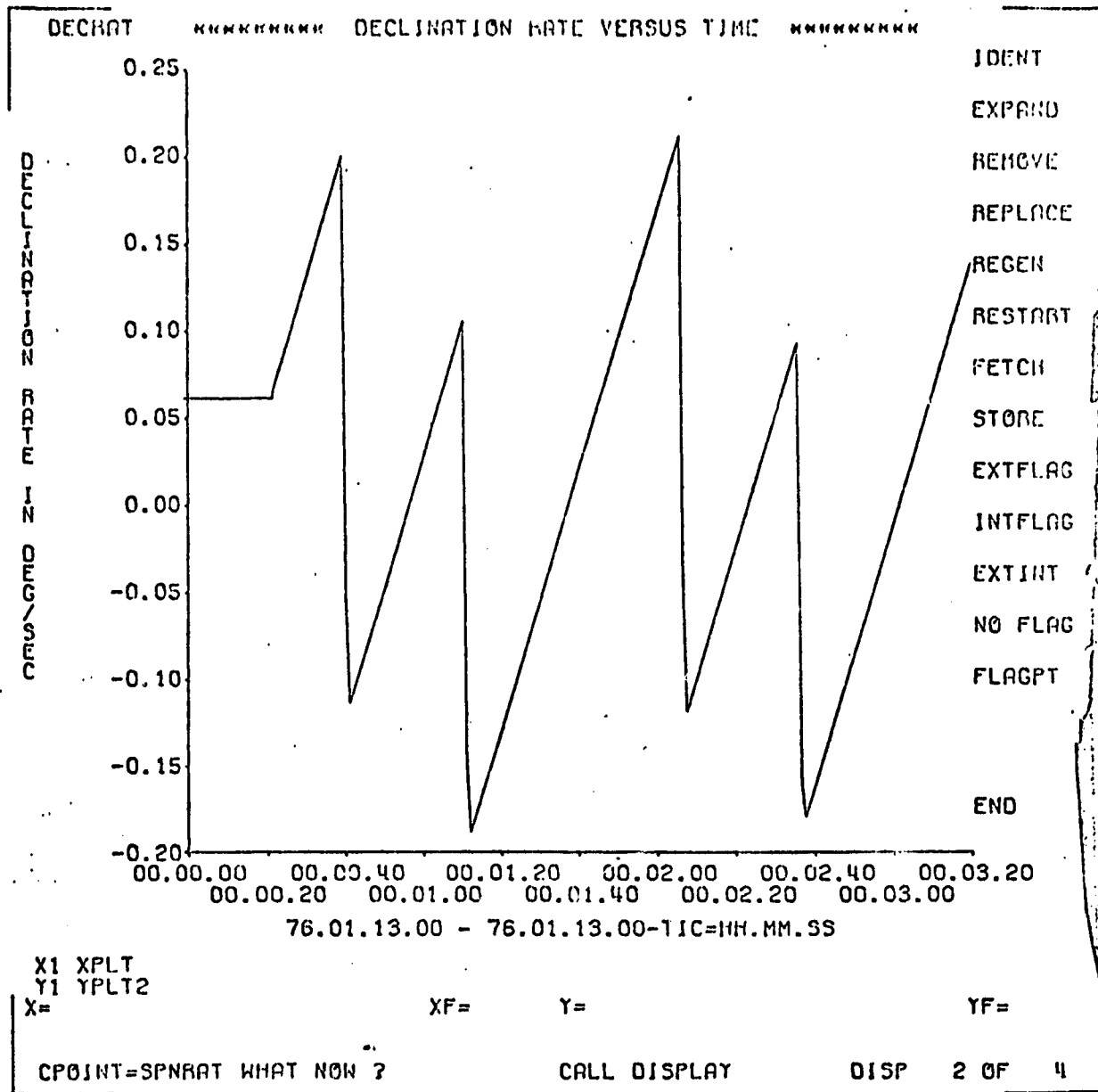


Figure 4-6. ω_y Versus Time for the First Three Minutes
of the SPINUP Maneuver

Table 4-25. Flexible Solar Array Tip Deflections and Deflection Rates During the First Six Minutes of the PRESUN Precession Maneuver

Solar Array #1 (23.79 Feet)				Solar Array #2 (22.79 Feet)			
In-Plane		Out-of-Plane		In-Plane		Out-of-Plane	
Deflection (Feet)	Deflection Rate (Feet/Sec)	Deflection (Feet)	Deflection Rate (Feet/Sec)	Deflection (Feet)	Deflection Rate (Feet/Sec)	Deflection (Feet)	Deflection Rate (Feet/Sec)
0.009	0.007	0.002	0.002	0.006	0.006	0.001	0.002

ORIGINAL PAGE IS
OF POOR QUALITY

PRELIMINARY DRAFT

ORIGINAL PAGE 19
OF POOR QUALITY

Table 4-26. A Comparison of Simulations With and Without Flexibility for the First Six Minutes of the PRESUN Precess on Maneuver

	<u>With Flexibility</u>	<u>Without Flexibility</u>
Maximum α_s	108.8°	107.8°
Minimum α_s	88.5°	89.5°
Maximum δ_s	0.5°	0.5°
Minimum δ_s	-4.6°	-4.6°
Maximum ω_x	0.098°/sec	0.096°/sec
Minimum ω_x	-0.119°/sec	-0.099°/sec
Maximum ω_y	0.238°/sec	0.207°/sec
Minimum ω_y	-0.185°/sec	-0.236°/sec
Maximum ω_z	0.001°/sec	0.002°/sec
Minimum ω_z	-0.096°/sec	-0.094°/sec
No. α -Controller Burns	11	8
No. δ -Controller Burns	0	0
No. PRESUN Burns	3	3

The entire PRESUN maneuver required 18 α -Controller burns, eight PRESUN burns, and no δ -Controller burns. The phase angle after the maneuver was less than 4 degrees off of the desired 270° (266.5°), and a damping burn was not required.

After control was turned over to ATTCON, seventeen α -Controller burns were commanded during the next half hour, and the spacecraft was controlled thereafter within constraints.

The effects of flexibility on the spacecraft attitude rates and the deflection of the solar array tips both in and out of the orbital plane are illustrated in the printer plots presented in Figures 4-7 to 4-13. These plots (three pages per parameter) include three PRESUN burns. The burns are described in Table 4-27; their effects on the spacecraft are readily discernible in the plots.

A typical PRESUN maneuver burn lasts approximately twelve seconds with a torque of 0.227959 foot-lb. This induces a solar array tip in-plane deflection of 0.26 inch, and an out-of-plane deflection of 0.03 inch. Due to the material damping of the array booms the deflection damps out prior to subsequent PRESUN burns and there is consequently no cumulative long-term motion due to flexibility.

The body attitude rates are modulated by flexibility effects as Figures 4-7 to 4-9 illustrate. This modulation is as large as 0.23 degrees/second, but damps out with the damping of the array tip deflections so that the cumulative effect on the rates is negligible. Should the material damping rate be less than that presented in Reference 18, a cumulative effect could occur which would adversely influence the GCAP software system. The crucial point is whether or not the flexing motions are adequately damped between PRESUN burns. With nominal parameters the damping appears to be adequate.

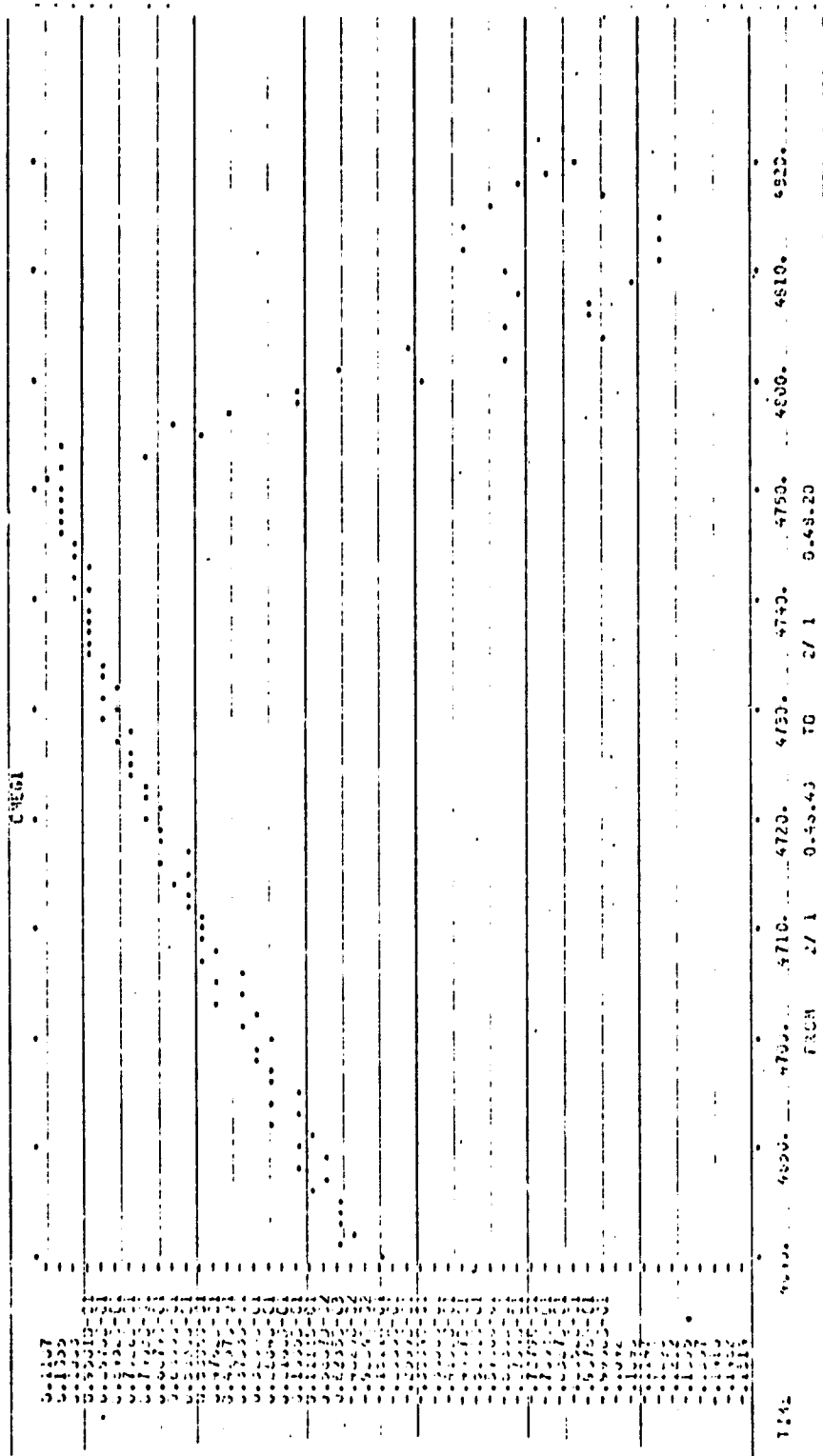


Figure 4-7. ω_x as a Function of Time During PRESUN Burn #2 (2 of 3)

o/s

PRELIMINARY DRAFT

ORIGINAL PAGE IS
OF POOR QUALITY

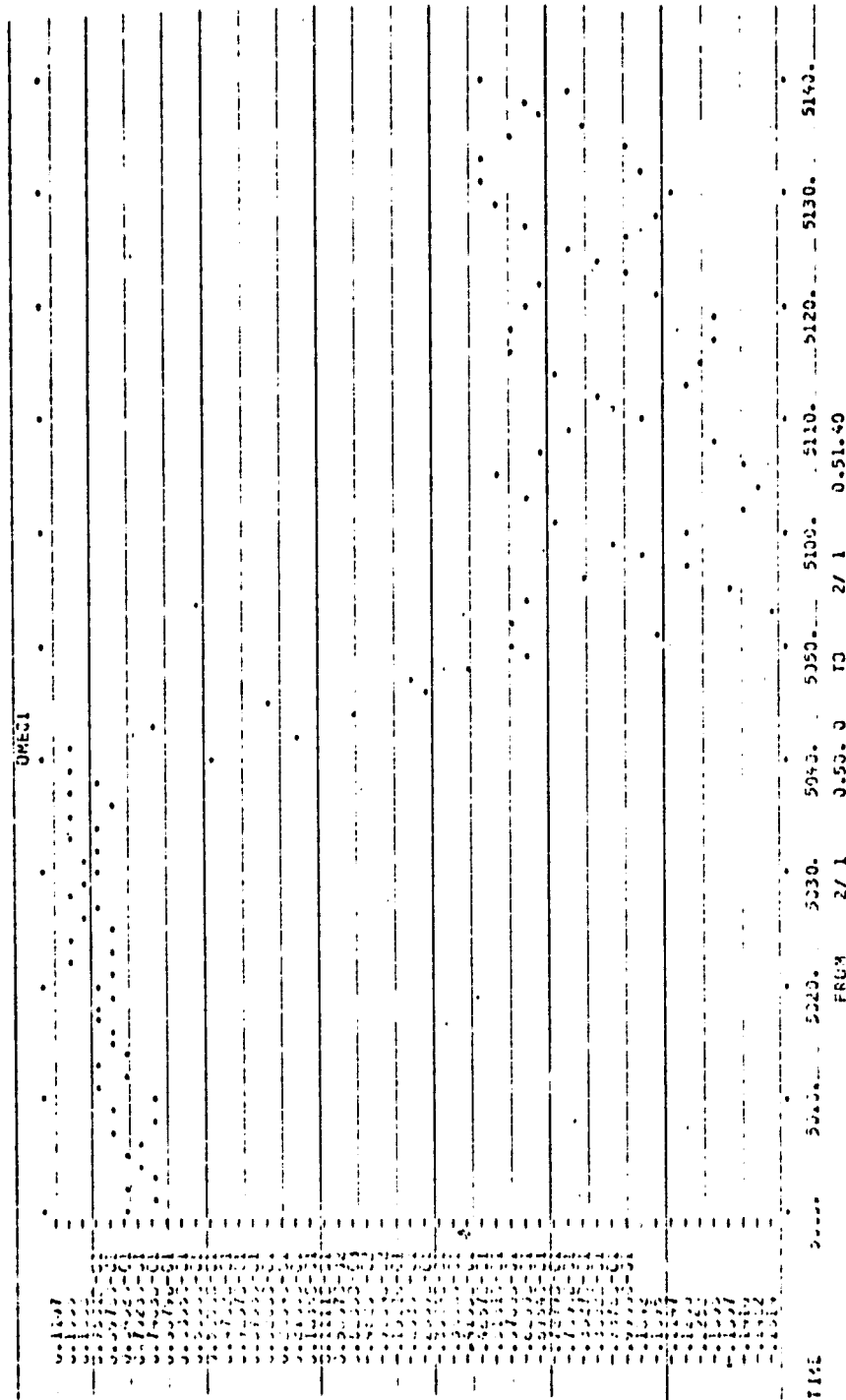
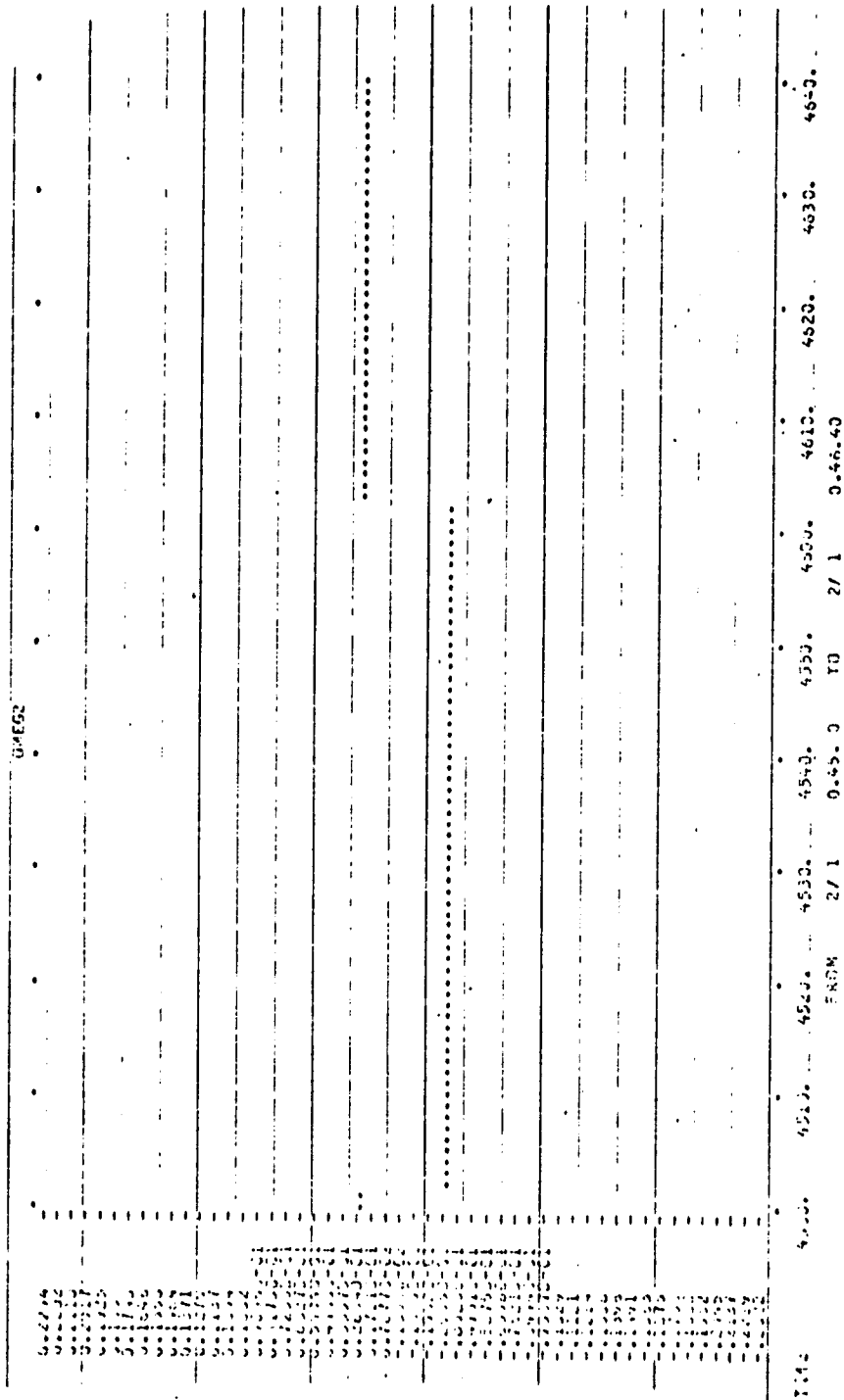


Figure 4-7. ω_x as a Function of Time During PRESUN Burn #3 (3 of 3)

o/s

PRELIMINARY DRAFT

ORIGINAL. PAGE 19
OF POOR QUALITY



PRELIMINARY DRAFT

ORIGINAL PAGE IS
OF POOR QUALITY

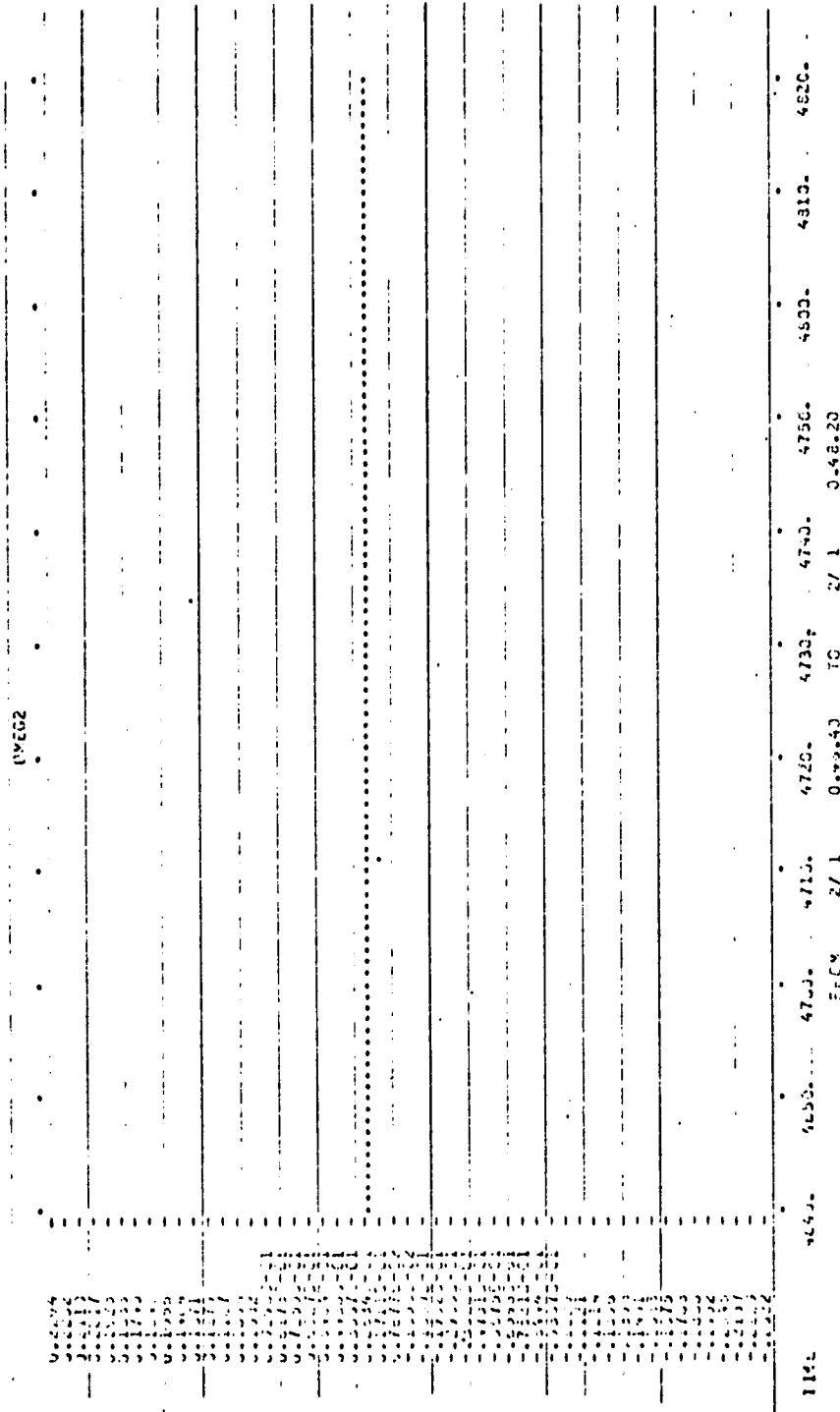


Figure 4-8. ω_y as a Function of Time During PRESUN Burn #2 (2 of 3)

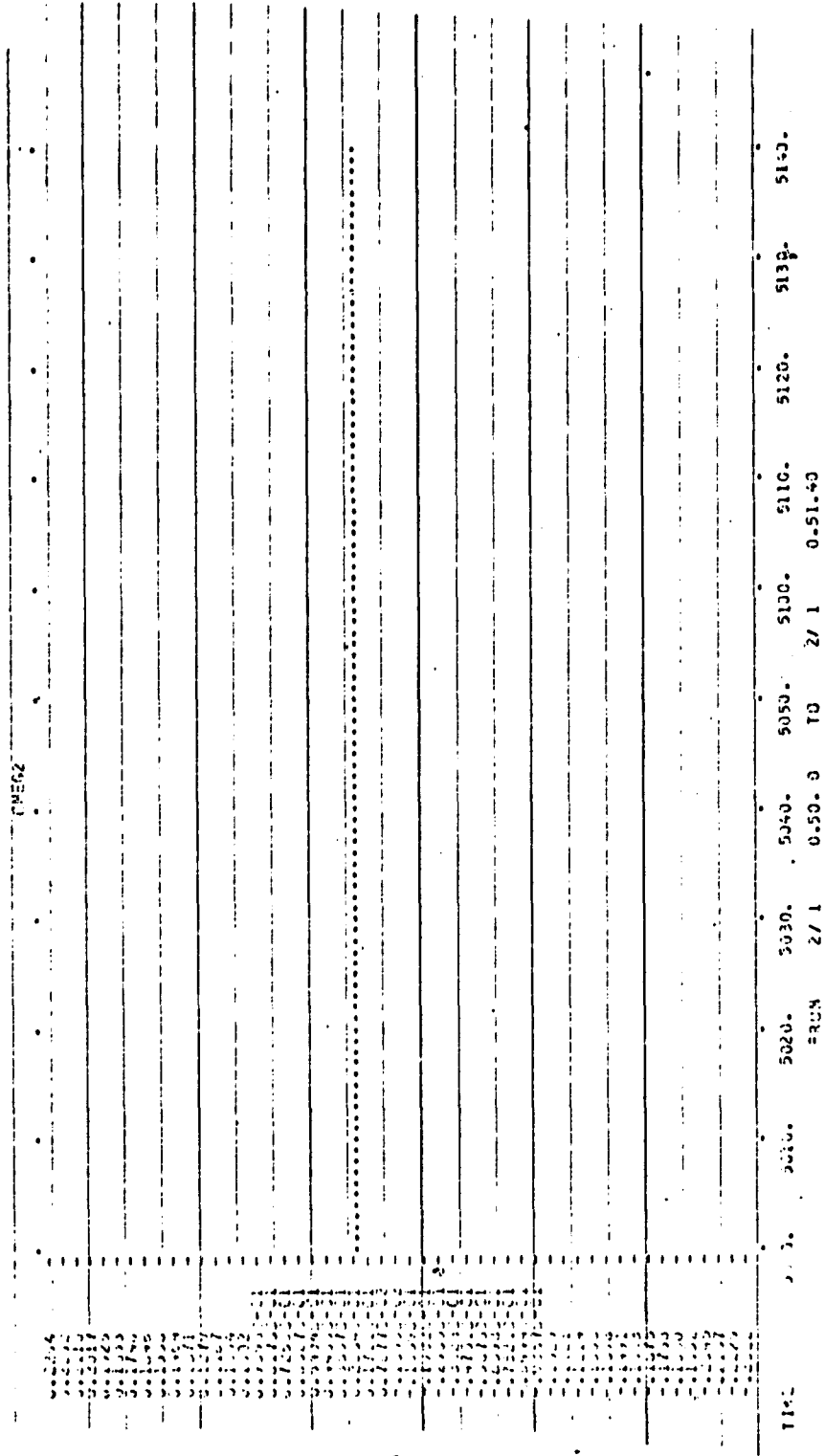


Figure 4-8. ω_y as a Function of Time During PRESUN Burn #3 (3 of 3)

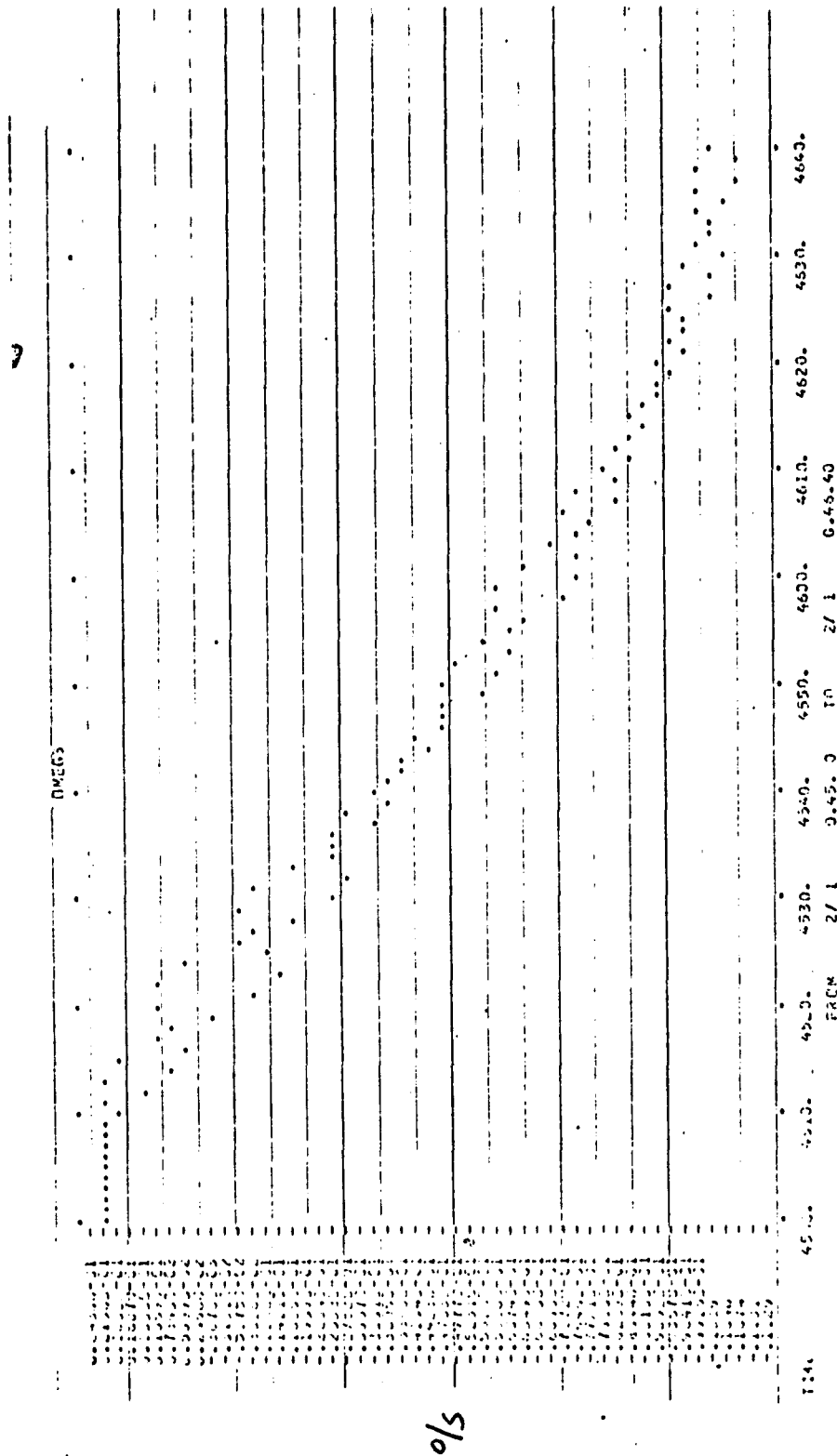


Figure 4-9. ω_z as a Function of Time During PRESUN Burn #1 (1 of 3)

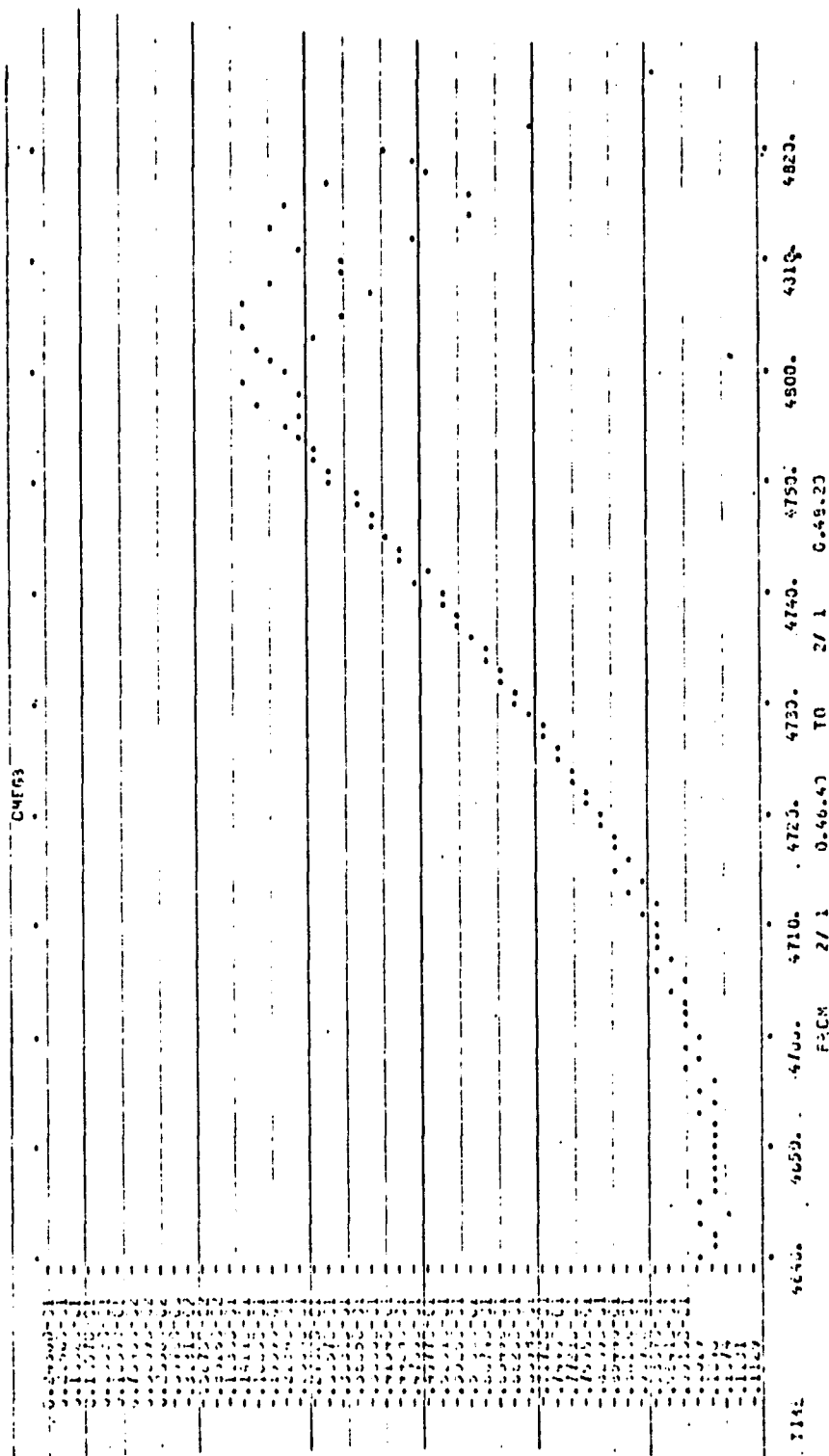


Figure 4-9. ω_z as a Function of Time During PRESUN Burn #2 (2 of 3)

PRELIMINARY DRAFT

ORIGINAL PAGE 19
OF POOR QUALITY.

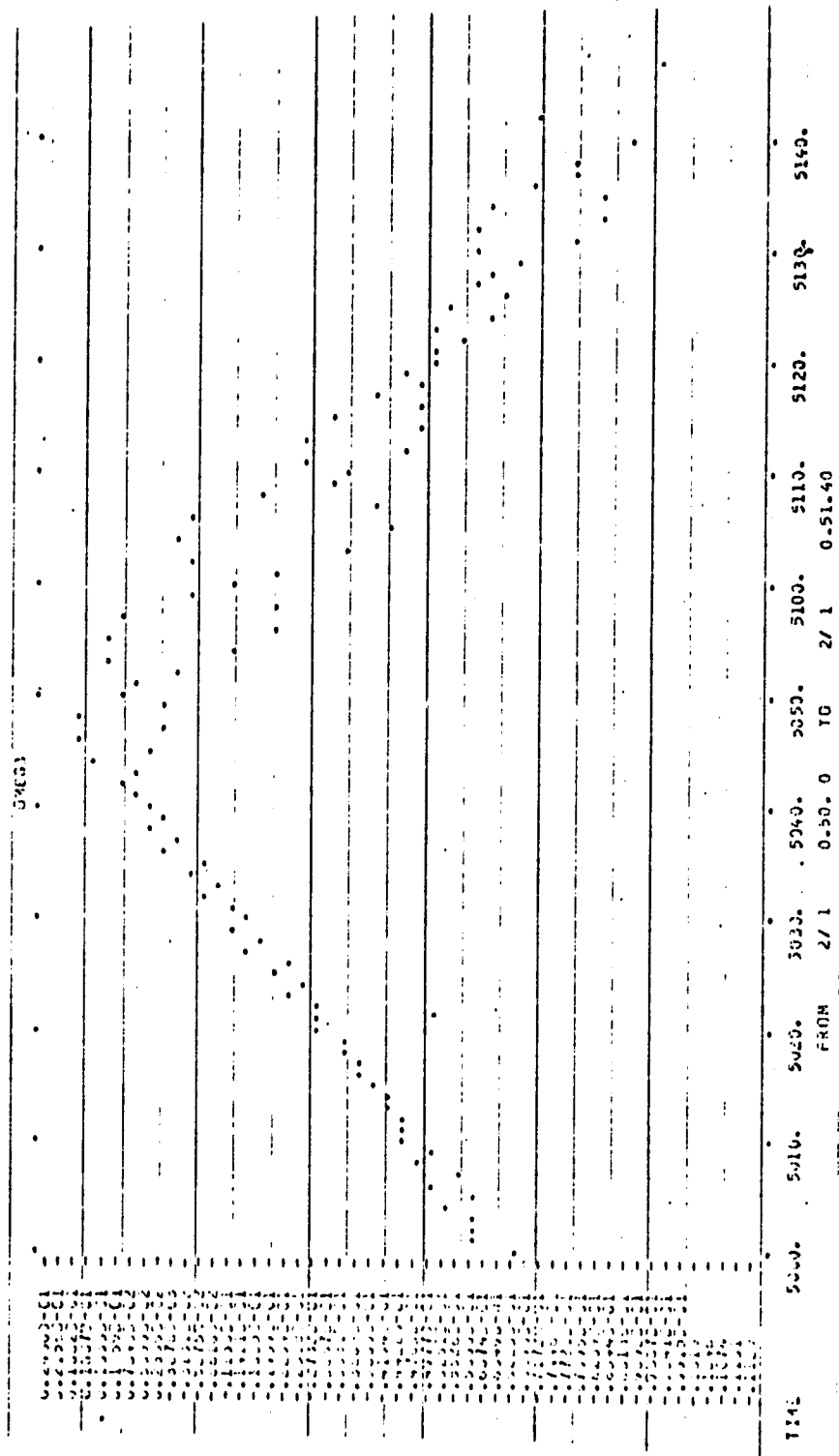


Figure 4-9. ω_z as a Function of Time During PRESUN Burn #3 (3 of 3)

PRELIMINARY DRAFT

ORIGINAL PAGE IS
OF POOR QUALITY

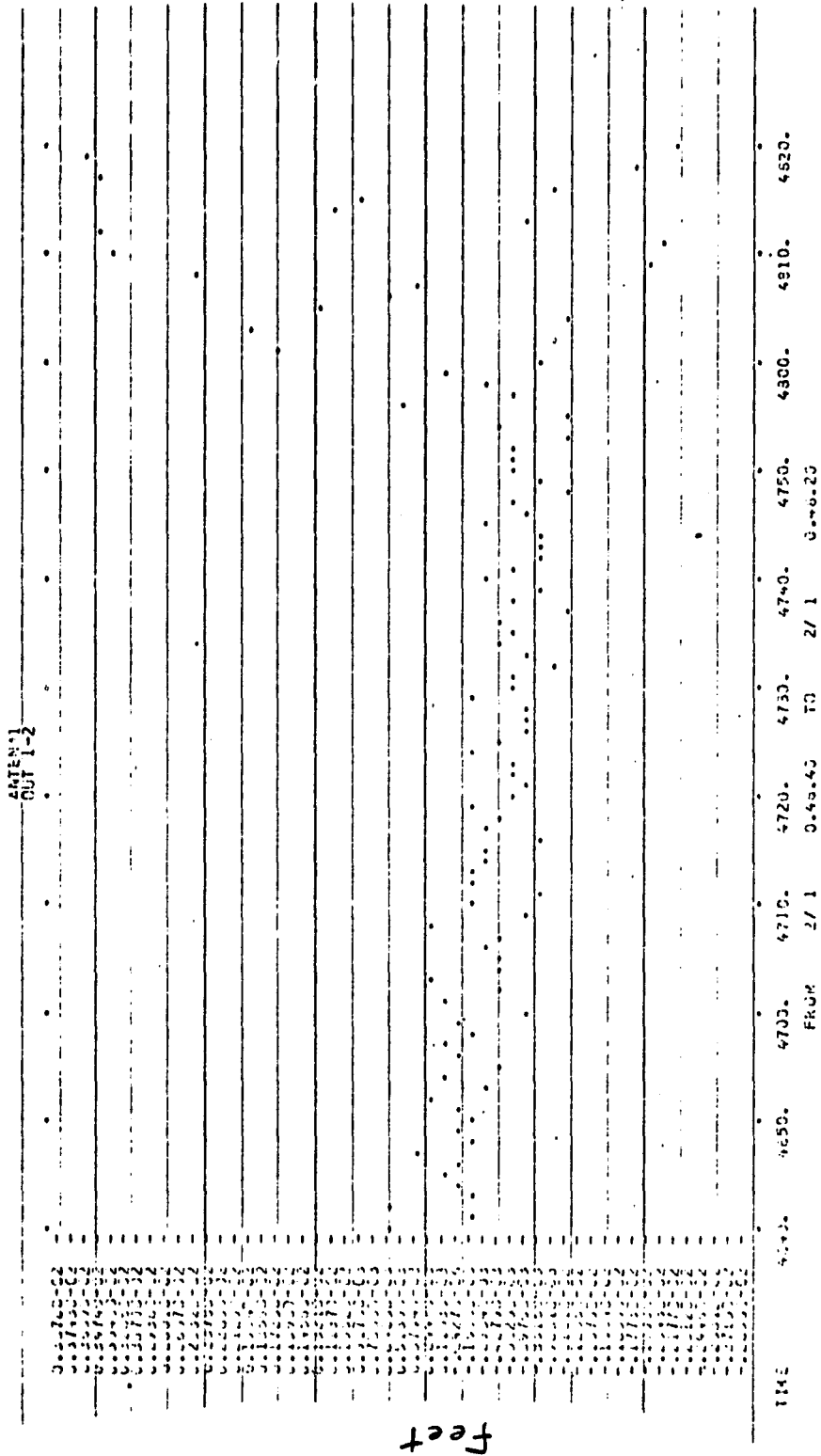


Figure 4-10. Out-of-Plane Deflection of Solar Array #1 (23.79 Feet)
During PRESUN Burn #2 (2 of 3)

**ORIGINAL PAGE IS
OF POOR QUALITY**

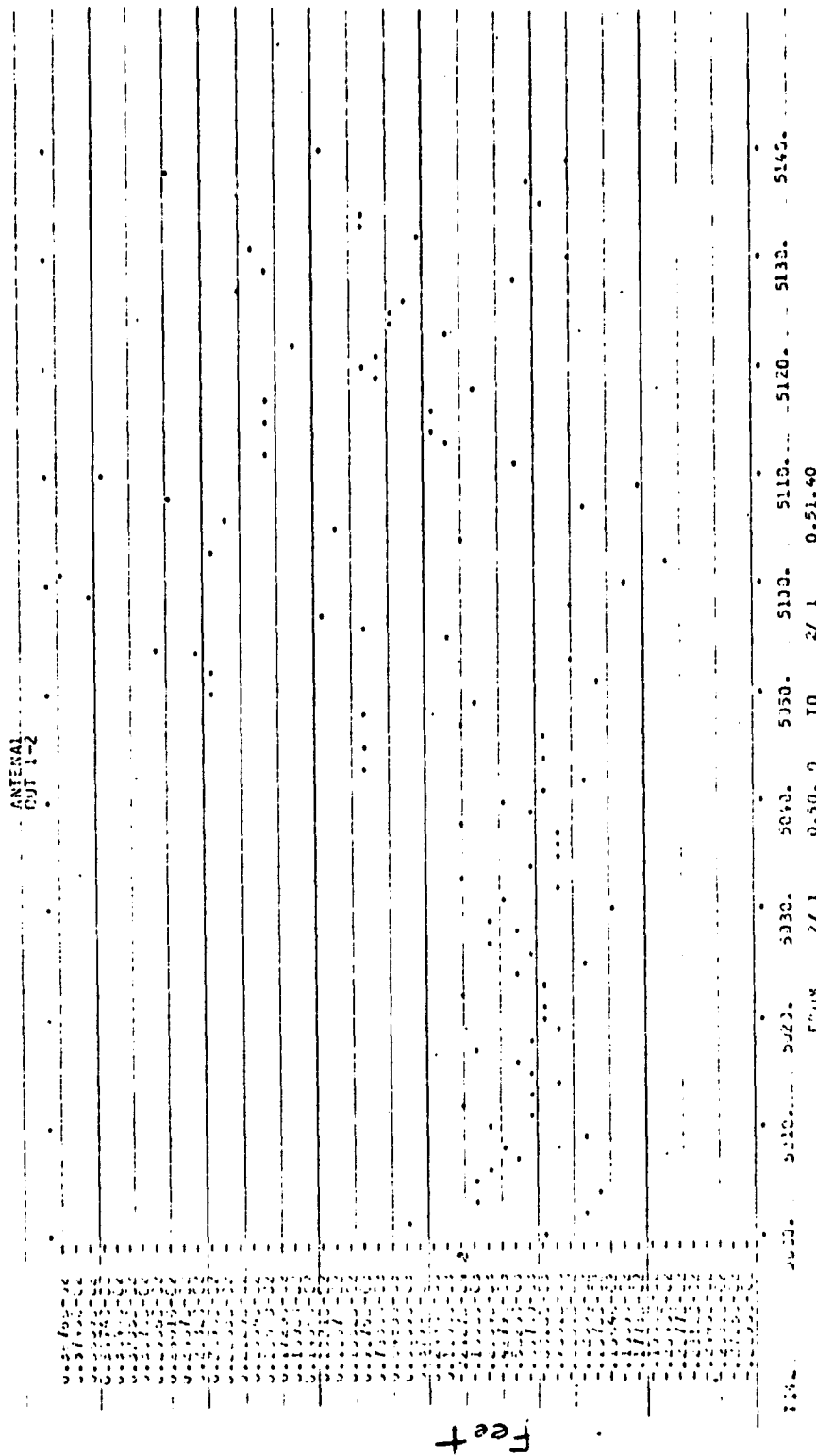


Figure 4-10. Out-of-Plane Deflection of Solar Array #1 (23.79 Feet) During PRESUN Burn #3 (3 of 3)

PRELIMINARY DRAFT

ORIGINAL PAGE 19
OF POOR QUALITY

ANTENNA
IN 1-3

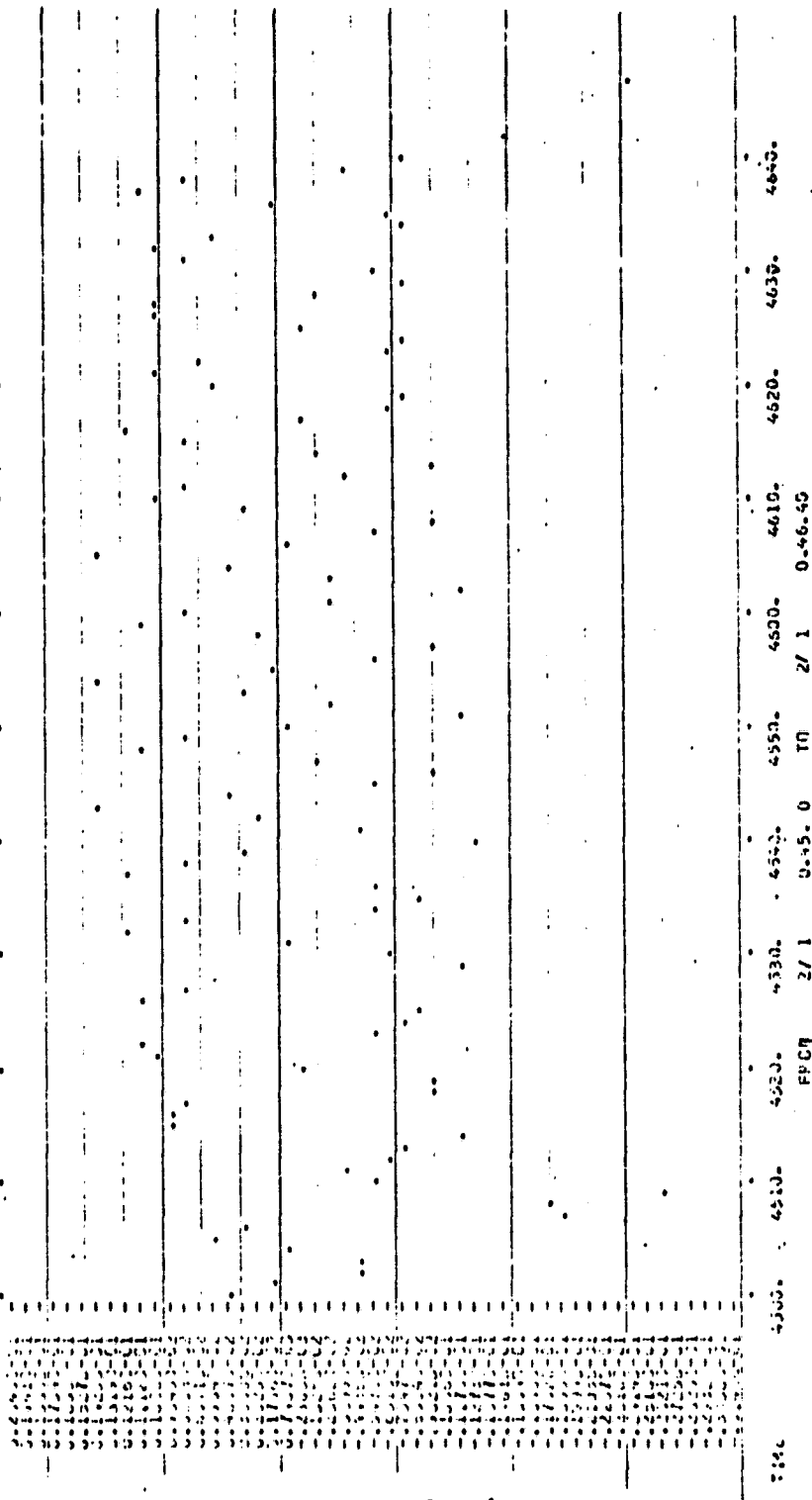


Figure 4-11. In-Plane Deflection of Solar Array #1 (23.79 Feet) During PRESUN Burn #1 (1 of 3)

ORIGINAL PAGE IS
OF POOR QUALITY

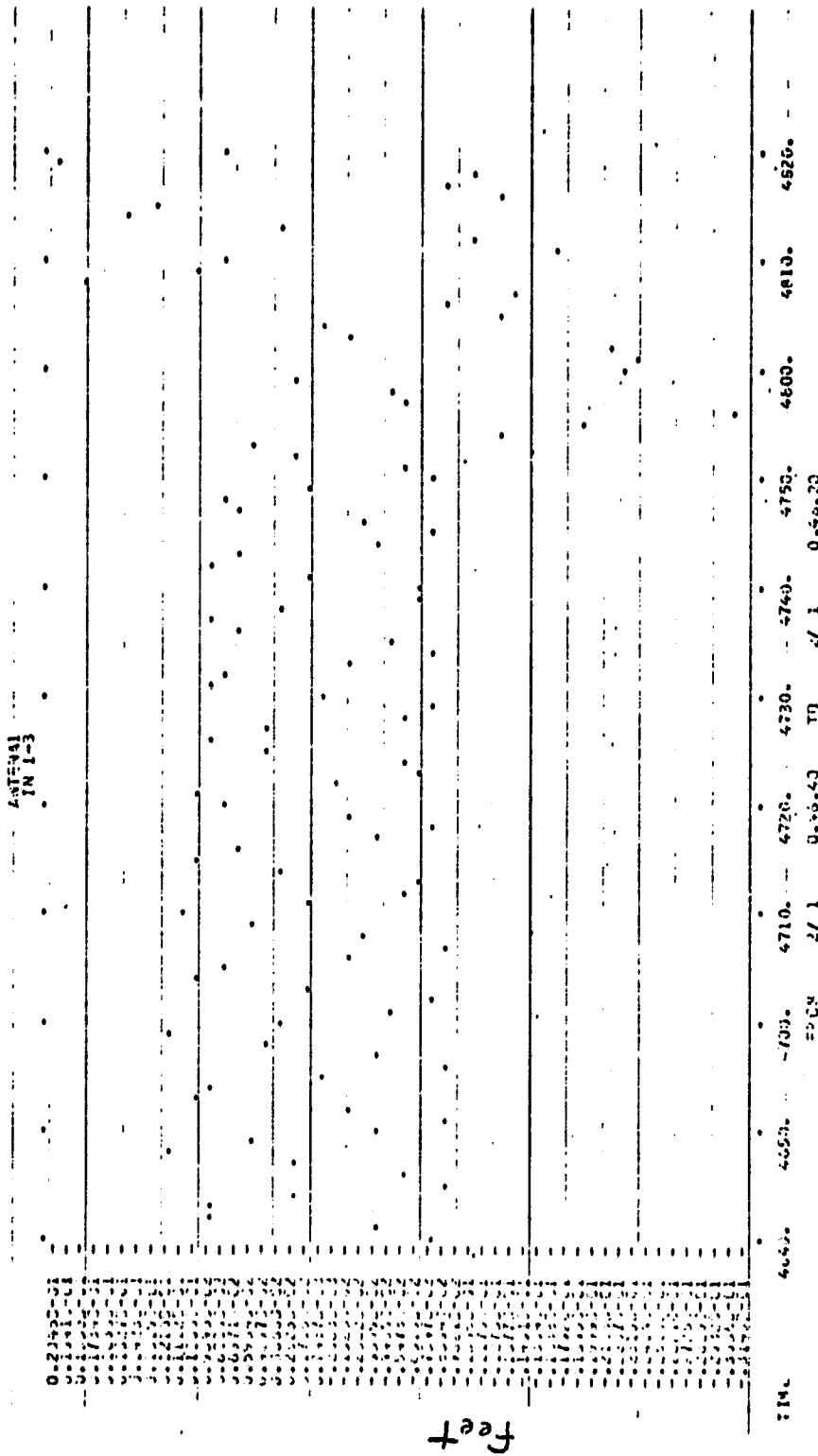


Figure 4-11. In-Plane Deflection of Solar Array #1 (23.79 Feet) During PRESUN Burn #2 (2 of 3)

PRELIMINARY DRAFT

ORIGINAL PAGE IS
OF POOR QUALITY

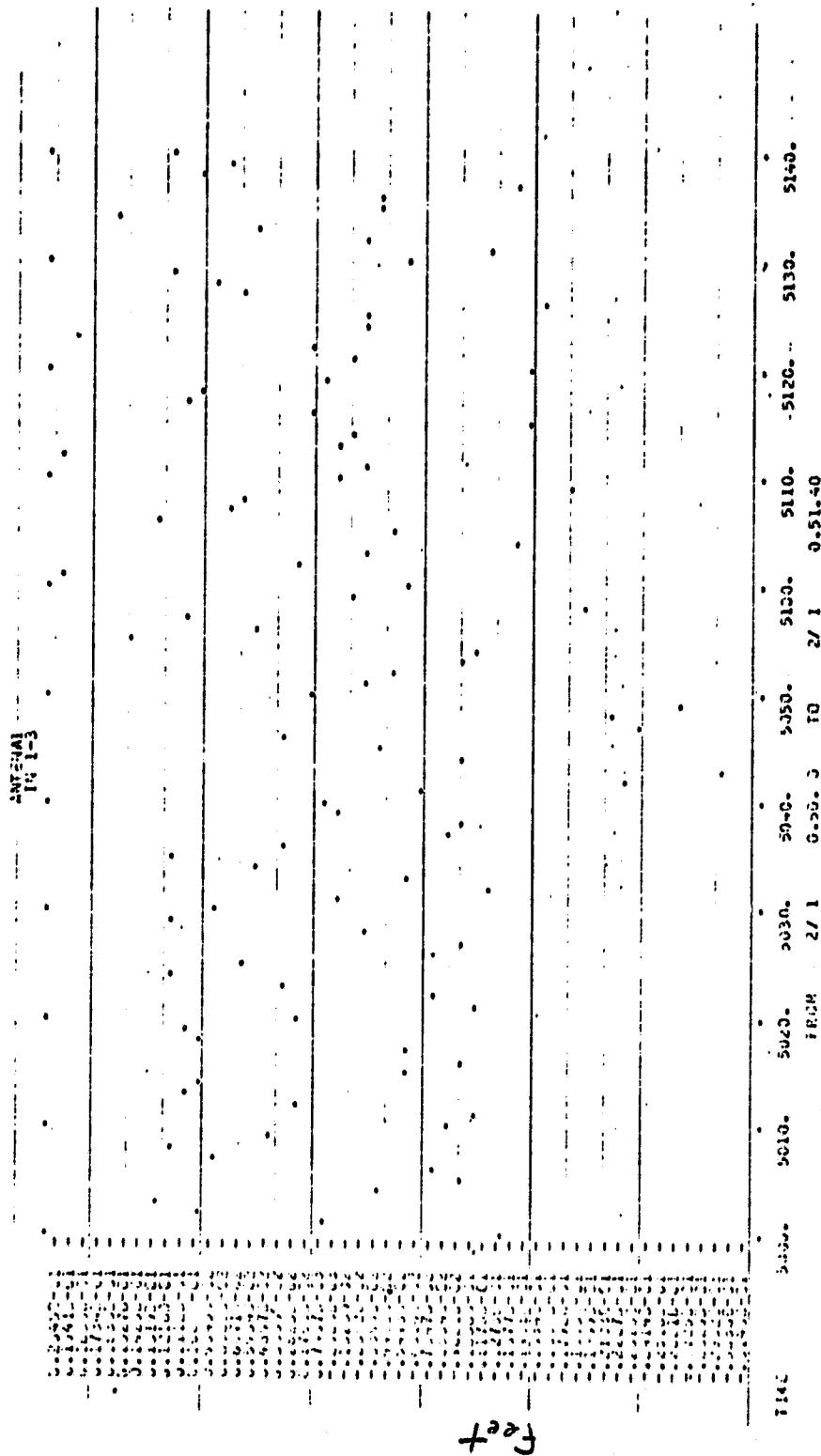


Figure 4-11. In-Plane Deflection of Solar Array #1 (23.79 Feet) During PRESUN Burn #3 (3 of 3)

PRELIMINARY DRAFT

ORIGINAL PAGE 19
OF POOR QUALITY

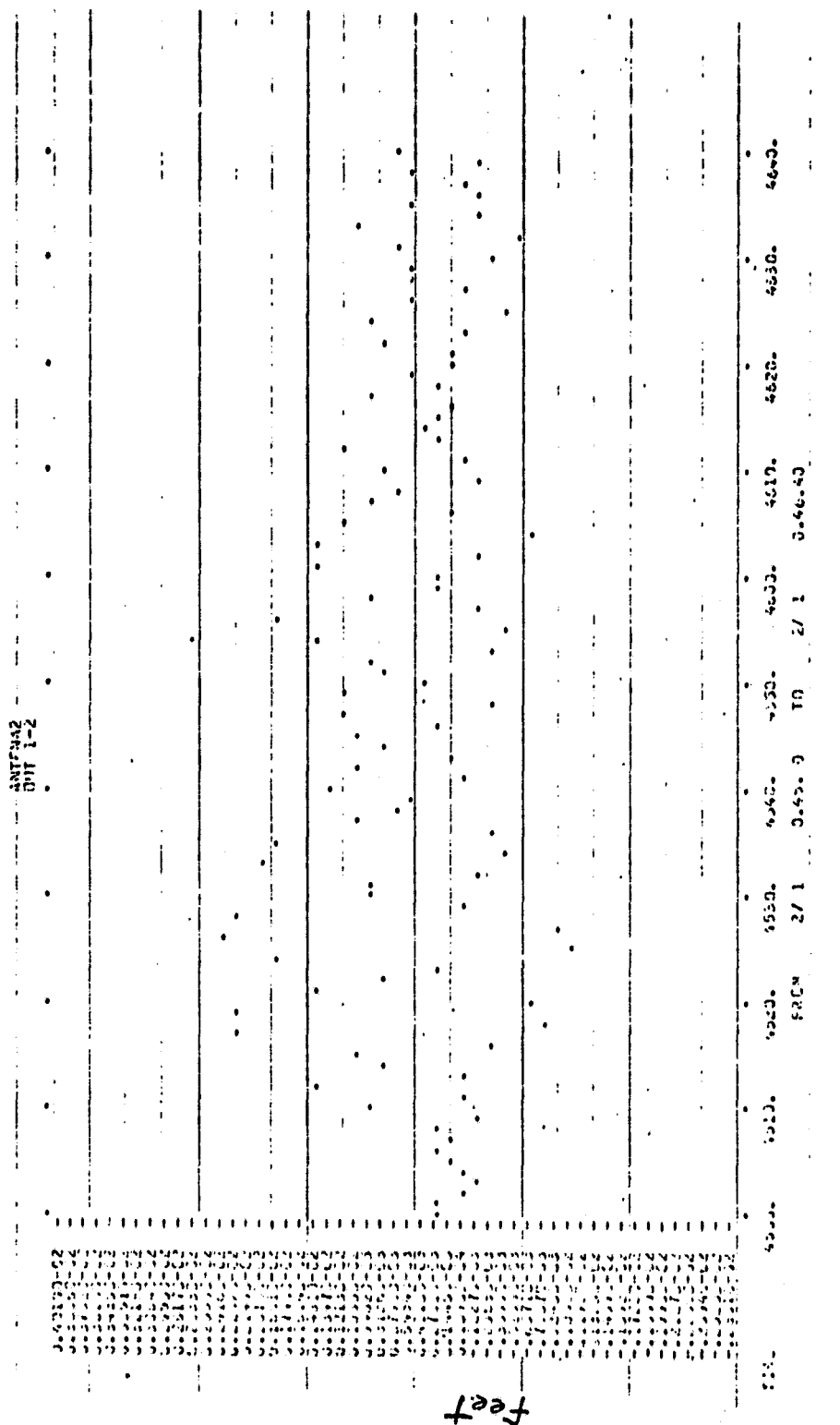


Figure 4-12. Out-of-Plane Deflection of Solar Array #2 (22.79 Feet)
During PRESUN Burn #1 (1 of 3)

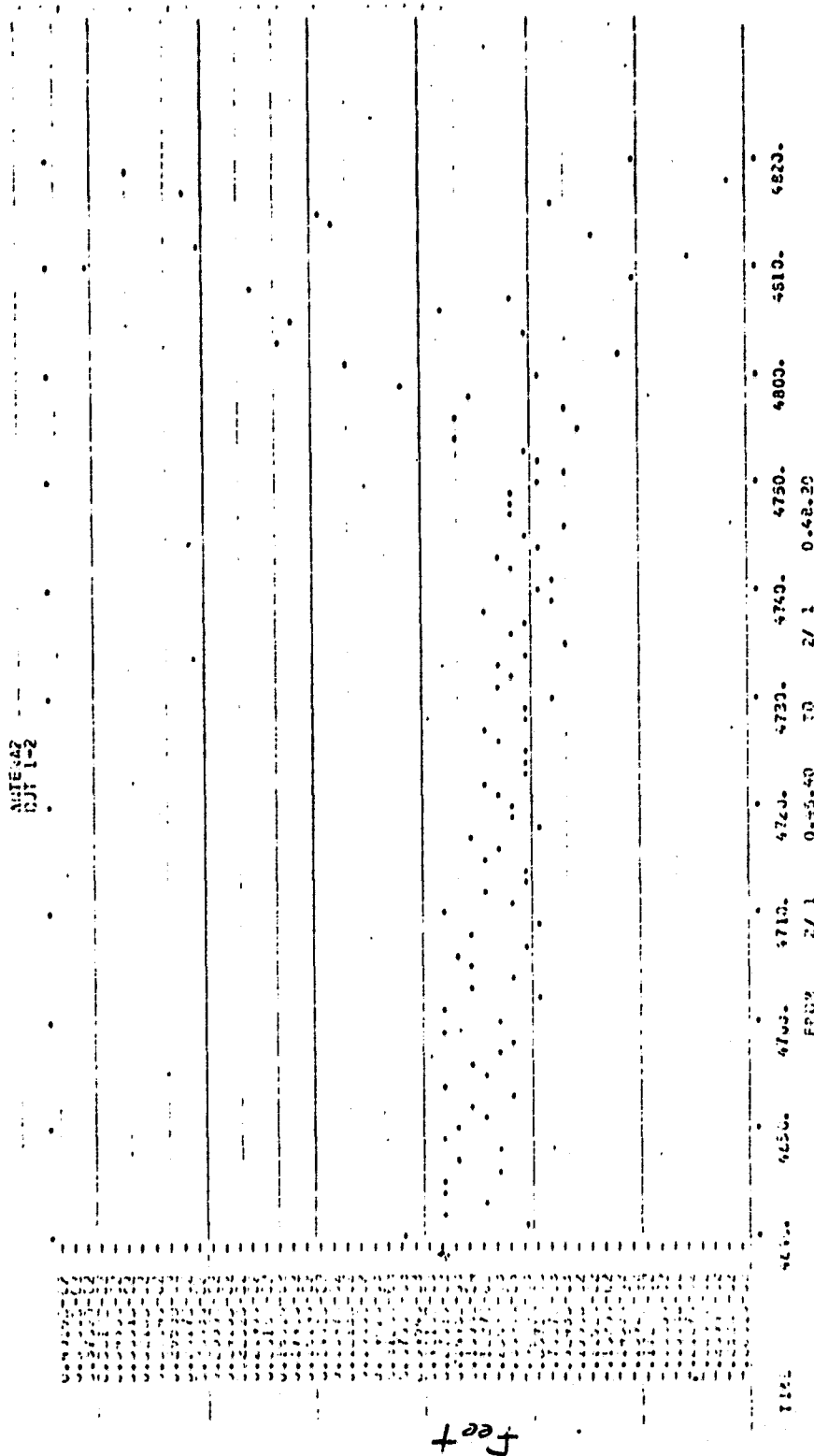


Figure 4-12. Out-of-Plane Deflection of Solar Array #2 (22.79 Feet)
During PRESUN Burn #2 (2 of 3)

PRELIMINARY DRAFT

ORIGINAL PAGE IS
OF POOR QUALITY

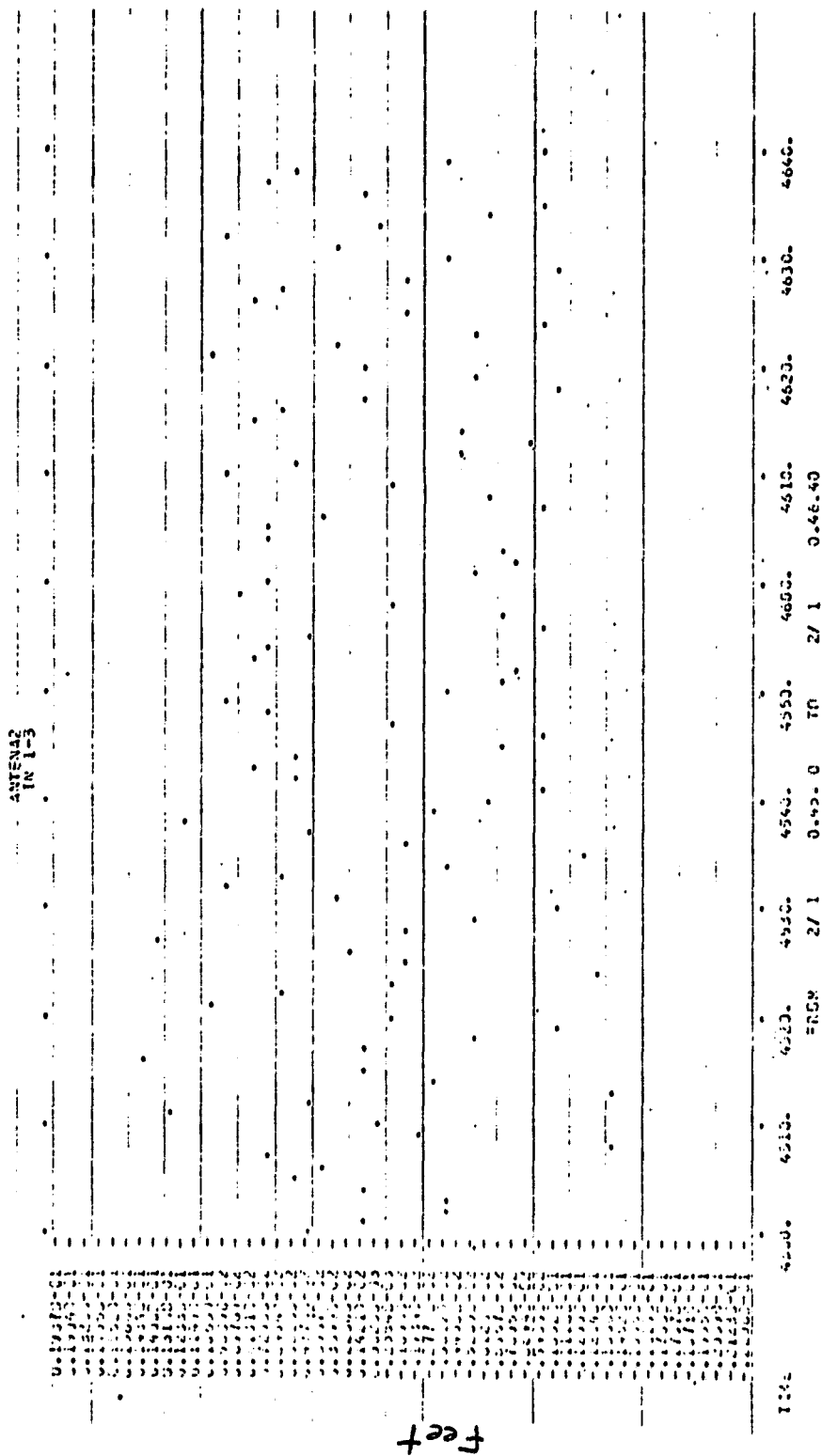


Figure 4-13. In-Plane Deflection of Solar Array #2 (22.79 Feet) During PRESUN Burn #1 (1 of 3)

PRELIMINARY DRAFT

ORIGINAL PAGE IS
OF POOR QUALITY

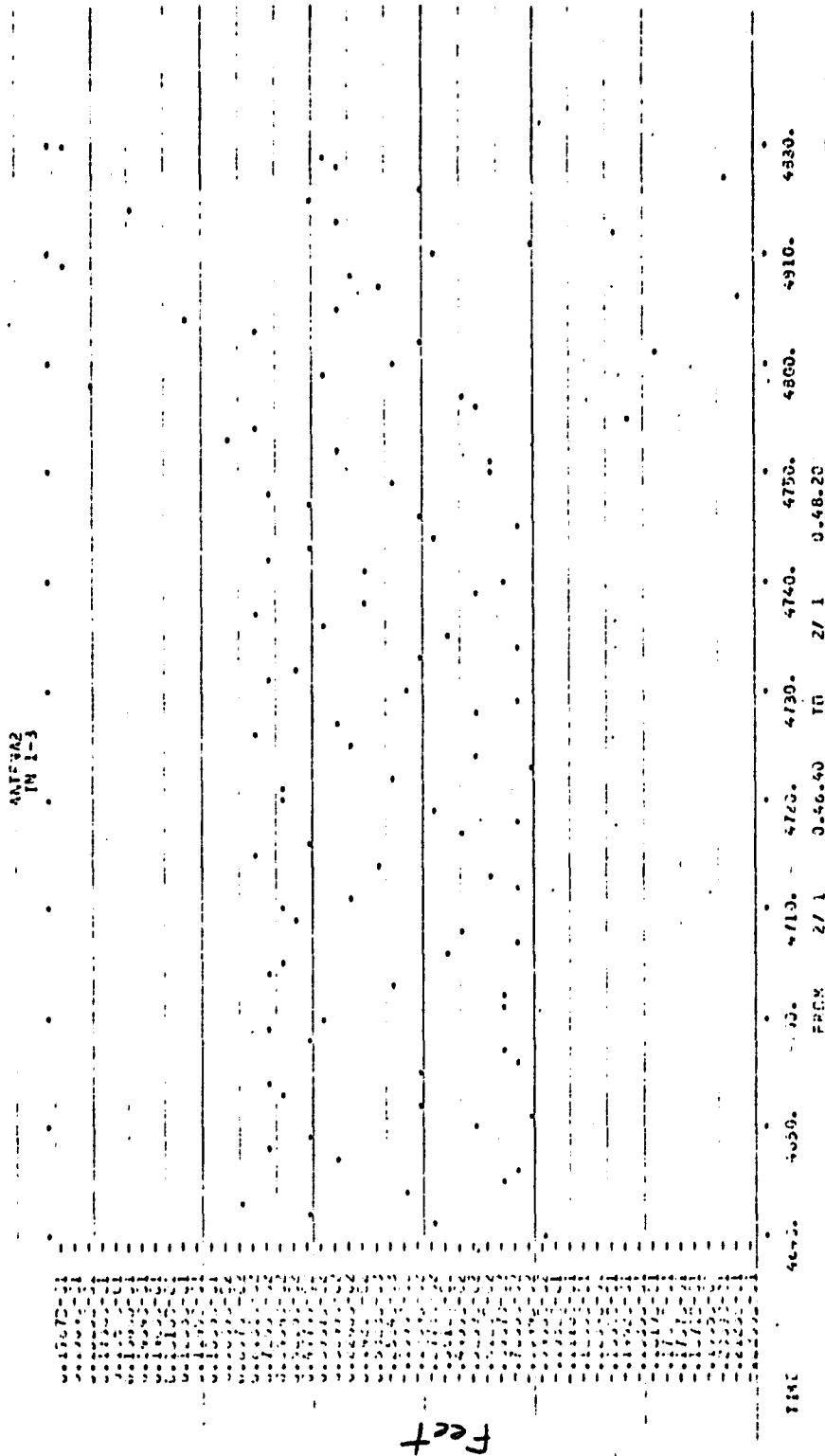


Figure 4-13. In-Plane Deflection of Solar Array #2 (22.79 Feet)
During PRESUN Burn #2 (2 of 3)

PRELIMINARY DRAFT

ORIGINAL PAGE 18
OF POOR QUALITY

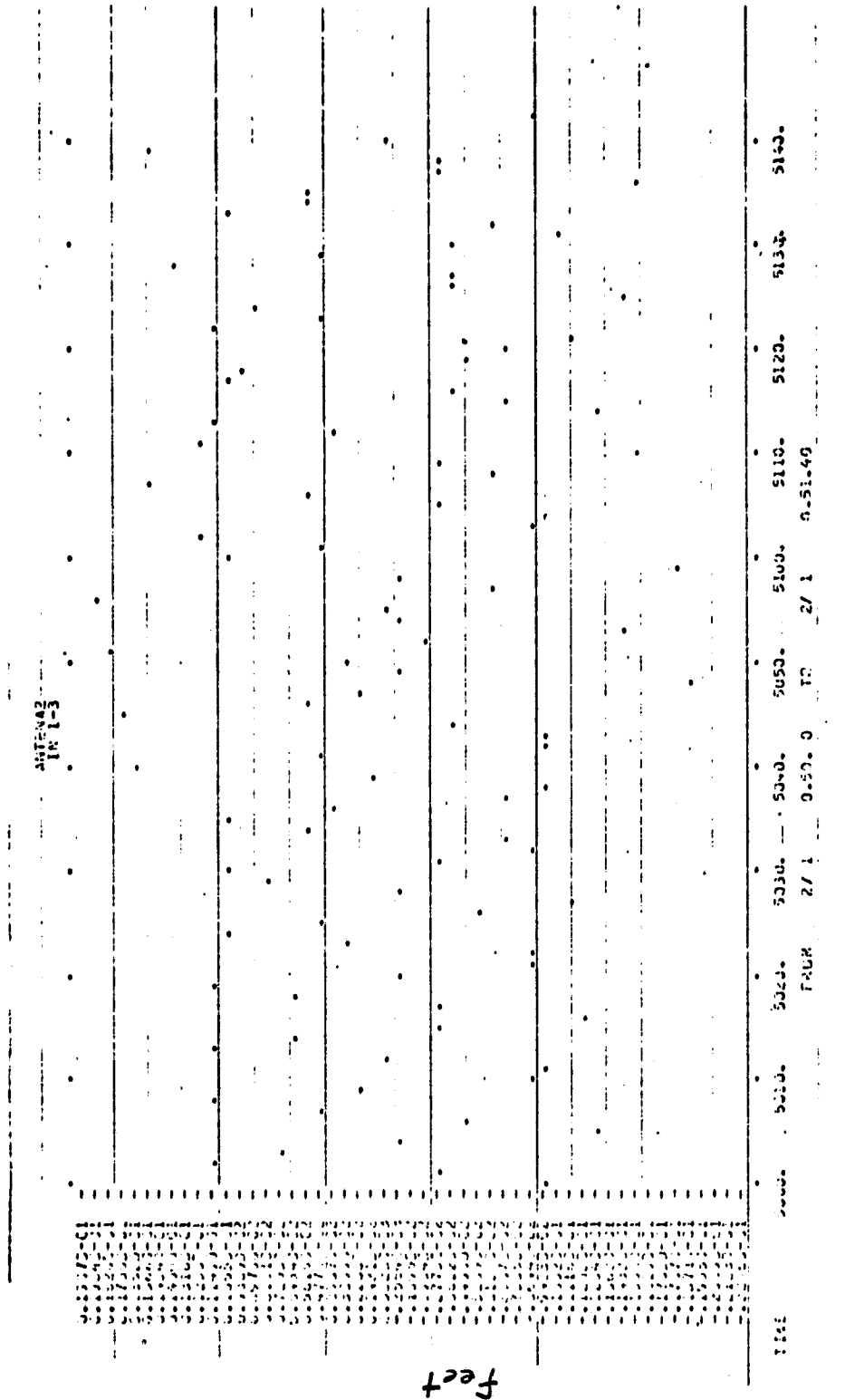


Figure 4-13. In-Plane Deflection of Solar Array #2 (22.79 Feet)
During PRESUN Burn #3 (3 of 3)

PRELIMINARY DRAFT

ORIGINAL PAGE IS
OF POOR QUALITY

Table 4-27. PRESUN Burn Parameters

	<u>Time of Initialization (Min:Sec)</u>	<u>Torque (Foot-lb)</u>	<u>Duration (Sec)</u>
PRESUN Burn #1	45:04	-0.227959	6.259
#2	47:52	-0.227959	12.531
#3	50:39	-0.227959	12.531

4.4.3 Failure Mode

A series of simulations was performed to determine how well the δ -Controller could maintain attitude should one solar array not be deployed properly. To achieve this, the wheel was commanded to spinup to full speed, but the torque given the spacecraft by the wheel was manually set to zero. Consequently, the δ -Controller attempted to maintain attitude during what it thought was wheel spinup (approximately one-half hour). After the wheel should have been at full speed, the δ -Controller was deactivated, so the spacecraft drifted in response to environmental torques. It was hence possible to compare the spacecraft's motion with and without δ -Controller commands. The solar array lengths were 23.79 feet and 1.0 foot. The principal moments of inertia were:

$$I_{xx} = 458.2 \text{ slug-ft}^2$$

$$I_{yy} = 69.0 \text{ slug-ft}^2$$

$$I_{zz} = 478.6 \text{ slug-ft}^2$$

During the "spinup" period (δ -Controller active) the spacecraft motion was as illustrated in Table 4-28.

Control was satisfactory, 17 α burns and 21 δ burns were issued in a 16 minute period with total durations of 23 seconds and 49 seconds respectively. The δ controller was deactivated and a 66 degree drift was observed in 14 minutes. The maximum deviation from the nominal Sun angle was about 3.5 degrees.

PRELIMINARY DRAFT

ORIGINAL PAGE 19
OF POOR QUALITY

Table 4-28. Spacecraft Motion With One Array at 23.79 Feet and One Array at 1.0 Foot, With Active δ -Controller During One-Half Hour

ϕ : 202.3 $^{\circ}$ to 268.7 $^{\circ}$
 θ : 80.6 $^{\circ}$ to 115.4 $^{\circ}$
 ψ : 270.00 $^{\circ}$ to 270.03 $^{\circ}$
 ω_x : -0.05 $^{\circ}$ /sec to 0.16 $^{\circ}$ /sec
 ω_y : -0.28 $^{\circ}$ /sec to 0.29 $^{\circ}$ /sec
 ω_z : 0.05 $^{\circ}$ /sec to 0.11 $^{\circ}$ /sec

Number of α -Controller Burns: 30

Number of δ -Controller Burns: 21

Maximum Sun Angle: 3.5 $^{\circ}$

PRELIMINARY DRAFT

APPENDIX A - DOP SUMMARY

This appendix contains a summary of the DOP. The material is taken verbatim from Reference 2.

ORIGINAL PAGE IS
OF POOR QUALITY

^{2.4} PRELIMINARY DRAFT

ORIGINAL PAGE IS
OF POOR QUALITY

2.2 First Day Activities

The operations to be conducted on Day 1 can be broken into five basic groups as follows (in chronological sequence):

- Configuration of both the spacecraft and ground station in preparation for despin (Events A1 to A9)
- Despin of the spacecraft from 60 rpm down to 2 rpm (Event A10)
- Active damping of any resulting spacecraft nutation (Event A11)
- Configuration of both the spacecraft and ground station in preparation for battery recharging (Event A12)
- Battery recharge and drift when waiting for Day 2 to start (Events A13, A14)

These activities are not orbit slot dependent. However, these activities are scheduled at the 90° orbit slot to:

- allow adequate time for battery recharge prior to commencing Day 2 activities
- provide an adequate rest time for the operations team prior to Day 2
- provide the optimum 3-axis attitude sensing since \bar{S} (line of sight from the spacecraft to the sun) and \bar{E} (line of sight from the spacecraft to the centre of the earth) are approximately at right angles to each other.

PRELIMINARY DRAFT

ORIGINAL PAGE 13
OF POOR QUALITY

To help illustrate the basic manoeuvre sequence, a series of summary level diagrams will be used throughout Sections 2.2 and 2.3.

The symbolic spacecraft which is used throughout these sketches is shown in Figure 2.2.1. (NOTE: It is assumed for purposes of the DOP development, that there is a region of $\pm 50^\circ$ away from the Negative Yaw (-Z) axis where "no telemetry" is available due to the gap in the belt antenna pattern. This is noted in Figure 2.2.1).

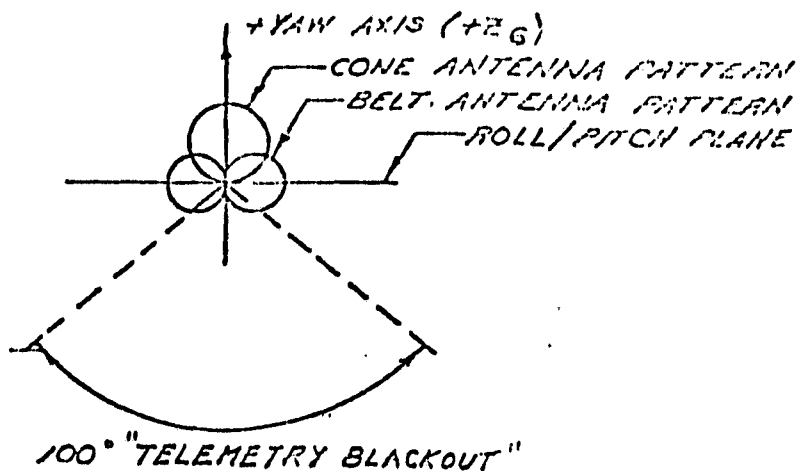
The First Day activities are illustrated in Figure 2.2.2.

VIEW ON FORWARD PLATFORM
END (ALONG POSITIVE YAW.)

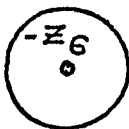


ORIGINAL PAGE 19
OF POOR QUALITY

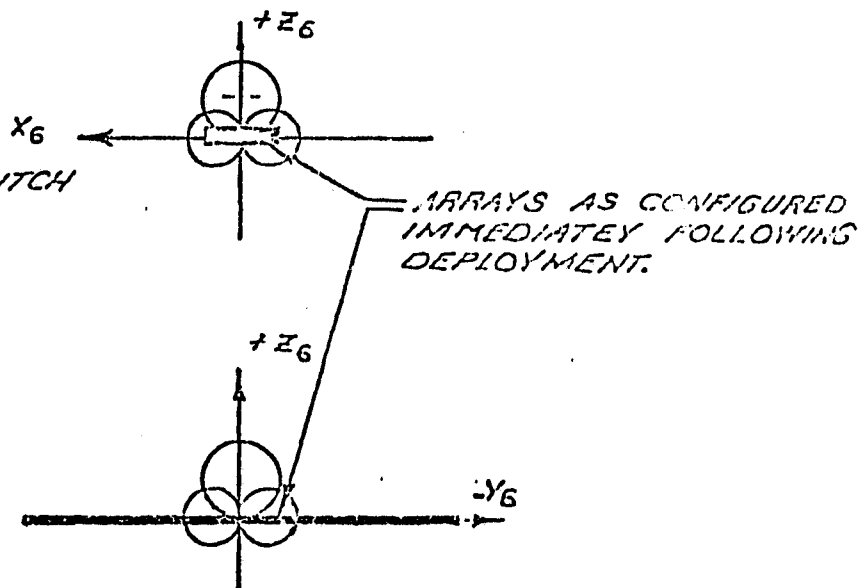
SIDE VIEW (STOWED)



VIEW ON APOGEE MOTOR
NOZZLE END (ALONG
NEGATIVE YAW).



SIDE VIEW ALONG PITCH
AXIS (DEPLOYED).



ALONG ROLL AXIS

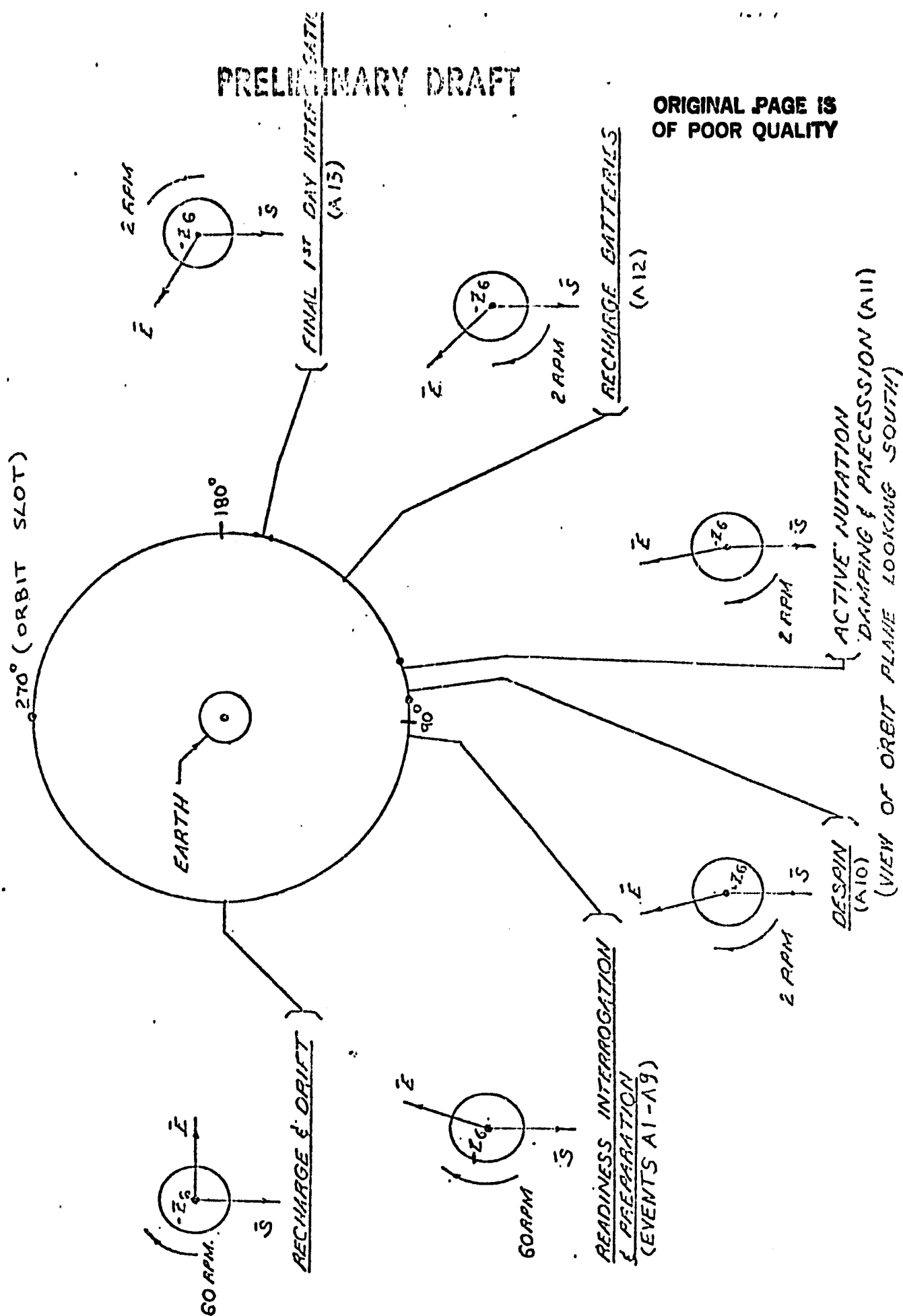
FIGURE 2.2.1

FIGURE 2.2.2

FIRST DAY ACTIVITIES

PRELIMINARY DRAFT

ORIGINAL PAGE IS
OF POOR QUALITY



2.3 Second Day Activities

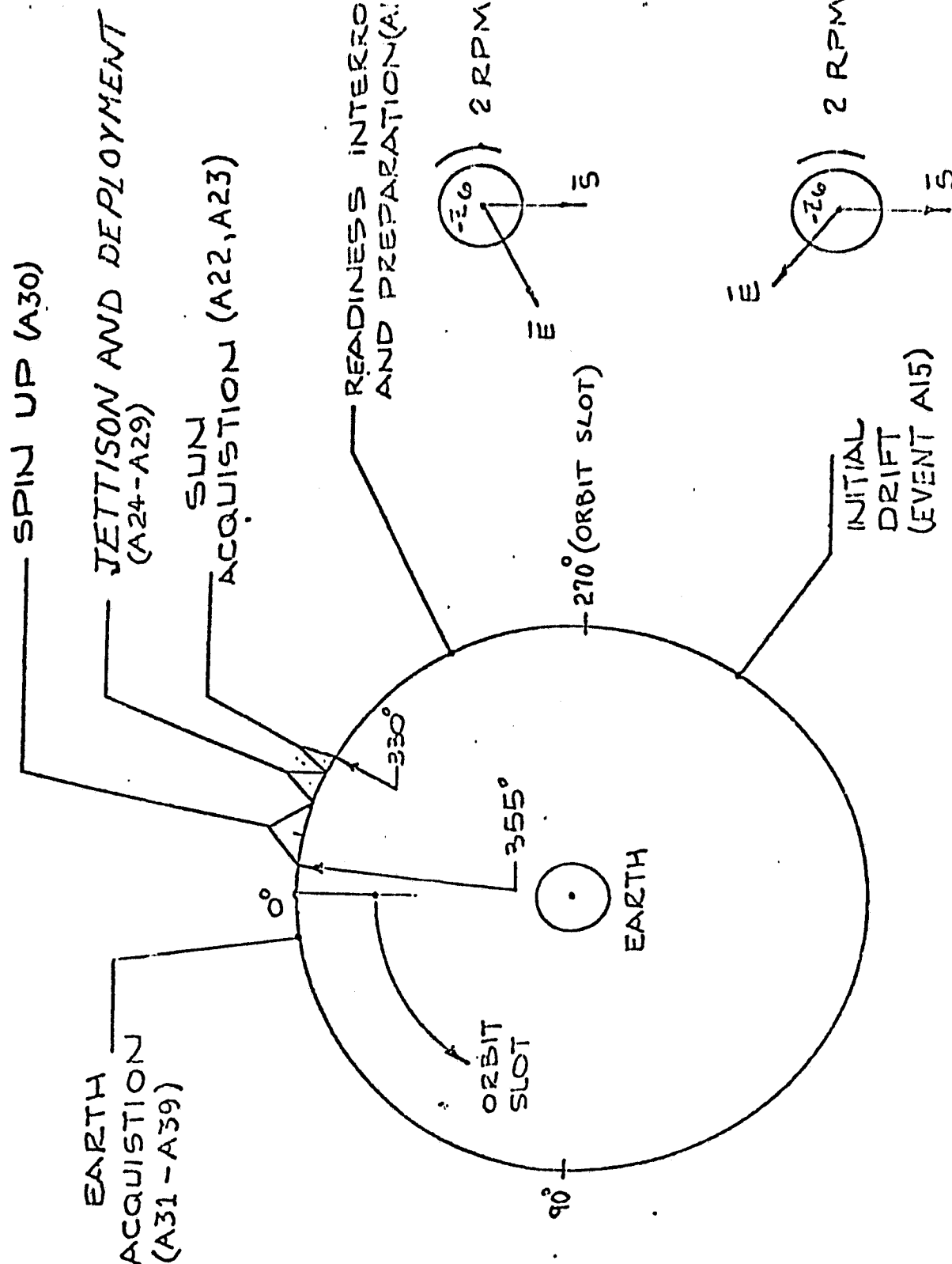
The operations to be conducted on Day 2 can be broken into ten basic groups as follows (in chronological sequence):

- Battery recharge and drift (Events A15, A16)
- Configuration of both the spacecraft and ground station in preparation for the Day 2 manoeuvres (Events A17 to A21)
- Final despin of the spacecraft from 2 rpm to 0 and acquisition of \bar{S} along the negative roll (-X) axis (Event A22)
- Acquisition of \bar{S} along the positive yaw (+Z) axis (Event A23)
- Jettison of the JBSA and deployment and checkout of the DSA (Events A24 to A26)
- Activation of thermal control heaters and configuration of spacecraft to allow battery recharge (Events A27 to A29)
- Spin-up of the momentum wheel (Event 30)
- Acquisition of \bar{E} along the positive yaw (+Z) axis with the spacecraft approximately in its required on-orbit operational attitude (Events A31 to A35)
- Final acquisition of the required on-orbit attitude and activation of on-board attitude control system (Events A36, A37)
- Configuration of spacecraft and ground station for initial on-orbit operations and transfer of control to On-orbit Flight Operations team (Events A38, A39),

The key Day 2 activities are specifically discussed in the following sub-sections. (shown also in Figure 2.3.1).

PRELIMINARY DRAFT

ORIGINAL PAGE 13
OF POOR QUALITY



(VIEW OF ORBIT PLANE LOOKING SOUTH)

FIGURE 2.3.1 SECOND DAY ACTIVITIES.

PRELIMINARY DRAFT

ORIGINAL PAGE IS
OF POOR QUALITY2.3.1 Final Despin and Sun Acquisition (Events A21 to A23)

This is the first major operation to be performed on Day 2. It consists of the following segments (see Figure 2.3.2):

- The spacecraft will be despun from 2 rpm to nominally zero and the negative roll axis ($-X$) will be aligned with \bar{S} and held there by ground-based software attitude controllers.
- The spacecraft is then to be rotated by -90° about the pitch axis so that the positive yaw axis ($+Z$) is aligned with \bar{S} and held there by ground-based software attitude controllers.

The earliest point in the orbit at which the positive yaw axis will be aligned with \bar{S} is at approximately the 330° orbit slot (varies slightly with sun declination). This point is chosen since it guarantees that the angle between the positive yaw axis and the Ottawa LOS will be $<130^\circ$ (ie: within the guaranteed telemetry/command patterns of the spacecraft antennas) regardless of the orientation of the pitch axis ($+Y$) about \bar{S} .

See Reference 6 for a detailed discussion.

2.3.2 JBSA Jettison and DSA Deployment (Events A24 to A26)

With the positive yaw axis maintained along \bar{S} by the ground-based software attitude controllers, the JBSA will be jettisoned followed directly by deployment of the DSA (see Figure 2.3.3).

PRELIMINARY DRAFT

By deploying the DSA with the sunline of sight normal to the solar cell faces, the following conditions are satisfied (note: deployment is planned to be from a spacecraft with nominally zero body rates):

- The BI-STEM and the back of the blanket will not at any time "see" the sun. Also the blanket should not coll down during deployment.
- There will be power available from the arrays almost immediately upon completion of deployment. This should minimize both the battery drain and the cool-down of the spacecraft subsystem after jettison.
- The control of the spacecraft attitude will be somewhat simplified since a geometric spacecraft axis (+Z) and not some intermediate axis will be maintained along \bar{S} .
- A good telemetry and command link through the conical beam antenna will be assured.

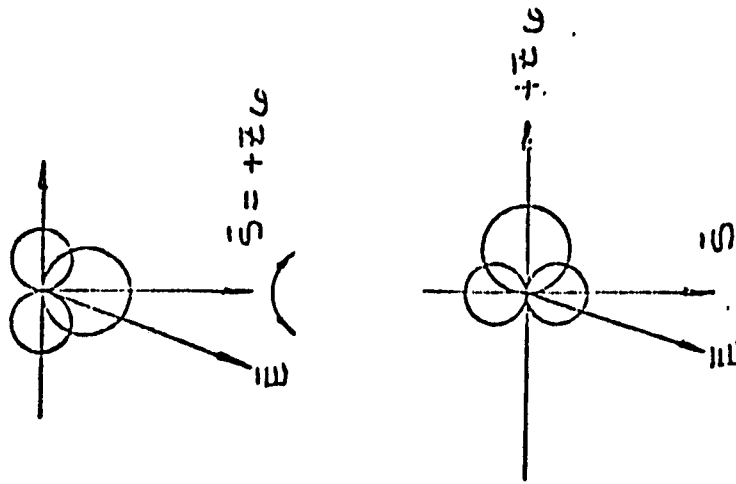
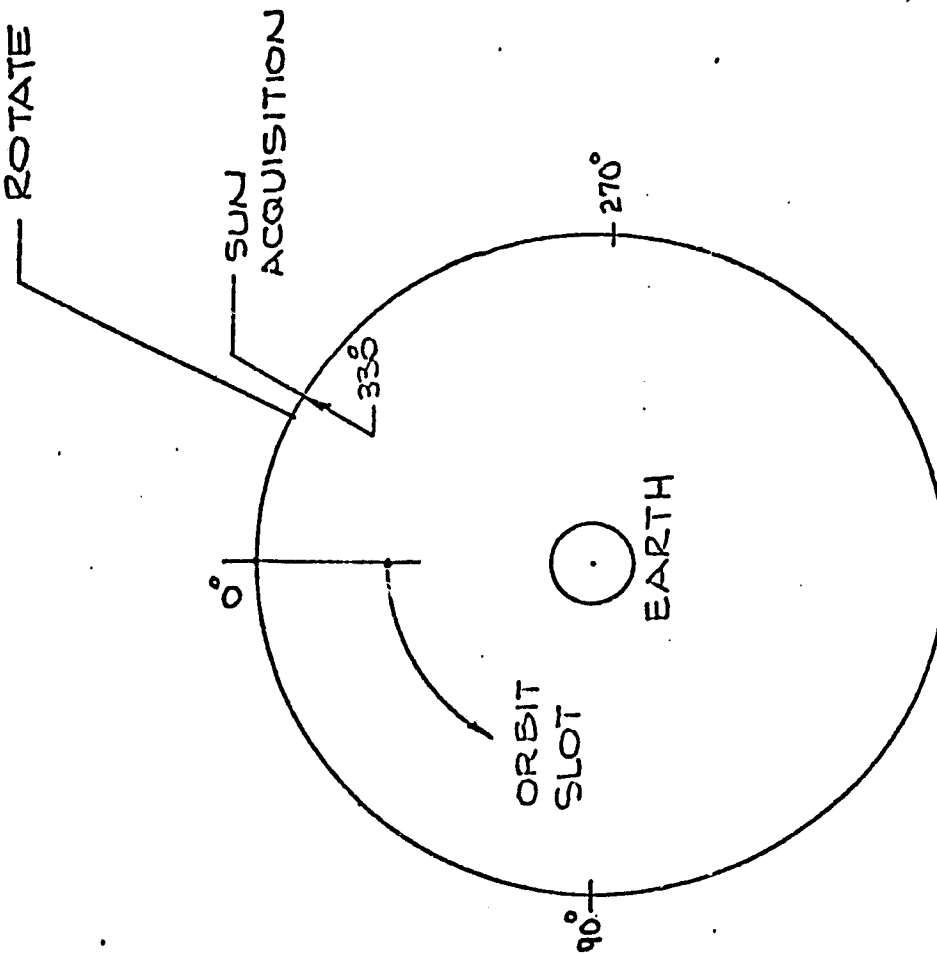
See Reference 6 for a detailed discussion.

At the completion of deployment, the +Y axis may be pointing anywhere about \bar{S} . Its orientation may also be slowly changing due to any residual yaw rate.

ORIGINAL PAGE IS
OF POOR QUALITY.

PRELIMINARY DRAFT

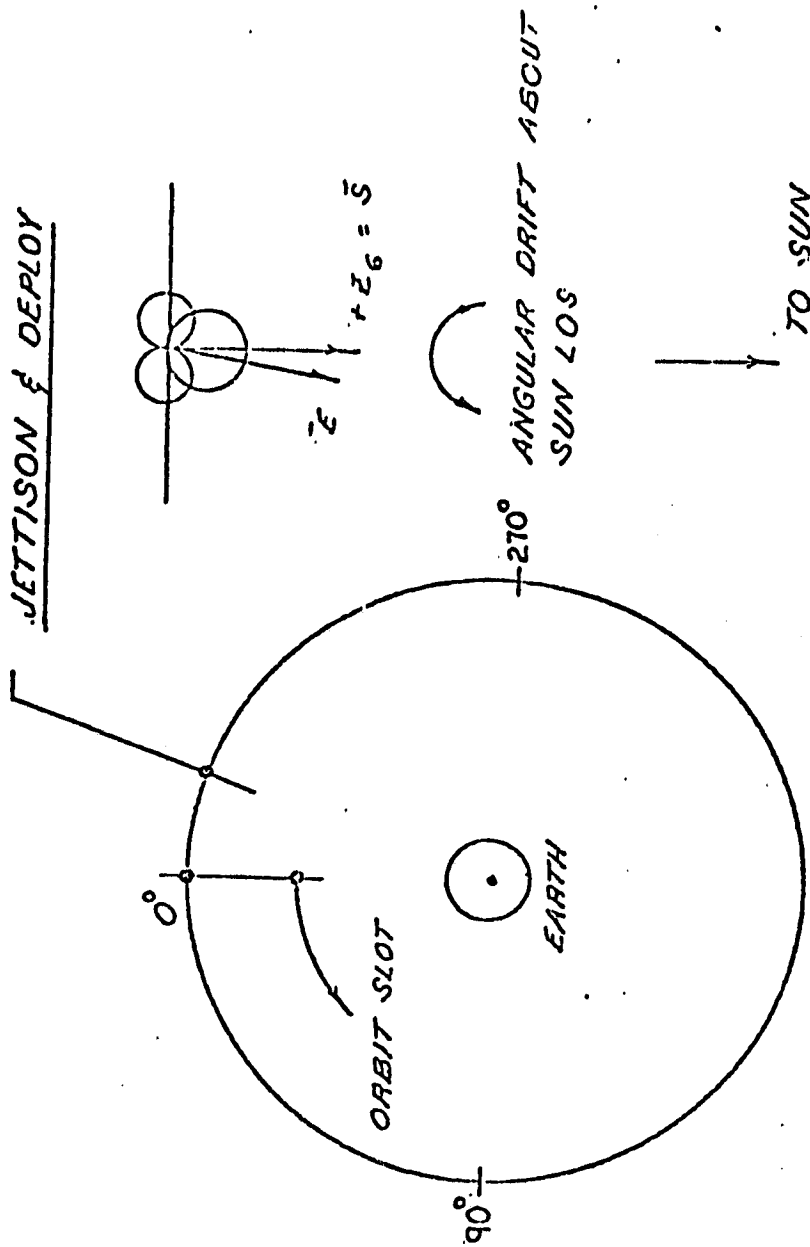
ROTATE ABOUT PITCH (90°)

ANGULAR DRIFT
ABOUT SUN LOS.WORST CASE T & C
ORIENTATIONS SHOWN

(VIEW OF ORBIT PLANE LOOKING SOUTH)

FIGURE 2.3.2 SUN ACQUISITION (EVENTS A22, A23)

PRELIMINARY DRAFT

ORIGINAL PAGE 13
OF POOR QUALITY

(VIEW OF ORBIT PLANE LOOKING SOUTH)

FIGURE 2.3.3. JETTISON AND DEPLOYMENT (EVENTS A24-A29)

PRELIMINARY DRAFT

ORIGINAL PAGE IS
OF POOR QUALITY2.3.3 Momentum Wheel Spin-Up (Event A30).

With the +Z axis being maintained along \bar{S} by the ground-based software attitude controllers, the momentum wheel will be spun up to its nominal speed of approximately 3750 rpm (see Figure 2.3.4).

Due to the residual rates (roll and yaw) which may exist at the start of spin-up, the pitch axis may be:

- nutating significantly and/or
- "tipped off" from being perpendicular to \bar{S}
(ie: \bar{S} in yaw/pitch plane but +Z \bar{S}) at the completion of spin-up.

Thus as part of Event A30 it may be necessary to carry out the following operations, in addition to the spin-up itself.

- damp the residual nutation cone of the pitch axis
and/or
- precess the pitch axis about the roll axis until the positive yaw axis is again maintained along \bar{S} .

See Reference 7 for a detailed discussion.

2.3.4 Earth Centre Acquisition (Event A31 to A35)

Upon completion of momentum wheel spin-up (Event A30), the +Z axis will be maintained along \bar{S} . However, the pointing orientation of the +Y axis about \bar{S} , although inertially fixed due to the spinning wheel, will be unknown.

PRELIMINARY DRAFT

To determine this orientation, an earth search rotation about pitch will be performed until an "earth strike" is recorded by the nonspinning earth sensor (NESA). The spacecraft will then rotate back until $+Z = \bar{5}$.

From the timing of the earth strike and the known ephemeris data, it is possible to determine where the +Y axis is pointing.

The spacecraft will then be precessed about the +Z axis until the +Y axis is southerly (NOTE: The rotation and precession are done in Event A32. Event A33 is a repeat of A32 to "fine-tune" the attitude.).

It should be noted that the earth search rotation must be done as close to the 0° orbit slot as possible. This ensures the best earth strike data possible. Upon completion of the rotation, there are no further orbit slot constraints on the ensuing manoeuvres.

To complete the earth acquisition, the following manoeuvres are done:

- precess the +Z axis (about the +X axis) into the orbit plane (Event A34).
- rotate the +Z axis (about the pitch axis) until $+Z = \bar{E}$ (Event A35).

This sequence is discussed in detail in Reference 12 and illustrated in Figure 2.3.5.

PRELIMINARY DRAFT**ORIGINAL PAGE IS
OF POOR QUALITY****2.3.5 ACE Capture and Transfer of Control (Events A36 to A39)**

At the completion of Event A35, the positive yaw axis will be maintained along \bar{F} and the positive pitch axis will be pointing approximately south.

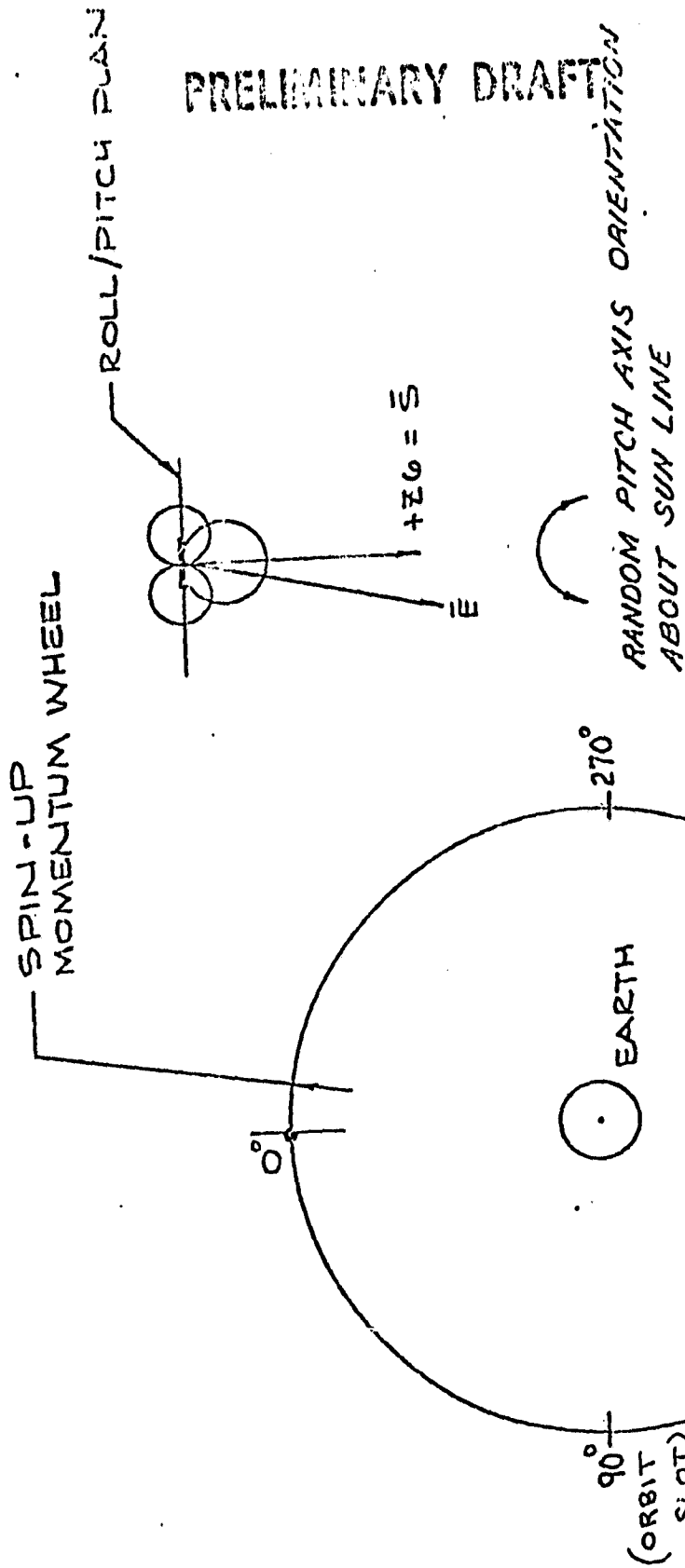
A series of small precessions about the roll and/or yaw axes (plus active nutation damping, as required) will be performed. These will "trim-up" the spacecraft attitude so that first the pitch wheel controller and then the offset controller can capture the earth. See Reference 10 for a detailed discussion.

Once the ACE onboard the spacecraft is maintaining attitude control (independently of GCAP), the final reconfiguration of the spacecraft hardware in preparation for On-Orbit Phase operations will be done.

This marks the end of the Attitude Acquisition Phase of the CTS mission.

PRELIMINARY DRAFT

ORIGINAL PAGE IS
OF POOR QUALITY



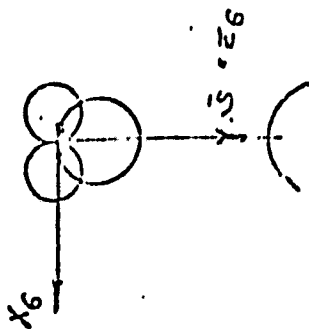
(VIEW OF ORBIT PLANE LOOKING SOUTH)

SPIN-UP (EVENT A30)

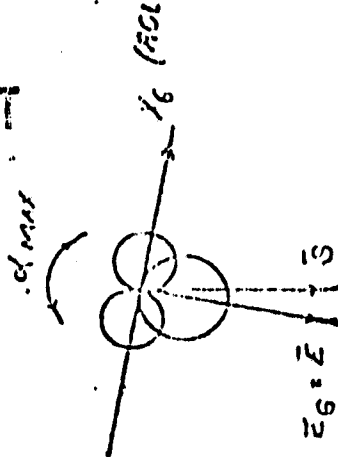
FIGURE 2.3.4

PRELIMINARY DRAFT

PRECESS ABOUT YAW

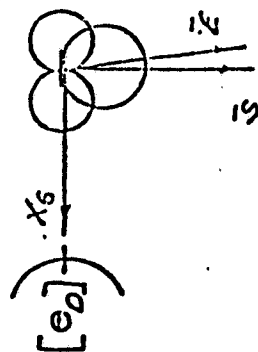


ROTATE ABOUT PITCH:
EARTH SEARCH

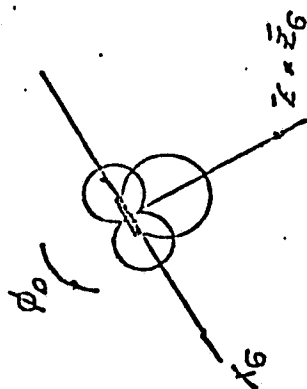


ORIGINAL PAGE IS
OF POOR QUALITY

PRECESS ABOUT ROLL
(EVENT A34)



ROTATE ABOUT PITCH;
ACQUIRE EARTH (A35)



ACE CAPTURE
(A36-A39)

θ_0 = SUN DECLINATION
 ϕ_0 = ORBIT SLOT
 α_m = MAXIMUM REQUIRED EARTH ROTATION
 ABOUT PITCH (\hat{x}),

VIEW OF ORBIT PLANE LOOKING SOUTH

FIGURE 2.3.5 EARTH ACQUISITION and ACE CAPTURE (EVENTS A31-A39)

PRELIMINARY DRAFT

ORIGINAL PAGE IS
OF POOR QUALITY

APPENDIX B - EVALUATION OF GCAP DATA SMOOTHING ALGORITHM - SMOOTH

The contents of the following memorandum were discussed with SED during meetings on August 27. Several clarifying points were raised:

1. Sun angle data is processed by SMOOTH.
2. During most of attitude acquisition the Sun is maintained along + yaw which is the boresight of NSSS number 5 and sensor transitions will be rare.
3. An upper limit on ATTCON command duration is accomplished by specifying the maximum number of executes (number of $1/512$ second burn intervals).
4. Additional preprocessing, such as proposed in the memorandum, has not been implemented.

PRELIMINARY DRAFT

ORIGINAL PAGE 19
OF POOR QUALITY

COMPUTER SCIENCES CORPORATION
SYSTEM SCIENCES DIVISION
8726 COLLEVILLE ROAD • SILVER SPRING, MARYLAND 20910

August 25, 1975

National Aeronautics and Space Administration
Goddard Space Flight Center
Greenbelt, Maryland 20771

Attention: Mr. G. Repass
Code 581.2, Bldg. 23, Room E-423

Subject: Contract No. NAS 5-11999
Task Assignment 635
Evaluation of GCAP Data Smoothing
Algorithm - SMOOTH

Dear Sir:

The attitude controller, ATTCON, is used by the ground control software throughout the CTS attitude acquisition sequence to issue thrust commands whenever preset controller angles and/or body rates exceed a preset deadband. A typical application of ATTCON is after Sun acquisition along the +Z axis and prior to jettisoning the body mounted solar arrays. The angle between the Sun line and the roll-yaw plane (δ_s) is controlled near the value 0° and the angle between the Sun projection on the roll-yaw plane, the + roll axis (α_s) is controlled at the value 90° , and the rate about the yaw axis (ω_z) is controlled near $0^\circ/\text{s}$. Deadbands are set about these null values to prevent excessive thruster activity.

Processed telemetry data is continually monitored by ATTCON and thrusts are commanded via a closed loop with the ground computer whenever a controlled variable leaves the deadband. The intensity of thruster activity depends upon the size of the deadband and the body rates. For a ± 1 degree deadband and rates near the rate gyro threshold, $0.2^\circ/\text{s}$, thrusts could be commanded every 10 seconds. This might be typical of conditions soon after Sun acquisition along +Z (Event A23). After several minutes ATTCON will have reduced the rates to near "steady state" values and infrequent attitude maintenance thrusts will be required every several minutes.

Mr. G. Repass

PRELIMINARY DRAFT

August 25, 1975

To prevent a single erroneous telemetered angle or rate from causing erroneous thrusting, ATTCON employs a smoothing algorithm. SMOOTH outputs the weighed mean of the last five valid samples. Samples are validated by comparing each new value with the last valid sample. Samples differing from the last valid sample by more than a preset amount are temporarily rejected, placed in a buffer and a flag set. If two consecutive samples differ from the last valid sample but agree with each other, the new value is accepted and the SMOOTH output is updated.[†] Figure 1 is a listing of the FORTRAN version of SMOOTH.

We do not feel that this procedure is sufficient to adequately discriminate against bad data and could result in large excursions from the desired controller attitude. As an example, non-spinning Sun sensor data is often garbled for several seconds when the Sun leaves the field-of-view of one sensor and enters another. In GEOS-3 several consecutive frames of data yielded valid angular readings but an incorrect Sun sensor identification. It would appear that the SMOOTH algorithm would interpret such an occurrence as a sudden 90° change in a controller angle and ATTCON would issue correction thrust commands.*

Figures 2 through 6 illustrate problems with actual sensor data for GEOS-3. Any smoothing algorithm should, at a minimum, successfully handle problems of this type. Note that GEOS-3 has three Sun sensors of a type identical to CTS.

A recommended update to SMOOTH would be as follows:

Pass the controller deadband (ϵ), null value (θ_0) and a tolerance parameter (N) to SMOOTH in addition to the controlled parameter (θ). Upon entry to SMOOTH the test

$$\theta_0 - N\epsilon < \theta < \theta_0 + N\epsilon$$

would be made. If θ were outside the extended deadband, $\theta_0 \pm N\epsilon$, it would be rejected. The tolerance parameter, N , would be selected based upon estimates of the maximum reasonable excursion from the deadband and varied depending upon the parameter and maneuver. A warning could be issued by ATTCON if an excessive number of values were being rejected.

[†] Gyro data is apparently processed by SMOOTH; however, it is not clear whether or not NSS data is processed by SMOOTH.

* It is our understanding that excessively long thrusts cannot be automatically commanded by ATTCON.

Yours truly,

COMPUTER SCIENCES CORPORATION



Dr. G. M. Lerner

PRELIMINARY DRAFT

REAL FUNCTION SMOOTH (NEW, DELTA, REJFLG, W1, W2, W3, W4, W5)

SAVED - ARRAY CONTAINING 5 SAVED VALUES
I.E. (NEWEST, NEXT, OLDEST, REJECTED)

NEW - THE DATA VALUE TO BE SMOOTHED WITH THE SAVED VALUES

DELTA - VALID CHANGE LIMIT

REJFLG - IF=1, INDICATES LAST VARIABLE WAS REJECTED ON A
DELTA CHECK

WX - WEIGHTS FOR THE SAVED TERMS

INTEGER REJFLG
REAL SAVED(5), NEW, DELTA, W1, W2, W3, W4

PERFORM INITIAL DELTA CHECK

IF (DELTA.GT.ABS(NEW-~~SAVED(1)~~)) GO TO 300

CHECK IF LAST VALUE WAS REJECTED
IF (REJFLG.EQ.0) GO TO 100

CHECK IF NEW=(REJECTED+DELTA)
IF (DELTA.LT.ABS(NEW-~~SAVED(5)~~)) GOTO 200

SAVE REJECTED VALUE
SAVED(4)=SAVED(3)
SAVED(3)=SAVED(2)
SAVED(2)=SAVED(1)
SAVED(1)=SAVED(5)
GOTO 400

SAVE AND REJECT THE VALUE
REJFLG=1
SAVED(5)=NEW
GOTO 999

CHECK IF LAST VALUE WAS REJECTED
IF (REJFLG.EQ.0) GO TO 500

ADD INTERPOLATED POINT
SAVED(4)=SAVED(3)
SAVED(3)=SAVED(2)
SAVED(2)=SAVED(1)
SAVED(1)=NEW-(NEW-~~SAVED(4)~~)/4
REJFLG=0

SMOOTH=W1*NEW + W2*SAVED(1) + W3*SAVED(2) + W4*SAVED(3) + W5*SAVED(4)
SAVED(4)=SAVED(3)
SAVED(3)=SAVED(2)
SAVED(2)=SAVED(1)
SAVED(1)=NEW

RETURN
END

Figure 1. FORTRAN version of GCAP SMOOTH

ORIGINAL PAGE IS
OF POOR QUALITY

PRELIMINARY DRAFT

Figure 2. Sun sensor data during transition from sensor 3 to sensor 1. About 60 seconds or 27 invalid frames were encountered. This occurred on April 12, two days after launch during attitude acquisition.

PRELIMINARY DRAFT

Figure 3. Sun sensor data after acquisition, June 28, 1975

ORIGINAL PAGE IS
OF POOR QUALITY

PRELIMINARY DRAFT

***** GESS *****									
***** DISPLAY ***** 75:227.02.01.17 *****									
***** FINAL OUTPUT ARRAY DISPLAY (1 OF 2) *****									
***** DATE OF BEGINNING OF DATA (YHRHDD.) 751628. *****									
REC. \$	F	FELDRX	FELDBY	FELDRZ	F	I	NA	N9	
ND.	F	M		S	D				
49	17.16.52	47.	-67.	-343.	3	20	72	✓	
50	17.16.55	47.	-67.	-343.	3	20	71	✓	
51	17.17.00	16.	-57.	-343.	3	20	70	✓	
52	17.17.05	55.	-67.	-343.	3	20	70	✓	
53	17.17.10	-51.	-57.	-343.	3	19	70	✓	
54	17.17.15	-495.	-483.	-465.	3	19	70	✓	
55	17.17.20	-51.	-57.	-343.	3	19	89	✓	
56	17.17.25	51.	-67.	-343.	3	19	70	✓	
57	17.17.30	51.	-67.	-343.	3	19	69	✓	
58	17.17.35	-51.	-57.	-343.	3	19	69	✓	
59	17.17.40	51.	-57.	-343.	3	19	69	✓	
60	17.17.45	51.	-57.	-343.	3	127	69	✓	
61	17.17.50	51.	-57.	-343.	3	19	59	✓	
62	17.17.55	51.	-57.	-343.	3	19	59	✓	
63	17.18.00	51.	-57.	-343.	3	19	59	✓	
64	17.18.05	51.	-57.	-343.	3	19	59	✓	
65	17.18.10	51.	-57.	-343.	3	19	59	✓	
66	17.18.15	51.	-57.	-343.	3	19	59	✓	
67	17.18.20	51.	-57.	-343.	3	19	59	✓	
68	17.18.25	51.	-57.	-343.	3	19	59	✓	
69	17.18.30	51.	-57.	-343.	3	19	59	✓	
70	17.18.35	51.	-57.	-343.	3	19	59	✓	
71	17.18.40	51.	-57.	-343.	3	19	59	✓	
72	17.18.45	51.	-57.	-343.	3	19	59	✓	
73	17.18.50	51.	-57.	-343.	3	19	59	✓	
74	17.18.55	51.	-57.	-343.	3	19	59	✓	
75	17.19.00	51.	-57.	-343.	3	19	59	✓	
76	17.19.05	51.	-57.	-343.	3	19	59	✓	
77	17.19.10	51.	-57.	-343.	3	19	59	✓	
78	17.19.15	51.	-57.	-343.	3	19	59	✓	
79	17.19.20	51.	-57.	-343.	3	19	59	✓	
80	17.19.25	51.	-57.	-343.	3	19	59	✓	
81	17.19.30	51.	-57.	-343.	3	19	59	✓	
82	17.19.35	51.	-57.	-343.	3	19	59	✓	
83	17.19.40	51.	-57.	-343.	3	19	59	✓	
84	17.19.45	51.	-57.	-343.	3	19	59	✓	
85	17.19.50	51.	-57.	-343.	3	19	59	✓	
86	17.19.55	51.	-57.	-343.	3	19	59	✓	
87	17.20.00	51.	-57.	-343.	3	19	59	✓	
88	17.20.05	51.	-57.	-343.	3	19	59	✓	
89	17.20.10	51.	-57.	-343.	3	19	59	✓	
90	17.20.15	51.	-57.	-343.	3	19	59	✓	
91	17.20.20	51.	-57.	-343.	3	19	59	✓	
92	17.20.25	51.	-57.	-343.	3	19	59	✓	
93	17.20.30	51.	-57.	-343.	3	19	59	✓	
94	17.20.35	51.	-57.	-343.	3	19	59	✓	
95	17.20.40	51.	-57.	-343.	3	19	59	✓	
96	17.20.45	51.	-57.	-343.	3	19	59	✓	
97	17.20.50	51.	-57.	-343.	3	19	59	✓	
98	17.20.55	51.	-57.	-343.	3	19	59	✓	
99	17.21.00	51.	-57.	-343.	3	19	59	✓	
100	17.21.05	51.	-57.	-343.	3	19	59	✓	

Figure 4. Noisy Sun sensor data, weak TM. 9 bad samples out of 43

PRELIMINARY DRAFT

Figure 5. Isolated instance of 3 Sun readings 10 degrees away from true value

PRELIMINARY DRAFT

Figure 6. Isolated instance of 2 consecutive Sun readings 77 degrees away from true value

PRELIMINARY DRAFT

ORIGINAL PAGE 19
OF POOR QUALITY

APPENDIX C - SUMMARY OF MEETINGS WITH SED ON AUGUST 27 AND 28

PRELIMINARY DRAFT

ORIGINAL PAGE 13
OF POOR QUALITY

COMPUTER SCIENCES CORPORATION

SYSTEM SCIENCES DIVISION

8728 COLESVILLE ROAD • SILVER SPRING, MARYLAND

(301) 539-1545

20910

September 4, 1975

National Aeronautics and Space Administration
Goddard Space Flight Center
Greenbelt, Maryland 20771

Attention: Mr. G.D. Repass
Code 581.2, Bldg. 23, Room E-423

Subject: Contract No. NAS 5-11999
Task Assignment No. 635
Meetings with SED on August 27 and 28
Simulation on August 27

Dear Sir:

This memorandum is an annotated summary of conversations which were held at CRC in Ottawa on August 27 and 28. In attendance were G. Lerner, J. Keat, and B. Blaylock of CSC; D. Kjosness, D. Basset, K. Magnussen and K. Krukewich of SED; G. Repass of GSFC; and H. Jackson of LeRC.

Included is a critique of the day 2 simulation and recommended areas for further investigation.

(1) Attitude acquisition and control via manual, wallboard displays.

Two HP2100 computers are used for support. One is used to create and drive CRT displays (four were used during the simulation) which are updated at 4 second intervals and to send manual commands; a second is used for the GCAP software and to initiate ATTCN attitude maintenance commands (a limited number of commands are sent by other GCAP modules and manual commands can also be sent). Present planning calls for control via the display computer in the event that the GCAP computer fails. Four 8 channel recorders will be used for support (a single 8 channel recorder was used during simulation with periodic channel reassignment) together with a single X-Y recorder.

Mr. G. D. Repass

PRELIMINARY DRAFT

September 4, 1975

The functions of the GCAP computer fall into several distinct categories:

(a) Attitude maintenance (ATTCON)

Most phases of the Attitude Acquisition require some sort of attitude maintenance, generally control of the spacecraft orientation relative to the Sun line-of-sight. A number of parameters are set by the GCAP operator to specify controller angles and rates, deadbands, and thrust duration (minimum impulse burn). The latter parameter specifies the magnitude of rate change to be used for control in the absence of gyro data and is of prime importance in determining the thruster firing frequency, angular excursions, and time constants of the system.

ATTCON uses smoothed telemetry data to automatically send attitude control burns at intervals ranging from a few seconds to a few minutes. During the simulation, ATTCON did not issue any commands during the 6 minute array deployment but did issue 36 momentum dumping pulses during the 11 minute momentum wheel spinup to maintain the yaw axis along the Sun line-of-sight.

(b) Data monitoring (AVERG, DAMP)

A data averaging routine is used to compute the mean of various TM variables (e.g. spin rate) which may then be used directly by analysts or input to GCAP for command computation.

DAMP monitors gyro and Sun or Earth data to determine amplitudes and phasing to select the optimal thruster, burn time and burn duration. Results are output for validation to the GCAP operator via the line printer. The operator may then enable DAMP for an automatic burn at the next opportunity.

(c) Rotation about pitch (after initial Sun acquisition and wheel spin up) and Precession about roll or yaw (ROTAP, PRECS)

ROTAP initiates and terminates pitch rotations via brief pitch thruster firings. Initiation is commanded and termination automatic dependent upon Sun angle monitoring. Manual operator intervention is also possible to terminate a rotation.

Roll and Yaw precessions are accomplished automatically after operator selection of the precession axis, direction, total arc length, and precession cone size.

It is apparent that many, if not all, of these functions could be performed manually via wallboard displays with varying degrees of difficulty. SED is in agreement with this conclusion. The most difficult period would probably be Sun maintenance during wheel spin up. This could be accomplished by greatly reducing the duty cycle (and consequently increasing the spin up time) so that momentum dumping thrusts would be required at fairly regular intervals of 30 to 60 seconds. Despite this capability, there is no need to initiate any attitude

acquisition maneuver from a backup facility whenever the spacecraft is in a stable configuration. This would apply to all maneuvers following array deployment and momentum wheel spinup.

Some measure of support could be provided at GSFC during critical time periods, in particular those periods during which the spacecraft is in an "unstable" configuration and commands must be sent to achieve or maintain positive power. We envision providing Ottawa with wall board type data and relaying requested commands (possibly via a Goddard affiliated station). The following, in increasing order of complexity, are the types of activities which could be supported in this fashion.

- An emergency single command (including multiple executes) capability
 - (a) If after despin from two RPM a failure occurs, Goddard could issue a spin up command to return to a positive power configuration.
 - (b) After initial Sun acquisition along yaw and jettison, Goddard could issue the array deployment command.
 - (c) After array deployment, Goddard could issue a yaw thrust command to provide an inertially stable configuration.
 - (d) During wheel spin up, Goddard could activate the CWS controller and/or activate the array autotrack system.
- Emergency attitude maintenance capability
 - (a) If after initial Sun acquisition along -roll or +yaw Ottawa experiences a limited failure, Goddard could maintain Sun lock until Ottawa can resume activities
 - (b) After array deployment, Goddard could issue periodic commands to maintain the yaw axis along the Sun line-of-sight.
 - (c) After wheel spin up, Goddard could issue periodic pitch thrusts to maintain Sun lock.
- Limited maneuver capability during mission critical events

This would apply only to events from the despin from 2 RPM through array deployment and wheel activation.

Note that some of these functions require only the sending of "blind" commands, others require detailed wall board displays.

Mr. G. D. Repass

PRELIMINARY DRAFT

September 4, 1975

The following calculated parameters (CP) would be useful/required to support the activities described. A more detailed description of the parameters is contained in Reference 2. Starred items are definitely required.

CP No.	Symbol	Description
* C0419		Battery A charge state
* C0420		Battery B charge state
C0601	ϕ_d	Orbit slot
* C0606	ω_{z1}	Spin rate from Δ Sun pulse time
* C0607	ω_{z2}	Spin rate from low speed spin rate counter
* C0608	θ_s	Angle of \hat{S} wrt XY plane
* C0610	α_s	Angle about pitch of \hat{S} projection into XZ plane
* C0613	δ_s	\hat{S} angle from XZ plane
C0617	β_s	Spin angle wrt \hat{S} on XY plane
C0618	θ_7	North array angle
C0619	θ_8	South array angle
* C0620		North array Sun angle
* C0621		South array Sun angle
C0638	γ_z	Nutation conc angle

The remainder are calibrated TM parameters

* P0649 ω_y (pitch)	
* P0650 ω_x (roll)	Rate gyro data
* P0651 ω_z (yaw)	
* P0660	Momentum wheel speed
* P0618	Wheel torque
P0704 } P0705 }	Jettison temperatures
* P0646	NSSS identification
* P0711	North Boom length
* P0712	South Boom length
P0709 } P0710 }	Elevation arm lock indicators
P02013 } P02014 } P02015 } P02016 } P02017 } P02018 } P02019 }	Boom deflection parameters
* P0713 } * P0714 }	array tension
P0616	CWS Controller mode

ORIGINAL PAGE IS
OF POOR QUALITY

(2) Orbit slot to initiate Earth Acquisition.

A number of arguments, none of them definitive, were presented by SED in favor of initiating Earth acquisition at the 0° rather than the 180° orbit slot. The primary reason for initiating day 2 activities near 0° was so that array deployment could be accomplished with maximum antenna gain and +yaw Sun-locked so that power input would be realized upon deployment without rotating the arrays. If the 180° slot were used for Earth acquisition, Sun acquisition through wheel spin up should still occur near 0° and one or more pitch rotations would be required to maintain a communications link prior to Sun lock along -yaw at the 180° slot. A second reason was that a Sun sensor is located along +yaw but -yaw is a region of Sun sensor overlap and NSS data could be degraded (-yaw is 60° away from the boresight of Sensors 4 and 5).

The general SED attitude towards the issue would appear to be:

- Sun interference is not expected to be a problem based upon NESA documentation. A sun interference flag is set in the NESA output if the Sun is within 3° of boresight.

If the 26° scan crosses near ($\sim 2.6^\circ$) of the Sun it would appear that the NESA output should be impacted. SED appears to assume that the Sun (diameter $\sim 0.5^\circ$) would add to the chord output. It would seem that the impact would be much greater.

We did notice a peculiar flip-flop between regions 2.1 and 4.1 (large negative roll, positive roll) in the NSES data when Sun presence was expected during the simulation. It was not clear whether this was a real effect or an artifact caused by the simulation model.

- In any event Earth acquisition will be initiated as early as possible regardless of orbit slot until an estimate of the ϕ_z angle (rotation or yaw angle about the Sun line) is obtained. A precession to place the pitch axis southerly, $\phi_z = 270^\circ$, will then be commanded and the acquisition repeated.

(3) Data Smoothing.

A discussion of the SMOOTH memorandum (Ref. 1) revealed that Sun sensor data is processed by SMOOTH. The examples cited in Reference 1 would have resulted in from zero ("noisy data") to one or possibly more minimum impulse burns. In the absence of rate gyro data, ATTCON only uses minimum impulse burns. Consequently, data of type shown would not be likely to significantly impact spacecraft control unless it persisted for an extended period. If gyro data exhibited similar characteristics (e.g. two consecutive, bad but equal values) a longer, more disruptive burn could be commanded. To counter this latter possibility, ATTCON is instructed to ignore all gyro rates above some selected limit. Also a maximum burn duration is specified in the software. Improvements to SMOOTH such as that proposed in Reference 1 will be considered by SED.

ORIGINAL PAGE IS
OF POOR QUALITY**(4) Momentum Transfer Maneuver.**

The merits of the momentum transfer maneuver were discussed with SED. Apparently the basic idea had been recommended by others and considered previously. It was rejected as a primary technique because of the need to accelerate the wheel in a power negative configuration and possible adverse effects on the wheel bearings from transverse body rates during spin up and subsequent high nutation amplitudes. Disturbance torques by the constant wheel speed controller (CWS) during array deployment were also mentioned. It was determined that although the wheel acceleration torque is fixed at 5 to 6 ounce-inches the wheel motor duty cycle is variable in 512 steps from 0 to 100%. CSC observed that by reducing the duty cycle both the power required and the subsequent nutation could be reduced. It was agreed that the power profile during the maneuver should be examined; conceivably at a low duty cycle it could be power positive. SED did not know about the relationship between the wheel acceleration time and nutation amplitude. The maneuver was considered for use under various non-standard procedures (NSP) and would be reexamined in light of the information presented. Copies of two AAS/AIAA papers on the maneuver were given to SED. The appendix to this note presents a hypothetical momentum transfer acquisition sequence with or without NSSS data.

(5) Nutation Damping.

CSC remarked that the nutation damping algorithms, MODE-1 and MODE-2, are derived assuming equal transverse moments of inertia whereas they are significantly different. However the phasing and burn duration computation are not grossly different and the algorithm used still reduces nutation by 80 to 90%. SED acknowledged that the algorithm had not been performing as expected lately and the problem had been attributed to a small timing error in the code. Moments of inertia presently used by SED are $I_x = 94.1$, $I_y = 69.0$, and $I_z = 114.5$; CSC was using $I_x = 94.5$, $I_y = 73.2$, and $I_z = 117.5$ slug-ft².

A brief explanation of the DAMP-3 and DAMP-4 algorithms was presented by SED (these modes use ATTCN to maintain a Sun or Earth locked attitude). Only pure X, Y, or Z torques are used by DAMP which explains the 4 damping opportunities per nutation period which was questioned by CSC.

(6) General - Pre simulation.

- The flight momentum wheel accelerates much faster (6 RPM/second) than the engineering model (3 RPM/second) at a 100% duty cycle.
- Rate feedback using tachometer data is no longer used by ATTCN for Sun maintenance during wheel spin up. Controller performance is better (reason unknown) without feedback.

G.D. Repass

PRELIMINARY DRAFT

September 4, 1975

- Rate gyro data was determined during tests to be much better than anticipated. Hysteresis and a "dead band" near zero rates were negligible. Gyro data is assumed valid over the entire range, a bucket size of 0.08 °/second is the primary data-limiting characteristic. For controller purposes, gyro rates below ± 0.3 °/second are generally ignored.
- The battery life at full load is approximately 2 hours. This could be extended appreciably by conservation measures such as turning off the rate gyro system.
- With both the belt and cone antennae on a TM link should exist virtually independent of attitude. SED believes commands could be sent (but data not received) down the apogee motor if necessary.
- NSES operation was discussed and documentation given to CSC. It was stated that the sign of the scan output is opposite the angular error. A negative pitch angle yields a positive scan output from scanner A. (Sign is the same as the required pitch null rotation).
- CSC observed that the attitude determination geometry for ϕ_s is worst at the 0 and 180 degree orbit slots and best at 90 and 270 for $\phi_s \approx 270^\circ$. In view of this the desirability of the $\phi_s = 270^\circ$ confirmation maneuver which occurs near the 20° slot should be examined. In any event, both the pitch and roll Earth strike angles should be used equally to determine and confirm ϕ_s .

(7) Day Two Simulation.

Initial conditions for a full day two simulation - spin down through WHECON enable - were supplied by CSC. The angular momentum vector was 1° off orbit normal. The spin rate was 2 RPM and a nutation half-cone of 2 - 3° was present. Spacecraft moments of inertia were 94.1, 69.0, and 114.5 slug-ft² for X, Y, and Z respectively. Thruster alignment was nominal and thruster forces were near nominal.

The simulation began at 8:20 PM after a 1 hour 20 minute delay due to problems with both the Σ -9 simulation computer and the HP2100 GCAP operating system.* The latter problem was overcome by switching to an older operating system.

In general, the simulation was quite successful requiring about four hours of wall clock time to complete the attitude acquisition sequence. Strip charts and CRT displays were available and critical parameters (excepting the GCAP computer control parameters) could be monitored.

The flight dynamicists used the GCAP computer, Hewlett Packard pocket calculators, and graphs to compute and verify commands. All members of the operations team appeared quite knowledgeable about spacecraft hardware as well as software operation.

* Unresolved external references in the GCAP load module.

ORIGINAL PAGE IS
OF POOR QUALITY

It should be emphasized that the problems noted below were quite minor and would not have inhibited an extremely successful acquisition assuming nominal spacecraft behavior.

- During the despin from 2 RPM the GCAP computer was assuming the wrong encoder was active and rate gyro data was ignored. Extremely sluggish controller response resulted and a 27° overshoot required about 30 minutes to correct.
- Attitude determination to compute the phase angle, ϕ_2 , about the Sun line was hindered by Sun presence and the use of graphical rather than tabular data (interpolation difficulties). The initial determination was $\phi_2 = -170^\circ$ (-180° was correct) and a 80° (rather than 90°) precession was commanded. The reconfirmation yielded $\phi_2 = 270^\circ$ (rather than 258°) and the final Earth lock sequence was initiated with the pitch axis 12° away from the desired southerly attitude. WHECON enable was finally achieved at the cost of additional roll precession maneuvers.
- The initial Earth search maneuver occurred at the 2° orbit slot with about 40 minutes of the "guaranteed" strike period remaining. Despite the fact that nutation damping was not required after wheel spin up (an artifact resulting from the exceptionally nominal spacecraft and initial conditions) and the elimination or cursory treatment of several events in the detailed operating procedures (DOP) the schedule was extremely tight.
- The angular difference between the north and south arrays ranged to 2.2° ; this implies a more serious "propeller effect" due to solar radiation pressure than previously indicated. This should not impact attitude acquisition but should be examined for on-station effects.

(8) Simulation Post-mortem.

The major CSC criticism involved the rigor of the DOP schedule and the SED tendency to prefer maneuvering over waiting.

Despite the fact that the only period during the acquisition that is time critical is from despin through array deployment (or possibly wheel spin up) * the DOP does not relax the pace.

CSC noted that during the simulation SED claimed that it was fortunate that the flight wheel could reach 3750 RPM so quickly thus accelerating the schedule. This, despite the fact that intense controller activity and array motion was expected. The duty cycle to be used in flight has yet to be determined but CSC's suggested 1 to 2 hour spin up time was felt excessive.

* Battery life at full load is about 2 hours. Thermal problems may require jettison within 33 minutes after despin.

Two controlled holds of approximately 10 hours after Event 30 (wheel spin up) and 5 hours after Event 32 (pitch axis southerly) were suggested by CSC for inclusion into the DOP.

The first would be to reduce the physical and psychological pressure to adhere to the schedule and permit the DOP emphasis to be on the time-critical battery power period. Initial Earth acquisition would slide to the 180° slot and would not be attempted unless the Earth strike probability was near 100%.

SED appears prepared to maneuver based on the negative interferences obtained from no Earth strike at say the 40° orbit slot.

The second hold would be to move the $\phi_3 = 270^\circ$ verification maneuver near the 270° orbit slot which is the optimal attitude determination geometry. Accurate southerly placement of the pitch axis will minimize subsequent precession maneuvers and expedite WHECON enable.

SED is reluctant to alter the DOP and prefers to streamline procedures and retain the opportunity to slip and alter procedures as the sequence unfolds.

(9) General - Postsimulation.

- The need to increase the GCAP computer visibility via a CRT display was discussed. Automatic input of parameters keyed by event was recommended to minimize human errors and expedite restart. The increased use of command mnemonics rather than HEX representations was recommended.
- Non-standard procedures are being considered with emphasis on the "safe-harbors" concept on attaining and maintaining stable attitudes. The return to a spinner either before or after array deployment was discussed.
- The wheel will spin up to saturation at 5000 RPM unless the CWS controller is activated.
- Day one tests of the low thrust engines at 60 RPM (where the passive nutation damper is functional) and an early day two check of the Z gyro at 1.5 RPM were being considered by SED.

(10) Recommendations.

- The level of information which can be provided at Goddard must be defined. Given this information, a list of scenarios, keyed to the DOP, can be drawn and specific backup commands and procedures established.

ORIGINAL PAGE IS
OF POOR QUALITY

- The momentum transfer maneuver should be examined in depth by SED with regard to thermal and power considerations. If feasible, full simulations should be carried out and the maneuver should be used as a backup in the event of NSSS or other system failure which would impact the success of the DOP.
- The rigor of the DOP schedule should be examined and inclusion of one or more "holds" should be considered.
- A tradeoff between maneuvering the spacecraft and waiting to gather more data should be established. Maneuvers based on negative inferences (such as using the lack of Earth strike to compute ϕ_s) should not be performed except on an emergency basis.

Yours truly,

COMPUTER SCIENCES CORPORATION

*D. Lerner*Dr. G. Lerner
Task Leader
Attitude Determination Area

cc:

GSFCLeRcCSCR. Werking
R. Coady

H. Jackson (4)

D. Stewart
K. Headrick
H. Hooper
Section ManagersK. Yong
J. Legg
B. Blaylock
J. KeatReferences

- (1) "Evaluation of GCAP Data Smoothing. Algorithm - SMOOTH",
Memorandum to G.D. Repass, August 25, 1975.
- (2) "Definition of GCAP Interface and Calculated Parameter Requirements,"
Memorandum to M. Evans from L. Flynn, April 9, 1975.

Appendix - Momentum Transfer Maneuver Attitude Acquisition

- (1) Day one activities are unchanged
- (2) Despin from 2 RPM to approximately $\chi = -1.23$ RPM *

where : $\chi = 30 H_w / \pi I_z$

H_w = wheel momentum ≈ 15 slug-ft²/S

I_z = yaw inertia ≈ 117 slug-ft²

- (3) Accelerate wheel to 3750 RPM and activate CWS controller. Duty cycle should be the minimum required to overcome friction consistent with thermal and power constraints. After spin up the total angular momentum of the system will still be $H_w = I_z \omega_z(0)$ along positive orbit normal. Spacecraft will be nutating with up to a 20 or 25 degree amplitude and a 40 second period. The nutation amplitude is proportional to $1/\sqrt{T}$ where T is the time required to spin up the wheel. A one-hour spin up (10 minutes correspond to a 100% duty cycle) implies a 8 to 10 degree half-cone angle. A residual body ω_y of 1 - 3°/S is achieved by activating the CWS controller while monitoring ω_y .

- (4) Damp nutation (null ω_x and ω_z) with a single burn using rate gyro data. The algorithm is burn duration = $\tau = \frac{2}{\alpha} \sin^{-1}(\alpha A_0 I / (2 T_b))$
initial gyro rate phase = $\beta_0 = \phi_0 - \frac{\alpha \tau}{2} - \pi$

where :

$$\alpha^2 = \alpha_x \alpha_z$$

$$\alpha_x = -\{ (I_z - I_y) \omega_y + H_w \} / I_x$$

$$\alpha_z = -\{ (I_z - I_x) \omega_y + H_w \} / I_z$$

$$I = 1/2 (I_x + I_z)$$

$$\phi_0 = \text{phase of selected thruster}$$

$$T_b = \text{torque magnitude of selected thruster}$$

$$A_0 = (\omega_x^2 + \omega_z^2)^{1/2}$$

This will reduce the nutation to a 3° or less half cone.

- (5) Acquire Sun in y - z plane with + yaw toward Sun by appropriately timed T_y to null ω_y using NSSS. Maintain Sun lock with $\alpha_s \approx 90^\circ$.
- (5a) Without NSSS data either Earth acquisition could be attempted using NSES data or an arbitrary ω_y null could be performed.

Note that the pitch axis should be within 8 to 10° of orbit normal.

* Nutation damping may be required after despin through zero.

- (6) Jettison Body Mounted Solar Arrays and Deploy Arrays. If NSSS data was used for Sun lock, the angle between the array normal and Sun line-of-sight will be the Sun declination \pm 10 degrees. If NSSS data was not used the arrays should be rotated until power input is observed. Auto-track is then engaged.
- (7) Rotate spacecraft about pitch until an Earth strike is obtained and maintain a minimum α_e angle using the pitch thrusters. Note that Earth strike is guaranteed independent of orbit slot.
- (8) Resume DOP activities with Event 35

This procedure requires far fewer maneuvers and is less dependent upon attitude sensors and closed loop control. It relies heavily on conserving the "hand-over" angular momentum direction.

The major disadvantage concerns the power profile during wheel activation and the probable battery state prior to array Sun acquisition.

Further investigation of this maneuver including a simulation comparable to that of August 27 appears warranted.

PRELIMINARY DRAFT

ORIGINAL PAGE 13
OF POOR QUALITY

APPENDIX D - LOSS OF SUN REFERENCE DURING MOMENTUM WHEEL SPINUP (LSL)

Several changes in response to the following memorandum have been made to reduce the chances of LSL:

1. The momentum wheel duty cycle has been reduced to 50%.
2. Array autotrack will be activated during spinup.
3. MODE-2 damping has been modified to accommodate nutation damping with a spinning wheel.

PRELIMINARY DRAFT

ORIGINAL PAGE IS
OF POOR QUALITY

COMPUTER SCIENCES CORPORATION

SYSTEM SCIENCES DIVISION

8728 COLLETSVILLE ROAD • SILVER SPRING, MARYLAND

4000 530 1045

20010

September 18, 1975

National Aeronautics and Space Administration
Goddard Space Flight Center
Greenbelt, Maryland 20783

Attention: Mr. G.D. Repass
Code 581.2, Bldg. 23, Rm. E-423

Subject: Contract No. NAS 5-11999
Task Assignment No. 635
Loss of Sun Reference During
Momentum Wheel Spin up

Dear Sir:

This memorandum addresses the problems of loss of Sun lock (LSL) during momentum wheel spin up and suggests procedures and algorithms for recovery of Sun reference.

Following the jettison of the body mounted solar arrays and array deployment (events A24 to A26) the positive yaw axis is maintained along the Sun line-of-sight via periodic control thrusts issued automatically by the attitude controller (ATTCON). The momentum wheel spin up (event A30) is commanded from this configuration with the array autotrack disabled. During wheel spin up, ATTCON issues momentum dumping burns at approximately 15 second intervals whenever the controller angles which are computed using non-spinning Sun sensor (NSSS) data leave a specified deadband. This procedure is somewhat changed from that used earlier in that rate feedback from the wheel controller is no longer used to command nominal dumping pulses which are then corrected using NSSS data. Although better performance is apparently achieved without using rate feedback, for reasons which are not clear, it would appear that a valuable data source is now being neglected and the probability for LSL during spin up is higher.

If no momentum dumping is performed, the reaction torque from wheel spin up will impart a spin rate of approximately 2.1 RPM (12.5 degrees per second) to the spacecraft; table 1 illustrates the time dependence of the pitch angle, α_s , during spin up in the absence of thrusting. If for some reason, e.g. invalid NSSS data or commanding problems during spin up, thrusts could not be issued, table 1 shows that at an acceleration rate comparable to the flight wheel at a 100% duty cycle a pitch error of 1.0° and a rate of $0.2^\circ/\text{S}$ would occur after 10 seconds.

Table 1

ORIGINAL PAGE IS
OF POOR QUALITY

Seconds	6 RPM/S		3 RPM/S	
	α_s (deg)	$d\alpha_s/dt$ (deg/s)	α_s (deg)	$d\alpha_s/dt$ (deg/s)
1	0.01	0.02	0.005	0.01
2	0.04	0.04	0.02	0.02
5	0.25	0.10	0.12	0.05
10	0.99	0.20	0.50	0.10
30	8.92	0.59	4.91	0.30
60	35.6	1.19	17.8	0.59
120	143	2.38	71.4	1.19
Maximum		12.5		12.5

This error is near the ATTCON commanding threshold. After 30 seconds the angular error would become significant and the angular rate beyond the capabilities of the array autotrack system if it were on (the DOP specifies autotrack off). After one minute array power would be dropping rapidly and the ability of ATTCON to recover automatically would be questionable. After two minutes array power would drop to zero, telemetry nulls would be likely, and ATTCON recovery probably not possible.

Although the time scale for recovery can be expanded by running the wheel at a reduced duty cycle, a reduction which is also desirable from an array dynamics viewpoint, the conclusion that LSL is conceivable would be unchanged. Experience on previous missions has shown that TM loss or sensor problems of a minute duration do occur and cannot be disregarded.

The impact of LSL during wheel spin up on the CTS mission cannot be adequately estimated without detailed, flexible spacecraft, simulations. Certainly, however, damage to the arrays at rates above 5 degrees/second would be likely.

A number of non-standard procedures (NSP) may be developed to (1) reduce the probability of LSL, (2) mitigate the consequences of LSL, and (3) recover from LSL. The following proposals (not recommendations) are a starting point for more detailed investigations and are not based on simulations already performed.

- Reduce the wheel duty cycle to yield a maximum spin up time consistent with acceptable mechanical performance.
- Use GCAP to automatically activate the CWS controller if the pitch error exceeds a TBD value; in the absence of NSSS data, after a TBD change of wheel speed; or in the absence of NSSS or wheel speed data, after a TBD time since valid data was received.
- Activate the array autotrack system during wheel spin up with automatic deactivation if the pitch gyro exceeds a TBD value.
- Acquire the capability at GSFC to activate CWS controller upon request.
- Develop within GCAP a "MODE-5" damping algorithm (described in the appendix to the September 4 memorandum) to be used for a spinning wheel without a Sun locked attitude.
- Deactivate ATTCON if controller angles or rates exceed a TBD extended deadband. Clearly ATTCON thrusting could be counterproductive if the pitch error approaches 180°.

ORIGINAL PAGE 15
OF POOR QUALITY

A Sun lock recovery procedure could consist of the following steps:

- (1) Activate the CWS controller.
- (2) Deactivate ATTCON.
- (3) Damp nutation using spinning wheel algorithm, DAMP-5.
- (4) Null pitch gyro rate when $\alpha_s \approx 90^\circ$, i.e. the Sun line in the pitch-yaw plane.
- (5) Activate ATTCON to maintain $\alpha_s \approx 90^\circ$
- (6) If necessary, rotate arrays to achieve maximum power input.

Simulations to investigate the dynamics of LSL will be performed with the open loop FSD/CTS simulator. ATTCON performance during spin up will be examined when the closed loop simulator is available.

Yours truly,

COMPUTER SCIENCES CORPORATION

Donald M Lerner

Dr. G. Lerner
Task Leader
Attitude Determination Area

GL:sm

cc:

GSFC

R. Werking
R. Coady

LeRc

H. Jackson (4)

CSC

D. Stewart
R. Headrick
H. Hooper
K. Yong
J. Legg
B. Blaylock
J. Keat
Section Managers

PRELIMINARY DRAFT

ORIGINAL PAGE IS
OF POOR QUALITY

APPENDIX E - ATTITUDE ACQUISITION VIA MOMENTUM TRANSFER (AAMT)

In response to the following memorandum, simulations have been performed at SED which have found thermal and power performance of AAMT comparable to that of the DOP. A NSP has been written to describe the implementation of the procedure (Réference 13).

PRELIMINARY DRAFT

ORIGINAL PAGE 18
OF POOR QUALITY

COMPUTER SCIENCES CORPORATION

SYSTEM SCIENCES DIVISION

8728 COLESVILLE ROAD • SILVER SPRING, MARYLAND

(301) 580-1545

20910

September 30, 1975

National Aeronautics and Space Administration
Goddard Space Flight Center
Greenbelt, Maryland 20771

Attention: Mr. G. D. Repass
Code 581.2, Bldg. 23, Room E423

Subject: Contract No. NAS 5-11999
CTS Attitude Acquisition Analysis
Task Assignment No. 635
Attitude Acquisition Via Momentum Transfer

Dear Mr. Repass:

This memorandum documents the results of the attitude acquisition via momentum transfer (AAMT) study for CTS. The study may be regarded as an existence proof of the feasibility of AAMT and has resulted in the recommendation that the ground station acquire the capability to implement AAMT. We do not suggest that AAMT is superior to the acquisition procedure contained in the detailed operating procedures (DOP) but rather that it appears to be a viable alternative in the event that one or more of the prerequisites of the DOP are not satisfied. In particular, the nominal DOP assumes (reference 1):

- A viable telemetry and command link between the spacecraft and ground station exists at all times.
- All spacecraft and ground stations hardware and software operate without failures.

Some deviation from these assumptions may, of course, be tolerated within the framework of the DOP. However, basic to the DOP is the requirement that the spacecraft be under active control at all times (during day 2) and consequently a continuous telemetry and command link between the spacecraft and ground station is essential.

ORIGINAL PAGE IS
OF POOR QUALITY

The AAMT ground support requirements are far less stringent since active control is needed only during several short periods. Specific subsystem failures, such as the non-spinning Sun sensor (NSSS) subsystem can also be tolerated. The number of required maneuvers and commands is far fewer than those listed in the DOP.

An element of risk is also inherent in AAMT since it relies heavily upon the performance of the momentum wheel under conditions of low duty cycle and substantial transverse body rates. In addition, acceleration of the wheel for a prolonged period prior to array deployment will require a substantial fraction of the available body array power. Maximum required wheel power is 50 watts at 100 percent duty cycle and minimum available body array power is 75 watts for the worst case orientation.

Although the disadvantages of AAMT cannot be disregarded, the obvious advantages justify the recommendation that the maneuver be given serious consideration as a non-standard procedure (NSP). Implementation of this NSP would appear to have minimal impact on the ground support software.

The remainder of this memorandum contains a description of the maneuver and the results of dynamic simulations.

The AAMT maneuver is described in papers by P. Barba and J. Aubrun of Aeronautics Ford Corporation (reference 2) and J. Gebman and D. Mingori of the Rand Corporation and UCLA, respectively (reference 3). Essentially the maneuver involves a transfer from an initial state at time zero,

$$\begin{aligned}\vec{H}_B(0) &= I_z \omega \hat{j} \\ \vec{H}_W(0) &= \vec{0},\end{aligned}\tag{1}$$

to a final state at time T,

$$\begin{aligned}\vec{H}_B(T) &\approx \vec{0} \\ \vec{H}_W(T) &= h_w \hat{j},\end{aligned}\tag{2}$$

where \vec{H}_B and \vec{H}_W denote the angular momentum of the body and wheel in inertial coordinates; \hat{j} is directed along the orbit normal (northward), and $I_z \omega \approx h_w$ are both positive. Conservation of angular momentum during wheel spin up insures that

$$\vec{H}_T = \vec{H}_B(0) + \vec{H}_W(0) = I_z \omega \hat{j} = \vec{H}_B(T) + \vec{H}_W(T).\tag{3}$$

Mr. G. D. Repass

PRELIMINARY DRAFT

September 30, 1975

The spin up of the wheel permits the relation $\vec{H}_w(T) = h_w \hat{j}_b$ in body coordinates to be obtained via control of the final wheel speed. However, although the length of $\vec{H}_w(T)$ in body (and inertial) coordinates may be controlled, the orientation may not.

Consequently the desired result, $\vec{H}_B(T) = 0$, cannot, in general, be obtained and the final attitude will consist of the wheel axis precessing and nutating about the conserved total angular momentum vector, $I_z \Omega \hat{j}$ (see Figure 1).

The precession period, about 43 seconds, is a function of the moments of inertia of the spacecraft and wheel and Ω ; however the offset angle, Θ , between the wheel axis and the momentum vector or orbit normal is a function of the moments of inertia, Ω , and the wheel acceleration time. The nutation, amplitude, or time variation of Θ , is small compared to Θ . In particular, it may be shown that as the wheel is accelerated, the energy of the body decreases and the wheel axis moves to conserve total angular momentum. If the wheel torque is sufficiently small, the process may be thought of as a quasi-static maneuver between successive, infinitesimally close, energy states. Intuitively, one would expect such a transition would yield a small offset angle. Conversely, a fast or sporadic wheel acceleration would violate the quasi-static assumption and a large offset angle might be expected. Numerous simulations were performed by Barba and Aubrun to confirm and quantify these observations.

Gebman and Mingori have obtained an analytical solution to Euler's equations during the momentum transfer maneuver by dividing the process into two asymptotic regions and a transition region. Perturbation expansions of the solution in each asymptotic region are obtained, using multiple time scales, and boundary matching procedures used across the transition region.

The result may be expressed in terms of the perturbation parameter, ξ , which is a function of the acceleration time,

$$\xi = \frac{h_w / T}{(I_z + I_w - I_y) \left(\frac{I_z + K_t}{I_x + K_t} - 1 \right) \Omega^2} \quad (1)$$

where: T = wheel acceleration time (assuming constant torque),
 I_x, I_y, I_z = body moments of inertia,
 K_t = transverse wheel inertia,
 I_w = axial wheel inertia.

PRELIMINARY DRAFT

$$\vec{H}_0(0) = \vec{H}_T = \text{total angular momentum}$$

$\hat{j} = \text{orbit normal}$

ORIGINAL PAGE IS
OF POOR QUALITY

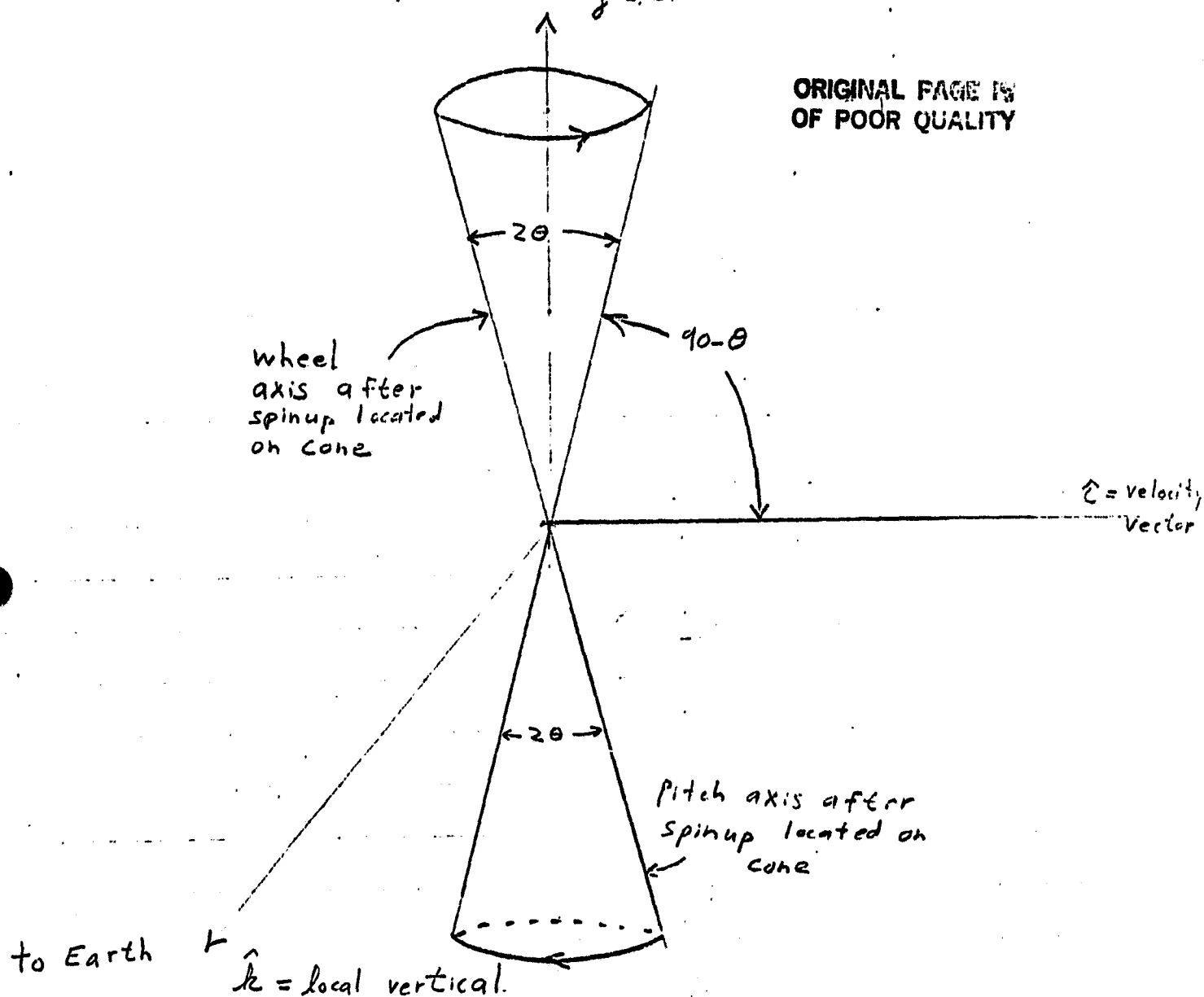


Figure 1. Momentum Transfer Geometry

The relation between the offset angle Θ , Ω , and the acceleration time is

$$\Theta = (G / \Omega T)^{1/2}, \quad (2)$$

where:

$$G = 0.980 \frac{\sqrt{1 + \frac{1}{2} \left(\frac{I_z - I_x}{I_y + K_1} \right)}}{\left(1 - \frac{I_y}{I_z + K_1} \right) \left(\frac{I_z - I_x}{I_y + K_1} \right)} \quad (3)$$

alternatively

$$\Theta = \varepsilon^{1/2} \left[0.939 \left\{ 1 + \frac{1}{2} \left(\frac{I_z - I_x}{I_y + K_1} \right) \right\}^{1/4} \right] + O(\varepsilon^{3/2}) \quad (4)$$

Hence the offset angle is inversely proportional to the square root of the acceleration time and, further, the validity of the perturbation expansion is governed by a size parameter which is inversely proportional to the 1.5 power of the acceleration time.

Using the values ,

$$\begin{aligned} I_x &= 94.1 \text{ slug ft}^2 \\ I_y &= 69.0 \text{ slug ft}^2 \\ I_z &= 114.5 \text{ slug ft}^2 \\ I_w &= 0.0332 \text{ slug ft}^2 \\ K_1 &= 0.02 \text{ slug ft}^2 \\ h_w &= 15.00 \text{ slug ft}^2/\text{second} \\ \Omega &= 0.1310 \text{ radians/second} \\ T &= 3750 \text{ seconds (about a 35 percent duty cycle),} \end{aligned}$$

we obtain,

$$\varepsilon = 0.0236$$

$$G = 8.02$$

$$\Theta = 0.128 \text{ radians} = 7.32 \text{ degrees}$$

Simulations by Gebman and Mingori indicate that for $\epsilon \approx 0.02$ up to a 12 percent error in the offset angle estimate may be expected.

At the initiation of wheel spin up, the total angular momentum vector must be equal (magnitude* and direction) to the desired angular momentum vector after spin up. The operational angular momentum is

$$\begin{aligned} \text{wheel} &: +15.0 \hat{j} \text{ slug} \cdot \text{ft}^2/\text{s} \text{ (3750 rpm)} \\ \text{body} &: +0.008 \hat{j} \text{ slug} \cdot \text{ft}^2/\text{s} \text{ (1 rpo)} \end{aligned}$$

where \hat{j} = orbit normal (north).

The operational pitch axis attitude is $-\hat{j}$ (south) and the wheel momentum is along the negative body pitch axis.

The handover angular momentum vector is $-720 \hat{j} \text{ slug} \cdot \text{ft}^2/\text{s}$. Consequently, a spin down through 0 rpm to -1.25 rpm is required to satisfy equations (1-3). Alternatively, a 180 degree precession could be performed at a low spin rate after handover.

The spin down to -1.25 rpm would be the simpler and preferable maneuver. Environmental torques acting on the spacecraft are insufficient to produce any significant precession, and resultant nutation, if any, could be damped easily.

A simulated spin down from +2 rpm to -1.27 rpm was performed with a thruster offset of 0.6 degrees and a torque of -1 ft-lb in order to obtain an estimate of attitude precession and nutation. The drift or precession angle, $\cos^{-1}(-\vec{J}_i \cdot \vec{J}_f)$ where \vec{J}_i and \vec{J}_f denote the initial and final angular momentum was 1.5 degrees and the nutation half-angle[†] was 1.4 degrees. Environmental torques (except gravity-gradient) were neglected but should not be significant during the 40 second despin (the magnitude of the spin rate was less than 1 rpm for 20 seconds).

Table 1 summarizes the results of a series of AAMT simulations consisting of three maneuvers:

- (1) Despin from 2 rpm to -1.27 rpm
- (2) Wheel acceleration
- (3) Nutation damping

*The initial magnitude should be somewhat smaller than 15 slug \cdot ft²/s to obtain a residual, positive pitch rate after wheel spin up.

$$\dagger \gamma_z = \tan^{-1} \left\{ \frac{[(I_x \omega_x)^2 + (I_y \omega_y)^2]^{1/2}}{I_z \omega_z} \right\} = 1.4^\circ$$

PRELIMINARY DRAFT

Table 1. AAMT Simulations

Wheel Acceleration Time (T) †	Net Wheel Torque (ft-lbs)	Final Wheel Speed (rpm)	Before Damping Burn (degrees)				After Damping Burn		
			θ_T	$\bar{\theta}$	γ_w	$\Delta\theta$	$\bar{\theta}'$	$\Delta\theta'$	γ'_w
1:04:10*	0.004	3850	7.2	8.7	8.4	3.8	9.2	1.1	1.1
1:04:10	0.004	3850	7.2	9.9	9.7	3.6	11.0	2.4	2.3
0:41:40	0.006	3750	8.9	12.1	12.0	3.5	7.4	1.6	1.6
0:31:15	0.008	3750	10.3	12.2	12.1	3.6	7.2	1.4	1.5
0:25:00	0.010	3750	11.5	13.2	12.7	3.5	13.5	2.4	2.3
0:16:40	0.015	3750	14.1	21.6	21.5	3.9	21.4	3.3	3.1
0:12:30	0.020	3750	16.2	17.6	16.7	3.6	15.7	4.7	4.6
0:09:37†	0.026†	3750	18.5	30.4	26.7	3.8	21.9	6.1	5.3

† hr:min:s

*Nutation damping burns after spin down through zero and wheel spin up were applied.

†100% duty cycle for flight wheel.

ORIGINAL PAGE 18
OF POOR QUALITY

In each case maneuver (1) was as described previously with a 0.6 degree thruster offset. The initial spin axis declination was -89 degrees and a pure 2 rpm spin was assumed. External torques (except gravity-gradient) were ignored. A nutation damping maneuver after despin was performed only in the first simulation because gyro rates, $\sim 0.2^\circ/s$, were near the gyro threshold. The first three columns give the wheel acceleration time, net torque, and final wheel speed. The theoretical (Θ_T) and observed ($\bar{\Theta}$) offset angles were obtained from equation (4) and the simulation respectively. The offset angle is given by

$$\bar{\Theta} = 90 + \overline{\sin^{-1}(A_{23})}, \quad (5)$$

where $A_{23} \equiv \bar{\gamma}_\theta(j)$ is the projection of the pitch axis along the orbit normal and the bar denotes time average. The agreement between Θ_T and $\bar{\Theta}$ is fair. Note that we expect $\bar{\Theta} > \Theta_T$ because of the initial 1.4 degree nutation⁺ and $\Theta_T \approx \bar{\Theta}$ only in the limit $T \rightarrow \infty$. The computed "nutation" angle is given by

$$\gamma_w = \tau_a \left\{ \frac{[(I_x \omega_x)^2 + (I_y \omega_y)^2]^{1/2}}{6 I_w S} \right\}, \quad (6)$$

where :

$$\begin{aligned} I_x &= \text{roll inertia} = 94.1 \text{ slug} - \text{ft}^2 \\ I_y &= \text{yaw inertia} = 114.5 \text{ slug} - \text{ft}^2 \\ I_w &= \text{wheel inertia} = 0.0382 \text{ slug} - \text{ft}^2 \\ S &= \text{wheel speed} = 3750 \text{ to } 3850 \text{ rpm.} \end{aligned}$$

The angle γ_w measures the nearly constant offset angle between the pitch axis and the total angular momentum vector. The time variation of the offset angle is given by

$$\Delta \Theta = \frac{\Theta_{MAX} - \Theta_{MIN}}{2} \quad (7)$$

The last three columns denote the attitude state after the nutation damping burn. The angular momentum vector and pitch axis are now nearly co-linear at an offset angle $\bar{\Theta}'$ with a time variation $\Delta \Theta'$. The angle $\bar{\Theta}'$ is bounded by

$$\bar{\Theta} - \Delta \Theta - \Delta \Theta' \leq \bar{\Theta}' \leq \bar{\Theta} + \Delta \Theta + \Delta \Theta'. \quad (8)$$

ORIGINAL PAGE IS
OF POOR QUALITY

+ Except the first simulation.

After damping, the nutation angle γ'_w is a measure of the pitch axis offset from the total angular momentum vector, hence

$$\gamma'_w \approx \Delta \theta'.$$

An AAMT sequence starting from a spin rate of -1.26 rpm is illustrated in Figures 2-4. The initial Z-axis attitude was $\alpha = 270$ degrees, $\delta = -89$ degrees.

A constant net torque, 0.004 ft - lbs or 0.77 ounce - inches, is applied to the wheel at $T = 0$ hours. This corresponds to a duty cycle of about 35 percent and requires approximately one hour for the wheel to reach nominal speed of 3750 rpm (15 slug - ft²/s). A maximum torque of 5 ounce - inches and a frictional torque of 1.5 ounce - inches were assumed.

There are a number of reasons for selecting a reduced duty cycle

- Maintaining the offset angle below 21.68 degrees guarantees an Earth strike using the non-spinning Earth sensor (NSES) at any orbit slot without need for a Sun reference.
- Active nutation damping may not be required for spin up times in excess of one hour.
- Reduced transverse body rates and resultant wheel bearing torques.
- Reduced power requirements.

As the wheel accelerates, momentum is initially transferred from the yaw axis to the pitch axis and the angle between the yaw axis and orbit normal increases from 0 to 80 degrees (Figure 4). Finally the pitch momentum peaks near 9 slug - ft²/s (-7.3 degrees/second) and is transferred to the wheel. The ω_y gyro rate is carefully monitored and the constant wheel speed (CWS) controller activated after a slight positive bias, 0.15 degrees/second, is obtained. If the initial spin rate based upon the pitch inertia and wheel inertia is correct, the final wheel speed will be close to the nominal 3750 rpm. The ω_y bias is chosen to maintain a body spin rate about the orbit normal to produce a power positive configuration, guarantee periodic Earth strikes by the non-spinning Earth sensors, and minimize loss of telemetry.

Figure 3 illustrates the gyro data about six minutes after activation of the constant wheel speed controller. This is a greatly expanded portion of Figure 2. The nutation half-cone angle may be calculated using equation 6.

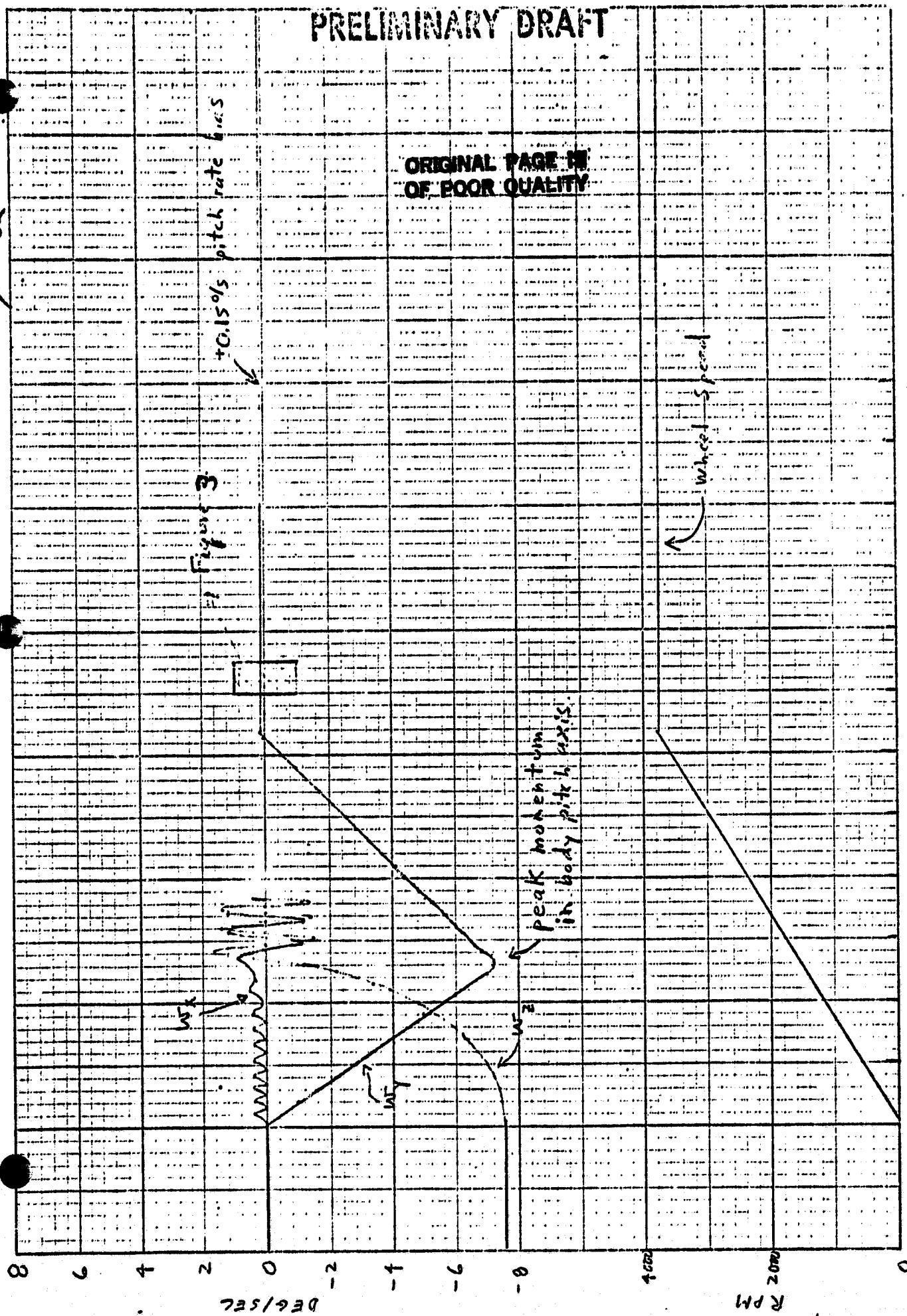
Figure 2

PRELIMINARY DRAFT

ORIGINAL PAGE IS
OF POOR QUALITY

Figure 3

+0.15% pitch rate bias



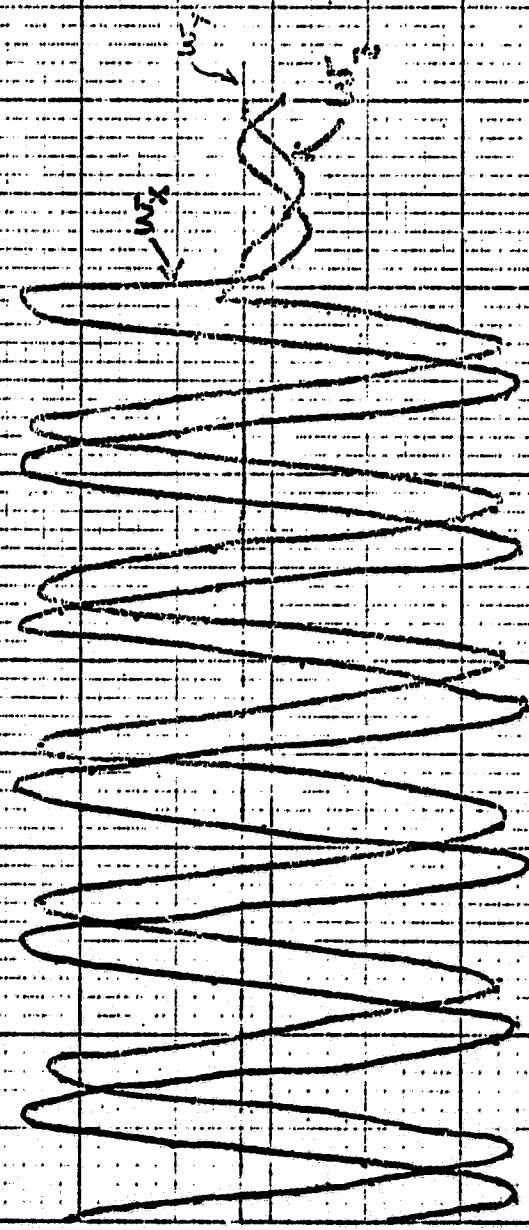
T (Hours)

PRELIMINARY DRAFT

ORIGINAL PAGE IS
OF POOR QUALITY

Figure 3

DAMP



1:10 1:11 1:12 1:13 1:14 1:15 1:16 1:17

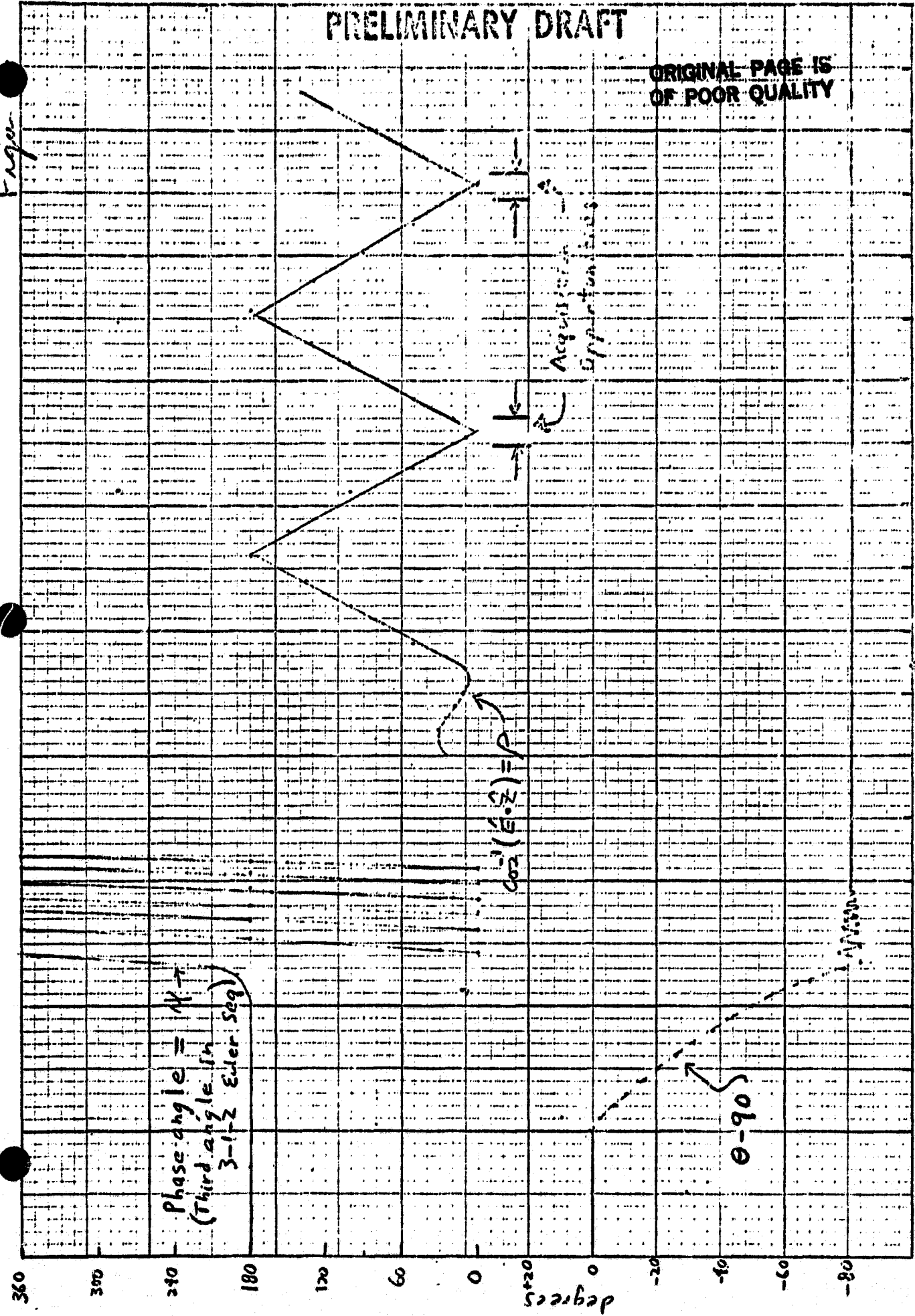
T (hours:minutes) →

ORIGINAL PAGE IS OF POOR QUALITY

PRELIMINARY DRAFT

ORIGINAL PAGE IS
OF POOR QUALITY

Figure



1 2 3 4 5 6 7 8 9 10 11 12 13 14 15 16 17 18 19 20 21 22 23 24 25 26 27 28 29 30 31 32 33 34 35 36 37 38 39 40 41 42 43 44 45 46 47 48 49 50 51 52 53 54 55 56 57 58 59 60 61 62 63 64 65 66 67 68 69 70 71 72 73 74 75 76 77 78 79 80 81 82 83 84 85 86 87 88 89 90 91 92 93 94 95 96 97 98 99 100

100 TO 1000000

Mr. G. D. Repass

PRELIMINARY DRAFT

September 30, 1975

At 1:14 we have $\omega_x = +1.18$ deg/s, $\omega_z = -0.59$ deg/s and $\gamma_w = 8.6$ degrees in substantial agreement with the analytical estimate, 7.3 degrees. Although conservation of angular momentum requires that the total angular momentum vector attitude is $\alpha = 90^\circ$, $\delta = +89^\circ$, after momentum wheel spin up, the negative pitch axis precesses about this attitude with a half-cone angle inversely proportional to the square root of the wheel spin-up time (see equation 2),

$$\Theta = \alpha / T^{1/2}$$

If Θ is in degrees and T in hours, the CTS configuration yields $\alpha = 8.8$.

A nutation damping maneuver was performed at 1:14:07 to reduce the nutation amplitude 1.2 degrees. * The damping impulse used was 1.92 ft - lb - sec. A residual nutation near zero was not achieved because the algorithm used, analogous to the SED DAMP2 algorithm, assumes equal transverse inertias. The algorithm has a tendency to overshoot and consequently only removes 80 to 90 % of the nutation with a single burn.

The burn duration, τ , and initial gyro rate phase $\beta_o = \tan^{-1} (\omega_x / \omega_z)$ are given by

$$\tau = \frac{2}{\alpha} \sin^{-1} (\alpha A_o I / (2 T_b)),$$

$$\beta_o = \phi_b + \frac{\alpha \tau}{2} - \pi$$

where :

$$\alpha = - \sqrt{\alpha_x \alpha_z},$$

$$\alpha_x = \{ (I_z - I_y) \omega_y + h_w \} / I_x,$$

$$\alpha_z = \{ (I_x - I_y) \omega_y + h_w \} / I_z,$$

$$I = \frac{1}{2} (I_x + I_z),$$

ϕ_b = phase of selected thruster,

T_b = torque magnitude of selected thruster,

$$A_o = (\omega_x^2 + \omega_z^2)^{1/2}$$

Note that β_o is reduced to compensate for the finite thrust duration. At the time of the thrust centroid β_o and ϕ_b are 180 degrees out of phase.

*Only rate gyro data is needed to compute the damping burn although use of Sun data (if available) could reduce the Sun-line, array normal angle.

Mr. G. D. Repass

PRELIMINARY DRAFT

September 30, 1975

After nutation damping the pitch axis attitude was $\alpha_y = 230$, $\delta_y = -80.7$ degrees and the body rate about the pitch axis was $\omega_y = 0.15$ degree/second. The angle between the yaw axis and the spacecraft to Earth vector, ρ , is illustrated on the right hand side of Figure 4. The minimum angle, determined by the complement of $|\delta_y|$ and the phase of the damping burn, occurs at regular periods, $T_n = 360/\omega_y$ seconds. In the example shown, Earth acquisition opportunities occur every 2400 seconds and last approximately $(2)(21.68)/\omega_y \approx 300$ seconds (21.68 is the NSES FOV).

The attitude acquisition sequence may be completed using either the Sun or Earth as a reference body.

Sun Reference

The reference angle α_s is monitored until the Sun is in the pitch-yaw plane ($\alpha_s = 90^\circ$) and the P1 or P2 thruster is fired to null ω_y . ATTCON is activated to maintain Sun lock. The body mounted solar arrays (BSA) are jettisoned and the arrays deployed. The angle between the Sun line and array normal will be $\beta \approx |\delta_{sun} \pm \theta|$ where $|\delta_{sun}| < 23$ degrees is the Sun declination and $\theta \approx 10$ degrees is the initial offset angle. Array autotrack is activated. The P1 or P2 thruster is fired to rotate about the pitch axis to obtain an Earth strike and the DOP sequence completed.

Earth Reference

NSES data is monitored until an Earth strike occurs at which time a pitch thruster P1 or P2 is used to null ω_y . The BSA are jettisoned and the arrays deployed. After deployment the arrays are slewed through an angle computed from the orbit slot or until the array power peaks. Array autotrack is activated. The angle between the Sun line and array normal will be $\beta \approx |\delta_{sun} \pm \theta|$. The P1 or P2 thruster is fired to rotate about the pitch axis to obtain an Earth strike and the DOP sequence completed.

Mr. G. D. Repass

PRELIMINARY DRAFT

September 30, 1976

To summarize, AAMT appears to be a viable procedure for CTS and we recommend that the ground station acquire the implementation capability as a NSP. The primary reservation concerning the maneuver, power and thermal constraints during spin up, should be examined fully via simulations by SED.

Yours truly,

COMPUTER SCIENCES CORPORATION

Donald M Lerner

Dr. G. M. Lerner
Technical Supervisor
Attitude Determination Area

cc: GSFC

R. D. Werking
R. E. Condy

LeRe

H. Jackson (4)

CSC

D. Stewart
Technical Supervisors
R. Headrick
H. Hooper
K. Yong
J. Legg
B. Blaylock
J. Keat

ORIGINAL PAGE IS
OF POOR QUALITY.

PRELIMINARY DRAFT

References

- (1) "CTS Attitude Acquisition Detailed Operating Procedures (DOP)", SED Document No. 5143-TR-101, April 15, 1975.
- (2) "Attitude Acquisition By Momentum Transfer", Peter M. Barba and Jean N. Aubrun, Paper No. AAS 75-053, July 1975.
- (3) "Perturbation Solution for the Flat Spin Recovery of a Dual-Spin Spacecraft", Jean R. Gebman and D. Lewis Mingori, Paper No. AAS 75-044, July 1975.

ORIGINAL PAGE IS
OF POOR QUALITY

PRELIMINARY DRAFT

APPENDIX F - DETERMINATION OF PHASE ANGLE ABOUT SUN LINE DURING CTS ATTITUDE ACQUISITION

ORIGINAL PAGE 18
OF POOR QUALITY

PRELIMINARY DRAFT

COMPUTER SCIENCES CORPORATION

SYSTEM SCIENCES DIVISION

8728 COLLEVILLE ROAD • SILVER SPRING, MARYLAND

(301) 580-1115

20910

ORIGINAL PAGE 19
OF POOR QUALITY

October 20, 1975

National Aeronautics and Space Administration
Goddard Space Flight Center
Greenbelt, Maryland 20771

Attention: Mr. G. D. Repass
Code 581.2, Bldg. 23, Room E423

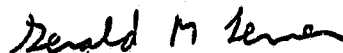
Subject: Contract No. NAS 5-11999
CTS Attitude Acquisition Analysis
Task Assignment No. 635
Determination of Phase Angle about Sun Line
During CTS Attitude Acquisition

Dear Mr. Repass:

Submitted herewith are two copies of the document entitled, "Determination of Phase Angle about Sun Line." The document addresses attitude determination accuracy during event A33 of the detailed operating procedures for the Communication Technology Satellite (CTS).

Yours truly,

COMPUTER SCIENCES CORPORATION



Dr. G. M. Lerner
Technical Supervisor
Attitude Determination Area

GML:sjm

cc: GSFC

R. Werking
R. Coady

LeRe

H. Jackson (4)

CSC

D. Stewart
Technical Supervisors
R. Headrick
H. Hooper
K. Yong

J. Legg
B. Blaylock
J. Keat
G. Tandon
F. Douglas
G. Urban

PRELIMINARY DRAFT

ORIGINAL PAGE IS
OF POOR QUALITY

Determination of Phase Angle about Sun line

During CTS Altitude Acquisition

This memorandum addresses the determination of the phase angle about the Sun line (ϕ_s) after momentum wheel spin up. We conclude that the uncertainty in ϕ_s after event A33 will be a minimum of 3.5 times the uncertainty in either pitch or roll if the event occurs near the zero degree orbit slot* as stated in the detailed operating procedures (DOP)¹. This implies an error in ϕ_s of the order of ten degrees prior to the initiation of the final precession and Earth acquisition maneuvers. The resultant impact will be to increase the number of trim maneuvers (event A36) and the time required to enable the on-board controller. We recommend that event A33 be delayed until the 270 (or 90) degree slot to provide the optimal geometry for achieving and verifying that $\phi_s \approx 270^\circ$.

Figure 1 illustrates the geometry for both event A32 (place + Y axis southerly) and event A33 (trim-up + Y axis pointing direction as required). The spacecraft is located at the center of the celestial sphere, the Sun is at a declination $\Theta_0 = -6$ degrees, and the orbit slot is $\phi_0 = 25$ degrees. The yaw axis is maintained along the Sun line by the attitude controller and the pitch axis is inertially fixed by the momentum wheel along a great circle 90 degrees away from the Sun. Because there is no attitude control (prior to wheel spin up) about the Sun line, the location of the pitch axis is arbitrary. The objectives of events A32 and A33 are (1) determine the pitch axis attitude, (2) precess the pitch axis to a southerly attitude, (3) repeat items (1) and (2) until $\phi_s = 270$ degrees (see figure 2).

The phase angle ϕ_s is defined as the counter clockwise rotation** of yaw about the Sun line required to place the +Y axis into the orbit plane such that $\phi_s = 90$ degrees is northward and $\phi_s = 270$ degrees is southward.

The philosophy of the DOP is to align the +Z axis along the Sun line so that near the zero degree orbit slot a rotation about the pitch axis will result in an Earth strike in the 21.68 degree non-spinning Earth sensor (NESA) field of view (FOV). From either the rotation angle to the Earth center, $\alpha_E = (\alpha_1 + \alpha_2)/2$ or the roll angle, δ_E , at $\alpha = \alpha_E$ the phase angle, ϕ_s , may be determined.

** ϕ_s increases clockwise about the Sun line

* A Sun declination of -16 degrees is assumed (February 5, 1976).

+ The values selected for Θ_0 and ϕ_0 are intended to be merely representative of the actual values.

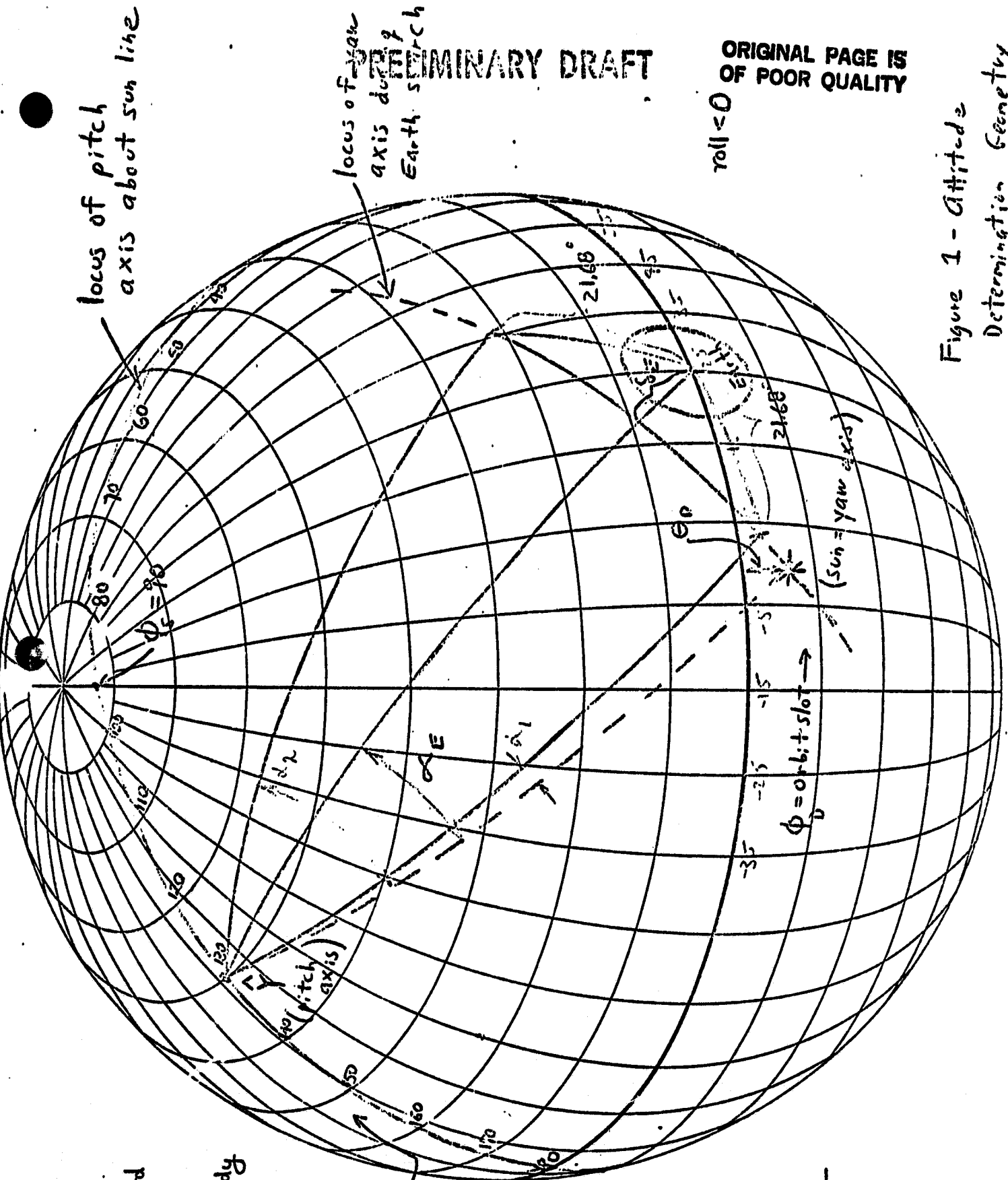
++ The 0 and 180 degree orbit slots are geometrically equivalent. Reference 1 discusses their relative merits.

PRELIMINARY DRAFT

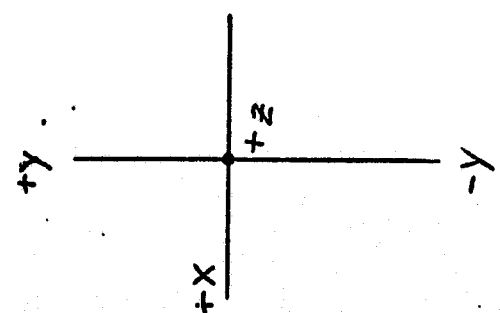
ORIGINAL PAGE IS
OF POOR QUALITY

roll < 0

Figure 1 - Attitude
Determination Geometry
on Celestial Sphere



\hat{X} = sun line
 \hat{Z} = north ward
 $\hat{Y} = \hat{Z} \times \hat{X}$
 ϕ_s rotates \hat{Y} body
 into \hat{Y}



PRELIMINARY DRAFT

ORIGINAL PAGE IS
OF POOR QUALITY

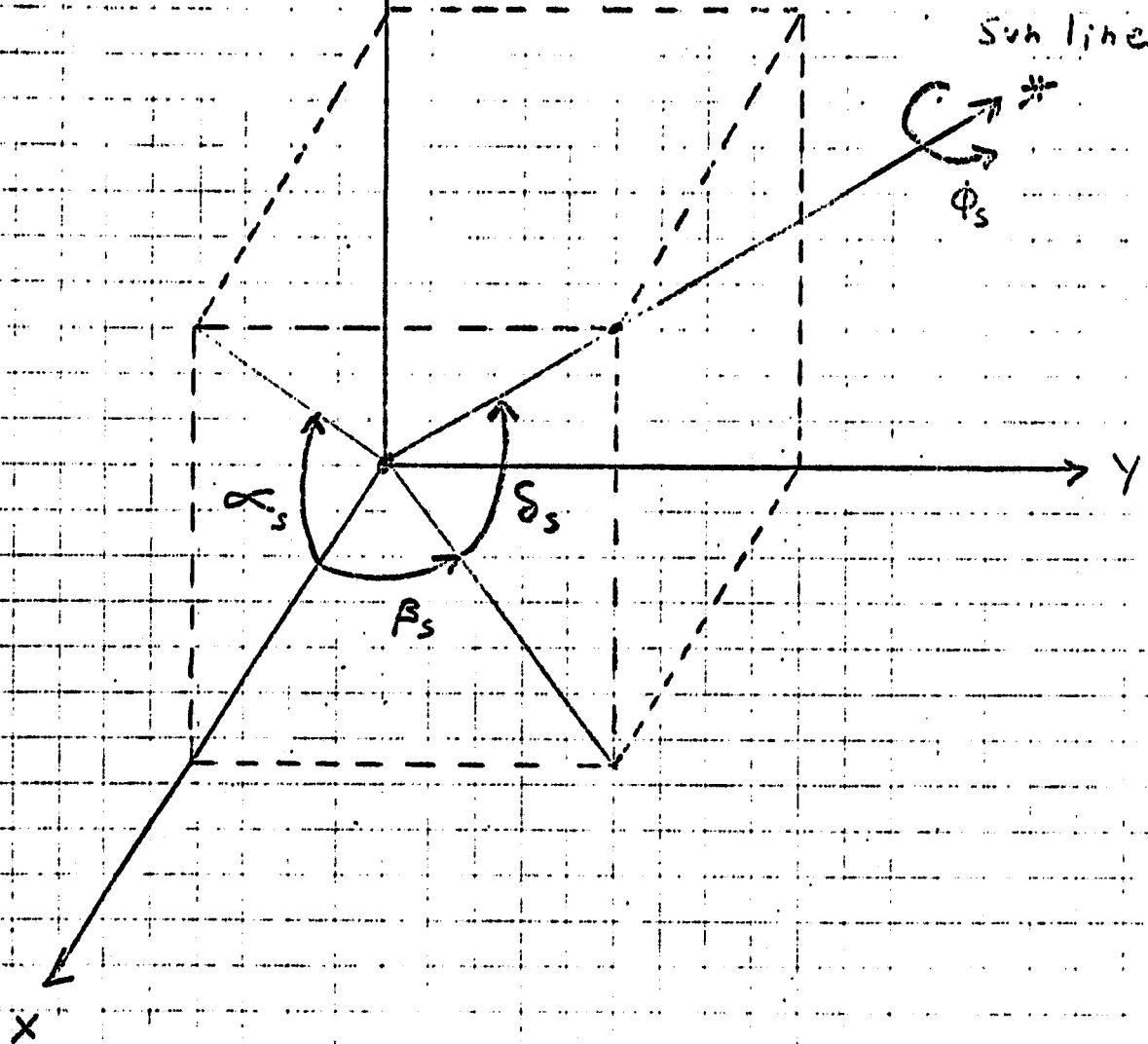


Figure 2 - Sun angle definition. The arrow denotes increasing ϕ_s not the counter clockwise rotation which defines the ϕ_s angle.

PRELIMINARY DRAFT

ORIGINAL PAGE IS
OF POOR QUALITY

Reference 2 contains the derivation of the relevant equations which are repeated here for convenience,

$$\begin{aligned}\phi_s^{(1)} &= \cos^{-1} Z - \text{ATAN2}(Y, X), \\ \phi_s^{(2)} &= 2\pi - \cos^{-1} Z - \text{ATAN2}(Y, X)\end{aligned}\quad (1)$$

where: $Z = \sin \delta_E / (\sin^2 \phi_D + \cos^2 \phi_D \sin^2 \theta_D)^{1/2}$,

$$Y = \sin \theta_D \cos \phi_D,$$

$$X = \sin \phi_D,$$

$$\theta_D = \text{Sun declination},$$

$$\phi_D = \text{Orbit slot}$$

The ambiguity in ϕ_s is resolved by the sign of the rotation angle,

$$\begin{aligned}\sin \alpha_E &= (\sin \phi_s \sin \phi_D + \cos \phi_s \cos \phi_D \sin \theta_D) / \cos \delta_E \\ \cos \alpha_E &= \cos \theta_D \cos \phi_D / \cos \delta_E\end{aligned}\quad (2)$$

Alternatively, ϕ_s can be computed from the pitch angle, α_E ,

$$\begin{aligned}\phi_s^{(1)} &= \cos^{-1}(Z) + \text{ATAN2}(Y, X) \\ \phi_s^{(2)} &= 2\pi - \cos^{-1}(Z) + \text{ATAN2}(Y, X)\end{aligned}$$

where $Z = \tan \alpha_E \cos \theta_D \cos \phi_D / (\sin^2 \phi_D + \cos^2 \phi_D \sin^2 \theta_D)^{1/2}$ (3)

$$Y = \sin \phi_D$$

$$X = \cos \phi_D \sin \theta_D$$

The ambiguity is resolved using δ_E information. Equations 1-3 have been written using the FORTRAN function ATAN2 to resolve quadrant ambiguity. Permissible geometries for obtaining an Earth strike for arbitrary ϕ_s , are greatly constrained by the 26 degrees NESA scan and the 8.686 degrees Earth radius

$$\delta_E = \cos^{-1} (\cos \theta_D \cos \phi_D) \leq \frac{26}{2} + 8.68 = 21.68^\circ \quad (4)$$

PRELIMINARY DRAFT

ORIGINAL PAGE 18
OF POOR QUALITY

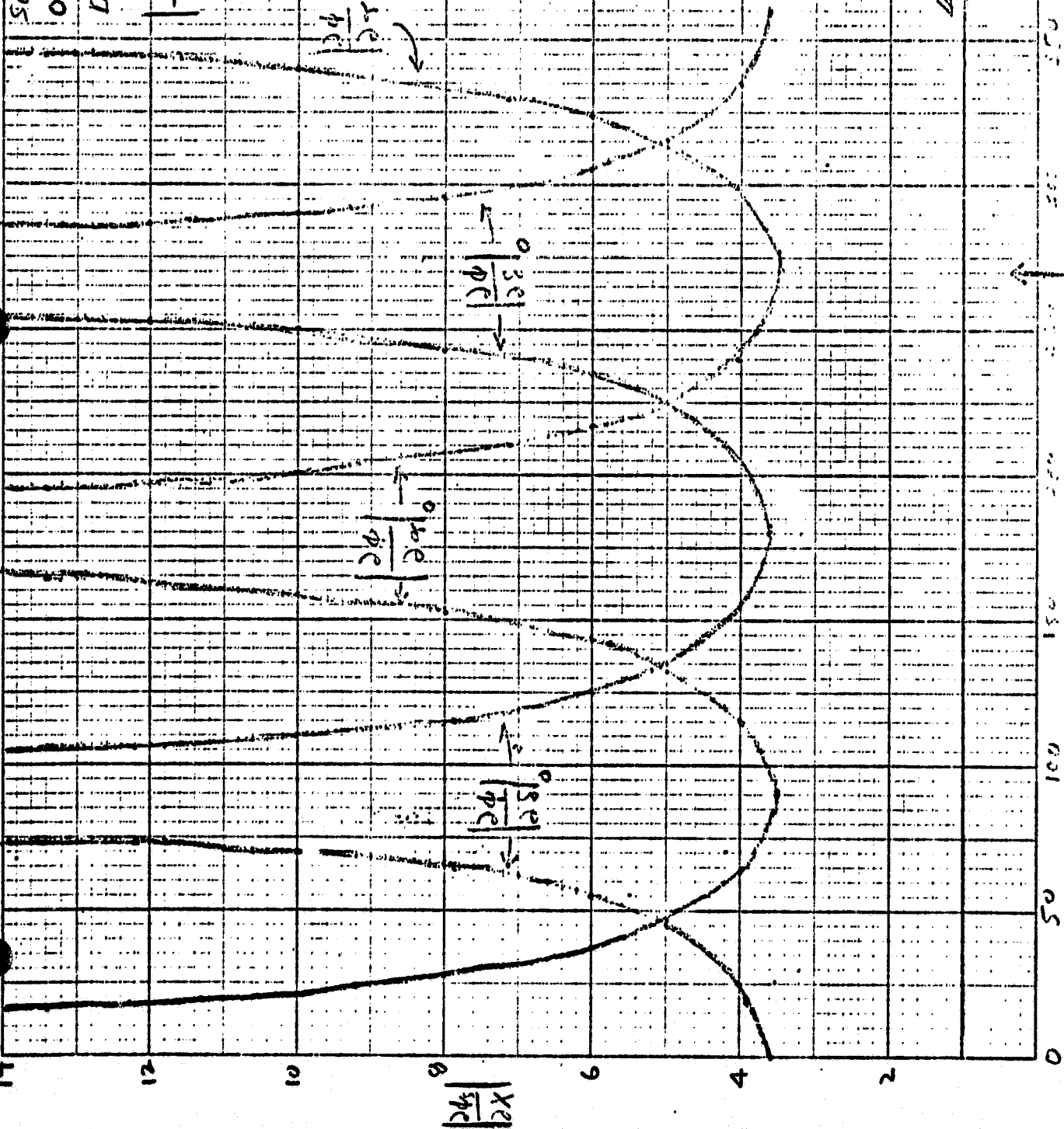
Sun Declination = -16°
Orbit + Slot = $0^\circ, 270^\circ$

Date 2/6/76

$$\left. \frac{\partial \theta}{\partial \alpha} \right|_{270} = \infty$$

$$\left. \frac{\partial \theta}{\partial \alpha} \right|_{0} = \text{orbit + slot}$$

$$\left. \frac{\partial \theta}{\partial \alpha} \right|_{270} = \frac{35}{24}$$



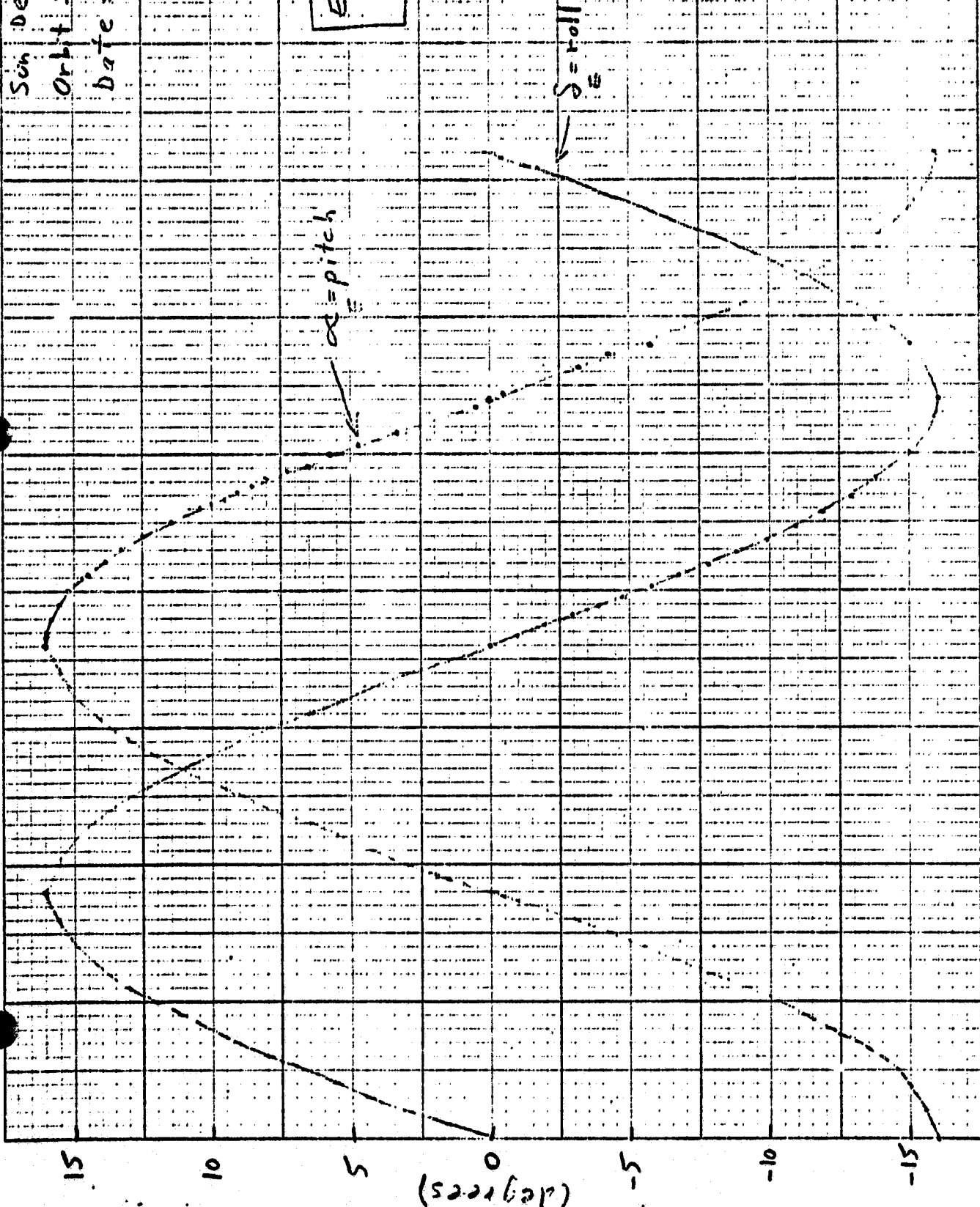
Phase Angle
About Sun line

Sun Declination = -16°
 Orbit Slot = 0°
 Date = 2/6/76

Earth station
 all Q_s

PRELIMINARY DRAFT

ORIGINAL PAGE IS
 OF POOR QUALITY



RECEIVED
 10 FEB 1976
 1000 HRS
 1000 HRS
 1000 HRS

Sun Declination = -16°

Orbit slot = 270°

Date 2/6/76

Lat+L Strike

$\phi_s = 90 \pm 21.78$ degrees
 $\phi_s = 270 \pm 21.78$ degrees

ELIMINARY DRAFT

ORIGINAL PAGE IS
OF POOR QUALITY

Roll angle at $\alpha = 0^{\circ}$
as a function of ϕ_s

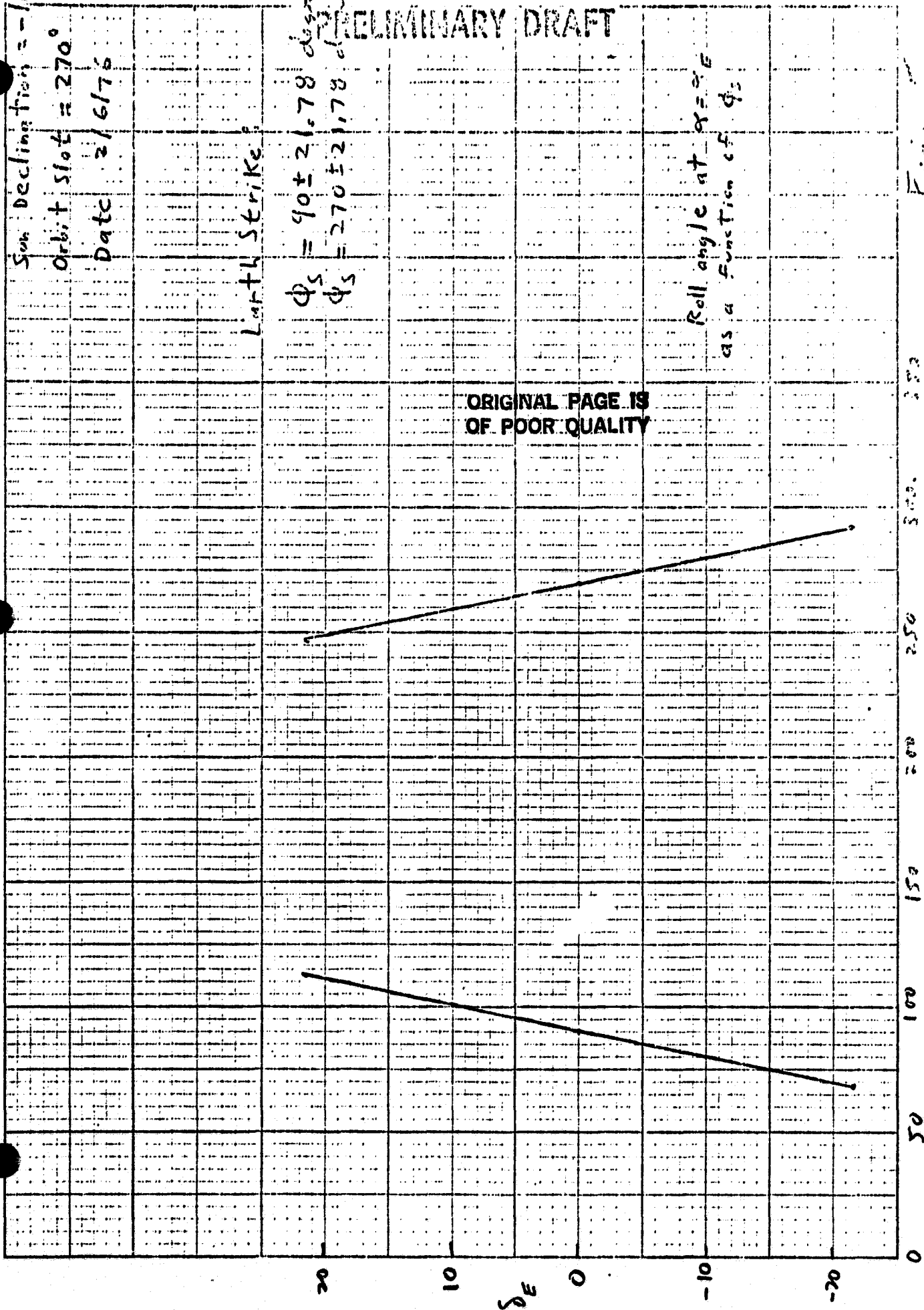


Figure 2

ϕ_s

PRELIMINARY DRAFT

ORIGINAL PAGE IS
OF POOR QUALITY

For small angles, the expression becomes

$$\delta_E = (\theta_D^2 + \phi_D^2)^{1/2} \leq 21.68^\circ \quad (5)$$

Consequently, Earth strike is guaranteed, independent of ϕ_S , only for an orbit slot near 0 (or equivalently 180) degrees, and ϕ_S may be determined only when the Sun and Earth separation is small. For high declinations, $|\theta_D| > 21.68$ degrees, an Earth strike is not guaranteed even at the zero degree orbit slot.

Unfortunately, the geometry which enables the computation of ϕ_S is paradoxically the geometry least favorable to an accurate determination of ϕ_S . Clearly for $\theta_D = \phi_D = 0$ the Earth is in the center of the field of view for $\alpha_E = 0$ but no phase angle information is available. In general the observability of ϕ_S is related to the partial derivatives of ϕ_S with respect to α_E and δ_E ,

$$\begin{aligned} \frac{\partial \phi_S}{\partial \delta_E} &= -\cos \delta_E / [\sin^2 \phi_D + \cos^2 \phi_D \sin^2 \theta_D - \sin^2 \delta_E]^{1/2} \\ \frac{\partial \phi_S}{\partial \alpha_E} &= -\left[\cos^2 \alpha_E \left(\frac{\sin^2 \phi_D + \cos^2 \phi_D \sin^2 \theta_D}{\cos^2 \theta_D \cos^2 \phi_D} - \tan^2 \alpha_E \right)^{1/2} \right]^{-1} \end{aligned} \quad (6)$$

If ϵ_δ and ϵ_α denote the uncertainty in δ_E and α_E , the resultant uncertainty in ϕ_S is

$$\epsilon_\phi \approx \epsilon_\delta \left| \partial \phi_S / \partial \delta_E \right| \quad (7)$$

$$\epsilon_\phi \approx \epsilon_\alpha \left| \partial \phi_S / \partial \alpha_E \right| \quad (8)$$

$$\epsilon_\phi \approx \frac{1}{2} \left[\epsilon_\delta^2 \left(\partial \phi_S / \partial \delta_E \right)^2 + \epsilon_\alpha^2 \left(\partial \phi_S / \partial \alpha_E \right)^2 \right]^{1/2} \quad (9)$$

where equations (7), (8), or (9) were obtained assuming $\phi_S = \phi_S(\delta_E)$, $\phi_S = \phi_S(\alpha_E)$, or $\phi_S = \frac{1}{2} (\phi_S(\delta_E) + \phi_S(\alpha_E))$ respectively.

PRELIMINARY DRAFT

ORIGINAL PAGE IS
OF POOR QUALITY

Figure 3 illustrates the partial derivatives for the orbit slot, $\phi_0 = 0^\circ$, and Sun declination, $\Theta_0 = -16^\circ$. This example is representative of the DOP geometry on February 6, 1976 prior to event A32. Two features are evident from the figure:

- (1) The attitude determination problem is symmetric in α_E and δ_E . For some values ϕ_s is insensitive to α_E , for others insensitive to δ_E .
- (2) Assuming nominal values, $\epsilon_s \approx \epsilon_\alpha \approx 3$ degrees, the best that one can do is $\epsilon_\phi \approx 10$ degrees. This implies the most judicious use of both δ_E and α_E information and is a fundamental limitation of the geometry.

Figure 4 illustrates the symmetric dependence of ϕ_s on δ_E and α_E . The phase angle is well determined by either α_E or δ_E near α_E or $\delta_E \approx 0$ and poorly determined near the extremes of α_E or δ_E .

This illustrates that it is fruitless to attempt to maneuver the spacecraft to $\phi_s = 270^\circ$ to an accuracy of better than approximately 10 degrees, and consequently, event A33 in the DOP should not be attempted near the 0 degree slot.

This problem was encountered during the August 27 simulation (reference 3) where a 12 degree error in ϕ_s , was falsely attributed to the graphical attitude determination technique.

In particular, for a desired precision, ϵ_ϕ , and an estimated ϵ_α and ϵ_δ , equation (6) may be used to compute the orbit slot, ϕ_0 , which is required.

The best geometry is near $\phi_0 = 90^\circ$ or $\phi_0 = 270^\circ$ where $\partial \phi_s / \partial \delta_E = 1$.^{*} However, as illustrated in figure 5, the best attitude determination geometry, guarantees an Earth strike over a limited range, $\phi_s = 270 \pm 21.68$. This attitude accuracy should be obtainable after the initial precession (event A32).

To summarize, we recommend the following change to the DOP : event A 33 (trim up + Yaxis pointing direction as required) should be eliminated or moved to an orbit slot consistent with the required accuracy.

PRELIMINARY DRAFT

ORIGINAL PAGE IS
OF POOR QUALITY

References

- (1) "CTS Attitude Acquisition Detailed Operating Procedures (DOP)"
SED Document No. 5143-TR-101, April 15, 1975.
- (2) "Redefinition and Simulation of Earth Acquisition Maneuvers"
SED Document No. 5144-TR-108, December 1974.
- (3) Memorandum from G. Lerner to G. Repass, Task 3000-63500,
September 4, 1975.

PRELIMINARY DRAFT

ORIGINAL PAGE 13
OF POOR QUALITY

APPENDIX G - SIGN OF NON-SPINNING EARTH SENSOR (NESA) TRANSFER FUNCTION

The following memorandum and response from E. A. McPherson of SED is concerned with the sign of the NESA output.

The issue is resolved by noting that:

1. The definition of pitch is

$$\alpha_E = + \tan^{-1} (E_{x6}/E_{z6})$$

2. The abscissa and ordinate of the figures defining NESA regions should be defined as $-\alpha_E$ and $+\delta_E = \sin^{-1} (E_{z6})$ respectively rather than the ambiguous "angular error about pitch axis" and "angular error about roll axis"

PRELIMINARY DRAFT

ORIGINAL PAGE IS
OF POOR QUALITY

COMPUTER SCIENCES CORPORATION
SYSTEM SCIENCES DIVISION
8728 COLESVILLE ROAD • SILVER SPRING, MARYLAND 20910
(301) 580-1646

October 9, 1975

National Aeronautics and Space Administration
Goddard Space Flight Center
Greenbelt, Maryland 20771

Attention: Mr. G.D. Repass
Code 581.2, Bldg. 23, Room E423

Subject: Contract No. NAS 5-11999
CTS Attitude Acquisition Analysis
Task Assignment No. 635
Sign of Non-spinning Earth Sensor (NESA)
Transfer Functions

Dear Mr. Repass:

A review of relevant NSES documentation has been made in an attempt to thoroughly understand the NSES output transfer functions. Several areas of confusion still exist and should be resolved to insure that the ground support and simulation software function properly. We note that simulations cannot validate the interpretation of NSES output functions but can lead to a mistaken sense of security. The interpretation of output functions can only be validated by using the spacecraft test data.

The remainder of this note refers to the attached figures which were copied from references 1 - 3. We assume that pitch and roll are defined by the relations

$$\begin{aligned}\text{pitch} = \alpha_E &= -\tan^{-1} (E_{x6} / E_{z6}), \\ \text{roll} = \beta_E &= \tan^{-1} (E_{y6} / E_{z6}),\end{aligned}$$

where $\vec{E} = E_{x6} \hat{i} + E_{y6} \hat{j} + E_{z6} \hat{k}$ is the spacecraft to Earth vector in body coordinates.

(1) With regard to figure 1 (O.3/1 in reference 1), the following interpretation is made:

- (a) The components of \vec{E} are $E_{x6} < 0$ and $E_{y6} > 0$ which implies pitch > 0 and roll > 0 .

PRELIMINARY DRAFT

(b) The EW(A) scanner output is

$$\text{SCAN} = \left(\frac{|CF| - |FD|}{2 \times 2.82^0} \right) 255 < 0 ,$$

$$\text{CROSS} = \left(\frac{15.909^0 - (|CF| + |FD|)}{2.82^0} \right) 255 < 0 .$$

ORIGINAL PAGE IS
OF POOR QUALITY

(c) The NS (B) scanner output is

$$\text{SCAN} = \left(\frac{|TS| - |SW|}{2 \times 2.82^0} \right) 255 < 0 ,$$

$$\text{CROSS} = \left(\frac{15.909^0 - (|TS| + |SW|)}{2.82^0} \right) 255 < 0 .$$

Consequently both the SCAN and CROSS output have a sign which is opposite to the pitch and roll angles. In general, for small angles, the sign of pitch is opposite to SCAN-EW and CROSS-NS and the sign of roll is opposite to SCAN-NS and CROSS-EW. These conclusions are in agreement with figure 2 (B.3.1 in reference 2).

(2) Assuming the preceding interpretation is correct, the following discrepancies/misinterpretations are noted :

- (a) Equation O.3/9 (reference 1) has the incorrect sign (enclosed figure 3).
- (b) If the abscissa in figure 4 (figure 3.15/4 in reference 1) is pitch in (a) and roll in (b), assuming scanner A, the sign of both output functions is incorrect.
- (c) Figures 5 and 6 (reference 3) which are apparently NSES test data, indicate a SCAN axis output in agreement with interpretation (1) but a CROSS axis output in disagreement. Again, we assume the abscissa is pitch in figure 5 and roll in figure 6.

Yours truly,

COMPUTER SCIENCES CORPORATION

Donald M. Lerner

Dr. G.M. Lerner
Technical Supervisor
Attitude Determination Area

cc: GSFCLeReCSC

R.D. Werking
R.E. Coady

H. Jackson(4)

D. Stewart
Technical Supervisors
R. Headrick
H. Hooper
K. Yong

J. Legg
B. Blaylock
J. Keat
G. Tandon

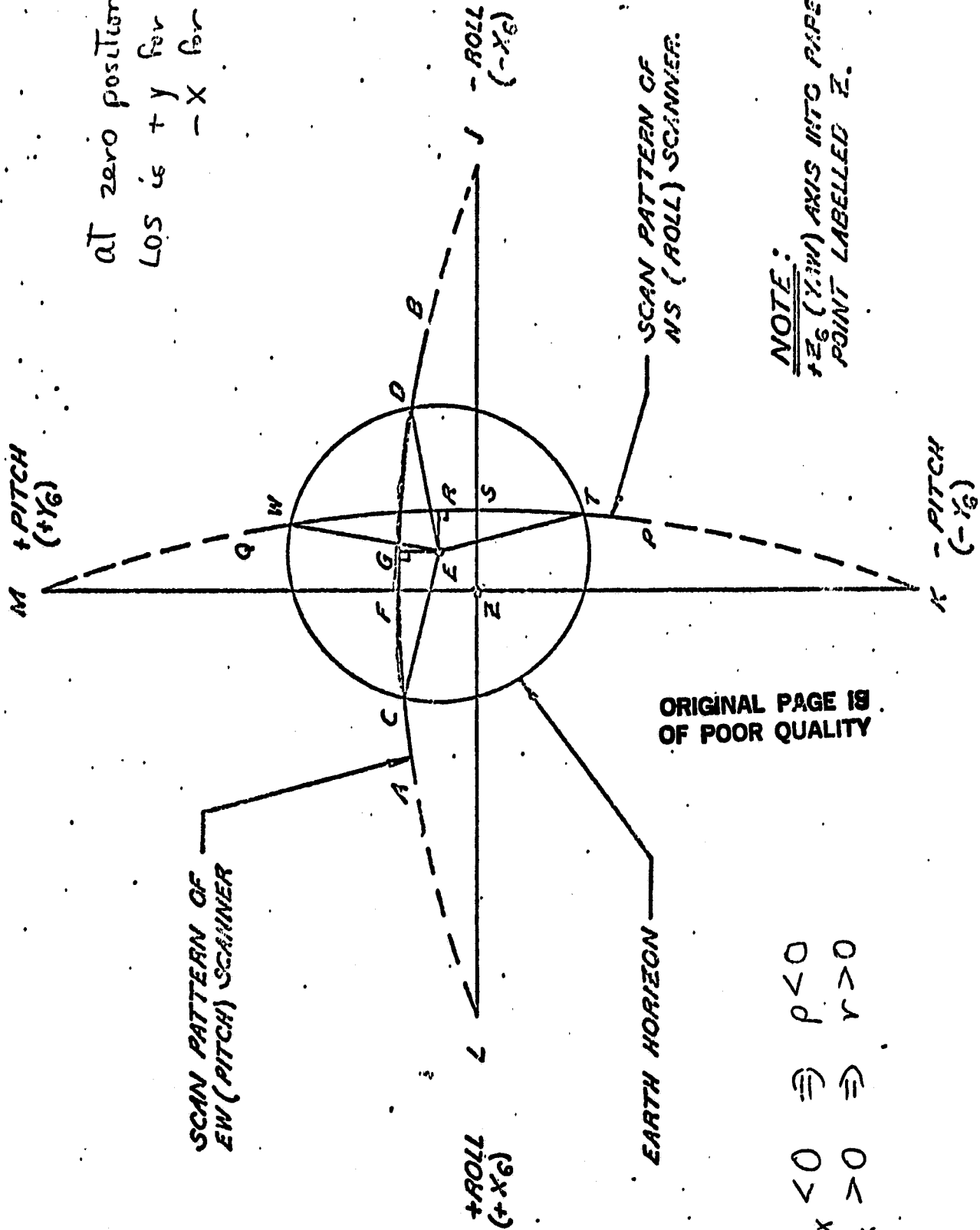
PRELIMINARY DRAFT

References

ORIGINAL PAGE IS
OF POOR QUALITY

1. CTS Spacecraft/Ground Station Batch Mode Simulation : Description, 5144-SW-102, November, 1974.
2. CTS Attitude Acquisition Detailed Operating Procedures (DOP), 5143-TR101, April 1975.
3. Functional Test Procedure, CTS Earth Sensor, TRW PD-07A-01A, March 1974.

at zero position
LOS is $+y$ for EW
 $-x$ for NS



NOTE:

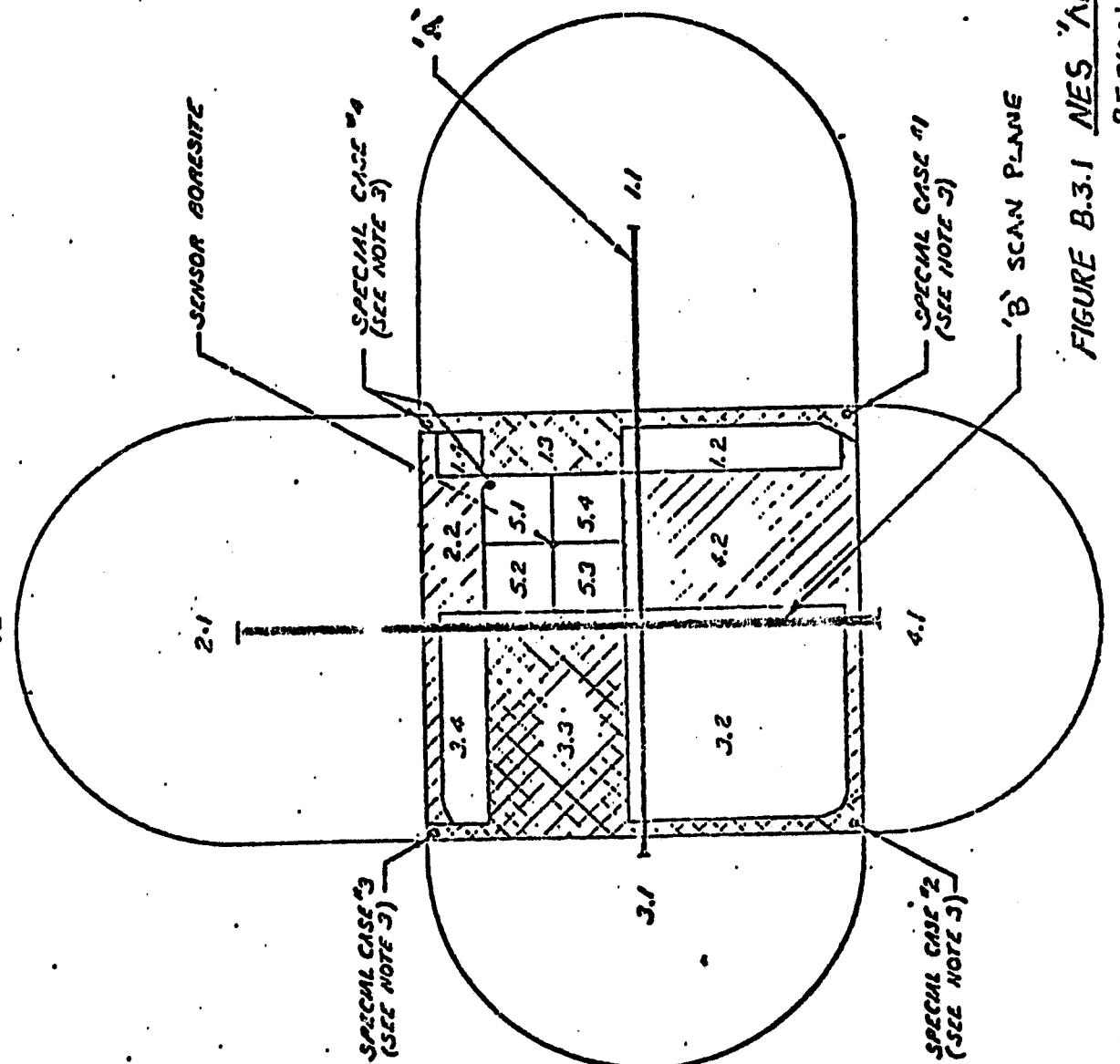
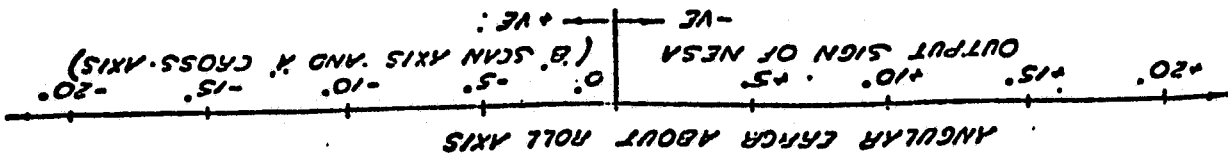
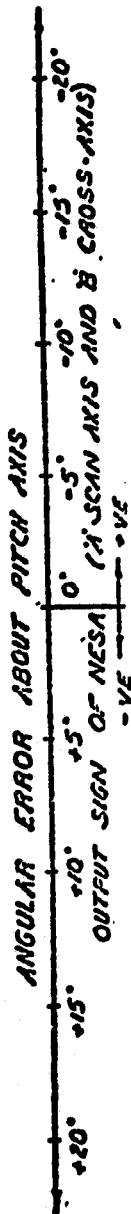
$\pm z_6$ (Y.M) AXIS INTO PAPER AT
POINT LABELLED Z.

**ORIGINAL PAGE IS
OF POOR QUALITY**

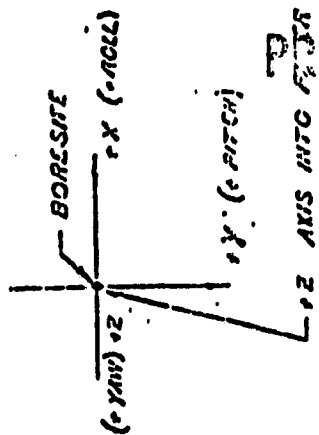
$$\begin{array}{cc} \begin{array}{c} \bigcirc \\ \vee \\ \rho \end{array} & \begin{array}{c} \bigcirc \\ \wedge \\ \rho \end{array} \\ \begin{array}{c} \Pi \\ \Pi \end{array} & \begin{array}{c} \Pi \\ \Pi \end{array} \\ \begin{array}{c} \bigcirc \\ \vee \\ \psi^x \end{array} & \begin{array}{c} \bigcirc \\ \wedge \\ \psi^x \end{array} \end{array}$$

FIG. 0.3// SCAN PATTERN GEOMETRY

Figure 1



S/C BODY FIXED
CO-ORDINATE FRAME.



PRELIMINARY DRAFT

NOTES:

1. REGIONS 5.1 TO 5.4 ARE LINEAR F.O.V. OF NESA.
2. REGION 0 INCLUDES AREAS OUTSIDE F.O.V. COVERED BY THE SPECIAL CASES ARE ~0.5° F.O.V.
3. OUTPUT OF NESA IS OPPOSITE IN SIGN TO THE ANGULAR ERROR.

ORIGINAL PAGE IS
OF POOR QUALITY

FIGURE B.3.1 NES 'A' 'B' FIELD OF VIEW
REGION DEFINITIONS

Figure 2

0. PRELIMINARY DRAFT

ORIGINAL PAGE IS
OF POOR QUALITY

(Note that $EKZ = -\alpha_E$, and α_E is used in developments for pitch and roll axis software controllers.)

The information on the angles is processed to give an output similar to that of the actual scanner. First consider the case where one horizon is on each side of the scan center as in Fig. 0.3/1. The actual scanner scan axis output gives a positive count over FD and a negative count over CF. The count is scaled so that when the angle FG is 2.82 degrees a maximum count of 255 is output. The simulation uses an equation to achieve this effect $N-S \text{ Scan} = \left(\frac{SIN - TS}{2 \times 2.82^\circ} \right) \times 235$

$$\text{East-West Scan Output} = \text{Integer} \left(\frac{FD - CF}{2 \times 2.82^\circ} \right) 255 \quad (0.3/9)$$

The cross axis output is the sum of the angles CF and FD with a fixed length subtracted to give a null output when the earth center is on the boresight. This results in the relationship:

$$\text{East-West Cross Output} = \text{Integer} \left(\frac{15.909 - (CF+FD)}{2.82^\circ} \right) 255 \quad (0.3/10)$$

A different situation arises when both G and D are on the same side of F, as shown in Fig. 0.3/3. Angle CF, as calculated by equation 0.3/4 is a negative angle. The scan axis output is proportional to the positive of angle CD. Since CF is negative and FD is positive

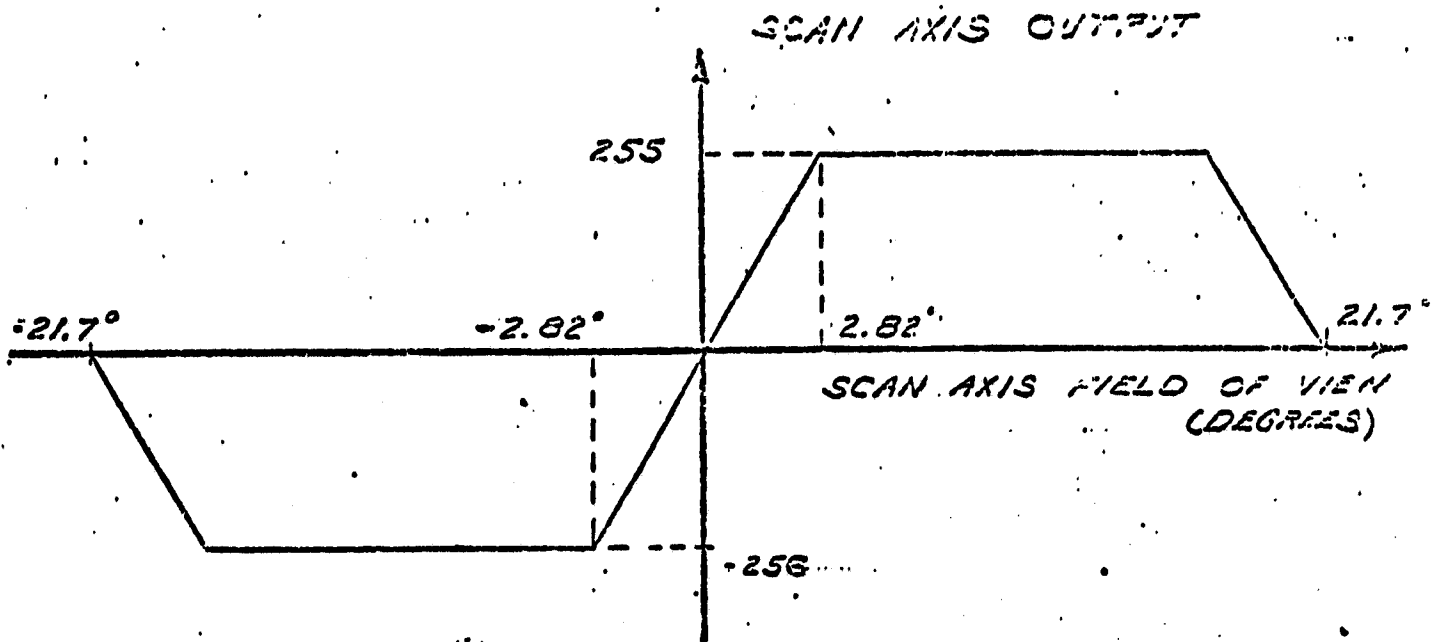
$$CD = FD - FC \neq FD - CF$$

and equation 0.3/9 is not accurate.

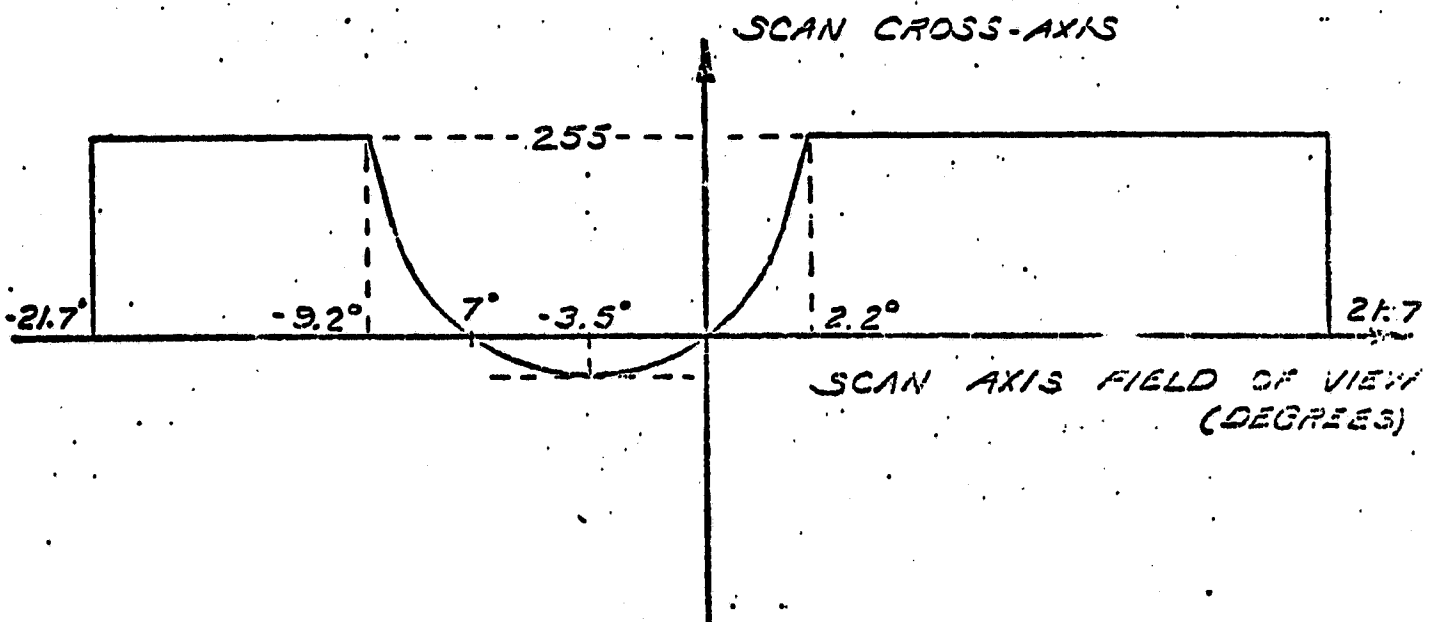
This problem may be solved by working with absolute values in the above equation. Then:

$$+ CD = |FD| - |FC| = |FD| - |CF|$$

Figure 3



(a) SCAN PLANE OUTPUT
(FOR NULL CROSS AXIS OUTPUT)



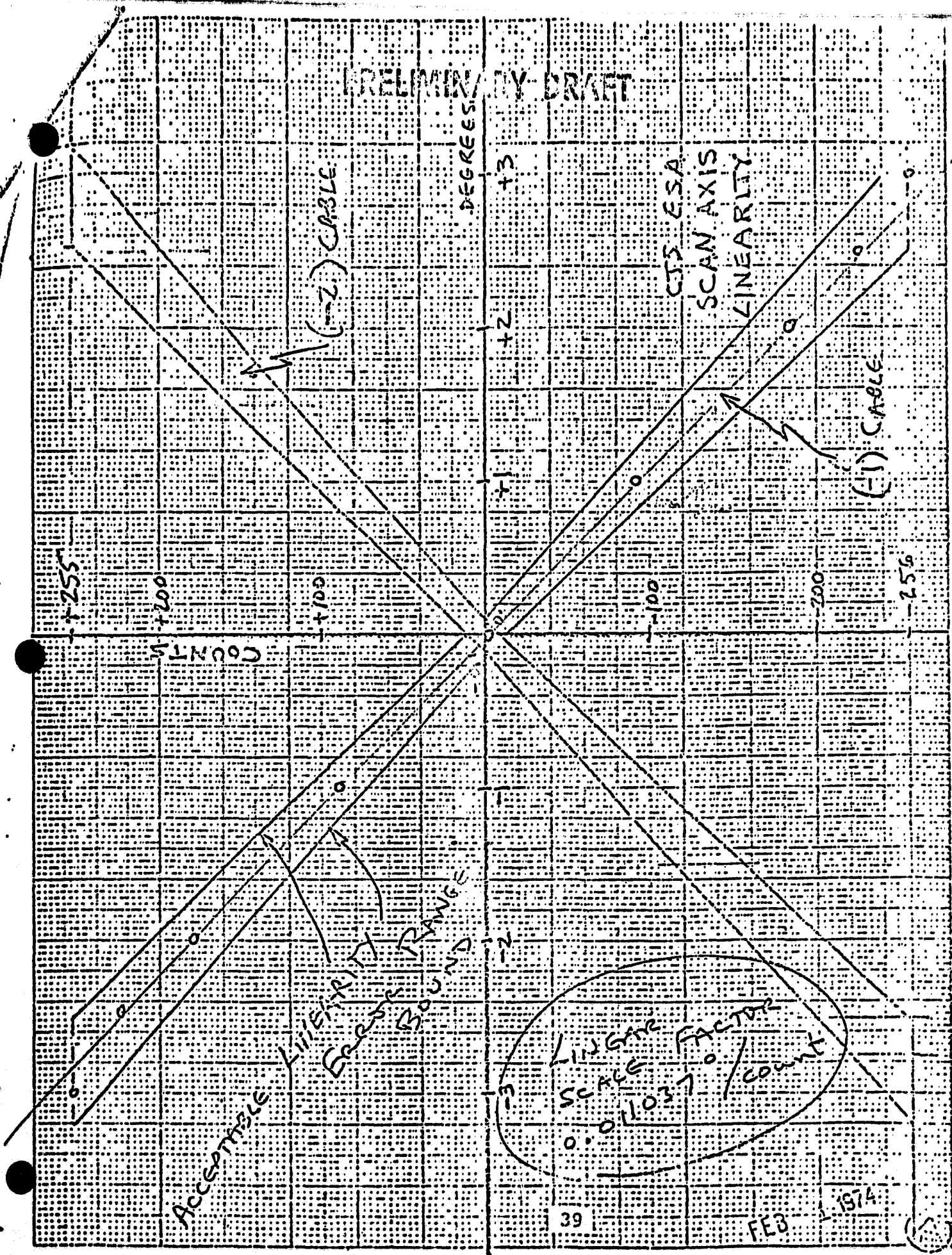
(b) SCAN CROSS-AXIS OUTPUT
(FOR NULL SCAN AXIS OUTPUT)

NOTE:

SINGLE EARTH HORIZON CROSSING CRITERIA ASSUMED.

FIG. 3.15/4 GENERALIZED EARTH SENSOR
SCANNER TRANSFER FUNCTIONS

PRELIMINARY DRAFT



ORIGINAL PAGE IS
OF POOR QUALITY

Figure 5

Date _____

DEGREES

COUNT

ACCEPTABLE LINEARITY RANGE BOUNDS

CTS GSA CROSS AXIS UNCERTAINTY

PRELIMINARY DRAFT

CTS-GSA
CROSS-Axis
UNCLAS-RTY

ACCEPTABLE
LINEARITY
RANGE
BOUND

**ORIGINAL PAGE IS
OF POOR QUALITY**

Figure 6

Date _____

(A)
 FEB 1967

PRELIMINARY DRAFT

SED 5140/189

CONFIDENTIAL

STE 300 COMMONWEALTH BLDG 77 METCALFE ST. OTTAWA ONTARIO K1P 6L6

November 28, 1975

Dr. G.M. Lerner
Computer Sciences Corporation
System Sciences Division
8728 Colesville Road
Silver Spring, Maryland

ORIGINAL PAGE IS
OF POOR QUALITY

Dear Dr. Lerner:

I'm writing this letter to confirm our telephone conversation early in November.

- 1) The label in Reference 1 should read
 $\alpha_E = \tan^{-1} E_{X6}/E_{Z6}$, NOT $\alpha_E = -\tan^{-1} E_{X6}/E_{Z6}$
as shown in the document. The figure is drawn correctly and shows positive α_E for positive E_{Z6} and positive E_{X6} .
- 2) In Reference 2, the (incorrect) definition was used as a starting point, and this causes the sign discrepancy stated in Paragraph 2a.
- 3) In Reference 2; Figures 4, 5 and 6 show the general form of the data, but signs are not specified. The assumptions of Paragraphs 2b and 2c (ie: sign of roll and pitch errors) is not justified.

.....2

PRELIMINARY DRAFT

ORIGINAL PAGE IS
OF POOR QUALITY

-2-

- 4) SED has confusing information on Reference 3.
Since SED uses ϵ_E and δ_E , I have corrected these
figures to show ϵ_E and δ_E .
- 5) As I stated in our telephone conversation; the
simulation has been compared to actual test data
taken during the mission compatibility testing,
and the signs of the NESA outputs were simulated
correctly.

I hope this helps to clear up any confusion which existed. Thank
you for taking the trouble to critically read our documents and for
bringing the discrepancies to our attention.

Yours truly,

E.A. McPherson

E.A. McPherson

EAM/it

cc: W.M. Evans
SED Ottawa

Attach.

PRELIMINARY DRAFT

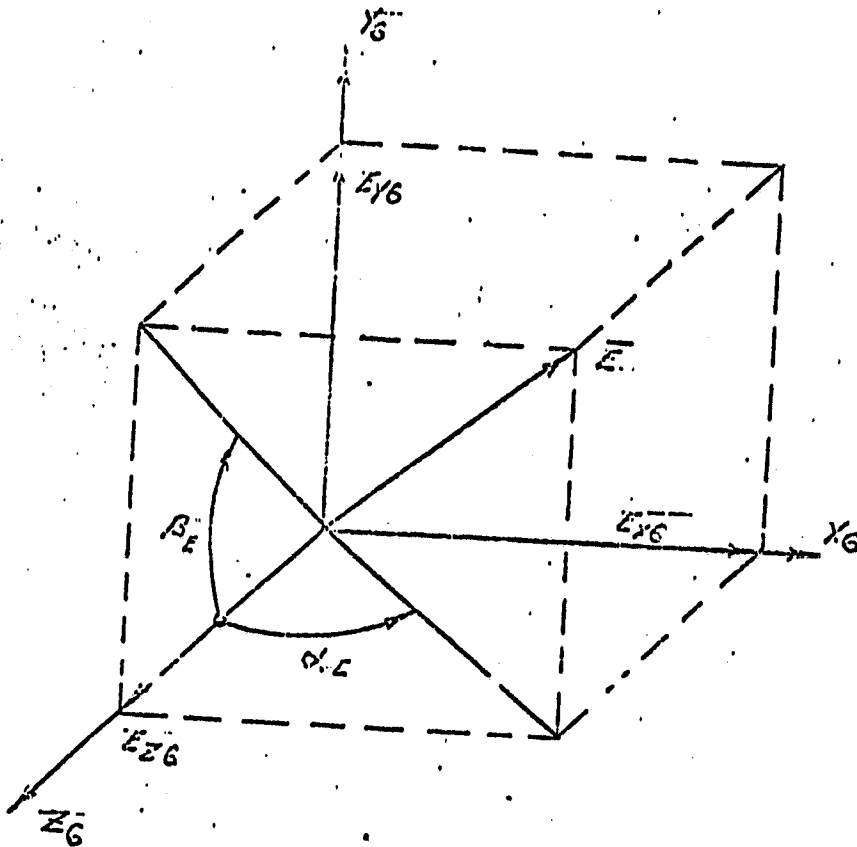
REFERENCES

ORIGINAL PAGE IS
OF POOR QUALITY

1. SED 5984-TR-102
Reverification of Earth Lock Maneuvers
Figure 4.2.2 Page 17
2. Letter TO Mr. D.G. Repas, FROM Dr. G.M. Lerner
DATED October 9, 1975
3. CTS 5144-SW-102
CTS Spacecraft/Ground Station Datch Mode Simulation.
Figures H.4.3, H.4.5 and H.4.7

PRELIMINARY DRAFT

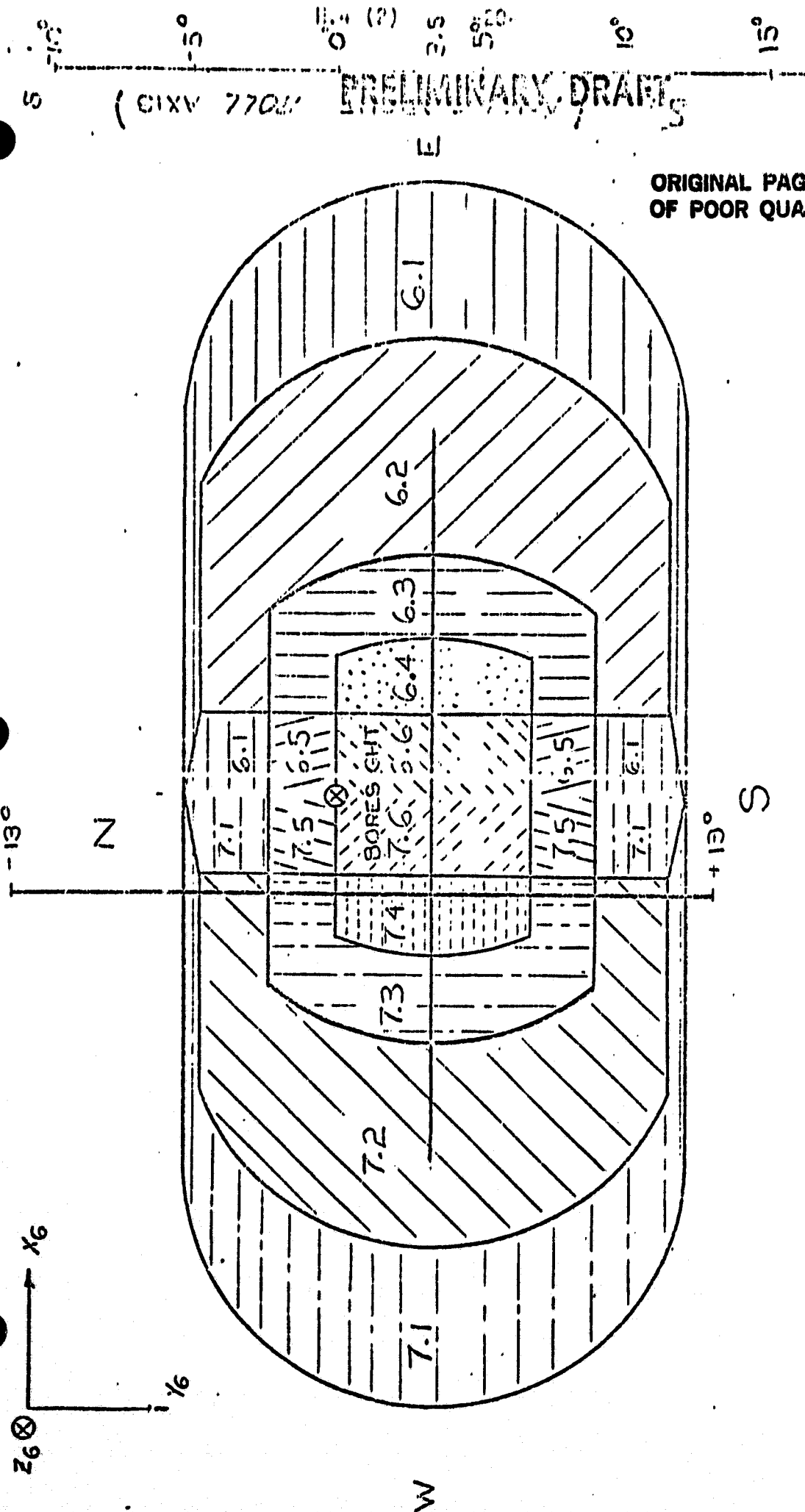
ORIGINAL PAGE 19
OF POOR QUALITY



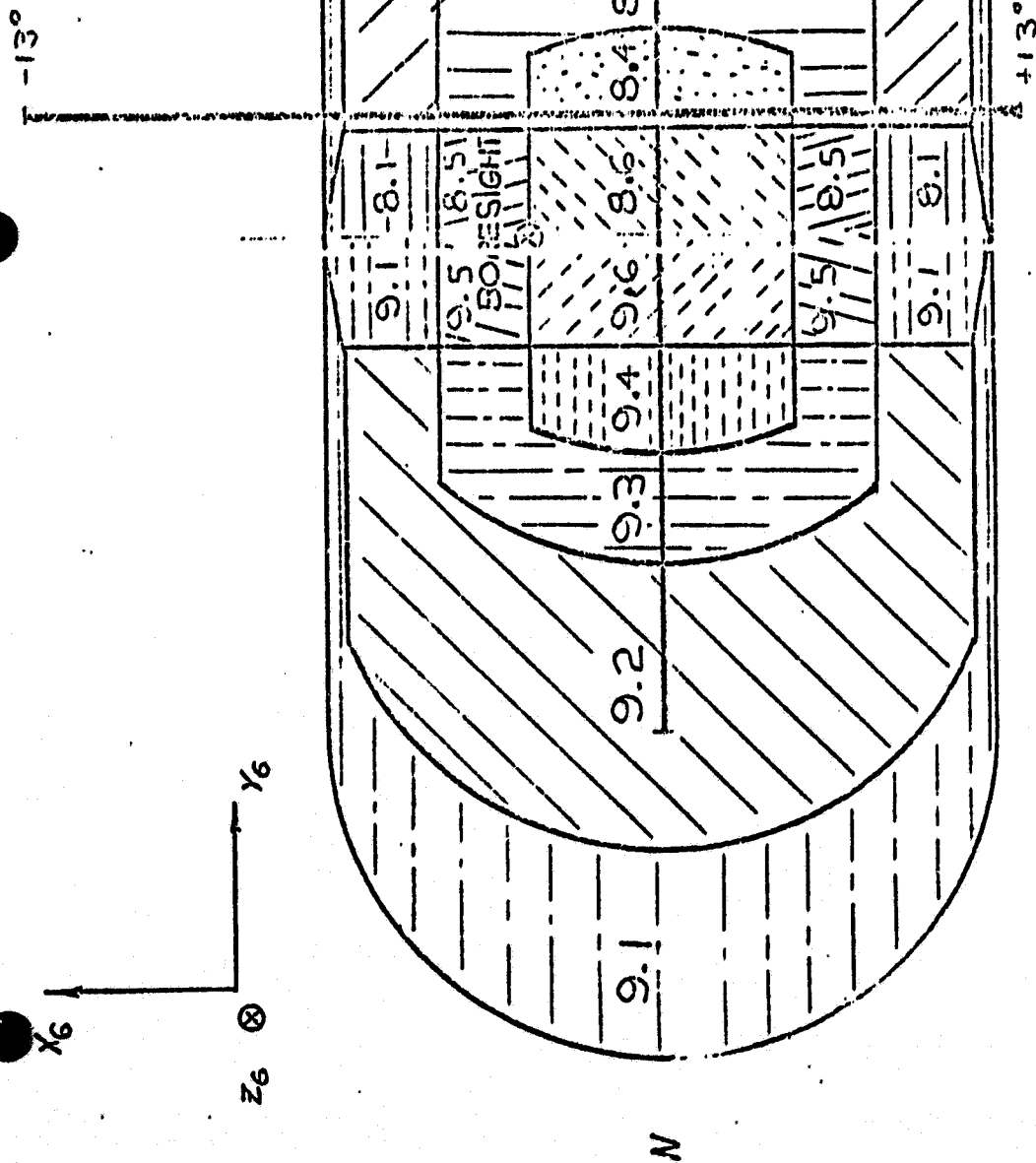
$$\alpha_E = \tan^{-1} \frac{E_{X6}}{E_{Z6}}$$

$$\beta_E = \tan^{-1} \frac{E_{Y6}}{E_{Z6}}$$

FIG. 4.2.2 DEFINITION OF EARTH SENSOR
ANGLE

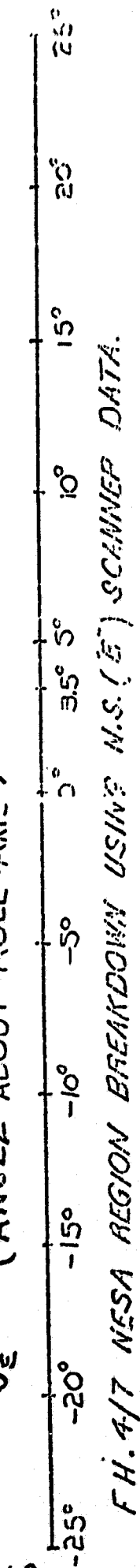


ORIGINAL PAGE IS
OF POOR QUALITY



SCALE: 1" = 5'

δ_ϵ (ANGLE ABOUT ROLL AXIS)



F.H. 4/7 NESA REGION BREAKDOWN USING N.S. (E) SCANNER DATA.

PRELIMINARY DRAFT

APPENDIX II - SUMMARY OF MEETINGS WITH SED ON NOVEMBER 19 AND 20

ORIGINAL PAGE IS
OF POOR QUALITY

PRELIMINARY DRAFT

COMPUTER SCIENCES CORPORATION

SYSTEM SCIENCES DIVISION

8728 COLLEVILLE ROAD • SILVER SPRING, MARYLAND

(301) 589 1545

20910

December 4, 1975

National Aeronautics and Space Administration
Goddard Space Flight Center
Greenbelt, Maryland 20771

ORIGINAL PAGE IS
OF POOR QUALITY

Attention: Mr. G. D. Repass
Code 581.2, Building 23, Room E-423

Subject: Contract No. NAS 5-11999
Task Assignment No. 635
CTS Attitude Acquisition Analysis
Meetings with SED on November 19 and 20
Simulation on November 20

Dear Sir:

This memorandum contains a summary of conversations held with SED at CRC in Ottawa on November 19 and 20 and comments regarding the Day Two simulation. A general discussion of changes to the DOP, GCAP software, and ground support hardware was held. In particular, the status of several earlier proposals was reviewed.

(1) Data Smoothing

CSC had expressed concern that GCAP Sun data smoothing algorithms were inadequate and proposed implementation of an extended deadband for data validation.

This proposal has not, and probably will not, be implemented but SED believes and CSC concurs that the possibility of incorrect, disruptive burns due to anomalous Sun sensor data has been reduced significantly. A number of procedural and software changes including increased GCAP visibility, reduced momentum wheel spinup duty cycle, and deactivated delta controller during spinup, have all lessened the possibility of incorrect ATTCN burns.

(2) Loss of Sun Lock During Spinup

The DOP now specifies a duty cycle of 50 percent during spinup which will yield a 30 to 35 minute spinup time rather than 10 minutes (100 percent duty cycle) previously. In addition, modifications to DAMP-2 have or will be made to accommodate nutation damping for the spinning wheel configuration without Sun lock.

(3) Attitude Acquisition Via Momentum Transfer (AAMT)

Several AAMT sequences have been simulated in detail to examine the timeline and power and thermal performance. Results have been encouraging and no serious problems with AAMT have been encountered. A detailed NSP utilizing AAMT has been written and several changes to the DOP have or will be made to cater to this NSP. The Day One precession maneuver to place the yaw axis normal to the Sun line will not occur unless specifically required to satisfy power constraints. This will preserve the required orbit normal attitude for AAMT. Inquiries to spacecraft personnel have been made to obtain approval to accelerate the wheel from a spinning configuration.

(4) Sign of NESA Transfer Functions

The sign of NESA output and associated documentation was resolved. The correct definition of pitch is $\alpha_E = + \tan^{-1} (E_X/E_Z)$ where \vec{E} is the spacecraft to Earth vector in body coordinates. Figures in the DOP describing the NESA regions should have the axes relabelled as follows: abscissa is minus α_E and the ordinate is plus δ_E . The sign of NESA output was verified in a number of ways during compatibility tests including comparison of NESA pitch output with Y-gyro output.

(5) Attitude Determination Accuracy

SED is aware of the geometric limitation of the ϕ_s determination accuracy and will not attempt a ϕ_s trim maneuver unless sufficient, accurate Earth search data is available.

A number of changes or proposed changes to the DOP and spacecraft hardware have occurred during the past two months. These include:

1. During the Day One despin, nutation damping will be performed, as required, at 16 RPM rather than 2 RPM and a precession to place the yaw axis normal to the Sun line will not normally occur.

These changes will preserve the orbit normal attitude and permit implementation of AAMT should circumstances warrant. Thruster calibration and check-out of various subsystems will also be performed at 16 RPM. The despin sequence is now 60→54→16→8→2→0 RPM.
2. Calibration of the X and Y gyros will be performed by observing the average values as a function of spin rate. A non-zero average, extrapolated to zero spin rate, will indicate a gyro bias.

3. Deployable solar array (DSA) autotrack will be turned on prior to wheel spinup. The stepping rate has been increased to 4.75 steps/second or 0.59 degrees/second (one step = 1/8 degree).
4. The wheel torque bias during spinup will be 255 or a 50 percent duty cycle.

SED noted that the nominal software freeze date was December 1 and that changes to the machine language code were time consuming and difficult to test adequately. A number of software changes were under consideration but only a small subset would be implemented.

The desirability of using a "barbeque" mode after wheel spinup (autotrack on, no active control) to obtain an improved geometry for determining ϕ_s was discussed. SED noted that for $\phi_s \approx 0$ or 180 degrees (arrays in orbit plane) telemetry nulls would occur near the 90 or 180 degree orbit slots.

CSC proposed a calibration procedure for the Z gyro which consisted of a phased spin down, 2 RPM to 0.25 RPM, with holds at 1.5, 1.0, 0.75, 0.5, and 0.25 RPM to obtain a spin rate from the spinning Sun sensor. Use of NSSS derived rates during the 90 degree pitch rotation (event A23) to calibrate the Y gyro was also proposed. SED observed that ample calibration data for the Z gyro would be available from NSSS derived rates.

CSC proposed a revision to the α controller algorithm during spinup. Tests at 100 percent duty cycle yielded more than a 50 percent reduction in the number of burns (32 to 14) for comparable angular errors. Two advantages of the algorithm, which uses both Y-gyro and α_s data are:

- (a) The algorithm is self-correcting. Burn durations are calculated using the Y-gyro and corrected using α_s errors. Operator action is not required to "trim" performance.
- (b) Performance is near optimal in the following sense. For a given spinup time, T , and a deadband, d , the minimum number of pulses satisfies $N = \sqrt{0.8 T/d}$. This relation assumes that when $\alpha_s - \alpha_{so} = +d$ a pulse occurs to yield $\alpha_s - \alpha_{so} = -d$.

*Assuming a body acceleration, a , and a limit cycle period, t , a burn will yield a rate change $\Delta \dot{\alpha} = -at$. After the burn, $\dot{\alpha} = -at/2$ and

$$-2d = (-at/2)(t/2) + a(t/2)^2/2$$
 or
$$t = \sqrt{16d/a}.$$

Since $T = Nt$ and $a = I_w \dot{\theta}_w / I_y T$, where $\dot{\theta}_w$ is the final wheel rate, we thus obtain
$$N = (I_w \dot{\theta}_w T / 16 I_y d)^{1/2}.$$

The advantages of the CSC algorithm are most pronounced at high duty cycles where manual trimming of ATTCON performance is difficult and less pronounced at low duty cycles where manual trimming is easier. However, tests of the CSC algorithm, which were performed subsequent to the meeting with SED, indicate that it also is advantageous at 50 percent duty cycle. In these runs the CSC algorithm maintained α within roughly 4° to 5° of 90° and required only 20 α burns. In the Day Two simulation at CRC, the SED algorithm required approximately 50 burns.

Results from a series of 100 percent duty cycle spinups were presented assuming Sun sensor anomalies of 10, 30, 50 and 120 second duration. Incorrect δ controller burns caused serious nutation and δ offset angles for the 60 and 120 second cases. CSC recommended deactivating the δ controller at 600 RPM. SED indicated that the δ controller would, most likely, not be used during spinup.

Other topics discussed included:

- Impact of attitude maneuvers on the CTS orbit.

The large ϕ_s precession maneuver could have a significant impact on the orbit. CSC proposed using the FSD program to evaluate orbit/attitude coupling.

- Damping algorithm.

SED noted that the timing of nutation damping burns is not optimal. It was agreed that, in general, two burns would be required to compensate for asymmetric moments of inertia and timing errors.

- Jettison of body mounted solar arrays.

CSC questioned the source of the "worst case" jettison impulse estimate. The value assumed coincident release of both arrays and would be much larger if the release were not coincident. The following parameters were obtained:

- (a) Panel weight ~ 7 pounds
- (b) Release velocity ~ 6 feet per second along geometric $\pm y$ axis
- (c) Center of mass offset ~ 3 inches

More precise values were available in the configuration control (SY104) document.

PRELIMINARY DRAFT

ORIGINAL PAGE IS
OF POOR QUALITY

- DSA deployment, flexibility.

The original DSA design was to permit deployment at 2 RPM and a document describing the spinning deployment was received. SED flexibility studies indicate a $\pm 5^\circ$ twist at the array tip and a resultant reaction torque on the body equivalent to ± 1 or 2 counts on the pitch gyro (± 0.16 degrees/second).

- Wheel acceleration profile.

The shape of the net wheel torque versus wheel speed was obtained at 100 percent duty cycle during compatibility tests and a table look-up interpolation procedure is used in the simulation model. At a reduced duty cycle, the table is used when the wheel is on and the bearing torque used when the wheel is off. The net torque is 4-1/2 to 5 ounce-inches at zero RPM, increases slowly to a plateau of 6-1/2 ounce-inches between 3700 and 4000 RPM, and drops rapidly near 4000 RPM to zero torque at 5000 RPM. The friction torque is 1-1/2 ounce-inches and decreases somewhat as the wheel bearings warm up. A duty cycle of 13 to 17 percent is required to overcome friction. Each bit on the wheel tachometer is 15 RPM. Below 2700 RPM the wheel cannot be torqued negatively because of a logic lockout.

- Sun interference on NESAs data. The NESAs model assumes:

- (a) Sun presence flag if the NESAs scan crosses within 3.5 degrees of Sun.
- (b) Data degradation at 2.6 degrees.
- (c) A 1.2 degree (100 count) addition to the scan output at 0.5 to 1.0 degrees. (1.2 degrees = Sun diameter + mirror field of view.)
- (d) The Earth will not be observed if the scan crosses within 0.5 degrees of the Sun.
- (e) The NESAs recovery time for Sun saturation is 10 seconds.

- Fuel budget.

Attitude acquisition will require only about 5 to 10 percent of the budget (less than 2 pounds). Returning to a spinner, even above 30 RPM, is therefore feasible without impacting the fuel budget.

PRELIMINARY DRAFT

ORIGINAL PAGE IS
OF POOR QUALITY

- c Spinning wheel precession maneuvers.

SED explained that yaw precessions are performed by using a roll thruster to induce an X-gyro rate and the rate is cancelled with a second, opposite roll burn, half a nutation period later. Roll precessions are performed in a similar manner using the yaw thrusters to induce a Z-gyro rate.

Day Two Simulation:

A simulation of the Day Two attitude acquisition from event A27 (prior to wheel spinup) through event A35 (acquire earth along +z axis) was observed. Several "faults" were incorporated into the simulation:

- (a) The rate gyro (RGP) subsystem failed.
- (b) The P2, R1, and O1 thrusters failed.
- (c) The prime ACE failed.

The simulation was quite successful after a slow start. About 1-1/4 hours were required to load the appropriate parameters into the GCAP and ground support computers. The most noticeable improvement was the increased GCAP visibility. A very useful display of relevant GCAP parameters, commands, and computations was available. Analysts in the "back room" now have a complete picture of maneuvers and the possibility of GCAP parameter errors has been greatly reduced. However, there is no parameter verify capability to prevent erroneous operator input. The simulation required about 3-1/4 hours to complete and no significant problems were observed although several items are worth noting:

- (1) The utility of the RGP failure as a training exercise was greatly diminished by the initial conditions, near zero rates on all three axes, and near nominal thruster alignment, calibration and performance. Nutation damping, when the RGP system is normally used was not required because of the wheel spinup occurred with zero yaw rate, environmental torques were neglected, and the thruster performance was nominal.
- (2) Attitude control during spinup was satisfactory, but far from optimal. The pitch angle ranged from 87 to 97 degrees (a 90 ± 3 degree deadband was selected), and 52 burns were required during the 33 minute spinup (every 38 seconds). Two burns were commanded at the lower deadband, a clearly undesirable feature, and the α_s rate change, was reset eight times by the GCAP operator in an attempt to optimize performance. For the achieved deadband, the

minimum number of burns would be 23 with a nominal α_g rate change of 0.56 degrees/second-burn.*

- (3) The use of the offset thrusters to perform the 70 degree yaw precession resulted in a 12 degree roll offset. Use of the offset thrusters was required because of the simulated failure of a roll thruster. The roll error was corrected by performing a roll precession using the yaw thrusters. It appeared that the maneuver selection was somewhat hasty:
 - (a) Dynamacists appeared surprised by the offset and questioned the feasibility of terminating the maneuver.
 - (b) An alternate possibility, using the yaw thrusters with roll along the Sun line was not considered until the debriefing. This choice would have delayed the acquisition (impractical for a simulation) but would not have resulted in a roll offset.
- (4) A yaw angle computation (ϕ_E) using Sun and Earth data was not available. The information would expedite final reduction of rates and angular errors since otherwise yaw errors can be detected and removed only through time consuming quarter-orbit coupling.
- (5) During the simulation, the NSS ID was 5 for the + yaw axis along the Sun line. This conflicts with NSS documentation (e.g. 5144-SW-102 Fig. 3.16/1) which states sensor 3 is along + yaw.

Recommendations:

CSC believes that the present attitude acquisition procedure is viable for a wide range of nominal and non-nominal hardware performance. SED has displayed the knowledge and has acquired the requisite hardware/software to implement a successful attitude acquisition. In the remaining weeks before launch, SED has placed the emphasis, rightly we believe, on training and finalizing operational procedures. The following areas should be considered:

(1) GCAP Restart

Every effort should be taken to minimize the time required to resume operations after a ground support failure. Logs or checklists for parameter entry, keyed to DOP event should be considered. A simulated failure of the GCAP computer (requiring use of the back-up, display computer) should be included as a training exercise.

* These numbers should be adjusted somewhat to account for time delays in data smoothing and transmission.

PRELIMINARY DRAFT

ORIGINAL PAGE IS
OF POOR QUALITY

(2) NASA/GSFC Commanding

NASA/GSFC should be prepared to command the spacecraft should a failure occur during a critical event. Only two commands would be anticipated, requiring only voice instructions from Ottawa.

- (a) Yaw burn of LTE to return to a spinner.
- (b) Activation of CWS controller.

(3) Attitude Control During Spinup

An attempt to minimize operator intervention during spinup should be made to reduce the possibility of an operator or hardware error. This could be accomplished by implementing a revised α controller algorithm or nearly as well, by selecting and maintaining a minimum $\dot{\alpha}$ (MINADT) of approximately 0.56 degrees/second. Alterations to MINADT would be required only if ATTCON performance was unsatisfactory and not merely to obtain optimal performance. Burns at the lower deadband definitely should be suppressed or an asymmetric deadband, $C'_S = 90 \pm 10^3$ specified.

(4) Maneuver Termination

It appeared during the simulation, that once initiated, maneuvers cannot be easily aborted. If this is the case, we would recommend that large precession maneuvers be preceded by a short precession in the desired direction to calibrate and validate the hardware selection.

(5) Yaw Versus Roll Thrusts for Event A.32 Precession

Present planning calls for the use of the roll thrusters to place the +Y axis southerly after wheel spinup. Unless the ϕ_S angle is near 0 or 180° and/or telemetry problems would occur, we recommend that a rotation to control $\pm X$ along the Sun line be performed after the ϕ_S determination and a yaw couple used to affect the precession for the following reasons:

- The roll thrusters will be poorly calibrated having been used only for brief ATTCON burns.
- The yaw thrusters will be well calibrated during the despin.
- Orbit perturbations cannot occur using the yaw couple and could be significant using the roll thrusters.

PRELIMINARY DRAFT

ORIGINAL PAGE 19
OF POOR QUALITY

- The 90 degree slot is favorable for $\pm X$ Sun lock, ϕ_s redetermination, and probable timeline consideration.

Yours truly,

COMPUTER SCIENCES CORPORATION

Derald Lerner

Dr. G. Lerner
Technical Supervisor
Attitude Determination Area

cc: GSFC

LeRC

CSC

R. Werking
R. Coady

H. Jackson (4)

D. Stewart
R. Headrick
H. Hooper
G. Tandon
K. Yong
J. Legg
B. Blaylock
J. Keat
Technical Supervisors

PRELIMINARY DRAFT

ORIGINAL PAGE 18
OF POOR QUALITY

GLOSSARY

Word and Acronym

AA	Attitude Acquisition
AAMT	Attitude Acquisition via Momentum Transfer
ADAMSSIM	Adams-Moulton Dynamics Simulator (Program)
ATTCON	Attitude Controller (Subroutine)
CRC	Communications Research Center
CTS	Communications Technology Satellite
CWS	Constant Wheel Speed
DAMP	Nutation damping (subroutine)
DELMAX	Maximum step size (seconds) for Adams-Moulton integrator
DELMIN	Minimum step size (seconds) for Adams-Moulton integrator
DESPIN	Despin (Subroutine)
DOP	Detailed Operating Procedures
DSA	Deployable Solar Arrays
ERTLCK	Earth lock (subroutine)
FASTOX	Fast orbit generator (subroutine)
FOV	Field of View
FSD	Flexible Spacecraft Dynamics (Program)
FSDGCP	FSD/GCAP Interface (subroutine)
GCAP	Ground Control Algorithms and Procedures
GEOS	Geodynamics Experimental Ocean Satellite
GESS	Graphic Executive Support System
JBSA	Jettisonable Body-Mounted Solar Arrays
JETDEP	Jettison and Deploy Solar Arrays (Subroutine)
LTE	Low Thrust Engines
MODE	Refers to nutation damping algorithm

PRELIMINARY DRAFT

ORIGINAL PAGE IS
OF POOR QUALITY

NESA	Non-Spinning Earth Sensor Assembly
NSSS	Non-Spinning Sun Sensors
PREDAY	Process Normal to Sun (Subroutine)
PRESUN	Precession About Sun (Subroutine)
PWC	Pitch Wheel Controller
RAE	Radio Astronomy Explorer
RGP	Rate Gyro Package
SPINUP	Spinup Momentum Wheel (Subroutine)
SSS	Spinning Sun Sensors
SUNAC	Sun Acquisition (Subroutine)
TCU	Thruster Control Unit
TOE	Transfer Orbit Electronics

Symbol

A	Attitude matrix, inertial to body transformation
A_{EW}	Transformation matrix from NESA-A frame to body frame
A_o	Amplitude of transverse component of $\vec{\omega}$
α_C	Controlled value for α_S for ATTCON
α_E	Angle from yaw axis to projection of \hat{E}_B in X-Z plane
α_S	Angle from roll axis to projection of Sun vector in X-Z plane
α_{SI}	Right ascension of the Sun vector in inertial frame
β	Pitch angle
β_E	Angle from yaw axis to projection of \hat{E}_B in Y-Z plane
β_S	Angle from yaw axis to projection of Sun vector in X-Z plane
C1, C2	Angles of horizon crossing in NESA frame
$\Delta \vec{L}_i$	Impulse for ith thruster
Δt	Time between PRESUN burns
δ_C	Controlled value δ_S for ATTCON

PRELIMINARY DRAFT

ORIGINAL PAGE IS
OF POOR QUALITY

δ_E	Elevation of \hat{E}_B from X-Z plane
δ_S	Elevation of Sun vector from X-Z plane
δ_{SI}	Declination of the Sun vector in inertial frame
\hat{E}_B	Spacecraft to Earth unit vector in body frame
\hat{E}_I	Spacecraft to Earth unit vector in inertial frame
\vec{F}_i	Force vector for ith thruster
$\gamma_{1/2}$	Nutation half angle
\hat{H}_B	Spacecraft to Earth horizon unit vector
h_W	Wheel momentum
I	Inertia transverse to DSA axis after deployment
\hat{I}	Moment of inertia tensor
I_W	Wheel inertia (0.0382 slug-ft ²)
I_{xx}, I_{yy}, I_{zz}	Diagonal elements of \hat{I}
I_1, I_2, I_3	Moments of inertia
\vec{L}	Wheel momentum vector in body reference frame
μ	Gravitational constant of Earth
NA, NB	NSSS output angles
ν	RGP output voltage
ω	RGP output rate (degrees per second)
$\vec{\omega}$	Angular velocity vector
ωt	Arbitrary line of sight angle in NESA frame
$\omega_1, \omega_2, \omega_3$	Components of $\vec{\omega}$ (also referred to as $\omega_x, \omega_y, \omega_z$)
ϕ	NESA scan plane tilt (3.5 degrees)
ϕ_E	Orbit slot
ϕ_S	Rotation angle of spacecraft about Sunline
\hat{R}	Unit vector, Earth to spacecraft
\vec{r}_i	Position vector of ith thruster relative to center of mass
ρ	Angular radius of Earth (8.7 degrees)
S	Wheel speed (RPM)

PRELIMINARY DRAFT

ORIGINAL PAGE IS
OF POOR QUALITY

\hat{s}_B^{EW}	East-west NESA line of sight vector in body frame
\hat{s}_B^{NS}	North-south NESA line of sight vector in body frame
s_{NESA}	Line-of-sight vector in NESA reference frame
s_1, s_2	Ordered NESA chord lengths
\vec{T}	Thruster torque
T_x, T_y, T_z	Components of \vec{T}
$\vec{\tau}$	Thruster torque
$\vec{\tau}_B$	Wheel bearing torque
$\vec{\tau}_W$	Wheel reaction torque
$\vec{\tau}_{gg}$	Gravity-gradient torque
θ, ϕ, ψ	3-1-3 Euler angles (inertial to body)
θ_D	Sun declination
θ_x	Angle between Sun and NESA line of sight at closest approach
\vec{v}_B	Sun vector in body frame
\vec{v}_{SS}	Sun vector in NSSS reference frame
v_1, v_2, v_3	Direction cosines of \vec{v}_B
y_1, y_2, y_3, y_4	Euler symmetric parameters

PRELIMINARY DRAFT

REFERENCES

ORIGINAL PAGE IS
OF POOR QUALITY

1. "A High Power Communication Technology Satellite for the 12 and 14 GHz Bands," C. A. Franklin and E. H. Davidson, AIAA Paper 72-580, April 1972
2. "CTS Attitude Acquisition Sequence Detailed Operating Procedures," 5143-TR-101 Issue 3, as amended November 17, 1975
3. "A User's Guide to the Flexible Spacecraft Dynamics Program" by J. V. Fedor, F. W. Hages, E. A. Lawlor, National Aeronautics and Space Administration, Goddard Space Flight Center, X-732-73-151, August 1973
4. "CTS Spacecraft/Ground Station Batch Mode Simulation Description," 5144-SW-102, November 1974
5. "Ground Control Algorithm and Procedures Program Logic Manual (GCAP)," 5147-SW-105, June 24, 1975
6. Memorandum from G. Lerner to G. Repass, Task 3000-63500, "Evaluation of GCAP Data Smoothing Algorithm - SMOOTH," August 25, 1975
7. Memorandum from G. Lerner to G. Repass, Task 3000-63500, "Meetings with SED on August 27 and 28, Simulation on August 27," September 4, 1975
8. Memorandum from G. Lerner to G. Repass, Task 3000-63500, "Loss of Sun Reference During Momentum Wheel Spinup," September 18, 1975
9. Memorandum from G. Lerner to G. Repass, Task 3000-63500, Attitude Acquisition Via Momentum Transfer," September 30, 1975
10. Memorandum from G. Lerner to G. Repass, Task 3000-63500, "Sign of Non-Spinning Earth Sensor (NSES) Transfer Function," October 9, 1975
11. "Determination of Phase Angle About Sunline During CTS Attitude Acquisition," CSC/TM-75/6197, G. Lerner
12. Memorandum from G. Lerner to G. Repass, Task 3000-63500, "Meetings with SED on November 19 and 20, Simulation on November 20," December 4, 1975

PRELIMINARY DRAFT

13. Memorandum from K. Krukewich to CTS Group, "Attitude Acquisition by Momentum Transfer," November 1975
14. "Communications Technology Satellite (CTS) Momentum Wheel Spinup Studies," CSC/TM-76/6002, J. E. Kent and B. T. Blaylock
15. "Geodynamics Experimental Ocean Satellite-C (GEOS-C) Prelaunch Report," NASA-X-580-75-23, G. Repass et al., February 1975
16. "MAPS/GEOS-C Operating Guide and System Description," 3000-17400-01TR, J. S. Legg, Jr., et al, December 1974
17. "Active Nutation Damping and Yaw Axis Precession of CTS Spacecraft Prior to Array Deployment," A. Bens, D. Bassett, D. Kjosness, and K. Magnussen, 5993-TR-103, July 1972
18. "A Structural Dynamics Model for Flexible Solar Arrays of the Communications Technology Satellite" by F. Vigneron, CRC Report No. 1268, Communications Research Center, Canada, April 1975
19. "The Effect of Structural Flexibility on the Stability of Pitch for the Communications Technology Satellite" by R. A. Millar and F. R. Vigneron, Department of Communications, Ottawa, Canada
20. Attitude Acquisition Holding Mode (24 hour) Spin Rate Study, D. Bassett and D. Kjosness, SED 5992-TR-101 (March 1972)
21. "Modification of the FSD Program for Linear Thrusting and Angular Momentum Computation," Computer Sciences Corporation, Contract No. NAS 5-24008, mod. 15 (1975)

ORIGINAL PAGE IS
OF POOR QUALITY